A NEW TECHNIQUE FOR LUBRICATION CONTROL BASED ON FRICTION CONDITIONS IN CNC MACHINE LINEAR GUIDEWAYS USINGSERVOMOTOR CURRENT SIGNALSIN FEED DRIVE SYSTEM

MAHDI SPARHAM

FACULTY OF ENGINEERING
UNIVERSITY OF MALAYA
KUALA LUMPUR

2015

A NEW TECHNIQUE FOR LUBRICATION CONTROL BASED ON FRICTION CONDITIONS IN CNC MACHINE LINEAR GUIDEWAYS USING SERVOMOTOR CURRENT SIGNALS IN FEED DRIVE SYSTEM

MAHDI SPARHAM

DISSERTATION SUBMITTED IN FULFILMENTOF THE REQUIREMENTS FOR THE DEGREE OF DOCTOR OF PHILOSOPHY IN ENGINEERING

FACULTY OF ENGINEERING
UNIVERSITY OF MALAYA
KUALA LUMPUR

2015

UNIVERSITI MALAYA

ORIGINAL LITERARY WORK DECLARATION

Name of Candidate: MAHDI SPARHAM I.C/Passport No: X95385380

Registration/Matric No: KHA100125

Name of Degree: DEGREE OF DOCTOR OF PHILOSOPHY IN ENGINEERING

Title of Thesis:
A NEW TECHNIQUE FOR LUBRICATION CONTROL BASED ON FRICTION CONDITIONS IN CNC MACHINE LINEAR GUIDEWAYS USING SERVOMOTOR CURRENT SIGNALS IN FEED DRIVE SYSTEM

Field of Study: MANUFACTURING PROCESSES

I do solemnly and sincerely declare that:

(1) I am the sole author/writer of this Work;
(2) This Work is original;
(3) Any use of any work in which copyright exists was done by way of fair dealing and for permitted purposes and any excerpt or extract from, or reference to or reproduction of any copyright work has been disclosed expressly and sufficiently and the title of the Work and its authorship have been acknowledged in this Work;
(4) I do not have any actual knowledge nor do I ought reasonably to know that the making of this work constitutes an infringement of any copyright work;
(5) I hereby assign all and every rights in the copyright to this Work to the University of Malaya ("UM"), who henceforth shall be owner of the copyright in this Work and that any reproduction or use in any form or by any means whatsoever is prohibited without the written consent of UM having been first had and obtained;
(6) I am fully aware that if in the course of making this Work I have infringed any copyright whether intentionally or otherwise, I may be subject to legal action or any other action as may be determined by UM.

Candidate's Signature Date

Subscribed and solemnly declared before,

Witness's Signature Date
Name:
Designation:

ABSTRAK

Kawalan Berangka Komputer pemesinan (CNC) pada masa ini adalah salah satu proses pemesinan yang paling penting untuk pembuatan dalam industry. Ini kerana mesin CNC yang menawarkan ketepatan yang menggalakkan dan pemesinan tepat. Walau bagaimanapun, tingkah laku geseran dalam guideways linear adalah salah satu cabaran yang paling penting dengan pemesinan CNC, sebagai geseran yang lebih tinggi menghasilkan gerakan dan ketepatan masalah. Pelinciran dalam guideways mesin CNC digunakan untuk mengatasi masalah tersebut. Pada masa ini, sistem pelinciran yang telah ditetapkan melalui perintah pengekodan CNC digunakan untuk melincirkan guideways dalam mesin CNC. Proses pelinciran dilakukan berdasarkan masa-masa tertentu dan jumlah suntikan minyak tanpa mengira nilai memotong kuasa, berat dan saiz bahan kerja, daya geseran pada guideways, dan keadaan proses pemesinan. Ini membawa kepada perlindungan kurang daripada guideways terhadap daya geseran yang tinggi atau penggunaan minyak yang berlebihan untuk mencapai kurang daya geseran dalam guideways.

Untuk sebab-sebab ini, satu teknik kawalan pelincir baru diperkenalkan berdasarkan keadaan geseran dalam CNC mesin guideways linear. Mengawal jumlah pelincir dan masa berdasarkan nilai daya geseran dalam guideways linear mempamerkan perbezaan utama antara teknik pelinciran baru dicadangkan dan sistem yang sedia ada. Pertama, nilai daya geseran dalam keadaan pelinciran kering dalam guideways linear dan dalam X dan Z dikira dari daya pemotongan diukur melalui analisis berkuat kuasa di guideways. Kedua, servomotor semasa diramalkan menggunakan neuro penyesuaian sistem inferens kabur (ANFIS) pemodelan, sebagai sistem ANFIS yang sesuai untuk meramalkan semasa motor dalam keadaan pelinciran kering kerana keadaan yang tak linear dalam proses pemesinan. Ketiga, daya geseran meramalkan dengan model ANFIS disahkan menggunakan skim ujian

baru untuk mengenal pasti purata meramalkan kesilapan dan ketepatan, yang didapati masing-masing 1.38% dan 98.62%, pada paksi-Z. Kerana kesilapan ramalan adalah rendah, model ANFIS yang digunakan untuk membina maklum balas minyak, unit kawalan pelinciran (LCU) dapat meramalkan nilai daya geseran berdasarkan perbandingan antara servomotor isyarat semasa dalam talian diukur dan diramalkan. The LCU menghantar isyarat kepada penggerak untuk mencetuskan pam minyak untuk menyuntik minyak. Jumlah suntikan minyak dan masa (interval sambutan pam (PRI)) dikenal pasti berdasarkan nilai daya geseran ANFIS-diramalkan dalam guideways linear. Nilai daya geseran meramalkan dikategorikan kepada Lima tahap yang bersamaan dengan lima servomotor paras semasa. Dalam setiap peringkat, PRI ditakrifkan secara optimum untuk melindungi guideways. Akhir sekali, prestasi pengawal itu disahkan palung satu set baru eksperimen di mana keputusan teknik pelinciran dicadangkan dibandingkan dengan keputusan sistem pelinciran biasa. Dalam ujian ini, beberapa parameter dipantau dalam kedua-dua sistem pelinciran, termasuk suhu, servomotor semasa, daya pemotongan, PRI, dan penggunaan minyak. Eksperimen pengesahan disediakan untuk tiga tahap tenaga, termasuk memotong rendah, sederhana dan tinggi, untuk memastikan ketepatan dan mengawal ketepatan pemesinan dalam keadaan yang berbeza Menurut hasil, suhu yang diukur, servomotor semasa, dan memotong nilai daya hampir sama dalam kedua-dua proses pelinciran. Walau bagaimanapun, minyak mengepam masa dan jumlah yang berbeza. PRI dalam teknik kawalan pelinciran baru menunjukkan pengurangan ketara penggunaan minyak sebanyak 67% untuk kemasan, 33% untuk perubahan sederhana dan 100% untuk perubahan kasar berbanding dengan mod pelinciran biasa. Teknik baru boleh mengawal bukan sahaja minyak pelincir yang berasaskan kepada keadaan geseran dalam CNC mesin guideways linear tetapi juga berguna dari segi keberkesanan kos dan mencegah pencemaran alam sekitar.

ABSTRACT

Computer Numerical Control (CNC) machining is currently one of the most important machining processes for manufacturing in industry. This is because the CNC machine offers favorable accuracy and precise machining. However, the frictional behavior in linear guideways is one of the most crucial challenges with CNC machining, as higher friction produces motion and accuracy problems. Lubrication in CNC machine guideways is used to overcome such problems. Currently, a predefined lubrication system via CNC coding command is used to lubricate guideways in CNC machines. This lubrication process is performed based on fixed times and amounts of oil injection regardless of cutting force value, weight and size of the workpiece, friction force on the guideways, and machining process conditions. This leads to less protection of guideways against high friction force or excessive oil consumption to attain less friction force in the guideways.

For these reasons, a new lubricant control technique is introduced based on the friction conditions in CNC machine linear guideways. Controlling the lubricant amount and time based on friction force values in linear guideways exhibits a major difference between the new proposed lubrication technique and existing systems. First, the friction force values in dry lubrication conditions in linear guideways and in the X and Z directions are calculated from the cutting force measured via force analysis in the guideways. Second, servomotor current is predicted using adaptive neuro fuzzy inference system (ANFIS) modeling, as the ANFIS system is ideal for predicting motor current in dry lubrication conditions due to the nonlinear condition in the machining process. Third, the friction forces predicted with ANFIS modeling are verified using a new testing scheme to identify the average predicted error and accuracy, which were found to be 1.38% and 98.62% respectively, on the Z-axis. Because the predictive errors are low, the ANFIS model is used to build an oil feedback, lubrication

control unit (LCU) to be able to predict friction force values based on a comparison between online measured and predicted servomotor current signals. The LCU sends a signal to the actuators to trigger the oil pump to inject oil. The oil injection amount and time (pump response interval (PRI)) are identified based on the ANFIS-predicted friction force values in the linear guideways. The predicted friction force values are categorized into five levels corresponding to five servomotor current levels. In each level, the PRI is defined optimally to protect the guideways. Finally, the controller's performance is verified through a new set of experiments where the proposed lubrication technique results are compared with ordinary lubrication system results. In these tests, several parameters are monitored in both lubrication systems, including temperature, servomotor current, cutting force, PRI, and oil consumption. The verification experiments are prepared for five cutting force levels, including low, medium, and high, to ensure correctness and control accuracy in different machining conditions. According to the results, the measured temperature, servomotor current, and cutting force values are nearly the same in both lubrication processes. However, oil pumping time and amount are different. The PRI in the new lubrication control technique shows significant reduction of oil consumption by 67% for finishing, 33% for medium turning and 100% for rough turning compared with ordinary lubrication modes.

The new technique can control not only the lubrication oil based on friction conditions in CNC machine linear guideways but is also useful in terms of cost effectiveness and preventing environmental pollution.

ACKNOWLEDGEMENTS

In the name of Allah, the Most Gracious and the Most Merciful, all praise to Allah, the most beneficent and magnificent, who provided me the courage and persistence to bring this work to successful completion, and who was with me through the most difficult times and always.

Accomplishing a dissertation is a major task and I could not have done it without the help of God and a number of people. Hence, it is my pleasure to acknowledge those who have contributed their effort directly or indirectly throughout my thesis work.

First of all, I would like to thank University of Malaya and the Ministry of Education for their financial contributions to this project. I would also like to thank the Ministry of Science, Research and Technology for the considerations to their students abroad, and I am not exception from this issue.

Secondly, I would like to express my deepest gratitude and appreciation to my dissertation supervisors, Professor Dr. Mohd Hamdi Abdul Shukor for the whole-hearted support and knowledge he has offered during my graduate studies and Dr. Ahmed Aly Diaa Mohammed Sarhan, who gave lots of advice, support, patience and hours of constant dedication to my research. It has been a pleasure and great experience working with them. My appreciation extends to Dr. Noor Azizi Bin Mardi for his kind help and allowing me access to equipment to complete the project.

Several people from University of Malaya should be acknowledged for their support as well: researchers, technicians, and administrative personnel. I particularly thank our friends at the Centre of Advanced Manufacturing and Material Processing (AMMP). I deeply appreciate your help and support for this research.

Last but not least, special gratitude to my lovely Father and Mother for their prayers, and my beloved wife Nafiseh Ganji for her love, support and understanding throughout the preparation of this project. I would never be this far without your support and encouragement.

Thank you so much.

Mahdi Sparham

9 January 2015

TABLE OF CONTENTS

LIST OF FIGURES

LIST OF TABLES

LIST OF ABBREVIATIONS

Abbreviation	Description
AC	Alternating Current
ADC	Analog to Digital Converter
AI	Analog Input
ANFIS	Adaptive Neuro Fuzzy Inference System
AO	Analog Output
API	Application Programming Interface
APT	Automatically Programmed Tool
CAD	Computer Aided Design
CAM	Computer Aided Manufacturing
CIMS	Computer Integrated Manufacturing Systems
CNC	Computer Numerical Control
CPU	Central Processing Unit
°C	Degree Celsius
DAQ	Data Acquisition
DAS	Data Acquisition System
DC	Direct Current
DI	Digital Input
DNC	Direct Numerical Control
DO	Digital Output
DOC	Depth of Cut
exp	Exponential
F	Force
f	Feed rate
FC	Cutting Force
F_k	Kinetically Friction force
FL	Longitudinal force
FLS	Fuzzy Logic System
FMS	Flexible Manufacturing Systems

Abbreviation	Description
F_p	Predicted Friction force
Fr	Radial Force
F_s	Statistically Friction force
Ft	Tangential Force
g	Gravitational Acceleration
a	Acceleration
GUI	Graphical User Interface
I_M	Measured servomotor current
I_P	Predicted Servomotor current
Kg	Kilo gram
Kw	Kilo Watt
°K	Degree Kelvin
LabVIEW	Laboratory Virtual Instrument Engineering Workbench
LCS	Lubrication Control System
LCU	Lubrication Control Unit
LED	Light Emitting Diode
m	Meter
MATLAB	Matrix Laboratory
MCU	Machine Control Unit
MDI	Machine Directly Indicate
MISO	Multiple-Input Single-Output
mm	Millimeter
mm/s	Millimeter Per Second
N	Newton
η	Viscosity
OFDM	Orthogonal Frequency Division Multiplexing
Pa	Pascal
PDI	Positive Displacement Injector
PID	Proportional Integral Deferential
PIOQL	Portable Intelligent Optimum Quantity Lubrication

Abbreviation	Description
PRG	Progressive Lubrication System
PRI	Pump Response Interval
PSU	Power Supply Unit
RMS (or rms)	Root Mean Square
RPM	Revolution Per Minute
RPS	Revolution Per Second
r	Radius
S	Spindle Speed
SLR	Single Line Resistance
STR	Samples to Read
t	Time
$T_{A, B, C, D}$	Thermocouples A, B, C, and D
T_{cr}	Critical Temperature
T_z	Torque in Z direction
UI	User Interface
VI	Virtual Instruments
W	Weight
π	Pi
ω	Angular Velocity or circular frequency
μ_k	Kinetic coefficient of friction
μ_S	Static coefficient of friction

CHAPTER 1: INTRODUCTION

1.1 Research Motivation

Linear guideways are widely applied in advanced machinery industries worldwide for different types of CNC machine (e.g., turning, milling, grinding, and gantry). All of these machines require accuracy and precision in the machining operations to manufacture quality products. The cutting operation in product manufacturing occurs with the displacement of machine tables on linear guideways. For this reason, linear guideways are significant parts and have sensitive locations in CNC machines to yield precision and accuracy. Friction and temperature are two major factors of deformation in guideways and non-smooth motion that prevents superior accuracy and precision in machine operations. An appropriate lubrication system reduces detrimental factors and helps improve the machining products. A new lubrication control technique based on the friction conditions in CNC machine linear guideways using servomotor current signals in a feed drive system is proposed in this research.

The consideration and application of new technology in advanced industries worldwide, including aerospace, nanotechnology, electronics and microelectronics, and manufacturing parts, medical equipment, and automotive equipment and machinery, etc. are of particular importance. These are also necessities and inseparable components in the modern world. To achieve these invaluable industrial feats and their suitable use, producing parts and products with high precision, accuracy and high sensitivity is essential.

Among these, CNC machine tools play a major role in the manufacturing and production of superior parts. Applying these machine tools is of utmost importance because

their production is of high precision and accuracy. Machining process precision and accuracy can reach more than a micrometer (0.001mm).

Manufacturing training in the past did not include studies on new techniques for lubrication control based on friction conditions in CNC linear guideways. Learning was purely through doing experiments in various laboratory classes. The current system came to be introduced later. Even when new lubrication was introduced as a study subject, the principles of measurement were never fully discussed and emphasis was on the descriptive study of instruments.

In this thesis, cutting parameters affecting cutting force, servomotor current effects on feed drive systems and thermal effects on the deformation of linear guideways on the machine table are studied. Moreover, estimation schemes for friction in the linear guideways of two machine motion axes for precision accuracy requirements are presented. The cutting force values correspond to different cutting conditions, spindle speed, depth of cut, and feed rate that are effective for friction conditions in machine linear guide ways in order to change cutting force values. The friction force on linear guideways of machine tools is calculated based on effective force analysis during cutting. The analysis of forces produced, such as normal force and cutting force is necessary for estimating the friction force. Friction force on the X- and Z-axes is estimated analytically.

The online measured servomotor current is used for comparison with predicted servomotor current in dry lubrication conditions. The decision between measured and predicted servomotor current is considered for checking two important issues: first, the necessity for lubrication in CNC machine linear guideways; and second, to understand the cutting operation duration. This decision is made to predict the friction force in linear guideways in dry lubrication conditions. Servomotor current and friction force prediction

using different cutting conditions is modeled via Adaptive Neuro-Fuzzy Inference System (ANFIS) method. The predicted friction forces are compared with those calculated and presented in chapter four, to investigate the prediction accuracy using ANFIS modeling.

Lubrication control in CNC machine linear guideways is processed according to the predicted friction conditions. In this process, the lubrication amount and time based on friction force values in linear guideways comprise the new lubrication technique proposed.

1.2 Objectives

This project is undertaken in order to contribute to the improvement of smart lubrication and friction control in CNC machine linear guideways using feedback servomotor current signals in a feed drive system. The following are the objectives of this research:

- To develop a new technique for lubrication control system based on friction conditions in CNC machine linear guideways using servomotor current signals in feed drive system.
- To control, optimize oil consumption and to effectively maintain or improve lubrication efficiency to protect the guide way and to provide environmentally friendly green technology.

1.3 Problem Statement

Today, CNC machine technicians generally have no background in thermal error, cutting force error, servomotor current error, and friction force error and their analysis. Developments have changed the way we look at experiments, planning and the science of lubrication control. The study of lubrication control has detached from the study of instruments, and attention has shifted to studying the lubrication process. Emphasis is more

on knowing how to create new lubrication control techniques based on friction conditions using servomotor current signals in a feed drive system rather than with *what*.

The frictional behavior in linear guideways is one of the most crucial challenges for CNC machining, as higher friction produces motion and accuracy problems. Lubrication in CNC machine guideways is used to overcome these problems.

A carriage moves on the table of a CNC machine in sliding form in order to cut in machining operations. We know that anywhere between two parts of friction and temperature stimulus there will be stick-slip motion, wear and corrosion of the parts. Thus, manufacturers are interested in these machines, particularly to facilitate this process with an actual lubrication system.

Currently, a predefined lubrication system via CNC coding command is used to lubricate the linear guideways in CNC machines. This lubrication process runs based on a fixed time and amount of oil injection regardless of cutting force value, weight and size of the workpiece, friction force on the guideways, and machining process conditions. This leads to less protection of the guideways in case there is high friction force, or excessive oil consumption to lessen the friction force in guideways. The most important matter in this thesis is the quality of correct lubrication. This thesis then emphasizes the effects of cutting parameters on friction and a systematic approach of lubrication is shown, after which the new control technique with smart, optimum lubrication quantities in a CNC machine is introduced. All measurements, modeling, assembly and control work are carried out with a high precision lubricant produced at the CNC laboratory, University of Malaya. The setup is instrumented with current and temperature sensors, and cutting force measurement at different locations to allow detailed physical models to be made and new control techniques to be developed and experimentally validated.

1.4 Overview of the Study

This study is organized as follows:

First is a literature review of machine tool precision and accuracy, including the precision manufacturing field and achieving accuracy by error compensation. The equipment employed is explained along with the measuring technique for recognizing friction force in CNC guideways. In addition, there is a discussion on potentially achievable effective lubrication when taking into consideration conventional types of lubrication systems, such as manual and automatic lubrication in CNC machines. Moreover, studies on optimization and reducing lubrication quantity consumption are presented in Chapter 2. Some objectives and roles that show the parameters' effects on CNC machine performance are also mentioned in this chapter.

Chapter 3 presents the methodology for three subsystems used in this research over the course of two sections: Section 1 introduces the new proposed lubrication system and experimental setup. This section addresses the measuring methods and lubrication control unit (LCU), as well as system performance. Section 2 in this chapter explains graphical user interface programming and Simulink, with block diagrams of temperature, cutting force and servomotor current signals. In the overall circuit diagram, all three block diagrams are placed within a general while loop using one output express VI. With this method, all data are written and stored in one file. In addition, we talk about a machining model and measurement techniques identified. Before the measurements, the method of installing the sensors on the machine and their relation with the measurement modules are described. In the sub-controller design, the control process is investigated in six steps.

Chapter 4 presents the estimation of friction on the linear guideways regarding cutting force and normal force in the static model. In addition, the following experimental results are

observed for the estimation of effective parameters on the control system: cutting force, friction force, and servomotor current. The effective forces on linear guideways are investigated and estimated, and figures, diagrams and graphs with several experimental improvements on this system are displayed. To obtain any of the measured parameters, circuit programming is designed.

ANFIS modeling to predict friction force in CNC guideways and servomotor current in a feed drive system with dry lubrication conditions to be employed in the new lubrication control system is presented in Chapter 5. In the primary section, servomotor motion and force analysis in the X- and Z-axis directions are considered based on the moving tool model. Then the servomotor current for the X- and Z-axes is measured based on the model of current designed in a block diagram. Two sets of training data are loaded in two ANFIS models to predict (1) friction force in guideways and (2) servomotor current in dry lubrication condition.

Chapter 6 deals with lubricating oil control for minimizing friction. A description as well as objectives and roles that exhibit the parameter effects on friction in linear guideways of CNC machine performance are given. Moreover, this chapter presents the experimental results of characterized motion in terms of current sensitivity and predicted friction force based on oil injection time or pump response interval (PRI). Then a comparison is made between servomotor currents, predicted friction force and oil consumption in ordinary and smart modes. Finally, chapter 7 concludes this work.

1.5 Research Methodology

The research methodology entails several subsystems: a) Mechanical parts design; b) electric and electronic setup design; and c) control design. Each subsystem includes one or more of the lubrication project sections, which is shown in the flow chart below. This

diagram represents a solution model to develop and design smart lubrication by analyzing, documenting and managing a process or program in various laboratory settings (Figure 1.1).

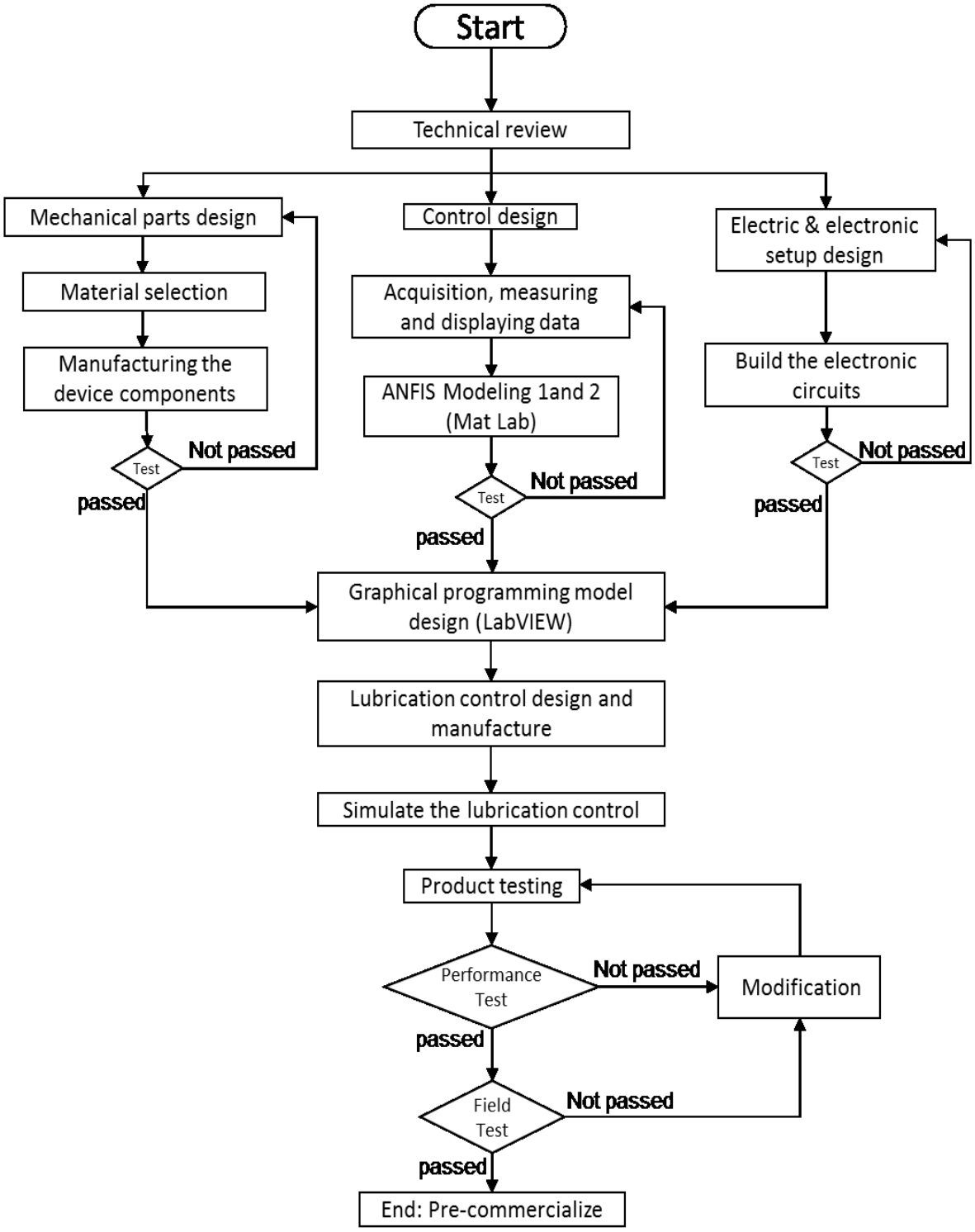

Figure 1.1 Research methodology flow chart

According to above flowchart, this methodology is divided to four major sections. Each of these can help us, for achieving to a technique for lubrication control system. The sections are including:

Section 1: Estimate the friction forces in linear guideways using cutting force analysis at dry lubrication conditions.

Section 2: Measure the servo motor current in feed drive system in dry lubrication conditions.

Section 3: ANFIS modeling to predict the servo motor current and the friction force in dry lubrication conditions.

Section 4: Build the lubrication control system based on friction conditions in CNC machine linear guideways using servomotor current signals in feed drive system.

CHAPTER 2: LITERATURE REVIEW

2.1 Introduction

CNC is short for Computer Numerical Control. CNC machines are controlled so that all axes move, while machining operations are done by a computer. This means that all data and information are processed using a computer and its memory. The microprocessor converts the data into electrical signals (pulses) to move the servomotor.

Achieving high accuracy and repeatability of accuracy with limited tolerance and high operation reliability are among the items required and that should be considered in designing CNC machines. Hence, the physical structure of mechanical CNC machines differs from traditional machines. In traditional machines, operator skill compensates for design defects and lack of machine accuracy. However, in the CNC machining process, due to the absence of direct operators, actions should be performed with high accuracy and reliability.

The APT programming language was developed in 1958. CNC machines were first invented in 1972 and in 1975, the first Fanuc system 5 and 6 series PSUs (power supply units) came on the market. The Sinumerik System 3 controller was manufactured in 1981. A microprocessor controller with 4-bit 1982 Sinumerik System7 emerged. By the end of 1982, 16-bit microprocessor controllers were being made with Sinumerik System 8. The Series 800 Analog Controller 810 Sinumerik was developed in 1985 (Kasa Narasimha Murthy, 2014). In 1986, the Sinumerik controller 850 came on the market and the Sinumerik controller 880 followed in 1988. In 1996, Siemens 810 and 840 Series Digital Controls were shipped. Now, with the help of computer and technological developments, various companies with diverse interests in a multitude of industries build controls with the speed and processing capabilities provided.

The hardware in CNC machines is not much different from ordinary machine bodies, but the controller is the main part, setting CNC apart from other machines. Usually, machines of other kinds (lathe, milling, grinding, etc.) are known for having a controller and operator training. After-sales services are generally based on the control system.

2.1.1 CNC Machine Components

The main components of a CNC machine are as follows:

a) Machine program,

b) Machine Control Unit,

c) Software Machine,

d) Servomotor,

e) Mechanical components,

f) Measurement system.

Various companies worldwide produce controllers and install them on CNC machines, including Siemens, Fanuc, HEIDENHAIN, Mitsubishi, Fagor, Fidia, GE, Allen-Bradley, Okuma, Bendix, and Hust. With the development of NC machines came many attempts to improve their capabilities. The advent of the computer caused dramatic changes in NC manufacturing technology systems and the first CNC machine was built in 1972 (d'Iribarne & Lutz, 2014).

The following are some basic differences between NC and CNC machines:

1- The NC machine runs a program to read line by line, and if there are wrong lines, a control unit is capable of detecting them.

2- In many CNC machines applications can be used for running tests and the moving tool path can be observed graphically on the machine monitor or PC. If modification is required, the program must be reformed.

3- Parametric coding in repetitive operations such as cycles can be easily written with coding program and it facilitates easy parametric coding of complex parts and geodesics. In addition, coding of such parametric coding is possible with APT language (Automatically Programmed Tool) and CAD/CAM software (L. Wang, 2014).

4- Since program correction in a CNC machine is done using software, any changes can easily be made and then saved. In addition, written applications can be connected effortlessly.

5- Tool radius offset can easily be done for curves and slope paths, thus significantly eliminating the volume of calculations. The advantage of most significance lies in the difference between NC and CNC, whereby NC machines read line by line and the program is not capable of compensating for the tool radius.

6- In CNC machines, the machining program can easily be transferred from the remote to the machine via DNC. The robot is easily connected to these machines in Computer Integrated Manufacturing Systems (CIMS). Generally, using CNC machines separately is not correct, and it is better to use the system in Flexible Manufacturing Systems (FMS) and CIMS.

The three main components of the machine hardware include:

- Drivers (Motors),
- Mechanical parts,
- Measurement system.

Drivers (Motors): In CNC machines, three kinds of driver systems are used: electrical, hydraulic and pneumatic. Due to the low power of pneumatic drivers, they are used less.

a) Electrical Drivers

Stepper motors: The motors have a simple structure, small size and reasonable prices. They are used in simple CNC machines, but precision is limited, torque is relatively low and power is less than 1hp (Figure 2.1). These motors are used in open-loop controls. For each input pulse to the motor, there is a rotation of a certain value of angle steps. In this kind of motor, the step angle differs (1.8, 2.5, 2.81, 5, 7.5, 45, 90 degrees). In a new type of motor, there is an even smaller step angle of 1 degree. Since controlling such digital motors is simple, they have good compatibility with the motor control unit. With a specific rotation angle of the motor, a ballscrew rotates and moves to a table with a ballscrew pitch. For example, if the ballscrew pitch is 6 mm and the accuracy of the encoder is 1.8 degrees per pulse to move a complete table over 12 mm (two full rotations of the ballscrew), 400 electrical pulses need to be sent. In addition, these motors can move along the table's X-, Y- and Z-axes in the rotary table's rotation.

Figure 2.1 Stepper motor used in CNC machine

These motors can be started and stopped quickly and there is no need for warmup. If needed, electro-hydraulic motors can be used at high torque, which are a combination of a stepper motor and a hydraulic system. Stepper motors can stop immediately when the pulses stop and do not require a clutch brake. Additionally, there is sufficient accuracy in terms of

the desired rotation and thus, feedback and closed-loop control are not necessary. When there is no closed-loop control and feedback, if, for whatever reason the pulse is continuous, measurement inaccuracy will result.

DC motors: DC motors are most widely applied in CNC machines (Figure 2.2). These motors have high power, steady speed and rapid reaction to velocity changes. By changing the voltage, it is possible to change the rotational speed, and by varying the current, the torque can be controlled. Maintenance of DC motors is important for the external collector and brushes. In some cases, the external collector and brushes cause motor noise, which has considerable impact on the track surface quality(Molina, Ponce, Ponce, Tello, & Ramírez, 2014).

Figure 2.2 Brushed DC servomotor for 3-axis CNC kit

AC motors: In these motors, the rotation control is based on frequency changes. This incurs much higher cost than DC motors. Advantages of AC motors include no rectifiers and cheaper maintenance due to the absence of external collector and brushes (Giri, 2013).

However, AC motors occupy a large volume (Figure 2.3). Prior to 1991, these were used to move tables and spindles.

Figure 2.3 AC servomotor with driver in CNC machine

b) Hydraulic motors

High power control with low force, speed control simplicity, force as stepper and quick reaction to direction change are hydraulic driver characteristics (Figure 2.4). The main disadvantages of hydraulic drivers are much leaking and they are expensive. System speed is also below electrical motor requirements. Hydraulic drivers are used in closed-loop controls (Prodan, Balan, Bucuresteanu, & Motomancea, 2013). Two types of hydraulic driver are rotary (motors) and sweep (cylinder and piston). For short longitudinal motion of the cylinder and piston, and for long longitudinal motion of hydraulic motors, ball screws are used.

Figure 2.4 A sample hydraulic motor

The mechanical components include machine bed, linear guideways, ball screw, machine table, and tool changer (turret).

The heart of a traverse system in a CNC machine is the nut and ball screw. When the motor's rotational motion is transmitted to the screw, the machine table finds a linear motion through the nut. Ball screws have much higher efficiency than ordinary screws. Efficiency usually reaches 90%, because it is in between the screw and nut balls. In ordinary screw and nut, there is sliding motion, while in ball screws there is a rolling motion.

2.2 Machine Tool Precision and Accuracy

Traditionally, the machining process is carried out by an operator who is responsible for safety and work quality (Pérez-Canales & al., 2011) . Improvements in machining processes have been observed thanks to the development of new lubrication methods based on injection automation approaches (Park & al., 2010). However, the inherent problems related to detection, prediction, control, and flexible changes for quality machining still exist almost everywhere. Machining precision mostly depends on the adequate lubrication and performance of a machine's individual units (Suresh Kumar Reddy & al., 2010). Accumulated errors occurring in machining are rooted in various thermo-mechanical and setup parameters as well as environmental conditions. The main factor that determines and covers the majority of these errors is the lubrication process (Tawakoli et al., 2009). Obviously, effective lubrication can be achieved when taking into consideration lubricant type, period of lubrication, amount of lubricant in each period, and precise functioning of the lubrication system (Jin-Hyeon & Yang, 2002).

Although computer numerical control (CNC) machines offer great precision and versatility in the fabrication of complex parts, machining is an innately slow and expensive process (Soundararajan, Zekovic, & Kovacevic, 2005). Attempts to improve the efficiency

of machining processes must be tempered by the call for maintaining part accuracy and avoiding dynamic instabilities that may incur damage to the moving parts, cutting tools, work pieces, or machine drive systems (Altintas, 2012). Machine accuracy entails how well the tool point is positioned anywhere in the envelope, and it comprises three aspects. The most common is positioning accuracy, or how precisely the carriage and cross slide, place the tool tip in the desired location. For roughly 80% of all turning jobs, an accuracy of 0.013 mm (0.0005") is acceptable and most machines currently available can easily achieve this. Precision is not only inherent to the machine but also depends on how the machine is handled. To allow a new or existing CNC machining center to attain its potential precision it is advisable to implement these techniques (Yun, Kim, & Cho, 1999).

2.2.1 Precision Manufacturing Field

Precision CNC machining seriously requires attention to detail, especially at the micron level. This process is exciting because people get to deal mostly with scientists and telecommunications developers. In addition, if cutting objects becomes boring, precision CNC machining may be the next step to take. There are several types of precision in CNC machining, one of which employs appropriate linear guideways to improve the way carriages travel and cut during machining. This is also known as exact difficult machining because of the low tolerance it has for error (Ramesh, Mannan, & Poo, 2000). As problematic as it may sound, experts have made it a point to become successful at this level. At a specific point in the machining stage no contact takes place between the machine and product, being considered a stress-free process (i.e. electric discharge machine (EDM), wire cut EDM CNC, etc.)

Enhancing CNC machine tool accuracy has always been the most important pursuit for researchers in the precision manufacturing field. Ribeiro et al. expressed that the economic

context has led industries to try and diminish equipment failure or unexpected breakdowns (Ribeiro & Barata, 2011). Consequently, such effort highlights the need for a user-friendly, knowledge-based fault diagnosis system for CNC machines.

Linear slide rail is a type of rolling guide, run by the power formed between the infinite-scroll circulation steel balls in the slider and slippery course. Along the slippery course load platform, the ball screw can easily perform high-precision linear movement (Figure 2.5). Compared with traditional sliding guides, the rolling-guided friction coefficient can drop to as low as 1/50 of the original, greatly decrease invalid movement, and therefore effortlessly achieve μm-class feed and positioning. Moreover, the bound unit design between the slider and slippery course allows the linear slide rail to withstand loads from all directions. Not only can a traditional sliding guide not match the above-displayed characteristics, but the machine, able to cooperate with the ball screw and use a linear slide rail for guidance, will greatly improve the accuracy and efficiency of the mechanical equipment.

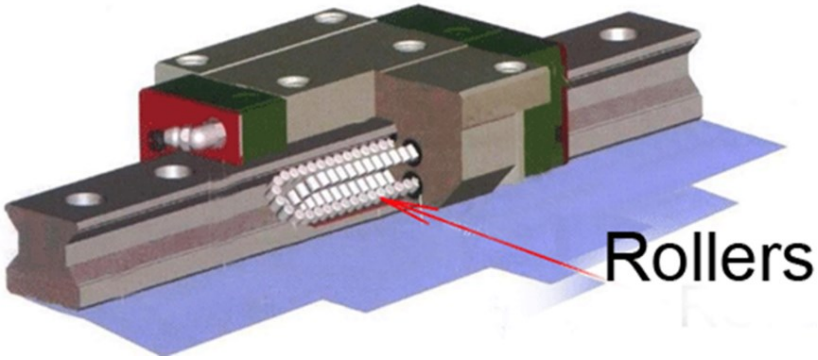

Figure 2.5 Linear slide rail using a type of rolling guide (Sutar & Deshmukh, 2013)

2.2.2 Achieving Accuracy by Minimizing Errors

The accuracy of any movement -- be it positional or locational change accomplished by the moving parts of CNC machines, is imperative. Accuracy is achieved by utilizing resources such as different high-precision parts for the base, guides, and basic components

of carriages and feed drive systems, or by reducing friction in the carriage mechanisms of movable subsystems. In accuracy and precision machining, friction in the moving components (ball screws, guideways, etc.) of machine tools is a major cause of significant errors. However, these characteristics are difficult to calculate and model. At low speeds, friction may cause relatively large errors, especially when a switch in the direction of motion of an axis is required (Armstrong-Hélouvry, Dupont, & De Wit, 1994). Due to the fact that friction in a CNC machine guideways forms a critical point, more and more researchers have recognized that the effect of friction must be carefully considered in the study of motion control in servo feed drive mechanisms in order to improve precision. Despite this being the case, it is difficult to measure friction in the control field, due to its failure in precise tracking control and nonlinear performance in low-velocity settings (Armstrong-Helouvry, 1993).

In order to improve product quality in high-tech industrial fields and precision product processes, a high precision position control system has been developed. However, this system faces a problem with friction between the contact surfaces of two materials. This denigrates precise motion because friction is susceptible to time-varying effects such as temperature, lubrication condition, material roughness, and degree of pollution. Thus, the tracking performance of servo systems is degradable because of the friction characteristics.

CNC machine accuracy and precision are influenced by a variety of errors categorized into four major sources. Displacement caused by thermal expansion is by far the greatest source, sometimes contributing as much as 70% of the total error. Mechanical deviation is around 20%, and comes in the form of errors introduced by wear and tolerance of various machine components. Forces acting on the parts as well as tool error and wear collectively constitute the remaining error percentage.

Rust, corrosion and thermal deformation of devices, and other parts and subsystems in precision CNC machines may be affected by the progression of heat generated by friction, the operation of hydraulic drives and electrical devices, and by the heat transferred by the linear guideways lubrication. The initiation of such deformation can be reduced or controlled by placing disposable heat sources adjacent to the machine tool guideways, using lubrication systems for temperature stabilization, or employing cooling devices in both the lubrication and cooling systems(Mickelson, 2006).

Static and dynamic errors affect the precision of highly accurate machines. Usually, the tolerance of geometrical parts and assembly errors precipitates problems called static errors. Errors such as this are common, and they are usually identified and controlled via established techniques. In contrast, dynamic errors can be monitored even when the machine is applied in a similar fashion. These types of error describe and compensate for errors that are to be modeled, as they are a function of time. Thermal and vibration errors are the most common dynamic errors, with thermal errors comprising almost 70% of total machining errors (Yun et al., 1999) in high-accuracy machines.

Kim et al. (2004) investigated thermal behavior and positional error in the machine tool's spindle. The machines included were those having linear motors governed by linear movements in both the X- and Z- directions (Jong-Jin & al., 2004). Pretot et al. (2000) and Ferreira (1987) recommended comprehensively studying the heat generated by linear motors (Pretot & al., 2000). It is also necessary to accurately evaluate the heat transfer characteristics by improving thermal mathematical models (Chow, 2010).

2.3 Friction in CNC Machine Linear Guideways

According Figure 2.6, friction between contact points in linear guideways and carriages is problematic for achieving machining precision and accuracy. Temperature increases due

to friction; consequently, friction is usually considered in motion control design for the sake of simple implementation (Tung, Anwar, & Tomizuka, 1991). However, the slideways generally used in the feed drive servomechanisms of CNC machine tools often induce significant static friction (Kato, 1974; Persianoff, Ray, & Vidal, 2003). Static friction cannot be ignored in practical applications because it can significantly deteriorate the reversal motions of feed drive servomechanisms.

Guideways are among the most critical elements in machine tools, as they guide the tool or work piece along a predetermined path (Schwenke et al., 2008), usually in a straight line or circle (Liu & Melkote, 2007). Guideway wear along with thermal and vibration errors are the largest contributors to positioning and dimensional workpiece errors in precision machining. For instance, machine tool carriages typically operate on slideways under high loads and slow speeds and thus must be able to get into motion quickly and smoothly and then continue at a constant speed.

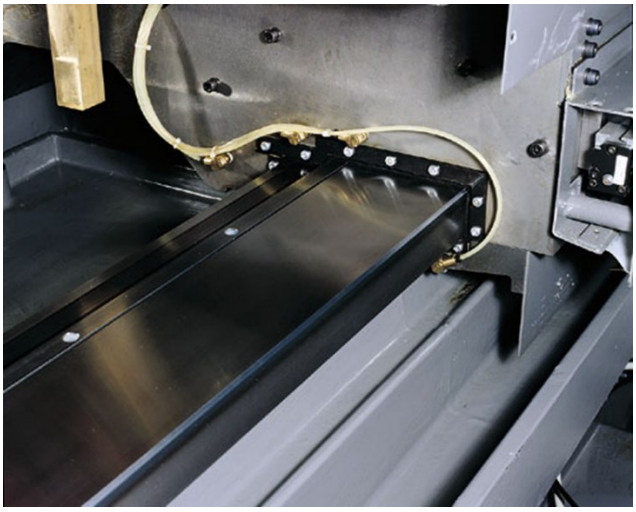

Figure 2.6 Contact points in linear guideways

Imprecise motions between parts and phase transitions in materials due to overheating are common problems in all types of machining. Problems can be detected by measuring temperature in dynamic parts (Lin & Tzeng, 2008). For instance, increasing heat due to

thermo-mechanical errors can be detected by thermal sensors, which are thermocouples positioned at appropriate points. Monitoring the temperature at critical points can provide real-time information about the quality of the machining process (Haitao & al., 2007; Pfefferkorn & al., 2009).

Excessive frictional resistance at startup compared to that during motion can cause undesirable erratic or jumpy motions, commonly referred to as machine tool chatter or stick-slip. Effective lubrication is important to prevent stick-slip problems. Extreme lubrication pressure properties are also required to prevent scoring of slideways and guides. Other benefits of using lubrication oil include decreasing friction, saving energy and preventing rusting and corrosion. Lubricants are employed in milling machines, lathes, planers, saw guides, grinders and jig borers for less guideways wear, longer life as well as better machining accuracy (Pateloup, Duc, & Ray, 2010).

Furthermore, friction plays an important role in the precise position control of many modern machines such as robots, machine tools, etc. However, it is challenging to deal with the issues concerning friction in the control field due to its deterioration effect on precise tracking control and highly nonlinear performance at low velocity (Armstrong-Helouvry, 1993). With respect to enhancing machine tool precision, progressively more researchers have realized that the influence of friction must be carefully considered when studying the motion control of servo-feed mechanisms. Various important machining processes and control tasks have been studied in the hopes of solving these matters, including in-process monitoring and lubrication control. Such tasks require reliable and industrially adaptable sensors that can provide informative signals regarding the state of the machine process.

According to Figure 2.7, lubricated sliding surfaces exhibit frictional behavior. The frictional coefficientμ, is caused by the oil viscosity, ɥ (cP), sliding speed, υ (mm/min^{-1}),

and the average normal force on the plane of projection, N (N). In zone Ⅰ, a solid-to-solid contact between guide surfaces is seen, since the oil film thickness is less than the surface roughness. Although the oil film prevents total seizure, partial seizure can occur as conditions approach boundary zone Ⅰ. This field is called boundary lubrication state. In zone Ⅲ, the oil film is much thicker than the surface roughness and prevents solid-to-solid contact. This is called the hydrodynamic lubrication state. Field Ⅱ indicates a middle stage called the mixed lubrication state. Many researchers have analyzed the frictional behavior of machine components, and some work has been carried out on practical machine tools. To simplify the stick-slip procedure, Kato et al. (1974) studied the characteristics of static friction during sticking and kinetic friction during slipping.

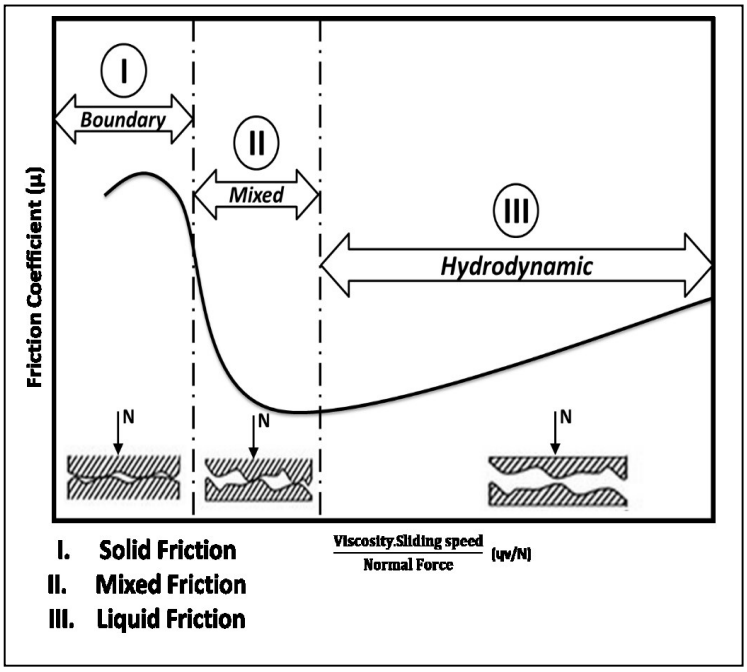

Figure 2.7Schematic representation of the Stribeck diagram(Kim & Chu, 1999)

The static coefficient of friction is larger than the kinetic coefficient of friction when two metal surfaces slide against each other. Under such condition, a machine tool slide will stay motionless until the feed force reaches a sufficiency to overcome the static friction. Then

the slide will be accelerated by the applied force, and the movement will be obeyed instantly by the tendency for the slide to slow down or come to rest. This unstable motion known as stick-slip motion is repeated in rapid succession until the slide reaches a certain velocity, which is called the critical velocity. Particularly in CNC (Computer Numerical Control) machine tools, this unstable motion should be removed even at very low sliding speeds.

However, static friction is position-dependent (Yeh & Su, 2011) and the interplay of moving parts in a transmission system can considerably affect the position dependency of static friction (Huo & Poo, 2013).

Friction occurs in all machines possessing relative motion and is salient in many servomechanisms and simple pneumatic or hydraulic systems. Realistically speaking, friction can lead to tracking errors, limited cycles, and undesirable stick-slip motion. Engineers have to deal with the undesirable effects of friction, and the lack effective tools make it all the more severe (Wang & al., 2001; Zhiping & al., 2013). In order to overcome this problem and achieve a high performance of servo control systems, an appropriate friction model (Olsson & al., 1998) to describe the friction characteristics is required. The LuGre model (Freidovich & al., 2010) is representative of such model. Researchers have utilized this model for it possesses a simple, implementable structure in the controller design, and it is capable of representing most friction characteristics with the notable exception of pre-sliding characteristics (Kim, Kim, & Han, 2009).

Tarng and Cheng used a nonlinear model to simulate and analyze the dynamic behavior of stick-slip friction on the contouring accuracy of CNC machine tools (Tarng & Cheng, 1995). Hou et al. (2013) investigated the tribological behavior of the thin-deep scraped and wide-shallow scraped surface topography of machine tool guideways (Kim & Chu, 1999). In order to evaluate the cutting force and cutting torque by the feed motor current, Stein et al.

(1986) evaluated the DC and AC servo feed motor drives in the machine tool as force and torque sensors, respectively (Stein & al., 1986; Stein, Wang, & al., 1990). Current control is necessary, as it is susceptible to increasing friction at the contact points of dynamic parts. Therefore, servomotor current was variably selected for measurement. Changes in current indicate that the mechanical movements are not smooth. The skip-slip motions of carriages and/or supporters cause the current in the servomotors to increase. In this thesis, the frictional behavior of an AC servo drive horizontal machining center is studied. The feed motor current is measured by a Hall effect sensor to calculate the feed force indirectly. The current of the variable feed motor can provide useful information about the stick-slip motion in carriages of the linear guideways since for turning operations the motor is aligned normally to the machine tables.

It is imperative to improve a dependable and economical intelligent monitoring system for friction processes. A successful monitoring system enhances the accuracy and precision of machine tool guideways, which leads to well-functioning cutting tools and workpieces in cutting processes. Cutting force is one of the important characteristic variables to be monitored during the cutting process (Tlusty & Andrews, 1983; Weck, 1983).

2.4 Servomotor Current in Machine Feed Drive Systems

Relocation moving carriages of CNC machines is one application of AC servomotors. The carriages can only have a reciprocating motion on linear guideways along the machine axes. The AC servomotor is best used in low power control applications (Figure 2.8). The main factors are current, speed, and torque specifications. An AC servomotor is usually a two-phase induction motor with some special design structures, which contains two stator windings oriented 90˚ electrically apart (Rubaai, Castro-Sitiriche, & Ofoli, 2008). The stator

windings are driven by voltages of equal magnitude and 90˚ phase difference. These results in electrifying currents i_1 and i_2 are phase-displaced by 90˚ and have the same values.

Kim and Jong (2004) analyzed the power and current of motors that act as alternate sensors in a machine tool. Electromechanical systems (i.e., feed and spindle axes) can be a function of power and current variations (Jong-Jin & al., 2004). These variations in the context of a dynamic system should be determined prior to using the sensors. This dynamic system can also serve as a low-pass filter. Accordingly, the mentioned system can be classified as a dynamometer due to its low bandwidth.

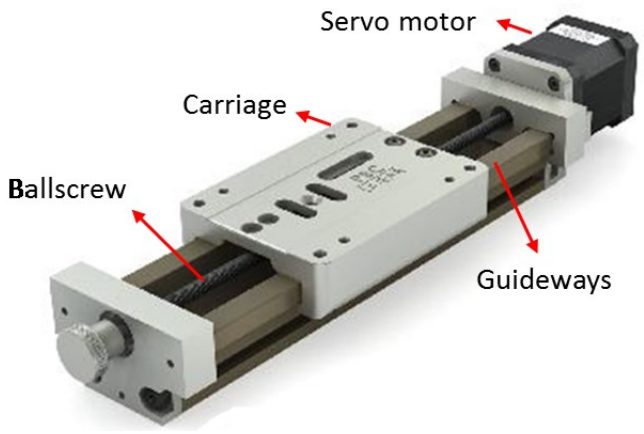

Figure 2.8 Moving carriage on linear guideways by a servomotor

Measuring small value power consumption in the cutting force process proves problematic for dynamometers (Byrne et al., 1995). Nowadays, engineers are more interested in using current and power values for measurement. This is because this method is user-friendlier, easy to operate, and more economical compared to dynamometers. Furthermore, the presence of a current evaluator in the motor drive encourages the installation and implementation of sensors. Measurement sensors also do not prevent the machining process from taking place.

Stein and Wang (1990) analyzed the spindle power consumption in a lathe machine center based on current sensors and voltage transformers (Stein JL, 1990). Altintas (1992)

evaluated the current of a DC motor in a vertical milling machine for feed drive systems (Altintas & Chicago, 1992). Additionally, Stein et al.'s proposed method is based on the measurement of feed system DC motor current in a CNC turning machine (Stein & al., 1986), while Lee et al. (1995) used AC servomotor current to estimate the cutting forces in CNC milling (Lee & al., 1995). Mannan and Broms followed Stein and Wang's methods in the setup process, based on the estimation of cutting torque and depending on spindle power (Mannan & al., 1989). This is used to determine the feed force in drilling, milling, and turning operations.

In the aforementioned studies, the ratio between current and power as well as cutting force and torque are measured with a dynamometer. This task was evaluated by Stein et al. (1990) to predict cutting torque and cutting force based on the feed motor current in AC and DC servo machine tool as torque and force sensors.

Current sensors have been used by many researchers to evaluate cutting force in the cutting process due to the inherent disadvantages of dynamometers. After some experiments, Stein et al. (1986) developed a dynamic lumped-parameter model in a feed drive system based on DC servomotors (Stein & al., 1986). Moreover, in the processes of turning, they determined the bandwidth, accuracy, and sensitivity of the current for cutting force. A study mirroring the work of Altintas (Altintas & Dong, 1990) was carried out by monitoring the drawn current, and now it is done in the context of the milling process.

However, both commercial dynamometers and motor current measurement have been used in parallel on spindle and feed drive systems to measure cutting force perfectly. The current behavior of an AC feed motor drive lathe machining center can be planned. A Pearson current monitor (Hall effect sensor) measures the feed motor current to determine the feed force and indirectly compare it with frictional behavior.

AC brushless motor currents for two X- and Z-axis feed drive systems were measured in terms of bandwidth and sensitivity in order to estimate their ability to be implemented in lubrication control based on motor current control during machining. The planning method for a motor current controller is as follows. (a) Current on the X- and Z-axes is found by a mathematical description method and is confirmed using real feed drive data measured with a Hall-effect sensor. (b) A servo system for X- and Z-axes feed and the lubrication control for motor current are considered. (c) The mathematical model based on motor current mode is implemented during machining to prove the current changes by modifying the depth of cut in real time for different feed rates. (d) The feed drive system current is measured with regards to bandwidth and sensitivity using Hall effect sensors that are fixed around the wire of the servomotor. (e) The tangential force is evaluated through the current of the spindle motor and using the preset relationship between the force measured by a commercial dynamometer and the current. In order to evaluate the current control system, a series of experiments with different depths of cut are carried out on the lathe machine.

2.5 ANFIS Modeling System to Predict the Friction and Servomotor Current

Soft computing techniques are useful when exact mathematical information is not available. These differ from conventional computing in that soft computing is tolerant to imprecision, uncertainty, partial truth, approximation, and met heuristics. Adaptive Neuro-Fuzzy Inference System (ANFIS) is a soft computing technique that plays a significant role in input-output matrix relationship modeling (Bramhane, Arora, & Chandra, 2014). It is used when subjective knowledge and expert suggestions are significant in defining the objective function and decision variables. ANFIS is preferred to predicting friction force based on the input variables due to the nonlinear condition in the coating process. In this research work the ANFIS modeling technique is applied to develop the rule model to predict the friction

forces in CNC linear guideways based on parameter and performance interaction. This relation, which is non-linear, can help obtain a predicted friction model. The predicted friction values are achieved from adapting training and testing data. The training data actually includes values of cutting parameters, measured servomotor current and friction force calculated by force analysis in guideways, which are determined as input/output data.

The neuro-adaptive learning method works similarly to neural networks. Neuro-adaptive learning provides a means for fuzzy modeling to learn information about a dataset. Fuzzy Logic Toolbox software computes the membership function parameters that best allow the associated fuzzy inference system to track the given input/output data (Adoko & al., 2013). The Fuzzy Logic Toolbox function that accomplishes this parameter adjustment of the membership function is called ANFIS. In ANFIS modeling, the testing dataset checks the generalization capability of the resulting fuzzy inference system. The idea behind using a checking dataset for model validation is that after a certain point in the training, the model begins overfitting the training dataset. In principle, the model error for the checking dataset tends to decrease as training takes place up to the point when overfitting begins, after which the model error for checking data suddenly increases (Maher & al., 2014). Overfitting is accounted for by testing the Fuzzy Interface System (FIS) trained on the training data against checking data, and choosing the membership function parameters to be associated with the minimum checking error if these errors indicate model overfitting.

To start training in ANFIS editor graphical user interface (GUI) the following steps are taken:

1. First, we need to have a training data set that contains desired input/output data pairs of the target system to be modeled.

2. Sometimes, it is also desirable to have an optional testing dataset that can check the generalization capability of the resulting fuzzy inference system, and/or a checking dataset that helps with model overfitting during training.
3. Overfitting is accounted for by testing the FIS trained on the training data against the checking data, and choosing the membership function parameters to be associated with the minimum checking error if these errors indicate model overfitting.
4. The training error plots will have to be examined quite closely in order to determine.
5. Usually, these training and checking datasets are collected based on observations of the target system and are then stored in separate files.

2.6 Control System Process via Design and Simulation

2.6.1 Open-Loop Control

According to Figure 2.9, in this type of control, linear control operations to be performed and the input system will cause a change in the output value. In other words, the output variable is determined by the control unit. However, the data output cannot be sent to the control unit. As a result, if an error occurs, the system will not be able to detect and compensate. Today's open-loop control systems are used only in educational CNC machines that do not require high precision for the product (Goodwin & al., 2001).

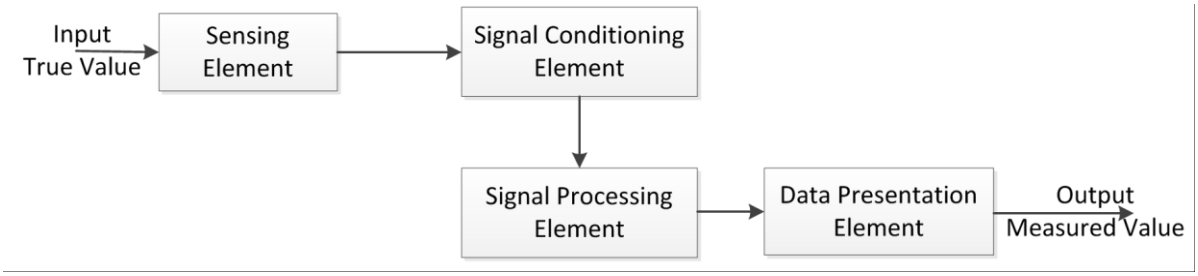

Figure 2.9 Schematic diagram of an open-loop measurement system

2.6.2 Closed-Loop Control

In closed-loop controllers, the control operation is performed much like in closed-loop controllers and not only the input but also the feedback will be effective on the output value. Regarding Figure 2.10, in this control system the data position of each axis is sent to the control unit via feedback and is then compared with the correct amount, so what the correction control unit needs will be corrected and sent to the system. A closed-loop control system that controls speed and position is called a servomechanism and the motor used in this system is called a servomotor. Closed-loop controls have high precision and accuracy.

In an NC machine tool program, after decoded conversion to the machine language and storage in memory, a calculation is performed. Next, the routing information and technical data are converted into output signals for switching and sending commands to the servomotor. Servomotor rotation is transmitted to the ball screws, which convert the rotational motion to linear motion. Eventually, linear motion is passed through linear guideways are passed to the tools under the measuring control system.

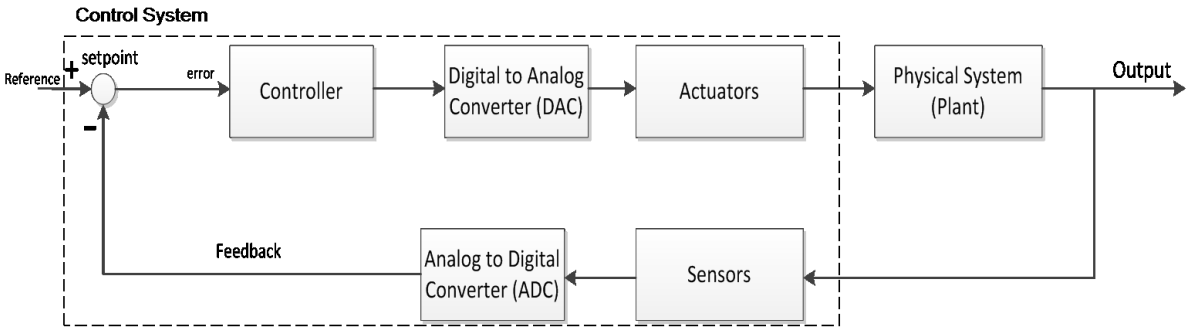

Figure 2.10 Schematic diagram of a closed-loop measurement system

(Goodwin & al., 2001)

2.6.3 Application of Closed-Loop Control

Depending on the result of applying a closed-loop control, two main benefits are achieved:

a. Compensation for disturbance in the controlled system. For example, in the servomechanism load, the control system changes the load cycle as necessary to keep the output variable (current consumption) fixed, independent of variations in output current, friction condition, etc.

b. Compensation for variations within the control elements. In the servomechanism example, the output variable is mentioned at the commanded level independent of changes in depth of cut, feed rate, cutting speed, etc.

The benefits of closed-loop control systems have already been confirmed, and servomechanisms are defined as closed-loop control systems by motors. Therefore, it can be said that the general application of servomechanisms is that the controlled variable can be controlled using a motor and significant variations of the control elements or disturbance of the controlled system are expected.

Servo drives in machine tools can accomplish difficult processes with high accuracy, such as create profiling. Although considerable setup time is generally involved in automating a machine operation, once the operation is set up, the servo drive tool can repeat it on a large number of pieces with minimum variation.

Makino and Ohde (1991) developed a motion control system for a direct drive actuator. The direct drive (DD) actuator is a high-torque, low-speed electric motor. It can drive a mechanism without a speed reducer and decrease the negative effects of non-linear backlash and low stiffness of gears, thereby yielding high precision, high speed and reliable positioning (Makino & Ohde, 1991).

Mei et al. (2001) considered the effect of stick-slip motion on a high-speed, high precision X–Y table of a milling machine using ball screw and roller type guideways in experimental and numerical simulation. A two-component mixed friction model was

involved in the mathematical model of the feed drive system. The study showed that the error caused by friction from the ball screw and roller guides could be accurately predicted by carefully tuning such parameters as surface roughness in the friction model. The dynamics and other characteristics produced by the stick-slip motion could be defined to some extent. With the mathematical model of the feed drive system developed by Mei et al. (2001), the effects of the dynamic parameters as well as the worktable rigidity, system dampness, etc. on system performance could be appropriately determined. The results obtained confirmed that friction error could be predicted off-line with the mathematical model (Mei, Tsutsumi, Yamazaki, & Sun, 2001).

Tarng and Cheng (1995) conducted a study of the contouring error of CNC machine tools due to stick-slip friction. Simulation and experimental studies indicated that quadrant protrusion produced by stick-slip friction is a primary contouring error in a circular test. It was also established that suitable adjustment of the velocity loop integral gain could efficiently suppress quadrant protrusions and torque disturbance in the circular profile.

Astrom and Wittenmark (1984) considered the problem of controlling a system with constant but unknown parameters. Their analysis was limited to separate time SISO systems. An algorithm achieved by incorporating a least squares estimator with a minimum difference regulator calculated from the estimated model was analyzed (Åström & Hägglund, 1984). The main results were two theories that characterize the closed-loop system achieved, given that the parameter estimates converge. The first theory identified that certain output covariance and certain control variable cross-covariance, as well as the output would vanish under weak assumptions on the system to be controlled. In the second theory, it was assumed that the system to be controlled was a general linear stochastic *n*th order system.

2.6.4 Control System Model Process

In this section, an orderly sequence is established for the design of feedback control systems. This will be followed throughout the rest of the thesis. Figure 2.11 shows the process described in steps:

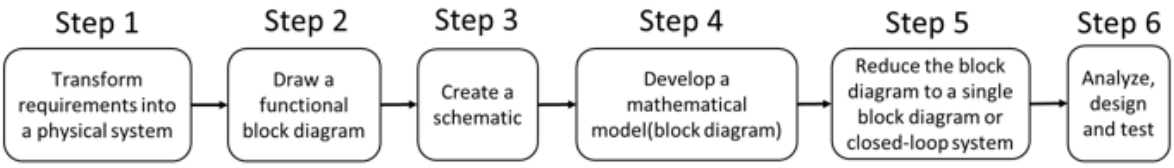

Figure 2.11 Process of control system modeling

1. Transform the requirements into a physical system: initially, the requirements are transformed into a physical system. Using the requirements, design specifications such as desired transient response and steady-state accuracy are determined. Figure 2.12 and Figure 2.13 show the schematics of the feed drive physical system in the X- and Z-axis directions.

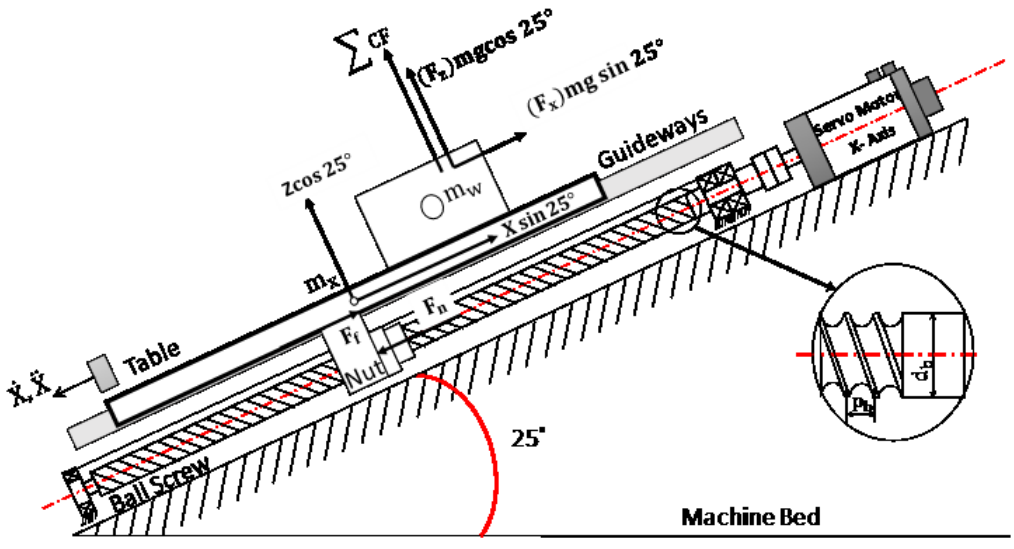

Figure 2.12 Schematic of X-axis feed drive physical system

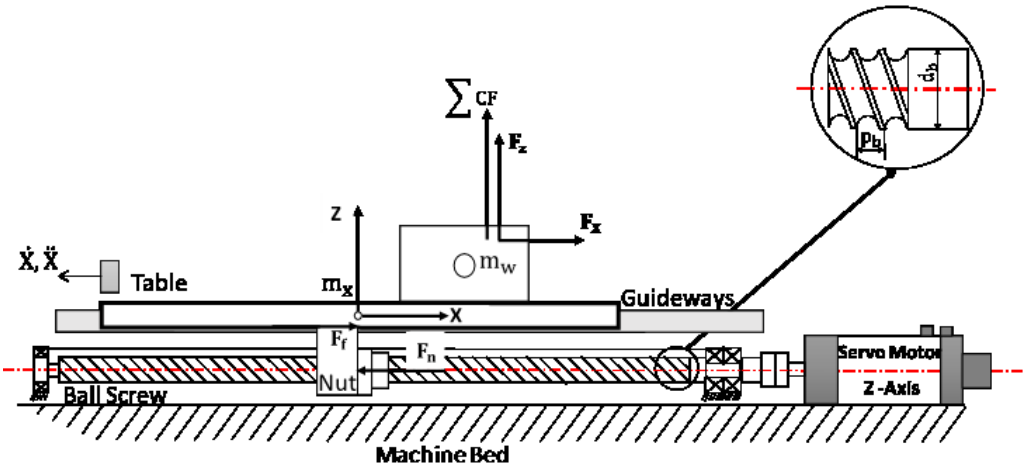

Figure 2.13 Schematic of Z- axis feed drive physical system

2. Draw a functional block diagram: the designer now translates a qualitative description of the system into a functional block diagram that describes the system's component parts and shows their interconnection (Figure 2.14). At this point, the designer may produce a detailed layout of the system from which the next phase of the analysis and design sequence can be launched: developing a schematic diagram.

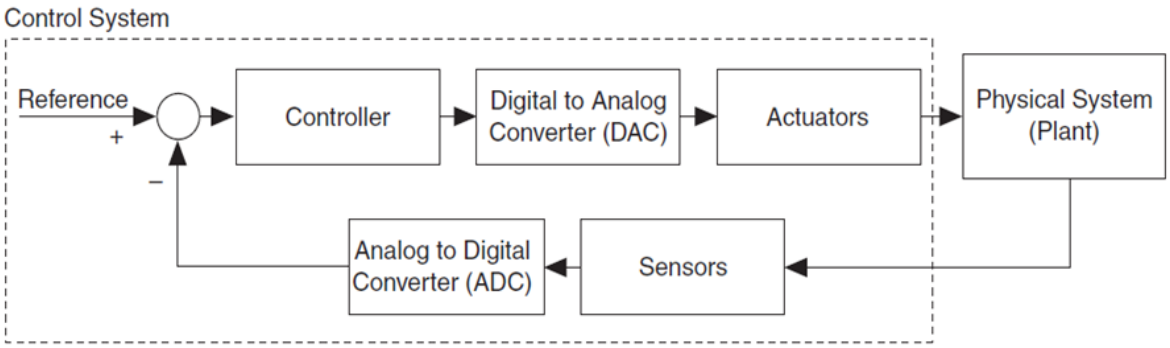

Figure 2.14 Functional block diagram of a closed-loop control system

3. Transform the physical system into a schematic: the control system designer can begin with the physical description and drive a schematic. The designer starts with a simple schematic representation and at subsequent phases of the analysis and design sequence, checks the assumptions made about the physical system through analysis and computer

simulation. The decisions made in developing the schematic stem from knowledge of the physical system, the physical laws governing the system's behavior, and practical experience.

4. Develop a mathematical model: once the schematic is drawn, the designer uses physical laws, Kirchhoff's laws for electrical networks and Newton's law for mechanical systems. The laws lead to mathematical models that describe the relationship between the input and output of dynamic systems.

According to the mechanical feed drive shown in Figure 2.12 and Figure 2.13, the differential equations governing the machine table motion can be written as follows:

$$(m_X + m_W)\frac{d^2x}{dt^2} + F_f\left(F_X, F_y, F_Z, X, Y, Z, \frac{d_x}{d_t}, \frac{d_y^2}{d_t^2}\right) + F_X = F_n \quad (2.1)$$

Where, F_n is the force applied by the nut on the table. F_f is the friction force between the table and guideways that will be estimated in the next chapter (refer to Figure 2.12 and Figure 2.13).

With regard to the motor motion, we have:

$$J_e\frac{d\omega_1}{d_t} + T_f + T_n = T_e \quad (2.2)$$

Where, T_f , T_n and T_e are friction torque, load torque, and electromagnetic torque, respectively. The feed drive of the servomotor includes several bearings causing frictional loss.

By using (Equation 2.1) and (Equation 2.2), the differential equation for a feed drive system is found as follows:

$$J_e\frac{d\omega_1}{d_t} + \frac{R_b}{\eta}\left(mg\,sin\,25° + F_fT_n\right) + \left\langle b1\left|\omega\right|\frac{2}{3} + T_0\right\rangle.sgn(\omega 1) = T_e \quad (2.3)$$

The rotational motion element is characterized by a parameter R_b considered in function of the pitch of screw P ((Equation 2.3, and Equation 2.4) :

$$R_b = \frac{P_b}{2\pi} \quad (2.4)$$

$$J_e = \frac{P_b^2}{4\pi^2\eta}(m_X + m_W) \quad (2.5)$$

Where, η refers to the efficiency of the screw and the equivalent inertia on the servomotor is represented by J_e(Equation 2.5).

To the differential equation, the transfer function is another way of mathematically modeling a system. The model is driven from the linear time-invariant differential equation using the Laplace transform. Although the transfer function can be used only for linear systems, it yields more intuitive information than the differential equation. It is thus possible to change system parameters and rapidly sense the effect of these changes on the system response.

Another model is the state-space representation. One advantage of this method is that it can also be used for systems that cannot be described by linear differential equations. Furthermore, state-space methods are used to model systems for computer simulation.

5. Reduce the block diagram to a single block diagram or closed-loop system: Subsystem models are interconnected to form block diagrams of large systems. In order to evaluate a system, it is necessary to reduce this large system's block diagram to a single block with a mathematical description that represents the system from its input to its output. Once the block diagram is reduced, the system is ready for analysis and design (Figure 2.15).

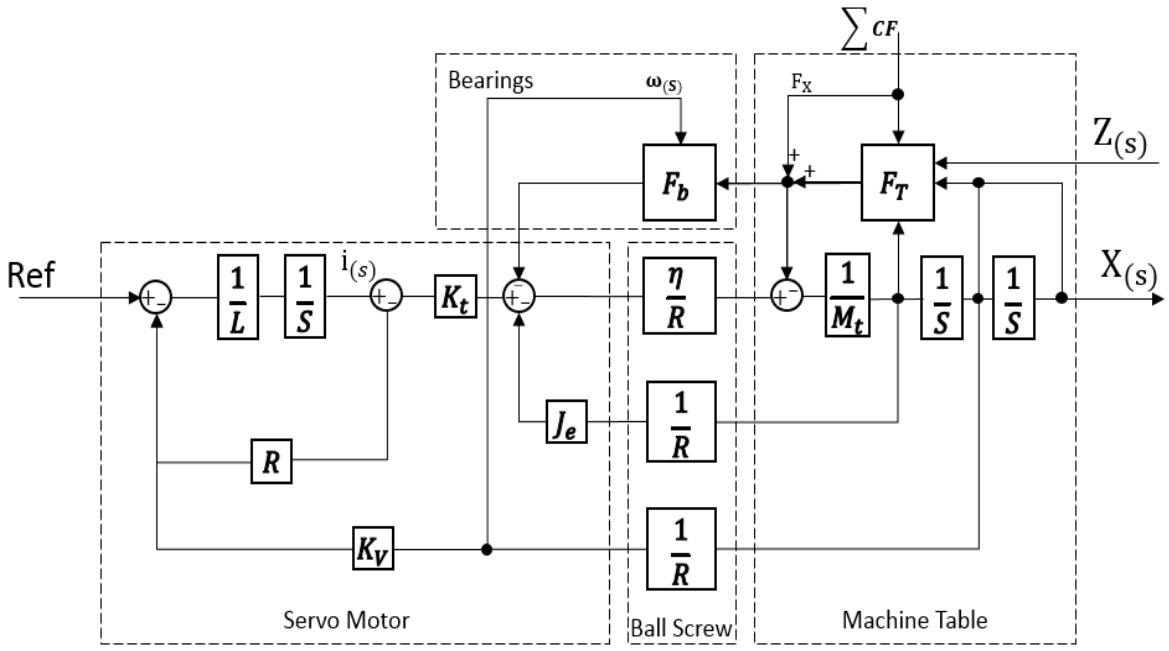

Figure 2.15 Block diagram of a feed drive system(Chiu & al., 2001)

Here, F_T is friction force on the table, F_b is friction force on bearings, and M_t is the machine table's total mass.

6. Analyze, design and test: the next phase of the process after block diagram reduction entails analysis and design. In this phase, the engineer analyzes the system to see if the response specifications and performance requirements can be met by simple adjustments of system parameters. If specifications cannot be met, the designer then designs additional hardware in order to obtain desired performance.

Test input signals are used both analytically and during testing to verify the design. It is not necessarily practical or illuminating to choose complicated input signals for system performance analysis.

2.7 Lubrication Operation

Since lubricating oil is meant to reduce friction, save energy and prevent rusting and corrosion, it is crucial to the lifespan of a linear motion guide. Correct prediction of lubricating oil consumption and timely refill are extremely important. Hsiao et al. (2004) studied these aspects of a linear motion guide (Hsiao & al., 2009).

The prediction results for lubricating oil consumption serve as reference for linear motion guide manufactures and users. They may also create a basis for tests pertinent to other sorts of linear motion guides, in the hopes that both testing time and cost can be reduced while enhancing profitability (Watson, 2013).

Oftentimes, the moving parts of a CNC machine come in contact with channels or feed lines, causing damage and requiring repair, realignment and downtime. Moreover, lubricated applications are quite difficult to control during micro-machining or high-precision applications. With respect to high-precision machining applications at least, with tolerance of less than a micrometer, employing automated lubrication control systems has become commonplace. The goal of the new lubrication method is to enable applying only the amount of lubricant needed to properly control the amount of current created by the servomotor as a result of the friction between machine tool guideways (Yong & al., 2014).

Machining precision mostly depends on adequate lubrication and the performance of a machine's individual units. The accumulated errors occurring in machining stem from various thermo-mechanical setup parameters and environmental conditions. The main factor that determines and can cover the majority of these errors is the lubrication process. Obviously, effective lubrication can be achieved when taking into consideration lubricant type, period of lubrication, amount of lubricant in each period, and precise lubrication system functioning (Jeong & al., 2002; Soundararajan et al., 2005).

Sometimes, the feed rate of the cutting process is manually decreased or increased by the operators based on different cutting conditions (Kumar & al., 2007). Thus, it is necessary to sense any overload on the tool and to maintain the cutting force at a constant level during machining, so efficiency can increase. Dölen and colleagues (2002) measured the cutting force that deviated from the spindle motor current of the lathe machining centers. The feed motor current for the axes was measured in order to compare it with cutting forces applied to the linear guideways. On the other hand, the spindle motor current remained independent of cutting direction. After the cutting force was measured from the spindle motor current, it was analyzed at a constant level of forces on the linear guideways. The following parameters were measured and used as performance indicators: temperature of linear guideways, motor current, cutting force, normal force, spindle speed, feed rate, depth of cut and friction force (Dölen & Lorenz, 2002).

The results of controlling the linear motion guide's period and amount of lubricating oil consumption can function as references for CNC machine tool manufactures and consumers (Kok Kiong & al., 2001). They can also form a basis for tests relative to other makes of CNC machine tools, with the hope that testing time, control programming and cost can be reduced and usefulness improved. The purpose of lubrication oil is to reduce friction, save energy and prevent rusting and corrosion, which renders it invaluable to the lifecycle of a linear motion guide. True estimates of lubrication oil consumption and apropos refill of lubricating oil are of paramount importance. Hsiao et al. (2009) evaluated the lubrication oil of a linear motion guide. The purpose of their research was to determine the measures of process performance in the case of good identification of the friction forces acting on linear guideways in a machining center. They used motor current and cutting force measures, and aimed to improve understanding of the physical changes in the carriages during machining.

Conventionally, two methods are used to lubricate guideways in CNC machines: manual and automatic lubrication.

I. Manual lubrication: Here, an operator delivers the lubricant by hand according to instructions provided by the CNC machine manufacturer (Anderson et al., 2012). This method does not guarantee correct, sufficient, controlled lubrication since it is dependent on operator experience.

II. Automatic lubrication: Here, time and amount of lubricant are controlled by electronic packages (Nikolakopoulos & Papadopoulos, 2008) that have some capabilities in programming and adjusting lubrication.

Manual and automatic lubrication procedures can be used independently or together based on the design provided by the machine manufacturer (Yukeng, Darong, & Linqing, 1985). Nevertheless, CNC machine characterization is extremely significant for the required process of eliminating bulk errors like axis linearity errors or spindle motion errors of the machine prior to implementing precision cutting operations (Benhabib, 2003). In addition, unexpected parameter changes and errors in precise machining necessitate alternatives (Jywe & Chen, 2005). Hence, the development of CNC machine tool guideway lubrication methods for more precise CNC machines is a current requisite of the machining industry to improve accuracy (Bushuev & Molodtsov, 2010; Desforges & al., 2011).

2.7.1 Optimization of Quantity Lubrication

Cost, environmental effects, and health issues are all relevant when considering the choice of a lubricant and application system in modem metal cutting processes. The need to use less quantities, and limit disposal and operator contact are all now very important (Chen, Mei, & Tao, 2011).

Since lubricating industrial machinery for smooth movement and without stick-slip motion in machine linear guideways is done with expensive industrial oils that are not recyclable or biodegradable, great damage to social and individual health can occur (Persson, 2014).

In recent decades numerous studies to reduce and optimize oil consumption have been done. Some studies present changes to design parts relevant to moving machine parts while in others, a variety of lubrication methods have been studied.

In a traditional method with machine tools to create a multi-axis motion, guideways and carriage were used. The operators of these machines must maintain the equipment and control machining precision and accuracy. The machine operators also need to manually lubricate the guideways proportional to the machining duration. Lack of attention to cleaning and maintaining the machine can cause irreversible damage to the machine and operator. Furthermore, the resulting output will not be accurate (Figure 2.16).

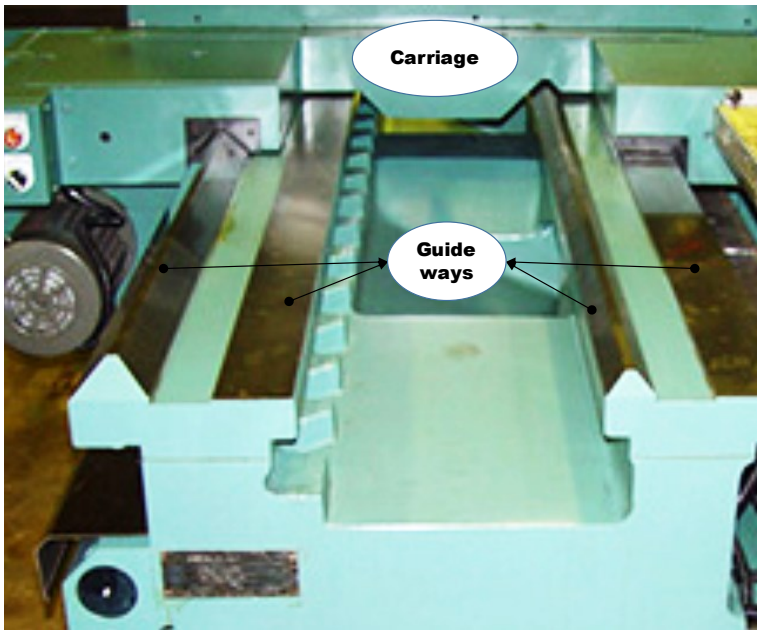

Figure 2.16 Carriage moving on the guideways

In traditional methods, oil consumption cannot be optimized and its performance depends on the operator. Low and improper oil use reduces the machine lifetime and causes faults in the products. Excessive oil intake also causes environmental damage and is associated with additional costs. Today, there are many modern machines with moving carriages on guideways, but there have been changes in application and lubrication methods.

Al-Bendera and Symens (2005) propounded using the hysteresis of friction in ball-bearing guideways. Frictional hysteresis is a feature that may be found in many machine elements for public engineering use. Plain and rolling element bearings that are commonly used in motion management of machine tools are classic models. They use hysteresis friction behavior on the guideways (Al-Bender & Symens, 2005).

Different block-rail designs in linear guideways have been considered by among the various ways to optimize oil consumption.

Linear guideways lead to high accuracy linear motion by using recirculating rolling components between the guide block and the rail (Figure 2.17).

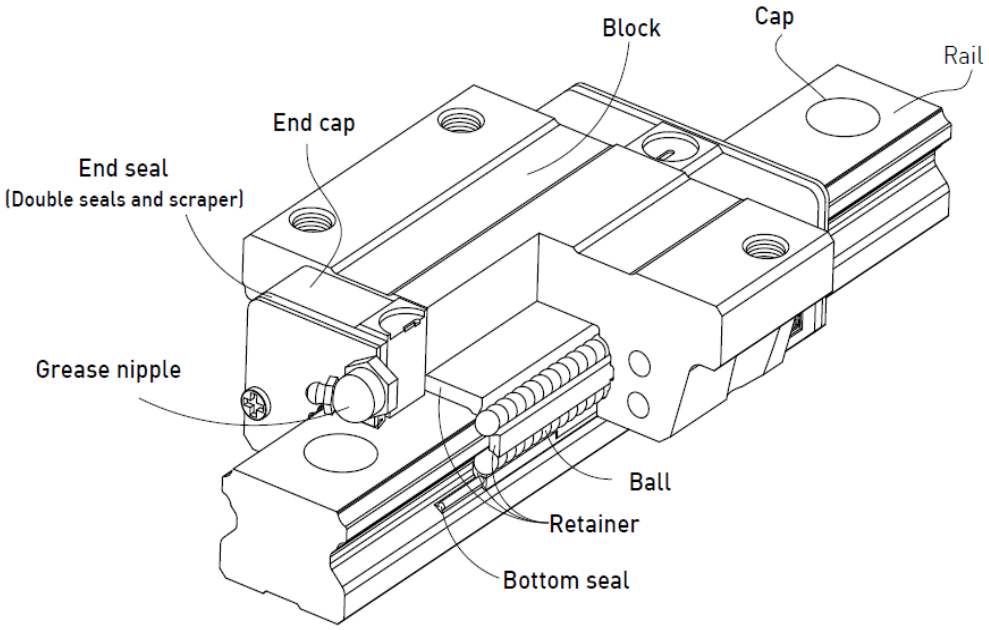

Figure 2.17 Construction of Block-Rail linear guideways(Yong-Sub et al., 2008)

The advantages of linear guideways include:

- Very high positional precision,
- Long life with high motional accuracy,
- High speed motion with low driving force,
- Equal loading capacity in all directions,
- Easy installation,
- Easy lubrication,
- Interchangeability.

Ikuo Tanabe and Watanabe developed and estimated permanent lubrication using grease with polymer for the slideways in machine tools. They found it is very suitable for both the environment and industry (Tanabe & Watanabe, 2011).

Kobayashi and Fujita patented a "Hydrostatic pressure linear guide device," which can be used as the worktable or tool-table of a work machining apparatus such as cylindrical grinding machine, cam grinding machine, crank shaft grinding machine, dicer, NC lathe etc. The hydrostatic pressure linear guide device includes a guide unit (guideway) with a pair of right and left rails on the upper surface of a bed, and a slide unit (slideway) with plural oil static pressure pockets on a lower surface and side wall of the slide unit (Kobayashi, 2006).

Optimum oil injection is required in an intelligent lubrication system to provide an economic process. As such, an injector motor pump responds over a time interval and injects oil into the system. The time interval is called a Pump Response Interval (PRI). The PRI needs to be flexibly defined in order to realize intelligent injection for optimum lubrication. Various PRI values were applied to determine the optimum, most economical condition for a particular machining operation, whereby the most effective PRI ensures minimum oil consumption and quality processing.

In another research, the real-time temperatures of the X- and Z-axes' linear guides were measured and compared with a presumed critical temperature (Tcr) to command the injection motor for intelligent, optimum lubrication using a special program and selected PRI. This intelligent approach reduced the oil consumption significantly.

Another way to optimize oil consumption is to use air bearings in the machinery. Although this method may seem expensive, it is a new technology to reduce oil consumption.

Air bearings use a thin film of pressed air to facilitate a 'zero friction' load bearing connection between surfaces that would otherwise be in contact with each other. The advantage of air bearings is that non-contact prevents problems such as friction, wear and high oil application. These problems are evident in traditional bearings at precise positioning time and machine deployment at high speed (Lau & al., 2013).

2.8 Summary

In this chapter, a basic background of linear guides was introduced. First, the development of machine tool precision and accuracy was presented, which is one of the most important reasons for lubrication control design in CNC machines. Then issues regarding the parameters required for measurement and control were briefly introduced. A concise introduction to the process of control systems was also given. The steps in the control design process were discussed. Next, traditional lubrication operations used in linear guideways were addressed, followed by a new lubrication control technique that serves as the topic of this thesis. This new technique for lubrication control is based on friction conditions in CNC machine linear guideways using servomotor current signals in a feed drive system. This background will be the technical basis that will help with the development of novel ideas in the following chapters.

CHAPTER 3: METHODOLOGY

3.1 Introduction

A new technique for lubrication and friction control in CNC machine linear guideways is introduced. Controlling the lubrication amount and time based on friction force conditions in linear guideways is one of the major differences between the new lubrication technique proposed and existing systems. The existing CNC guideways lubrication systems are working based on fixed time and amount of oil injection. The lubrication is done regardless of cutting conditions, weight and size of workpiece and/or friction force values in guideways.

First, the friction force values in the linear guideways in the X and Z directions are calculated from a cutting force analysis on the guideways. Second, the correlation between the calculated friction force and measured servomotor current signal is performed using adaptive neuro fuzzy inference system (ANFIS) modeling, as the ANFIS system is ideal for predicting friction force based on servomotor current due to nonlinear conditions in the machining process. The friction forces predicted with ANFIS modeling are verified with a new testing scheme to identify the average predicted error and accuracy. As the predictive percentage errors are low, the ANFIS model is used to build the lubrication control unit (LCU) with oil feedback to enable the prediction of friction force values at different online servomotor current signals and cutting conditions. Hence, the LCU sends a signal to the actuator to trigger the oil pump to inject oil. The oil injection time and amount or pump response interval (PRI) are identified based on the friction force values in linear guideways. Finally, the controller performance is investigated through a new set of experiments. The lubrication results of the proposed technique are compared with ordinary lubrication results. In these tests, several parameters are monitored in both ordinary, existing lubrication systems and our new lubrication technique.

3.1.1 Lubrication Pump Identification

A lubricator consists of a motor-driven gear pump with a built-in flow relief valve that controls the distribution line pressure during “OFF” time, as required for PDI systems. A pressure switch and low-level switch are available to monitor pump cycles and low oil levels in the reservoir.

A built-in timer controls the operating cycles of the lubricator. Three modes are required to operate the lubricator: “Pause” period (pump motor off), “Pressure build” period and “Pressure hold” period. At the end of the Pause period, power is supplied to the lubricator’s electric motor, commencing the Pressure Build operation and increasing oil pressure.

Once pressure to operate the system is attained, the lubricator’s built-in pressure switch closes, advancing the controller to Pressure Hold mode. The pump motor continues to run until the Pressure Hold time is complete. Then the controller advances to the Pause mode and remains in this mode for the preset interval. The controller shuts off the pump, allowing the lubricator’s relief valve assembly to relieve pressure from the system network, and allowing all injectors to reset for the next cycle.

Generally, the SM-AC controller is a multi-purpose controller for different lubricating systems, such as Single Line Resistance (SLR) or centralized lubrication, PDI system, and Progressive Lubrication System (PRG). This programmed controller is compact and reliable. It can deal with almost all kinds of rough industrial conditions due to its high protective grade and anti-vibration feature.

Real-time fault alarm is an outstanding feature of this excellent controller as well as its data memory function during power off.

There is one 4-digit display and three LED lights on the panel. The digital screen displays the operation mode and program. The three LED lights indicate: power supply (Green), pump running (Red) and low-level alarm (Yellow).

There are some keyboards for manual pump setting on the control panel. The keys are as follows:

S: Function setting and program review,

R: Data store, reset and run,

↩ : Remove cursor,

↑ : Data setting .

a) Control board wiring diagram: As seen in Figure 3.1 the control board wiring comprises:

- Terminal 1 and 2: Power input for customer connection
- Terminal A0, A1, A2: alarm output (A0 and A1 normal close; A0 and A2 normal open)
- The terminals below are wired by the factory:
- Terminals 3 and 4: Motor load (the voltage should be compatible with the power supply).
- Terminals 5 and 6: Low-level signal input. Closed at low level.
- Terminals 7 and 8: pressure and cycle signal input.

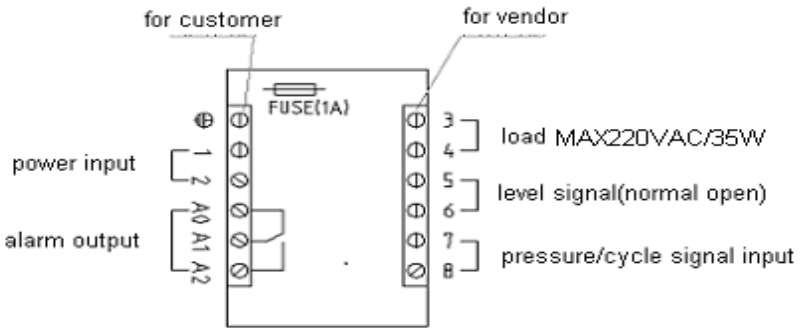

Figure 3.1 Control board ring diagram of the lubrication pump

b) Procedure:

- Power on: The controller runs the previous program set before power off. The following steps are taken if reset is required.
- Data Setting:
  - i. Press "S" and "R" simultaneously to enter setting mode, and the cursor flashes.
  - ii. In the setting mode press ↺ and ↑ to modify the data.
  - iii. Press "S" to set the next parameter.
- Run & Stop:
  - i. After all data are preset, press "R" to save the data and start the system.
  - ii. Whenever the system is running, pressing "R" will reset the system.
  - iii. Pressing "S" and "R" simultaneously can stop a running system.
- Program Review: In order to review the preset data, press the "S" key whenever the system is running. After releasing the key, the display will be restored.
- Fault Alarm: When any malfunction is being checked, the controller will cut off output by activating an inner relay.

A pressure switch mounted on the pump or online is a key monitoring unit for the whole system. Normally, the system should build up rating pressure to activate the pressure switch

to close for a proper amount of time (called alarm time) after the pump starts. In order to build up enough pressure at the end of the lines, the pump will keep running for four additional seconds (called a 4-second delay) after the pressure switch is closed. Then the pump stops and completes one discharge cycle. The system starts to count down idle time and prepare for the next period. If there are any faults in the system, such as leakage, clogs or malfunctioning units, the pressure switch cannot be triggered in the preset alarm time, so the controller will give off an alarm signal and the LED shows "EEPP." (If data needs to be modified, press the "R" key first to enter data setting mode).

Users can adjust the alarm time according to the line length and discharge volume needed. Controller programming is achieved using a 4-digit LED display and four soft function keys. Press S and R simultaneously to begin programming. Select operating Mode (as described above) using the ↑ key to change options and S to select an option.

Proceed with setting up the various pump on-time and off-time parameters as described in the chart below. Use the ↑ key to change the number and ↺ to move across the display. Press R to save all the data and start the system, or press S to go back and make further changes. To run the controller press R to set the system at any time. The controller will begin with a new cycle. Press S and R simultaneously to stop the system when running. Press S to review the data stored.

3.2 New Proposed Lubrication System Experimental Setup

Experimental studies were done on a CNC lathe machine (OKUMA LB15-II) with maximum cutting length and diameters of 425 mm and 250 mm, respectively, and with various workpieces weighing up to 500 kg (4905 N). The table travelled about 520 mm when undergoing any cutting. An OKUMA OSP7000L control was installed on the CNC machine

for this research. The operation framework of the experimental setup and processing system used in the experiments are shown in Figure 3.2.

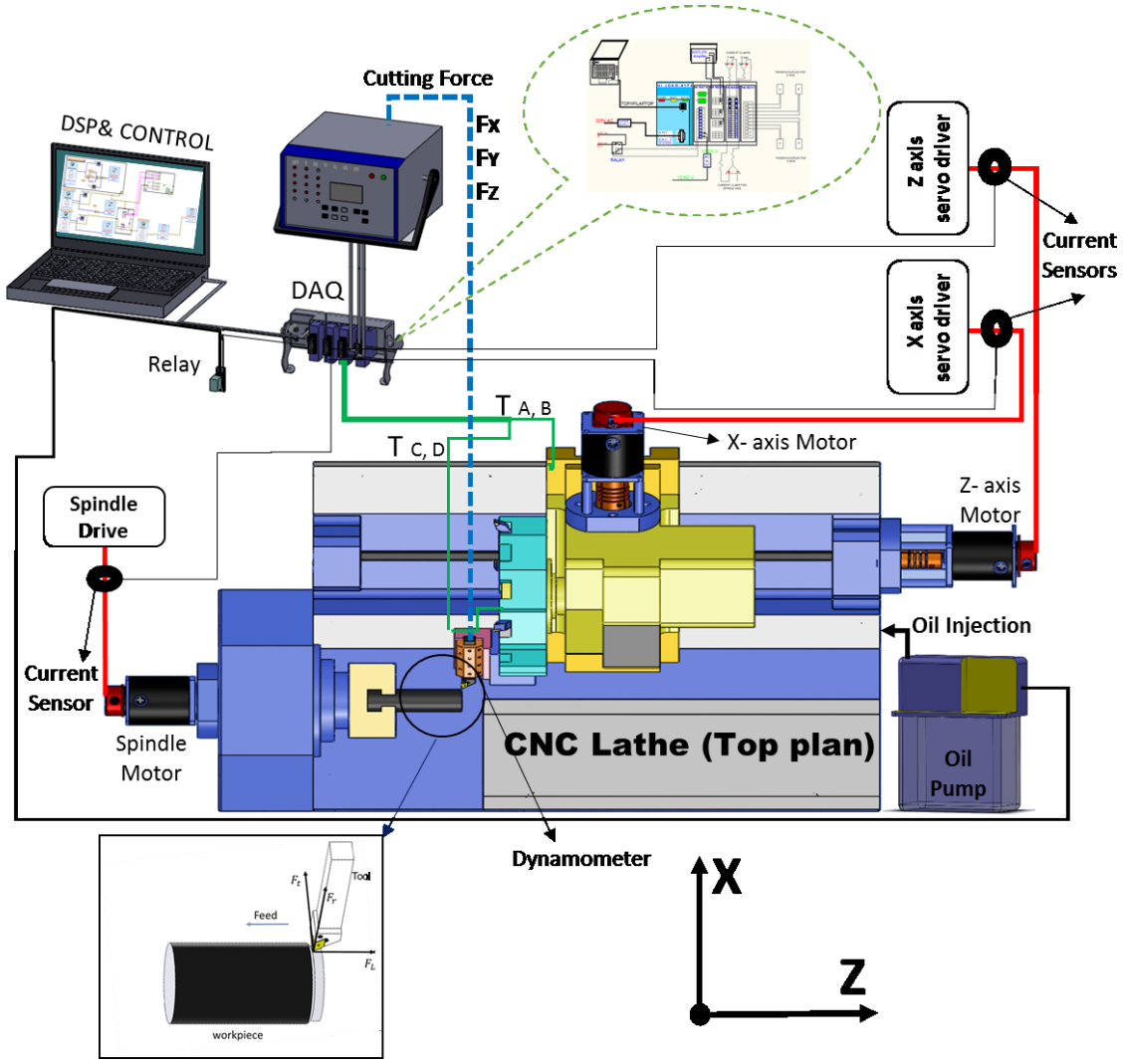

Figure 3.2 Schematic representation of the system experimental layout

The X and Z-axes have a 25-degree slope relative to the horizontal line. The moving table includes a turret and tool changer, and it moves on the axes at this angle in its own direction. In other words, the side view of the machine tool shows that the slideways are at a 25-degree slope from the horizontal line of the machine bed (Figure 3.3).

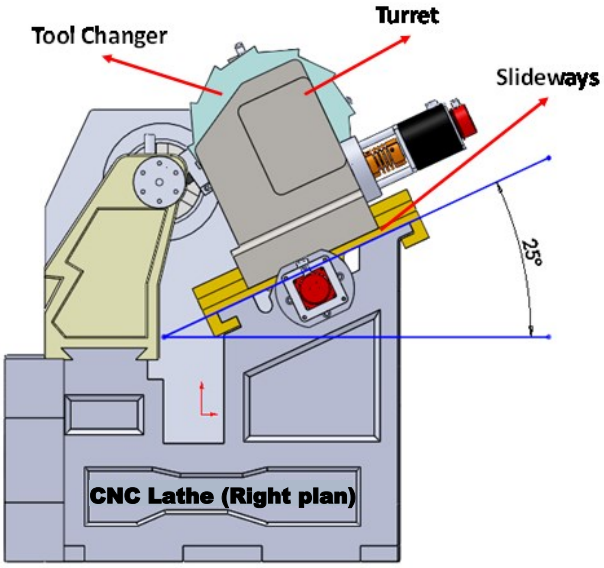

Figure 3.3 Outline of the moving table on slideways at a 25-degree slope (side view)

For the machining process on a given surface, only one cutting tool is utilized. The insert is a SANDVIK Carbide Insert DNMG 332-PM4015, and the workpiece material is normal mild steel. The tool data and cutting parameters are summarized in Table 3.1.

Table 3.1 Tool data and cutting parameters

Cutting conditions	Parameters
Cutting tools	SANDVIK Carbide Inserts DNMG 332-PM4015
Spindle speed (rpm)	250- 500- 750- 1000
Feed Rate (mm/rev)	0.1- 0.25- 0.4- 0.5
Depth of cut (mm)	0.5-1-1.5
Cutting length (mm)	130
Number of teeth	Single
Insert angle	60˚
Tool holder diameter (mm)	25*25 (mm^2)

Two brushless linear AC servomotors (OKUMA BL- MC) were used for the X and Z direction feed drives of the machining center. The angle of rotation from the motor encoder was acquired at 2048 pulses per revolution using a counter board. An OKUMA VAC-MB-A302A motor was used for the spindle drive (Table 3.2). The cutting force in the X and Z

directions and servomotor current signal in the X and Z directions as well as spindle motor current signal were measured using a dynamometer and three Hall effect sensors, respectively. The electrical circuit system and schematic drawing of the experimental setup is shown in Figure 3.4.

Table 3.2 Machine driver specifications

Specifications	**X-axis Servomotor**		**Z-axis Servomotor**		**Spindle Motor**	
Type	BL-MC150E-12SB		BL-MC200E-20SN-A		VAC-MB-A302A	
Output	1.8	KW CONT.	4	KW CONT.	15-11	KW CONT.
Torque	16.2	N.M	21	N.M	ASDFASDF	
Voltage	133	V	137	V	170	V
AMP.	~ 8.02	A 3PHASE	~ 14.7	A 3PHASE	~98-89	A 3PHASE
Speed	1200	min^{-1}	2000	min^{-1}	440/4500	min^{-1}
Freq.	80	HZ	133	HZ	300	HZ
Pole	8		8		-	
Encoder	ER-FC-2048		ER-FC-2048D		-	

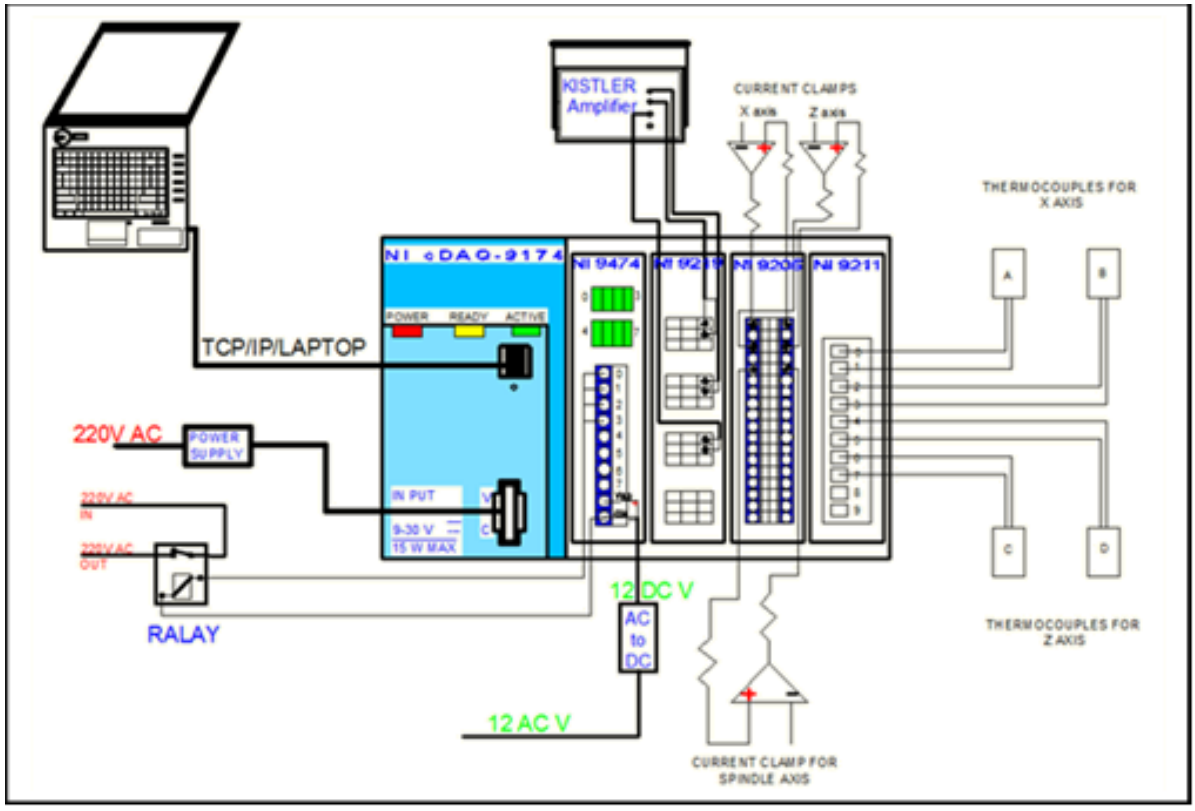

Figure 3.4 The electrical circuit system and schematic drawing of the experimental setup

The DAQ system includes four major parts: sensors, measurement modules, compact DAQ chassis, and actuators. Signals are sent from the dynamometer, thermocouples and current clamps to the measurement modules. These modules process cutting force values, temperature errors and current variables from the servo drivers, which arrive at the controller.

In traditional CNC machine tools, there is a metal-to-metal contact between the linear guideways and the guiding table. Hydrostatic linear guideways including the X and Z directions were used in these experiments, because the oil is pumped into small pockets in the guiding table, which are in contact with the linear guideways (Figure 3.5). The fluid pressure gradually reduces to atmospheric pressure as it leaks out from the pockets through the gap between the guiding table and linear guideways. The hydrostatic linear guideways provide a nearly frictionless condition for the carriage movement. For efficient operation, it is very important that the oil and guideways are kept clean. Moreover, the hydrostatic guideways need very large surface area to provide adequate support. According to the above description, the lubrication pipelines of existing guideways are shown in Figure 3.6.

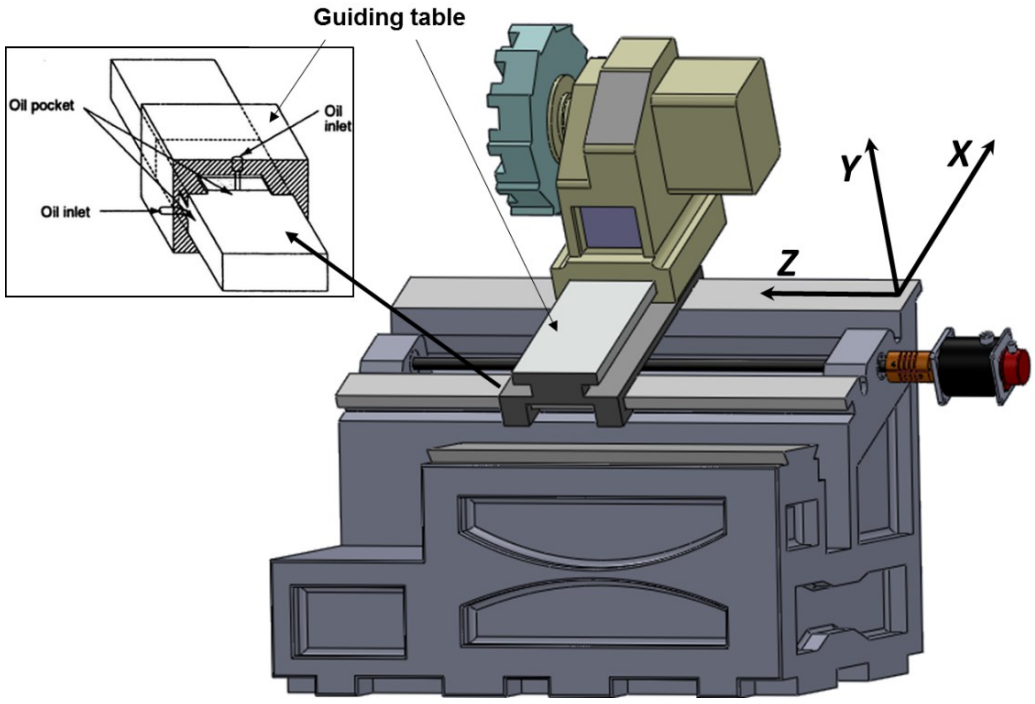

Figure 3.5 A drawing of existing guideways in the X and Z directions

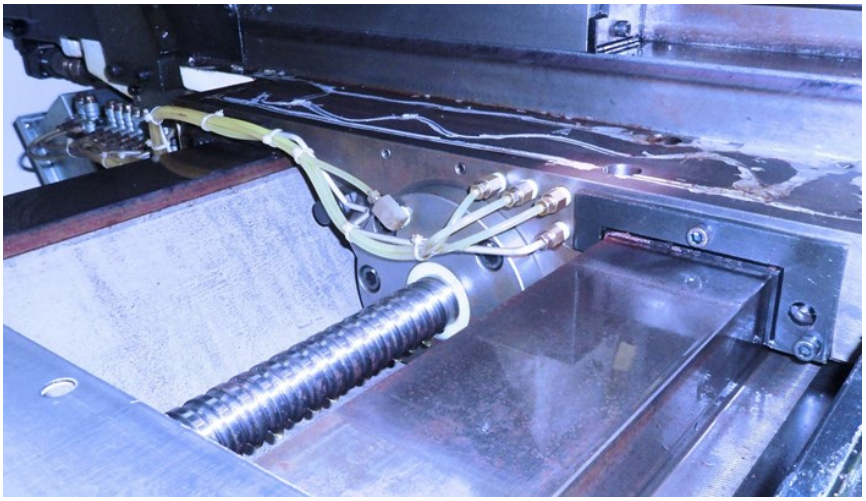

Figure 3.6 The lubrication piping on existing guideways

3.2.1 Measuring Method Structure

Thermocouple: the guideway temperature is measured with four thermocouples mounted on the biaxial linear guideways (T_A, T_B, T_C and T_D). Adhesive thermocouple type K is used. The thermocouple specifications are listed in Appendix C (Table C.1). According to Figure 3.7, T_A and T_B are for measuring the temperature of the X-axis linear guideways, while T_C and T_D are for measuring the temperature of the Z-axis linear guides. The contact points between the carriages and linear guides are considered the most sensitive to temperature change due to the friction caused by relative movements. The temperature readings in the temperature signals are sampled at 100 Hz and the temperature signal input range is experimented at 0-50˚C. The signals are recorded in a DAQ module (Model 9211, NI- C series, 24-Bit Thermocouple Input Device) for processing.

Current clamps: Three current sensors made by Pearson Electronics, INC, are fixed onto the servomotor wire to measure motor current of the feed and spindle systems. Hall-effect current transducers (Model 410 Pearson Electronics, INC, Palo Alto, USA) on the wire of the U-phase spindle motor current outputs, and 2 Hall-effect current transducers (Model

2879 Pearson Electronics, INC, Palo Alto, USA) are fixed on the wire of the U-phase motor current of the feed system (Figure 3.8).

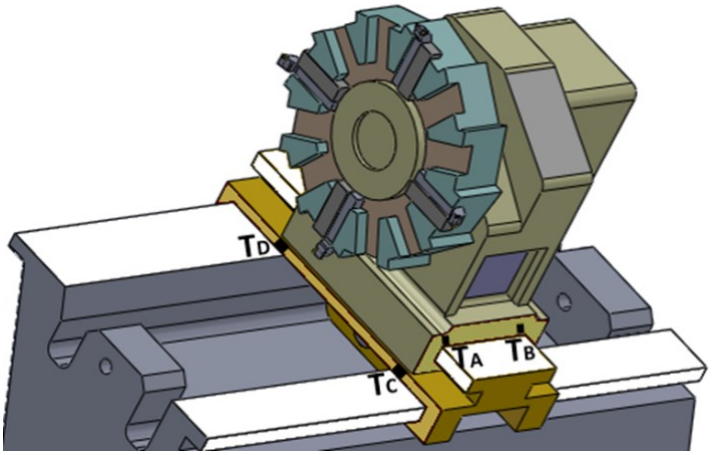

Figure 3.7 Locations of thermocouple installation

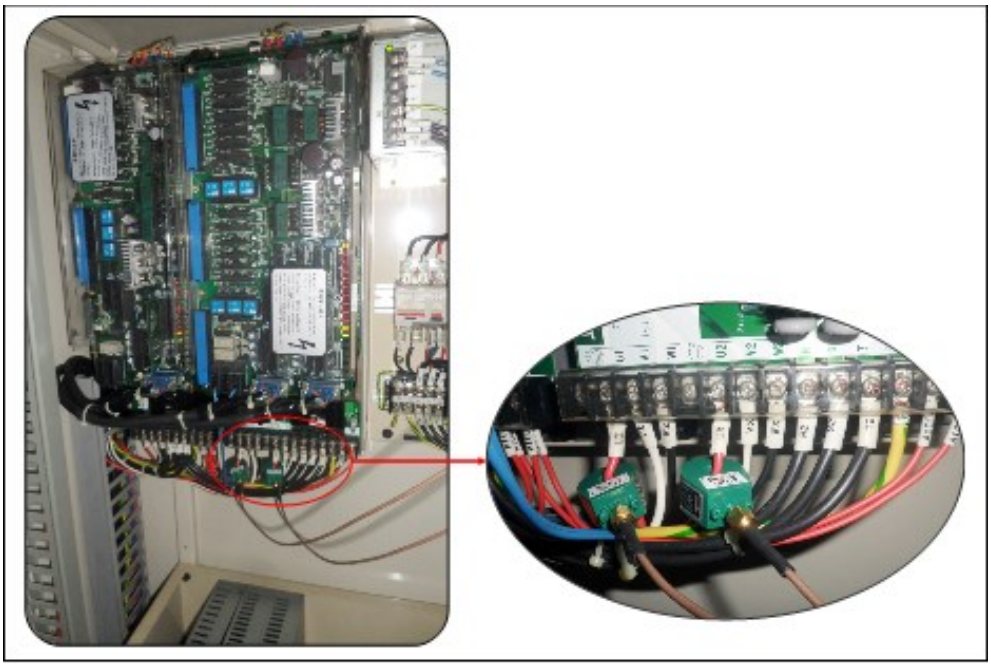

Figure 3.8 Current clamps fixed on the X and Z-axes; servo driver wires

Current data signals are sampled at 1 kHz. The voltage signal input range for the spindle motor is ±10 V, and for the feed drive systems, it is ±2 V, captured with a DAQ module (Model 9205, NI- C series, 16-Bit Analog Input Module).

Dynamometer: A tool dynamometer (Model 9121, Kistler Instrument AG, and Winterthur, Switzerland) was installed on the turret of the LB15-II (Fig. 3.2). The dynamometer has several quartz-based piezoelectric force transducers in steel housings. When force is acting on the dynamometer, each transducer produces a charge proportional to the force component that is sensitive to that axis. The 9121 model measures force on the X, Y, and Z-axes. The charge is then converted into voltage signal by a multi-channel charge amplifier (Model 5019 B 141, Kistler). Force data signal and voltage signal input ranges were sampled at 1 kHz and ±10 V, respectively, with a DAQ (data acquisition) module (Model 9219, NI- C series, 24-Bit Universal Analog Input).

Controller: The control algorithm was written in Laboratory Virtual Instrument Engineering Workbench (LabVIEW) version 11.0.1, control design. A PC software set (NI-Lab VIEW 2011) was employed to illustrate the machine-tool conditions, and to simplify the improvement of block diagram, identification and control algorithms. The software is ideal for any measurement or control system, which uses icons instead of lines of text to create applications. Numerical simulations, curve fitting, interpolation and displaying data plots, are written and run in MATLAB version 7.12.0.635 (R2011a-The MathWorks, Inc., Natick, MA, USA).

Display and control: An experiment was designed to obtain the data for deriving the relationship between current and friction. Two different signals were acquired: cutting force, and servomotor current for feed drives and spindle on drive systems. Figure 3.2 illustrates an image representation of the experimental setup.

Experimental studies were conducted on a two-axis CNC turning machine, comprising an industrial laptop, a Compact DAQ USB chassis designed for use with C Series I/O modules, and a mechanical system equipped with a commercial servomotor. An industrial

laptop with an Intel "Pentium" processor T4400 2.2 GHz CPU was used to provide functions and include an interface for human and machine operation, implementing documentation methods, and recording data values during the tests.

Lubrication pump: Lubrication is the process or technique employed to reduce wear of one or both surfaces in close proximity that are moving relative to each other. A substance called a lubricant is interposed between the surfaces to carry or help carry the load (pressure generated) between the opposing surfaces. The lubricator includes a motor-driven gear pump with reasonable structure, excellent performance, complete function, wide applicability, good self-absorption and high volume efficiency. As a self-contained motorized gear pump, automatic lubrication VERSA Ⅲ is compact and efficient. It is suitable for most industrial lubricant from 20cst to 2000cst and meets a variety of lubricating requirements. The pump is programmed to discharge accurate amounts of oil at predetermined intervals from several minutes to several hours. Model coding of the lubrication pump is VERSA 4BBCDA and it represents the reservoir capacity, 4 liters of which material is ABS or metal. The model is used in Positive Displacement Injector (PDI) systems. Its units are available complete with built-in level switch, pressure switch, and programming controller (SM-AC) or external controller. The power supply voltage is 230 V AC 50/60 HZ for motors with M12 × 1 connector. The pump specifications are shown in the table below (Table 3.3).

Table 3.3 Motor pump specifications

Delivery Volume	108 ml/min
Rated Pressure	1.4 MPa
MAX. Delivery Pressure	2.5 MPa
Oil Viscosity Range	20~2000 cst
Filter Precision	90μm
Volumetric Factor	≥75%
Power Supply for Motor	230V 1 Phase 50/60 Hz
Velocity of Motor Shaft	1350 rpm
Input Rating	60 Watts
Controller	SM-AC

This kind of lubricant pump is equipped with a 4-liter capacity reservoir, a single-phase motor, liquid level switch and pressure switch that can be employed according to different applications. When the pump is switched on, the 230 VAC motor drives a gear pump, which delivers oil to the main distribution line. A power circuit diagram for the lubricant pump is shown in Figure 3.9.

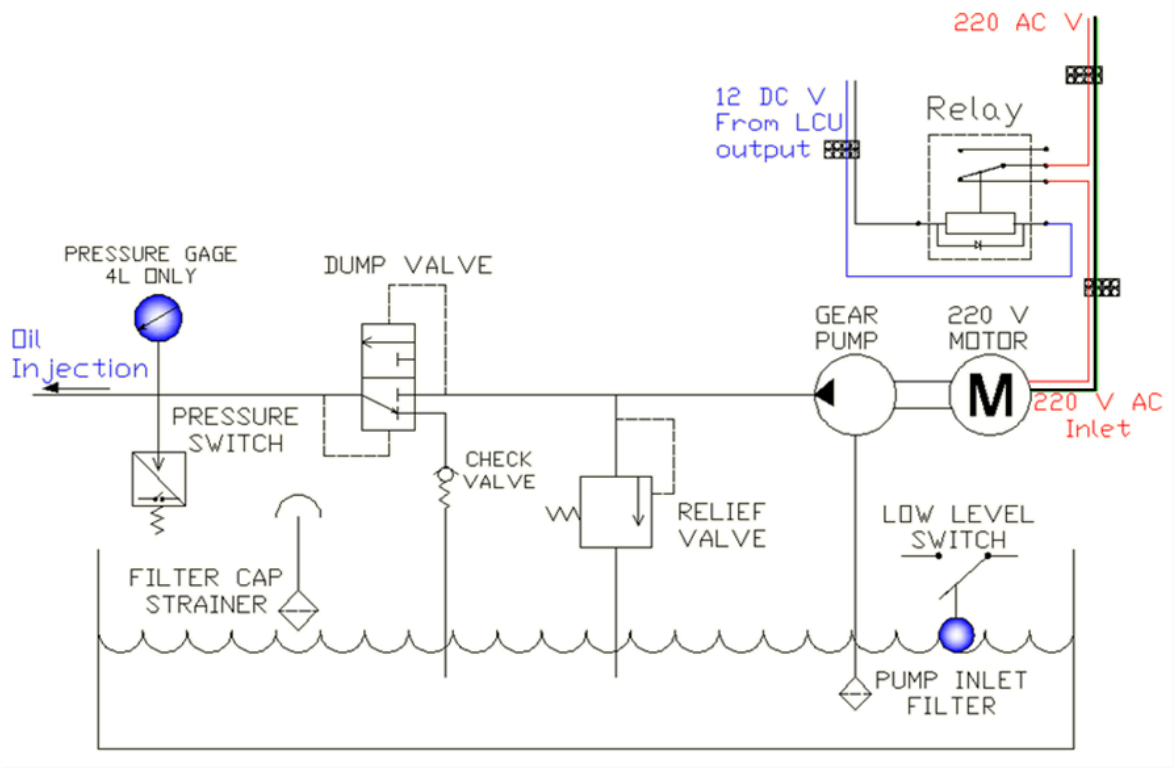

Figure 3.9 Power circuit diagram for the lubricant pump

3.2.2 Structure of the Lubrication Control Unit (LCU)

NI cDAQ-9174 is a 4-slot NI Compact DAQ USB chassis designed for small, portable, and mixed-measurement test systems. It has four 32-bit general-purpose counters/timers built in. The cDAQ-9174 is combined with up to four NI C Series I/O modules for a custom analog input, analog output, digital I/O, and counter/timer measurement system. The configuration of the modules used in cDAQ-9174 is shown in Table 3.4. The NI Compact DAQ serves as the interface for sending motion commands and for receiving feedback signals from the

servomotor drives with a sampling period of 1.0 msec. The mechanical system of the turning machine is mainly composed of a horizontal axis and biaxial linear guideways. Two Okuma BL-Type drive the biaxial linear guideways, which is the main object of this study.

The AC servomotor was prepared with inherent velocity and torque control loops, which can be changed by loads on the biaxial linear guideways. Here, the loads' command signals are sent to each driver via a 16-Bit AI (Analog Input) resolution installed on the Compact DAQ chassis. This module supports a low-power sleep mode at the system level, depending on the chassis that the module is plugged into. A rotary encoder is directly connected to the servomotor, and the produced encoder signals are used to indicate the motor's angular positions. A 16-Bit ADC converter that is applied on the cDAQ is used to receive analog signals from the servomotor in order to obtain the cutting and thrust force values that actuate the biaxial linear guideways.

Table 3.4 Specifications and configurations of modules in data acquisition

Modules	channels Used	Sample to read	Rate (HZ)	Scaled units	Signal input range	Type of measure output
NI 9211	4/4	10	100	Temperature	0-50 ˚C	TA ,TB, TC, TD
NI 9205	3/4	100	1K	Voltage/ current	± 10 V, ± 2 V	M.Cs, M.Cx, M.Cz
NI 9219	3/4	100	1K	Voltage/ cutting force	± 10 V	Fx, Fy, Fz
NI 9474	4/4	-	-	A/D converter	0-1 A 5-30 VDC	- Analog - Digital

3.2.3 System Performance

Conventionally, a predefined lubrication system via CNC coding command is used to lubricate guideways in CNC machines, where the time and period of lubrication are controlled by the machine maker by default. However, users can modify the lubrication motor's OFF or ON timer (pump response interval) in relation to the machine's action rate,

cutting force, and other such parameters. For example, in the OKUMA LB15 II CNC lathe machine, the motor OFF time was defined as 5 minutes while the ON timer was set at 30 seconds. If lubricant delivery volume in the pump unit is 0.1l/min, it means that after 10 cycles, oil consumption will be 0.5 liters every 1 hour approximately. Under these conditions, 4 liters of the pump reservoir volume transfers throughout around 8 hours of machining. This is a standard situation; however, some operators may change parameters without any understanding of oil consumption control.

The development of CNC machining requires an optimum lubrication process that does not rely on the operator. This requirement can be met by adding a new lubrication control technique to the process and automatic commands according to friction force conditions on the linear guideways.

An external lubrication pump was used to create changes in "OFF" and "ON" time, and to design a lubrication control system for this research method. The external pump is controlled by the new proposed lubrication control system. The oil outlet then injects oil to the linear guideways. It is a novel approach in machining technology, whereby the lubrication condition during the machining process can be identified using current signals from sensitive current sensors fixed on the servomotor wires and cutting force signals from the dynamometer installed on the turret of the machine tools. In these cases, the current and force data signals reflect the friction, wear and loading conditions. Signal analysis and signal commanding are performed by the LCU.

The LCU consists of several modules, each of which is a micro controller already programmed to capture data from the sensors. The modules then send command signals to the actuator to trigger the oil pump to inject oil. A schematic of the measuring system is shown in Figure 3.10.

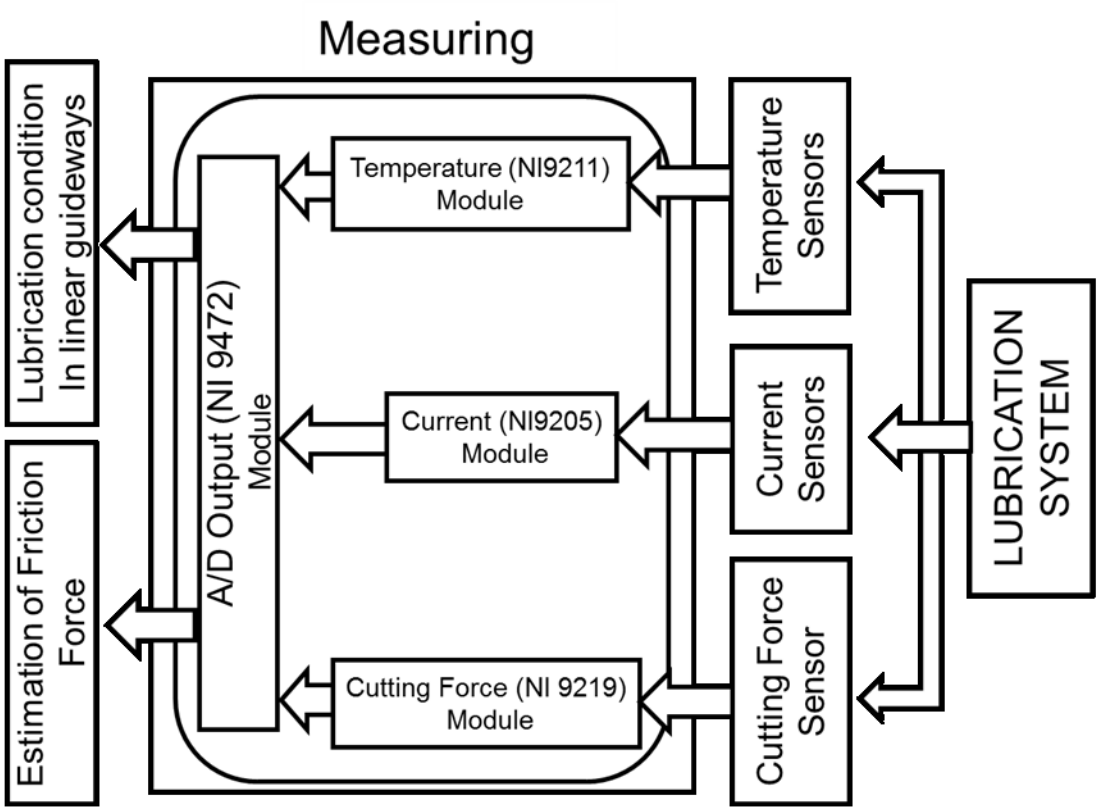

Figure 3.10 Schematic of the measuring system

Parameter identification is an experimental method based on several subsystems. Each subsystem includes one or more lubrication project sections, which are described below using the measured data.

Three main variables are considered in the research: temperature of linear guides on the X and Z-axes, effective cutting forces on the moving table, and servomotor current for the X and Z spindle directions. As previously mentioned, temperature on the X- and Z-axes was measured with four thermocouples (T_A, T_B, T_C and T_D). The type of adhesive thermocouples is thermocouple K. T_A and T_B measure the temperature of the X-axis linear guideways, while T_C and T_D measure the temperature of the Z-axis linear guides. The temperature readings are sent to LCU for processing.

The real time X and Z-axis servomotor current is measured to control the power load on the motor due to the friction/lubrication process. The measurement is done by two current monitors (model 2879) fixed on the wire of the motor to detect output current. The sensitivity and dimensions of the current monitor are presented in Appendix C (Table C.2). The result is sent to LCU for processing. Temperature and current changes with time are measured to control the quality of CNC performance and command for the optimum required lubricant using a certain program developed for this purpose. The real time, measured temperatures and the current are reported in digital numbers and displayed in graphs on the screen of the computer connected to the system via the port RS-485 interface for USB on the modules (refer to Table 3.4). The operator can observe the changes and values of measured quantities.

The presented data can show the influence of the applied load, speed, friction, and other parameters on the CNC machining process. Parameter monitoring is helpful as it provides information about possible unexpected happenings. The mode of monitored quantities is selected by the operator. It is possible to observe one or more measured quantities at the same time on the screen, thus allowing the operator to compare the data for the optimum working mode.

Simulation tools help engineers investigate the behavior of stick-slip motion when designing a lubrication system for machine guideways, which is one of the important goals of this study. In this regard, a method is developed, and the corresponding differential equations are created. In order to simulate real-time conditions, friction coefficient data are experimentally obtained and evaluated with the help of a function.

In this thesis, the measurements and control algorithms are written in LabVIEW, which is a graphical programming language that uses icons instead of lines of text to create programs. LabVIEW contains an inclusive set of virtual instruments (VIs) and functions.

Most LabVIEW virtual instruments have three key tasks: acquiring some kind of data, analyzing the acquired data, and presenting the results. A VI consists of a front panel window, which is the user interface, and a block diagram, which is the graphical source code. The front panel window and block diagram provide various toolbars, shortcut menus, and palettes to help create VIs.

When data acquired by the instruments are connected to a computer, the data need to be recorded and stored for future reference. This process is called writing data to a file. However, when there is a need to access the stored data from a file, the process is called reading data from a file.

LabVIEW provides file I/O VIs to read and write data to a file. In an executable VI, all the sub-VIs, functions, and structures must be wired with the correct data types for the terminals. Sometimes a VI does not run, or it runs in unexpected ways. LabVIEW can be used to debug VIs and correct problems.

Before a computer-based measurement system can measure a physical signal such as force, the physical signal must be converted into an electrical one, such as voltage or current. After a signal is measured, the measurement is communicated to the computer through a data acquisition (DAQ) device.

A typical DAQ system has three basic types of hardware: a terminal block, a cable, and a DAQ device. After a physical phenomenon is converted into a measurable signal with or without signal conditioning, it is necessary to obtain the signal. To acquire the signal, a terminal block, a cable, a DAQ device, and a computer are needed. This hardware combination can transform a standard computer into a measurement and automation system.

By using LabVIEW, it is possible to control and acquire data from instruments with the Instrument I/O Assistant, virtual instrument software architecture (VISA), application programming interface (API), and instrument drivers.

3.3 Graphical User Interface (GUI) Programming and Simulink

There are many design patterns for LabVIEW. Most applications use at least one design pattern. As a pattern gains approval, it becomes easier to recognize when a design pattern has been used. This recognition helps to read and make changes to VIs that are based on design patterns. In a programming design, two main components are the block diagram and front panel window, and these are used simultaneously. The front panel window is a user interface (UI) for the VI. It is created by controls and indicators which have input and output terminals, respectively (Figure 3.11). In block diagram windows, a series of graphical codes called "function palettes" graphically show the design created in the front panel (Figure 3.12). It can be used to control front panel components via graphical symbols of functions.

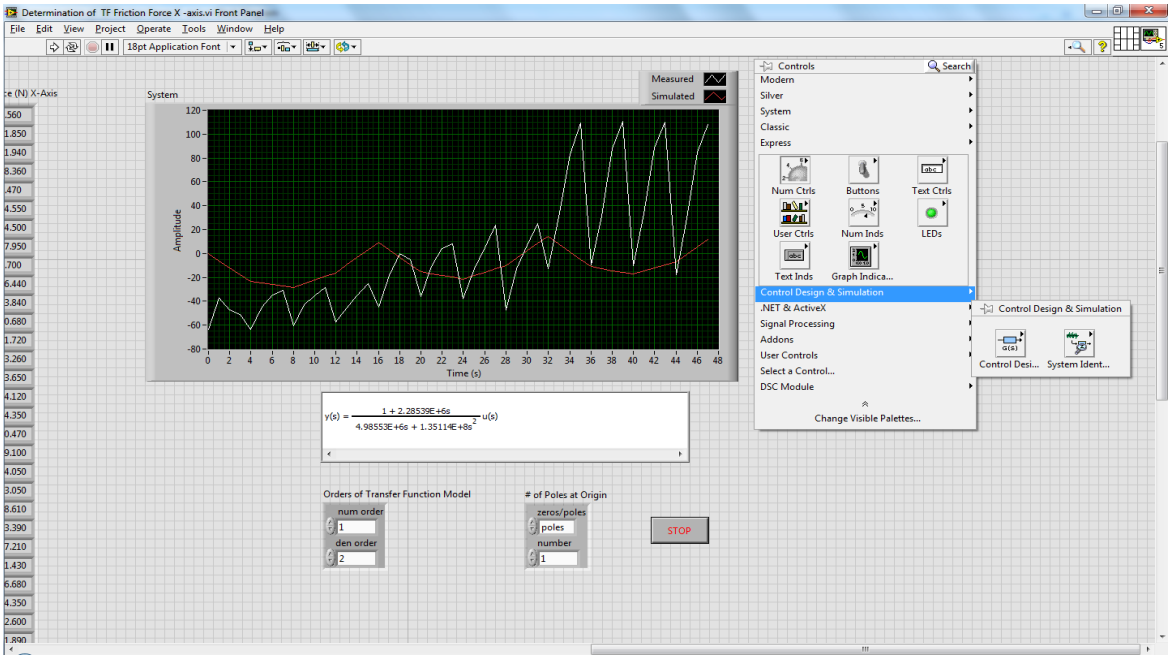

Figure 3.11 Graphical representation of controls in the front panel window

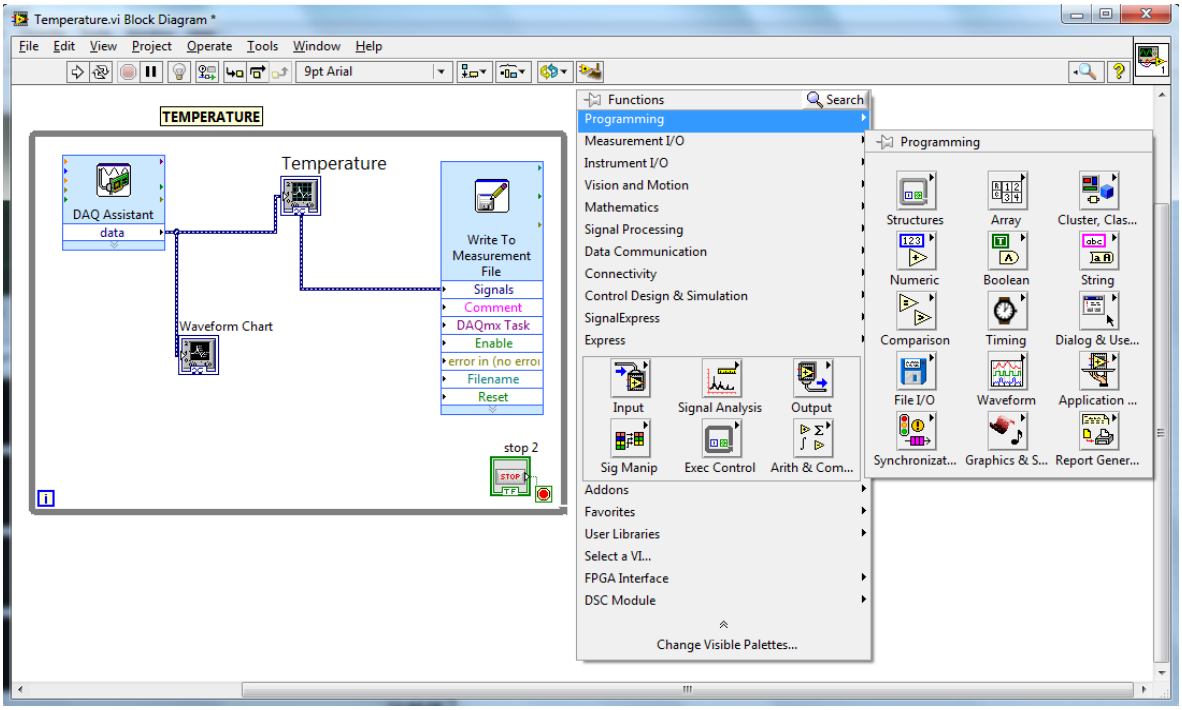

Figure 3.12 Graphical representation of functions in block diagram window

3.3.1 Temperature Measurement

In this design pattern, the front panel and block diagram were documented. A while loop is drawn from the drop-down functions menu. The loop consists of a DAQ Assistant for creating input/output data and configuring them with dialog boxes. In addition, a "write to measurement file" for defining the file name, format and action is saved to a file where we want to store the signals. According to Figure 3.13, a waveform chart is placed between the acquiring task and measurement data.

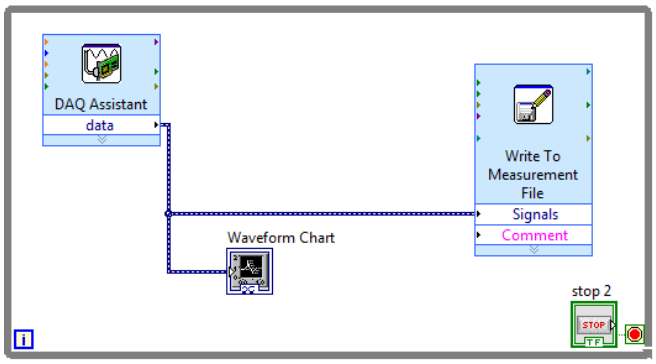

Figure 3.13 Temperature Block Diagram

In configuring the temperature design pattern, the number of thermocouples that were applied according to module type and relevant channel are defined in the channel settings section. Moreover, signal input range, scale unit, and thermocouple type are specified in this section. In the timing settings, acquisition mode, samples to read (STR), and rate of frequency can be adjusted appropriately to the sensor. The values shown in Figure 3.14 are TA settings. The values are equal to other thermocouples (TB, TC, and TD).

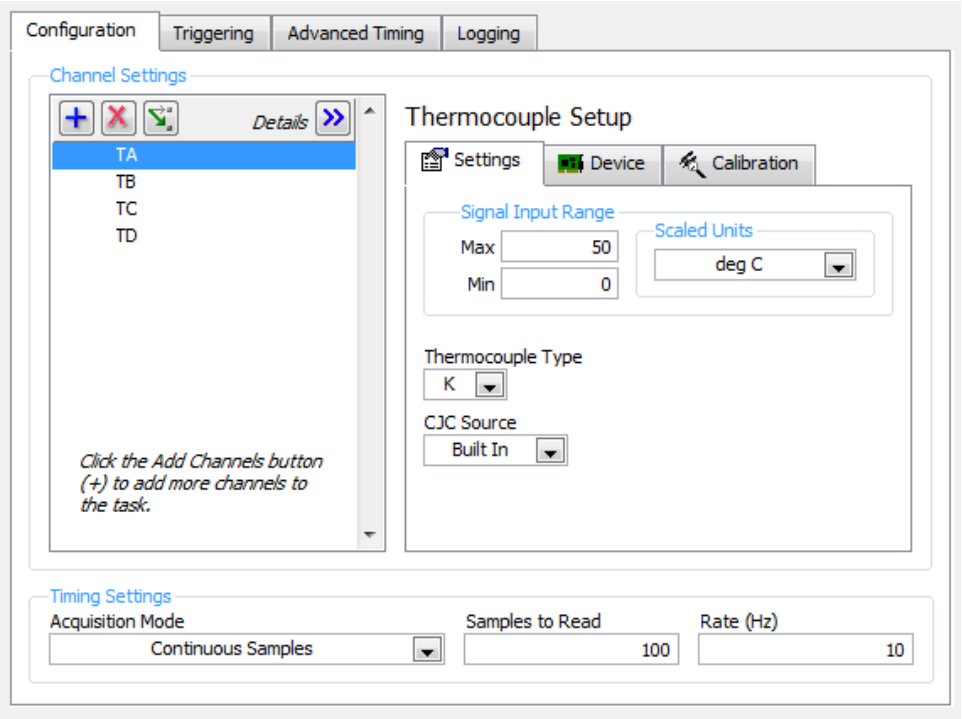

Figure 3.14 DAQ Assistant configuration for temperature

3.3.2 Cutting Force Measurement

According to Figure 3.15, in the block diagram of cutting force measurement the output signals of each force ($F_L, F_R, and\ F_t$) as shown in Figure 3.16 is multiplied by some numbers. This value is measured and calculated for measurement device (dynamometer) calibration. The coefficient values for every force are given below:

$F_X = F_L \rightarrow 126.937\ (N),$ $F_Y = F_R \rightarrow 126.974\ (N),$ $F_Z = F_t \rightarrow 275.248\ (N)$

These values are called calibration coefficients and are essential for calculating the exact cutting force value.

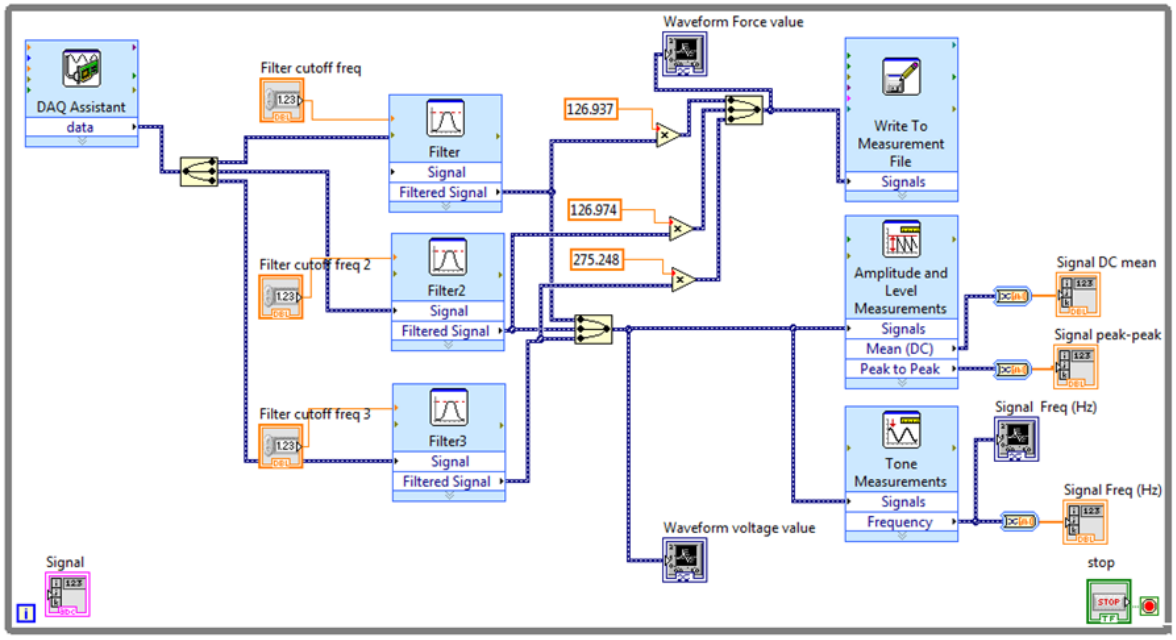

Figure 3.15 Cutting force block diagram

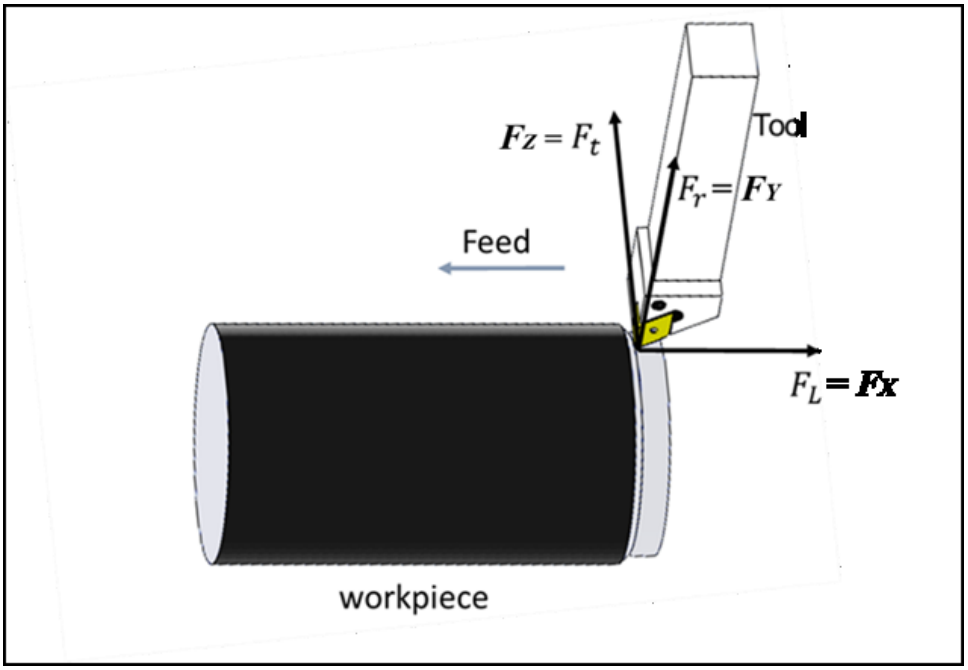

Figure 3.16 Cutting force directions

As noted in the introduction, there are three important tasks in programming: data acquisition, analysis, and display of data results. In a design pattern of cutting force circuit, each one of the categories has been used. In the Analyze category, the low pass filtering type with 50 HZ cutoff frequency was configured (Figure 3.17) in the "configure filter" window. The filters will remove noise, such as noise whose power spectrum changes over time.

Another component of the analysis category is amplitude and level measurement. This task is responsible for measuring the signal voltage. For cutting force measurement, the amplitude measurements on DC and peak-to-peak are specified (Figure 3.18).

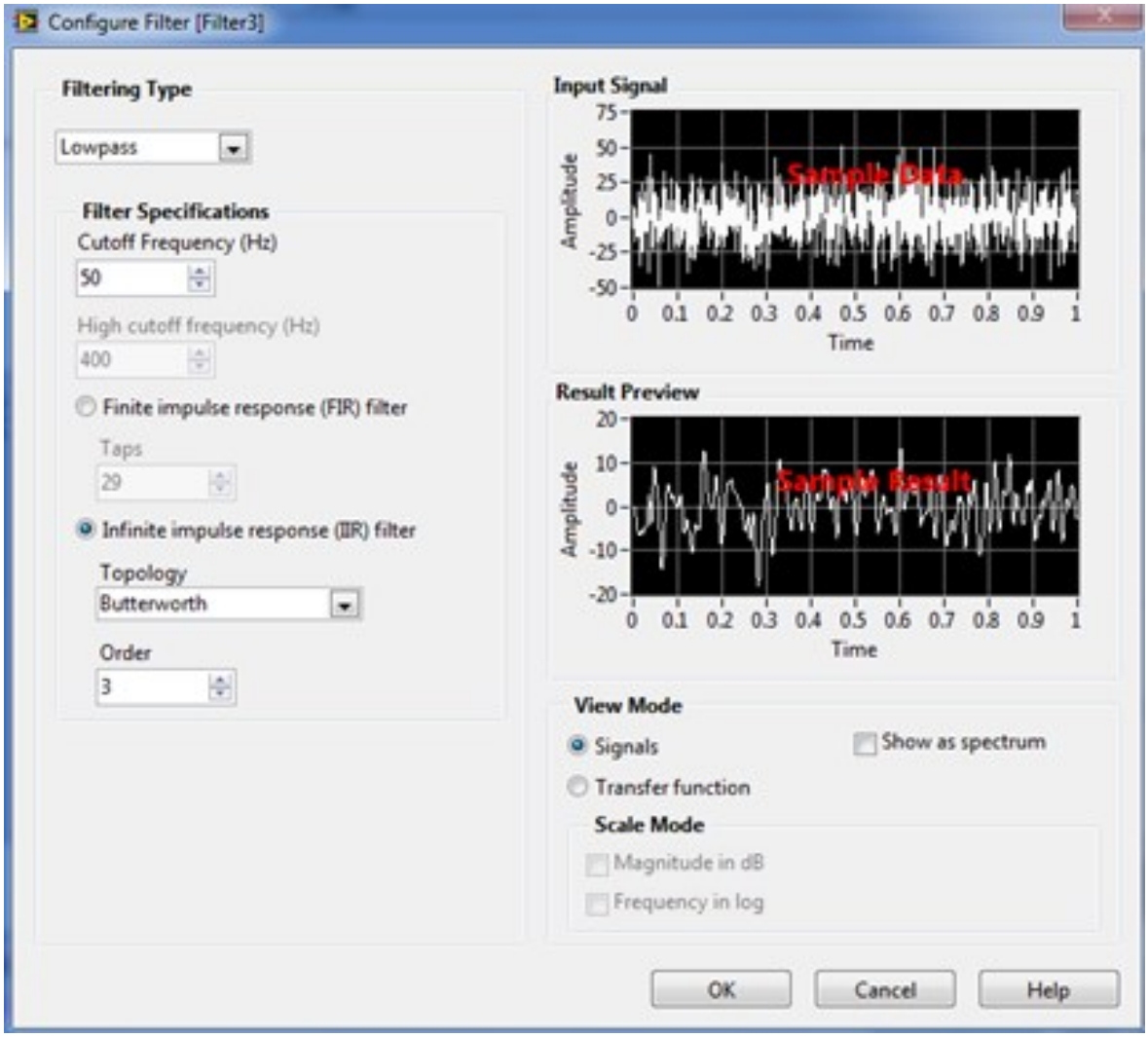

Figure 3.17 Filter configuration window

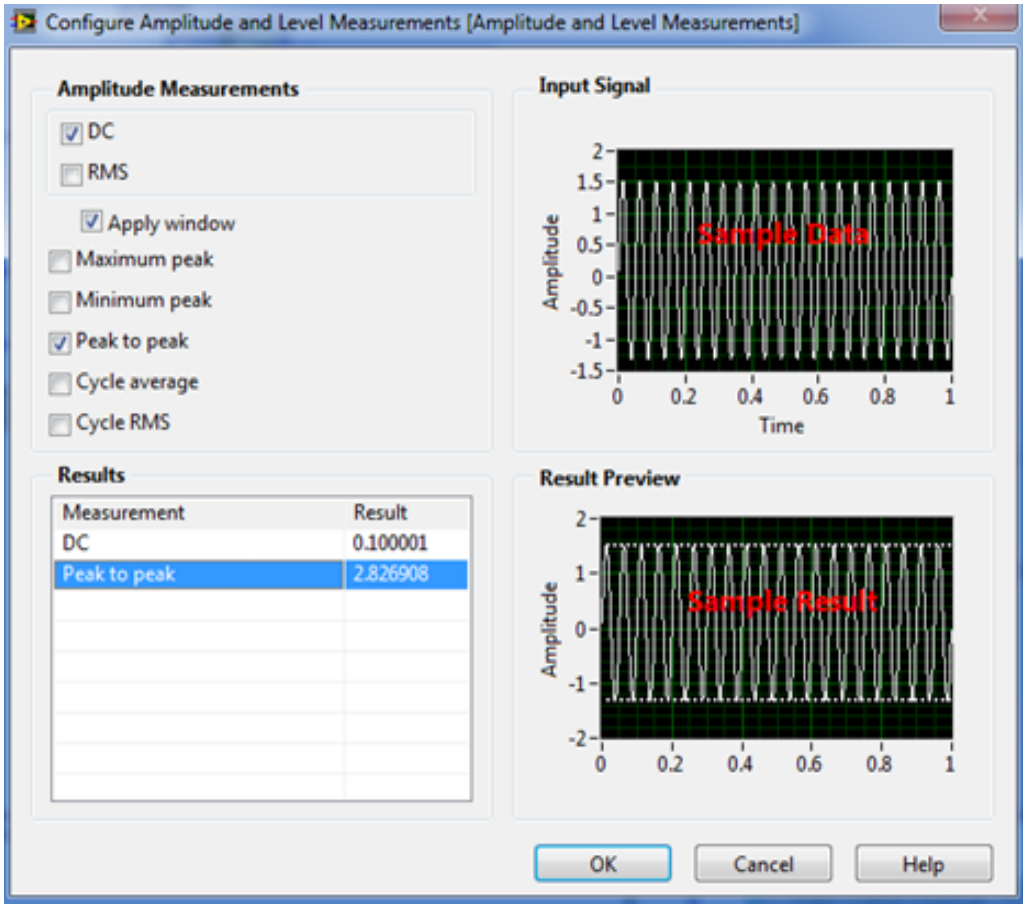

Figure 3.18 Amplitude configuration window

Figure 3.19 shows one of the measures considered. The window is related to measurement selection. Frequency and its approximate value are closely defined to experimental results. A result preview in terms of amplitude and frequency can be displayed as well. After building a task, it should be configured for continuing measurement. Channel-specific settings include input limits, scaling, and terminal configuration. The timing of task-specific settings can also be configured.

In this task, scaling is not necessary. To configure the cutting force measurement task, the following steps are carried out:

i. Determine the input limits. Default values of 10 for max and -10 for min are applied for signal measurement.

ii. Select "Terminal Configuration" for the signal.

iii. In the configuration tab under the "Timing Settings" section, select N samples for the acquisition method. Enter 100 for STR, and enter 1000 for rate of frequency (Hz) (might default to 1k), as shown in Figure 3.20.

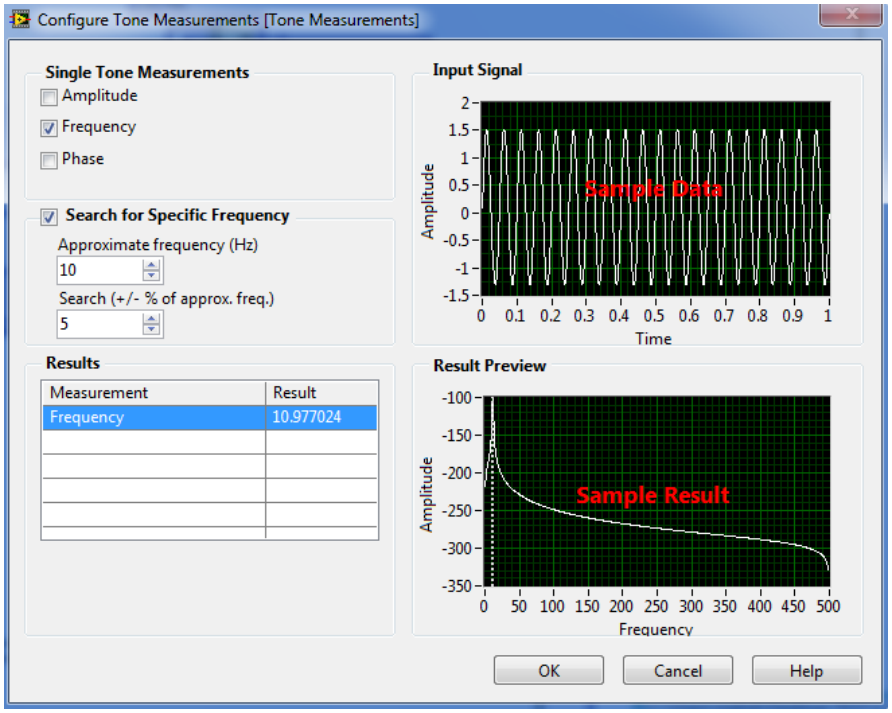

Figure 3.19 Tone configuration window

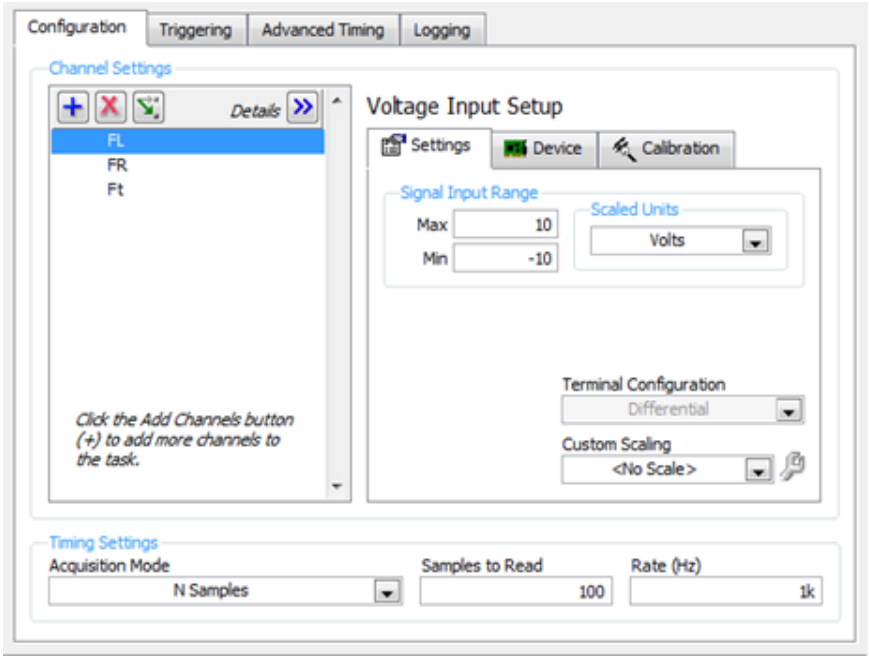

Figure 3.20 DAQ Assistant configuration

3.3.3 Servomotor Current Measurement

As explained in section 3. 2. 1, three current sensors are looped around the servomotor wires to measure motor currents of the feed and spindle systems. Hall-effect current transducers on the wire of the U-phase spindle motor current outputs, and two different types of Hall-effect current transducers (Model 2879) are fixed around the wire of the U-phase in the X and Z-axis motor currents of the feed drive systems.

Regarding the block diagram shown in Figure 3.21, the methods of filtering (cutoff frequency), amplitude/level measurements (peak-to-peak), and signal frequency (HZ) are configured. Moreover, a calibration coefficient is used according to the sensitivity of the sensors. Current sensor sensitivity for the X and Z-axis servomotor current measurement is 0.01 volt/Ampere. Therefore, its value is multiplied by 100. Since the sensitivity of the spindle motor's sensor is 0.1 Volt/Ampere, a coefficient of 10 is chosen accordingly. To configure the DAQ assistant, current data signals are sampled at 1 kHz. The voltage signal input range of the spindle motor for experimentation is ±10 V, and for the feed drive system, it is experimented with ±2 V with a DAQ module (Model 9205, NI- C series, 16-Bit Analog Input Module) as shown in Figure 3.22.

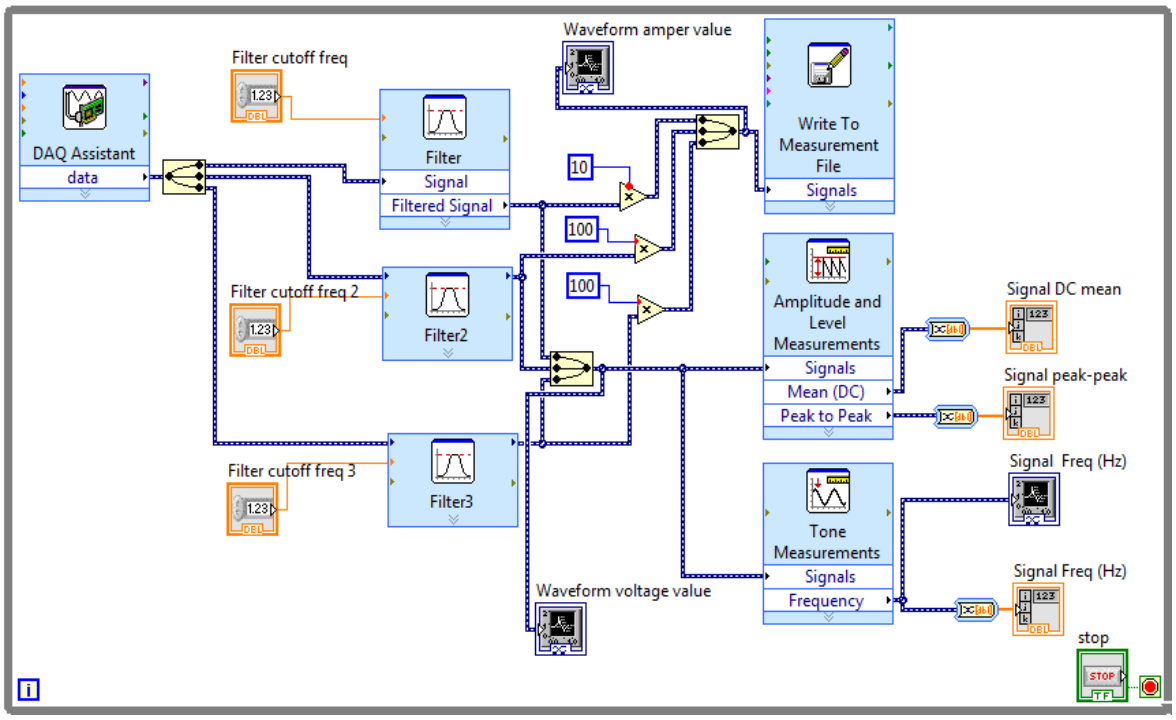

Figure 3.21 Block diagram for servomotor current measurement

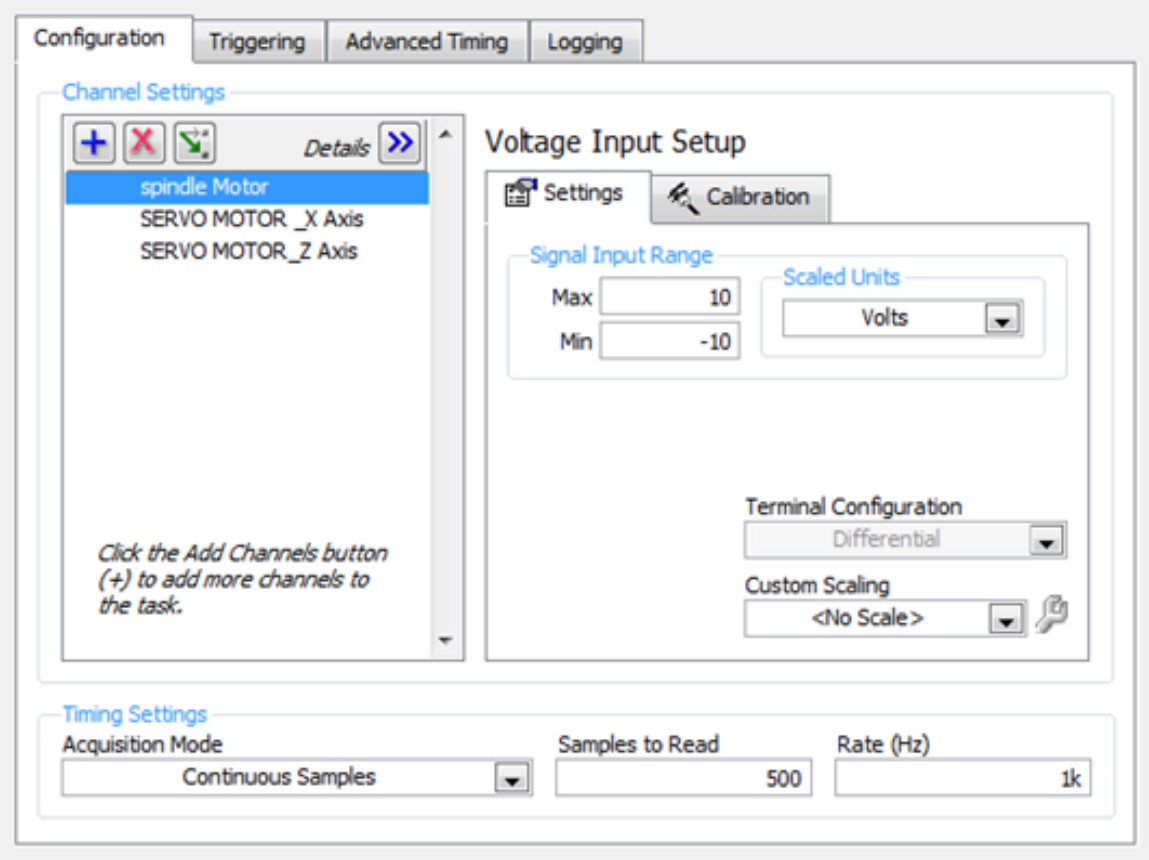

Figure 3.22 DAQ Assistant configuration for cutting force

3.3.4 Overall Circuit Diagram

After the parameter configuration in terms of signal type, timing settings, channel settings, amplitude, filtering, and tone, the block diagrams can be placed inside a while loop. Once again, all three block diagrams are placed within a general while loop using one output express VI. With this method, all data are written and stored in one file. Figure 3.23 shows this design method.

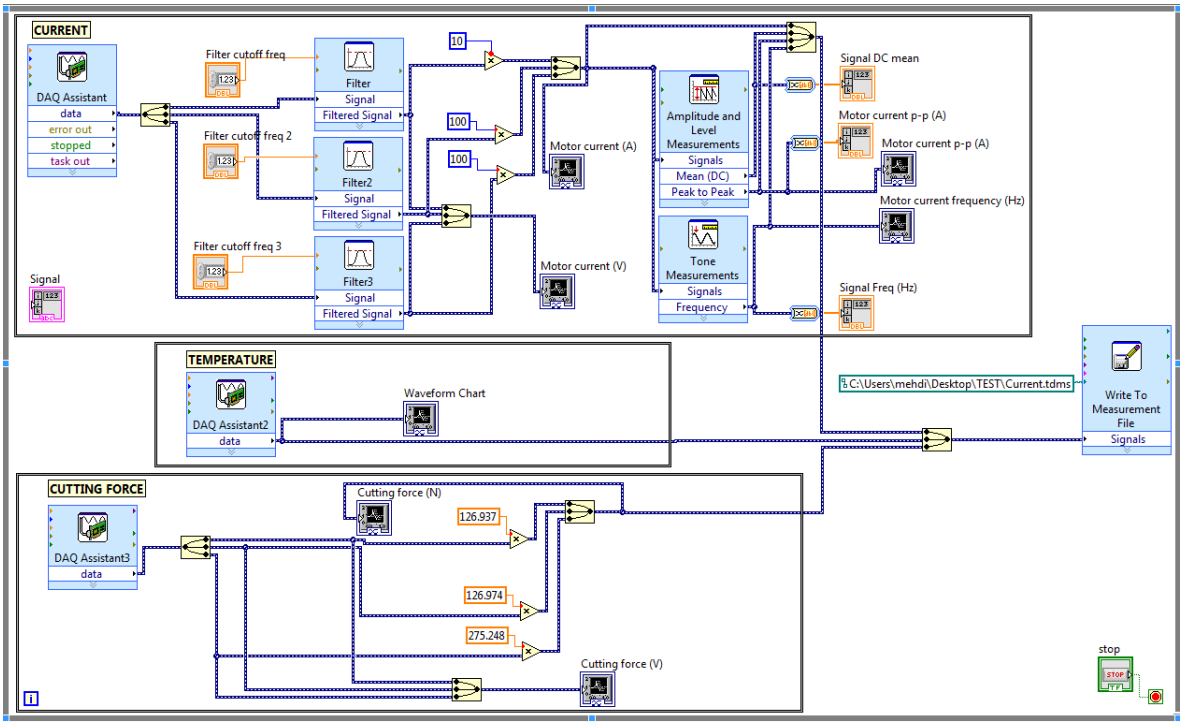

Figure 3.23 The overall block diagram for the initial measurements

In this section, a model of machining and technique measurements is identified. Before the measurements, the method of sensor installation onto the machine and their relation with the measurement modules are described.

The mechanical subsystem includes four main parts: sensors, controller, actuator, and monitor to control the lubrication in linear guideways. Previously, lubrication systems for CNC machine linear guideways were used via coding command techniques. These were necessary for master operators responsible for defining oil injection time and amount of oil

injected based on machining volume. This process was performed based on fixed time and amount of oil injection regardless of cutting force value, weight and size of the workpiece, friction force on the guideways, or machining process conditions. That led to less protection of guideways in case of high friction force with less lubrication provided or excessive oil consumption in case of less friction force in guideways (Nikolakopoulos & Papadopoulos, 2008). This technique did not guarantee accuracy, since the time and amount of lubrication were controlled subjectively by the operator. In this case, lubrication time, period, and amount of lubricant are managed by electric/electronic parcels (Yukeng et al., 1985), which have some abilities in programming and varying the lubricating operation.

Environmental temperature should be considered when setting machining parameters. The most sensitive temperature points are the contact points of carriages and guideways where friction appears during relative movements (Figure 3.24).

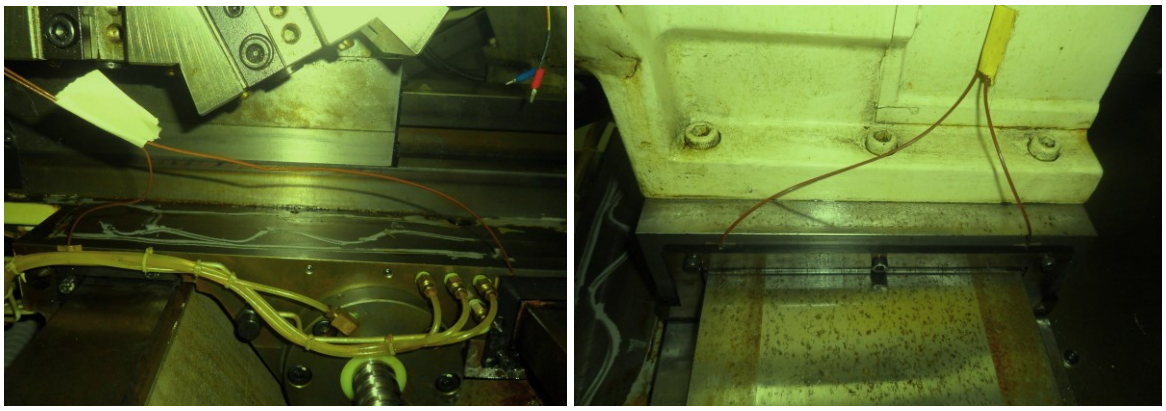

Figure 3.24 Installation of sensitive thermocouples on linear guideways

In order to set the machining process in relation to the environmental temperature, which varies from time to time, a critical temperature (Tcr) was defined. This temperature can be flexibly set according to the environmental temperature during machining time throughout the day. This novel approach provides superior safety and longer, more precise machining. The rate of real time temperature variation in the machining process is slower.

Therefore, over a long time of machining, the temperature variation in linear guideways is low.

Another variable considered in the research is the servomotor's current in the X and Z directions. The real-time X and Z-axes' servomotor current is measured to control the power load on the motors, that changes due to the friction/lubrication process. According to Figure 3.8, two current monitors (Model 2879) carry out measurement with current clamps fixed on the servo driver wire to detect output current. The results are sent to the LCU for processing.

A differential measurement configuration intended to obtain accurate measurements and less noise requires two inputs for each measurement. Figure 3.25 shows the current sensors connected to the module using differential connection.

Differential connection mode for connecting the cutting forces and thermocouples to the modules are used similar to connecting the current sensors as shown in Figure 3.26 and Figure 3.27 respectively.

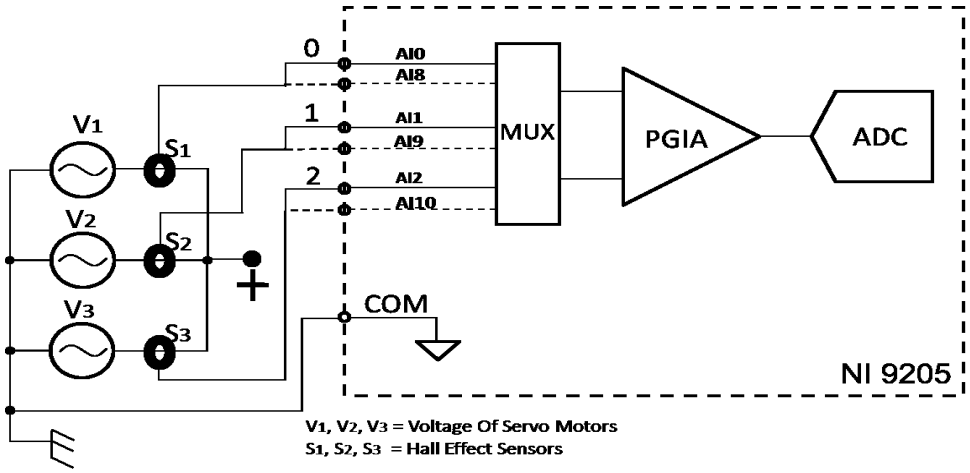

Figure 3.25 Connecting current sensors to the measurement module

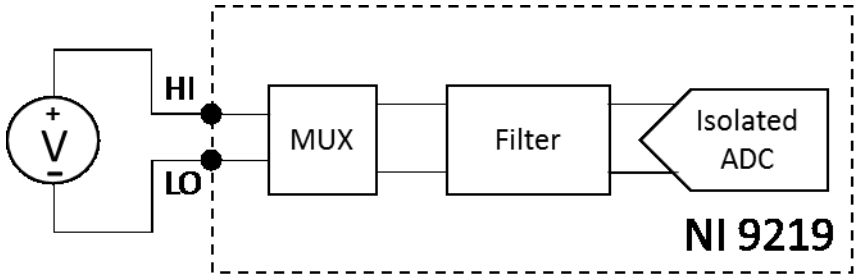

Figure 3.26 Connecting cutting force sensor to the measurement module

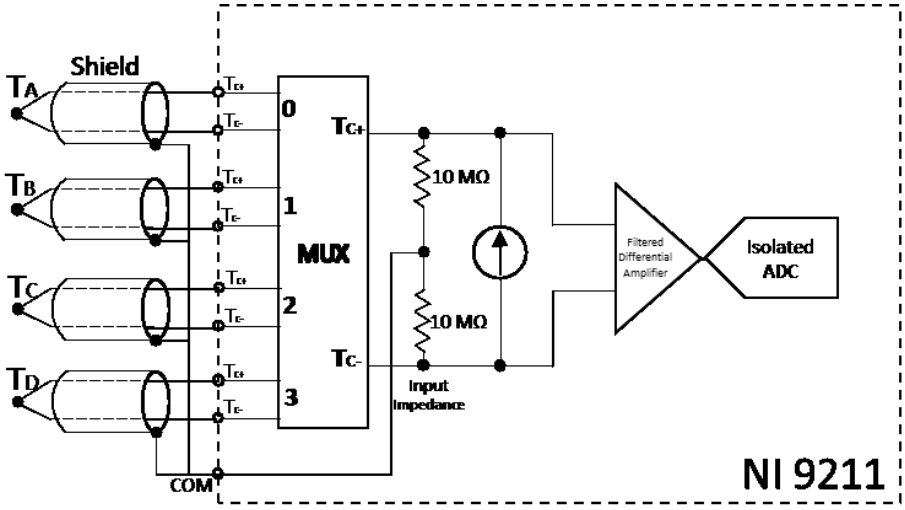

Figure 3.27 Connecting thermocouple sensors to the measurement module

For turning, the spindle speed (S) is preset in revolutions per minute (rev/min) as an integer number (250, 500, 750, and 1000 rpm) in three experiment groups.

The coefficient of friction changes in tandem with velocity for almost all linear guideways materials. Stick-slip motion occurs in cases where the coefficient of friction has a maximum rate at zero sliding velocity, and reduces with increasing velocity. In this case, the slope of the friction coefficient's sliding velocity curve is negative. It is established that friction depends on surface roughness; therefore, friction occurs from normal/cutting forces. Moreover, it was specified by some authors that kinetic friction is true friction; however, static friction is the sum of true friction plus the cohesion between surfaces (Tabor, 2001).

The measured values of friction data are found during motions of the moving parts that are placed on each feed drive servomechanism of the CNC turning machine.

Figure 3.28 schematically shows the moving tool model during the experiments. According to Figure 3.28, the sample moving model of the cutting tool starts at point "A," undergoes the cutting process, and returns to point "A". Furthermore, regarding the behavior of the model presented in Table 3.5, during the C-D path (147 mm), the cutting operation occurs. The depth of cut, feed rate and cutting speed already defined in each experiment are generated during this time. The moving part moves along the motion path and undertakes several forward and backward motions. In each experiment, the cycle shown in Figure 3.28 is repeatedly run in order to obtain the average behavior of friction.

$$Movement\ value\ (mm) = (|X_2 - X_1|, |Z_2 - Z_1|) \tag{3.1}$$

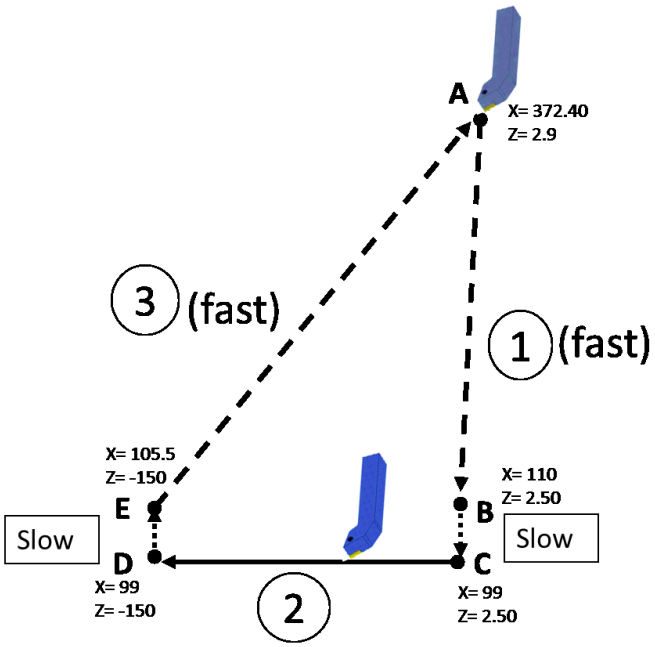

Figure 3.28 Moving tool model

Table 3.5 Specifications of tool movement changes

path	Type of motion	Movement (mm) Eq. 3.1	Feed rate (mm/rev)	Depth of cut (mm)	Cutting Speed (m/min)
AB	fast	(262.4, 0.4)	0	0	0
BC	Slow motion	(11, 0)	0	0	0
CD	Cutting speed	(0., 147.5)	0.10 0.25 0.50	0.5 1.0 1.5	66 132 265
DE	Slow motion	(6.5, 0)	0	0	0
EA	fast	(266.9, 152.9)	0	0	0

Measuring current is necessary because it is sensitive to increasing friction at the contact points of dynamic parts. Therefore, the servomotor current was selected as the variable to be measured. The changes in current indicate the friction conditions in the linear guideways. The skip-slip motions of carriages and/or supporters cause the current to increase in the servomotors. These undesirable mechanical movements of the parts result in damage to the sliding surfaces in a short time. In the long term, the non-smooth displacement of parts leads to reduced machining precision. Therefore, detecting real-time current is required to gain on-time information concerning machining process conditions. Existing problems in machining are detected by a current clamp monitor, after which the signals are sent to the LCU for data analysis. Therefore, it is necessary to simulate the problem and study the interaction between the current clamp and the LCU in controlling the required oil for the machining process. Obviously, the detection of any mechanical problem requires more lubricant to facilitate smooth movement. The current is considered to be using the cutting forces and strong stick-slip friction, with unstable sliding behaviors (Cheok, 1988; Karnopp, 1985). Thus, the behavior of the servomotor with stationary motion differs from that of a rotating feed motor. In these servomotors, the current level is considered a model of static

and dynamic behaviors. Long-term forms are presented in the static current levels, while short-term effects are described by the dynamic behavior. To determine the static current, the servomotor current levels change during the cutting process. However, during machining with constant cutting force the current remains similar to the initial pre-cutting levels.

The Intelligent Control Toolkit (ICTL) is essential to ANFIS graphical model applications for making and completing block diagrams in the control model of LabVIEW.

Code rules of MATLAB programming language were used, and to achieve predictive friction, all commands were written in the Script space. Some of these commands are given below:

```
[s,d,f,i,fr]=textread('trnData.txt','%n %f %f %f %f');
trnData = [s,d,f,i,fr];
numMFs=[3 3 3 2];
mfType='gbellmf';
epoch_n=50;
in_fis = genfis1(trnData,numMFs,mfType);
out_fis = anfis(trnData,in_fis,epoch_n);
for i = 1:1000000
inputvalues = csvread('parameters.txt');
pred_fric = evalfis(inputvalues,out_fis);
fid=fopen('friction.txt','w');
fprintf(fid,'%6.4f %12.8f\n',pred_fric);
fclose(fid);
pause(0.1);
end
```

One easy and reliable way to convert the real data which, was achieved from the ANFIS model is used standalone executable program file to write a text file for implement in LabVIEW software tool. When an `.exe` file is opened, it launches the program contained within without the need for additional software. The LabVIEW software tool is used for programming and online monitoring the data.

The programming languages code rules is used and to achieve predictive motor current, all of comments were written in the Script space. Some of these commands are given below:

During the experiments the .exe file is run. For this work, the MATLAB compiler `(MCR)` must be installed.

To create a standalone executable program in MATLAB the following comment is needed:

```
mcc -m myapp.m -d 'C:\Users\mehdi\Desktop\azizi'
```

In addition, to create an `.exe` file, the `deploytool` command opens the Deployment Tool window, which is the graphical user interface (GUI) for MATLAB Compiler. It should be stored in a file name similar to the name of the input and output files.

Figure 3.29 shows the relationship between executable programming in MATLAB and LabVIEW. In this connection, a `.txt` file is written by the `.exe` file. This text will be read by the LabVIEW program. Another `.txt` file corresponding to the .exe file needs to be recreated by the LabVIEW program. This text will be read by the `.exe` file. This cycle of reading and writing is developed in a graphical modeling LabVIEW environment and is then placed in a `whileloop` structures. To establish the LabVIEW program, it would be required to run the .exe file.

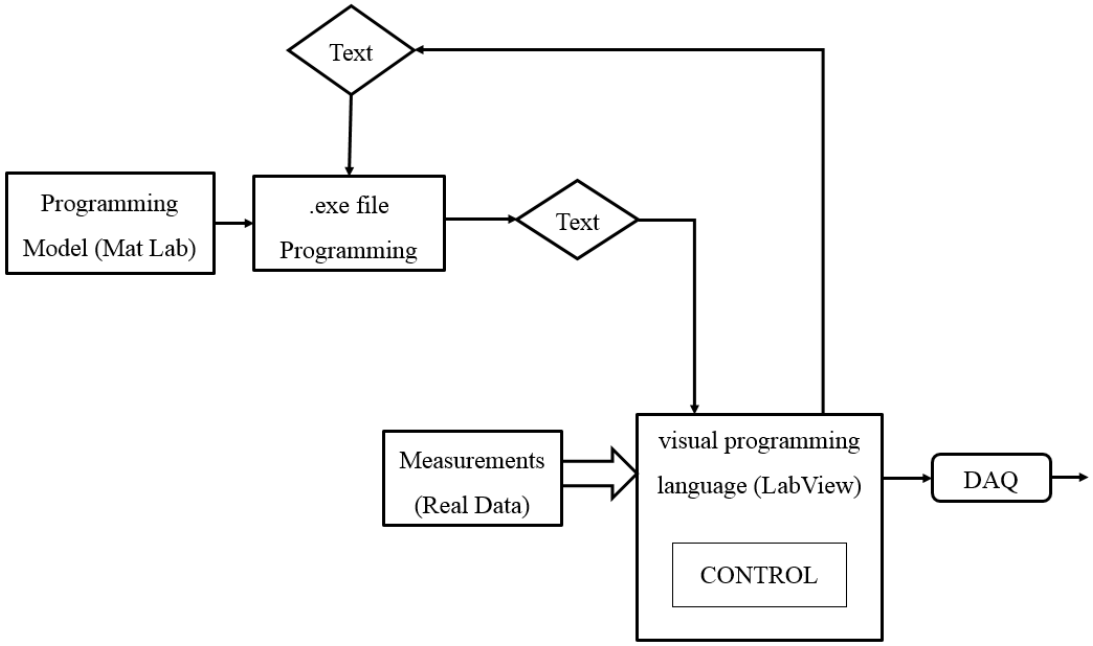

Figure 3.29 Schematic of relationship between LabVIEW and MATLAB

Figure 3.30 and Figure 3.31 show a while loop in block diagrams for predicting friction force and motor current, respectively. This data is read by LabVIEW to create a predicted friction and store it in another .txt file called friction. This file is used to control lubrication in the next step.

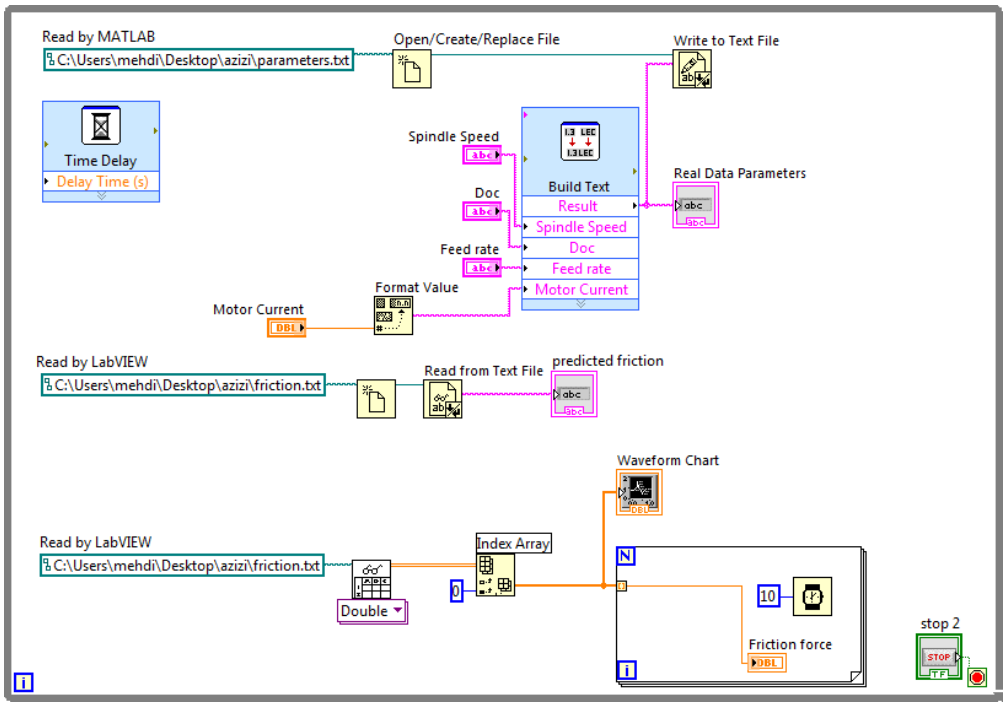

Figure 3.30 While loop with block diagrams to create reading and writing text files

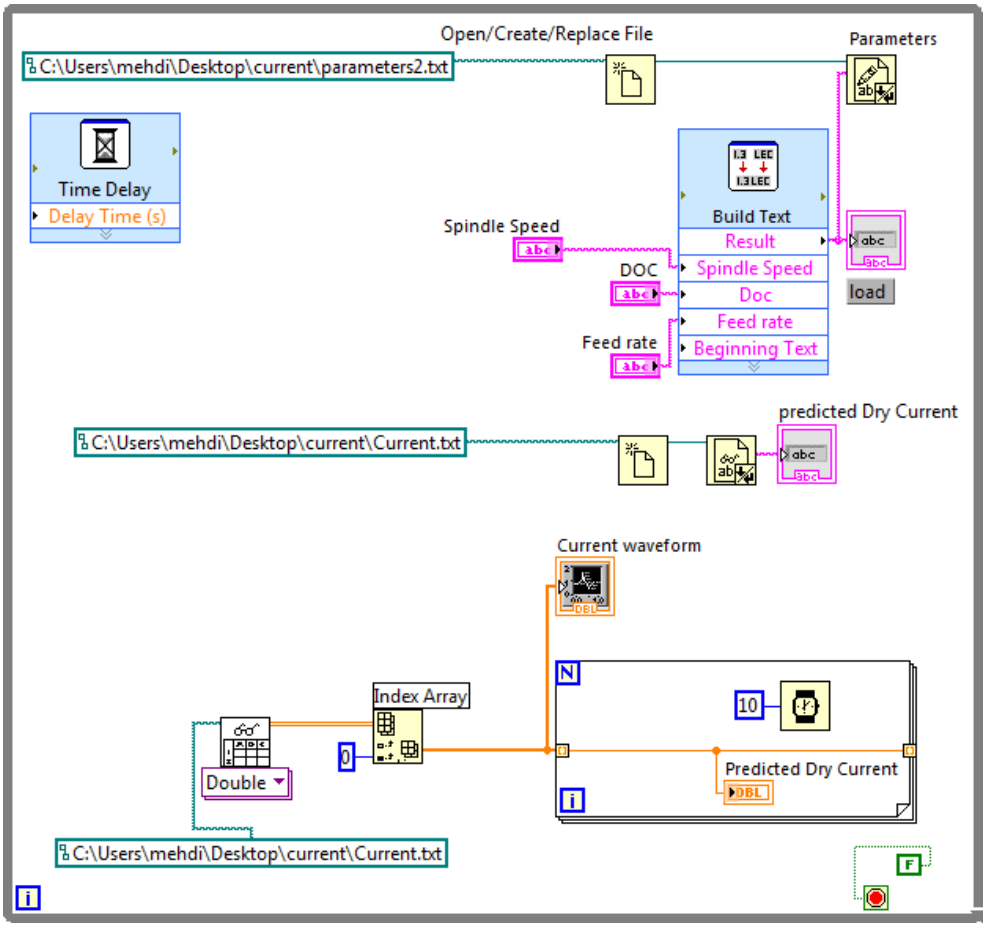

Figure 3.31 While loop with block diagrams to predict the servomotor current

3.3.4.1 Measuring system parameters loop

Figure 3.32 shows the block diagram of measuring system and write to measurement file.

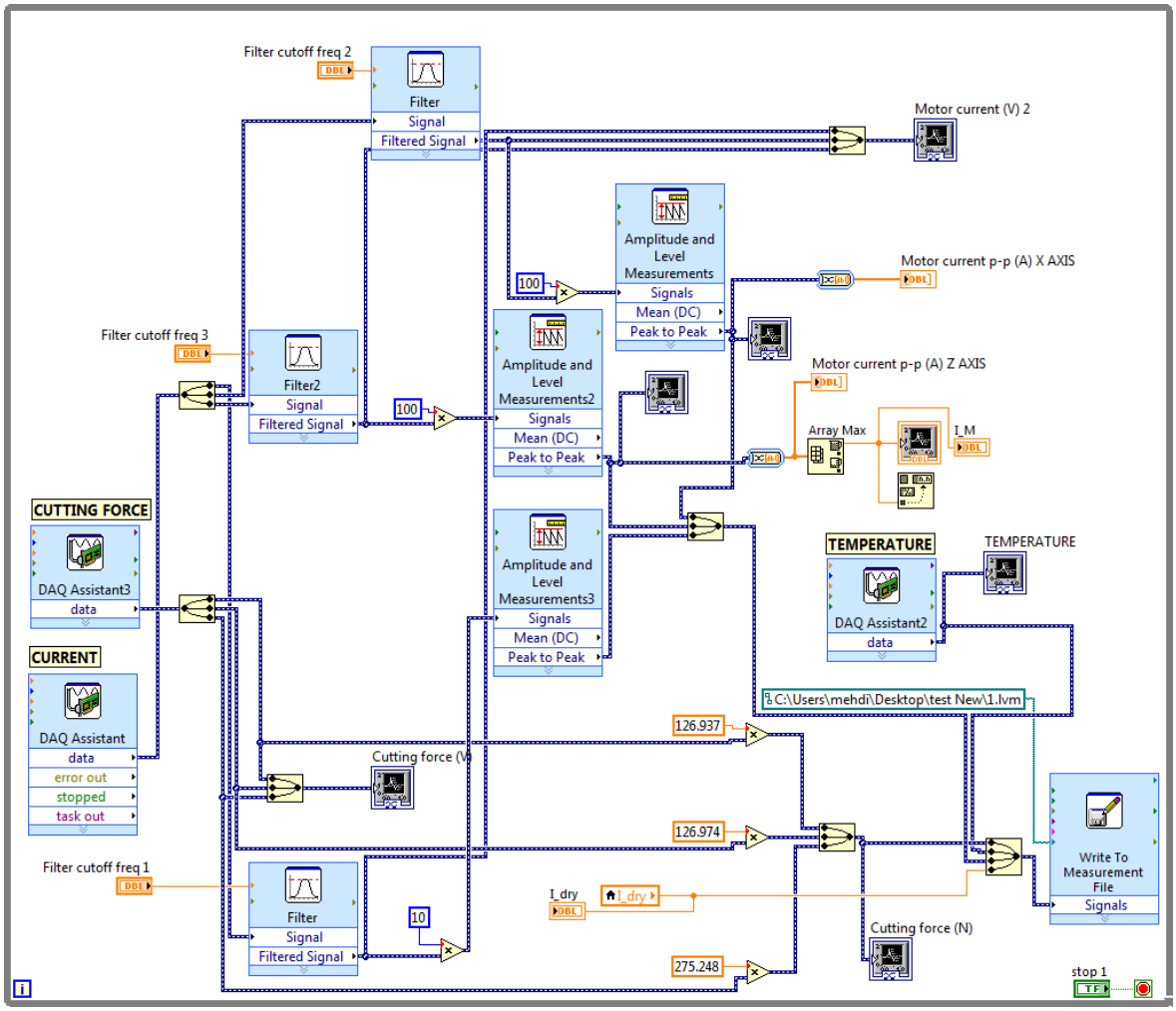

Figure 3.32 block diagram of measuring system and write to measurement file

Each one of the output signals is a Boolean type, so, actually it is not able to trigger actuators. To make the output signal to be transformed into physical form, it should be used of a Build Array ( ).The data signal is sent to DAQ Assistant Express VI. Figure 3.33, shows a simple example of this conversion. For this purpose, it is necessary to configure the DAQ Assistant as a digital output with physical channel port0/lin0.

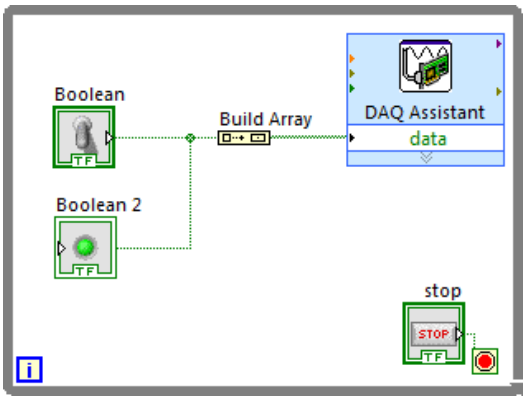

Figure 3.33 Block diagram of data connection to digital output

Regarding to specification and configuration of this A/D Converter unit (NI 9474), the module is supported by TTL (transistor-transistor logic) compatible digital signals. A TTL signal has two states, logic high and logic low (Hi/Low):

Logic Low = 0 V to +0.8 V

Logic High = +2 V to +5 V

When the A / D converter connected to a 12 DCV power supply, the logic high would be 12 V. Common digital generation applications include controlling relays and driving external devices, such as an LED.

3.3.4.2 Text files reading and writing loops

Figure 3.34 and Figure 3.35 are shown the loops in block diagram to create the parameters for read and write the predicted friction force and predicted servomotor current by ANFIS model in dry lubrication conditions.

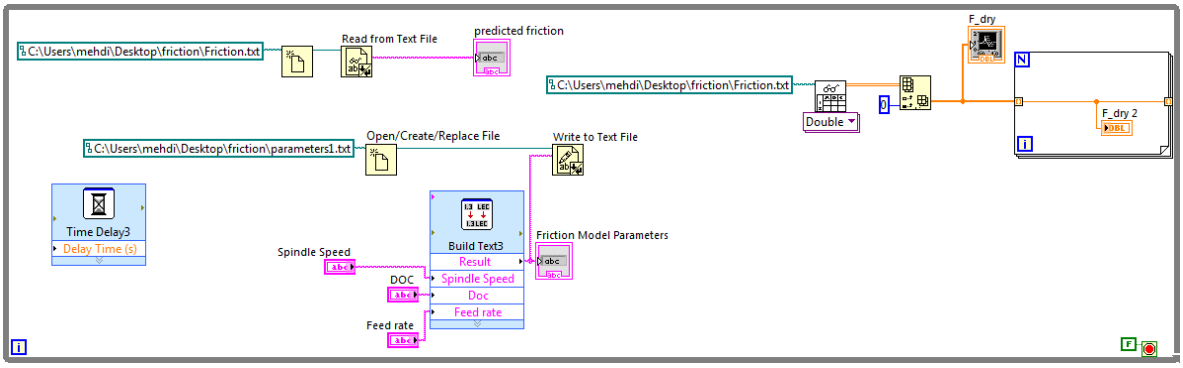

Figure 3.34 Create the parameters to read and write the predicted friction

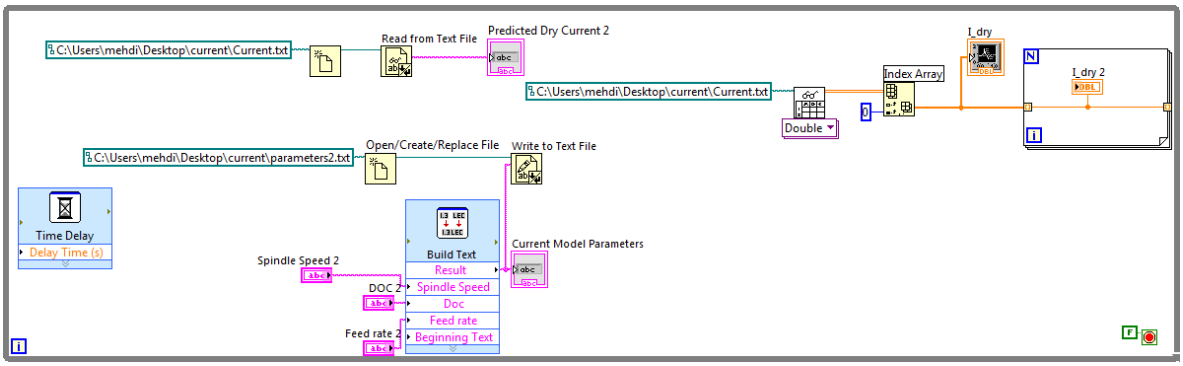

Figure 3.35 Create the parameters to read and write the predicted current

3.4 Summary

In this chapter, after introducing the various system components, the subsystems were identified in two sections. First, the mechanical subsystem was presented including the main components of CNC machines such as servo driver, machine control unit, measurement model structure, machine/lubrication control unit specifications and identifications. Then the lubrication pump setup and settings were explained and one mode for the pressure control system was recommended. In the second section, the electrical components between the major electrical subsystem parts of the electrical circuit system were presented. In this section, two segments of the design process were considered: measurement and control system. In the measurement design process, a differential measurement configuration was

intended to obtain accurate measurements and less noise. The differential connection mode for connecting the thermocouples and cutting force to the modules was explained.

In the programming design process, the effective parameters needed to calculate and predict friction force were investigated in order to apply them to designing a control model. First, design patterns were created in LabVIEW for sequential programming. The design patterns were confirmed to make it easier to recognize when a design pattern has been used. Circuit programming for temperature, cutting force, and servomotor current was designed separately. Subsequently, an overall circuit was created for simultaneous parameter measurement.

This methodology is relating to the objectives, because it is divided to four sections. Each of these can help us, for achieving to a technique for lubrication control system. The sections are including:

Section 1- Estimate the friction forces in linear guideways using cutting force analysis at dry lubrication conditions.

Section 2- Measure the servo motor current in feed drive system in dry lubrication conditions.

Section 3- ANFIS Modeling to predict the servo motor current and the friction force in dry lubrication conditions.

Section 4- Build the lubrication control system based on Friction Conditions in CNC Machine Linear Guideways using Servomotor Current Signals in Feed Drive System.

CHAPTER 4: ESTIMATION OF THE FRICTION FORCES IN LINEAR GUIDEWAYS IN DRY LUBRICATION CONDITION

4.1 Introduction

In this chapter, the friction force in the linear guideways of CNC lathe is estimated using cutting force values. The cutting force components including, longitudinal, radial, and tangential forces are measured during cutting process. These cutting force values are corresponding to different cutting conditions, spindle speed, depth of cut, and feed rate in order to the changing of cutting force values.

The friction force on linear guideways of machine tools is calculated, based on the effective force analysis during cutting. The analysis of the effective forces such as, normal force and cutting force for estimating the friction force is necessary for rigid body modeling statically. Friction force in X, and Z-axes is estimated analytically. The coefficient of friction measurement and the relation between the estimated friction force and cutting force are discussed, accordingly.

4.2 Cutting Force Components

Cutting force is a force that is created by the cutting tool on the work piece during the turning operation. According to Figure 4.1, the main cutting force (F_t) is tangential force and it is related to the force applied in the spindle direction. F_r is the radial force in the X-direction, whereas F_L (Longitudinal force) is the force in the Z-direction performed on the work-piece. These cutting force components are measured using dynamometers, with specifications given in the previous chapter. (Refer to section 3.2.1).

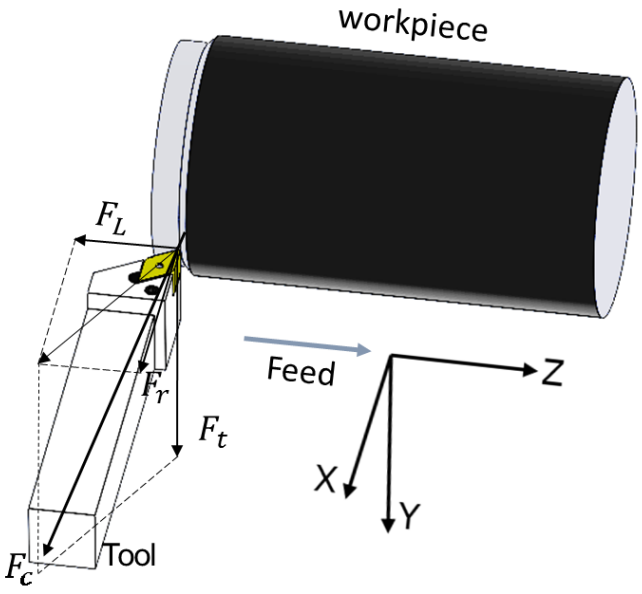

Figure 4.1 Cutting force components and their directions

The cutting force components (F_L, Fr, and Ft) in turning are measured for different cutting conditions. Figure 4.2 shows the sample of measured cutting force including longitudinal, radial, and tangential forces at 1000 (rpm) spindle speed, 1.5 (mm) depth of cut, and 0.5 (mm/rev) feed rate conditions in one cycle of cutting (refer to Figure 3.28). The values of cutting force based on cutting conditions that were measured, are shown in Table 4.1, Table 4.2, and Table 4.3 with different depth of cut, respectively.

According to Table 4.1 to

Table 4.3, variation in cutting conditions have a direct impact on cutting forces. Meanwhile, the contribution of feed rate and depth of cut is significant. Although, increasing the spindle speed is accompanied with reduced cutting forces because the higher spindle speed reduces the friction force between tool and workpiece.

Estimation of resultant cutting forces (F_C) is obtained using below equation:

$$F_C(N) = \sqrt{F_t^2 + F_r^2 + F_L^2} \tag{4.1}$$

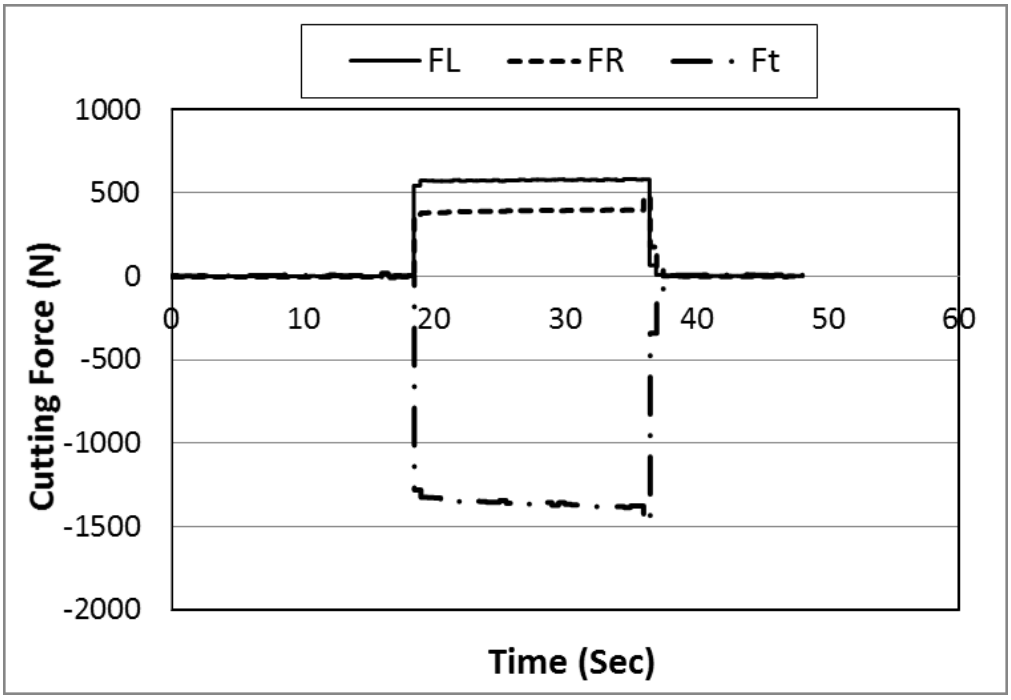

Figure 4.2 A sample of measured cutting force in one cycle of cutting

Table 4.1 Measured values of cutting force at depth of cut = 0.5 mm

NO.	Cutting Conditions		Cutting Forces (N)			F_C
	speed (S) rpm	Feed Rate (f) mm/rev	Longitudinal (F_L)	Radial (Fr)	Tangential (Ft)	
E1	250	0.1	42.33	33.11	61.87	81.95
E2		0.25	145.24	50.83	243.82	288.32
E3		0.4	244.125	80.235	360.22	442.49
E4		0.5	319.4	98.235	461.58	569.84
E5	500	0.1	92.845	50.499	103.371	147.84
E6		0.25	156.415	55.086	222.583	277.57
E7		0.4	231.532	62.175	311.651	393.19
E8		0.5	265.157	72.96	362.832	455.28
E9	750	0.1	109.542	75.34	102.95	168.15
E10		0.25	176.254	78.34	219.5	292.20
E11		0.4	222.534	89.95	297.43	382.20
E12		0.5	264.123	97.53	360	457.03
E13	1000	0.1	125.481	85.923	95.312	179.48
E14		0.25	180.535	89.932	202.3	285.67
E15		0.4	225.425	92.321	293.1	381.11
E16		0.5	239.338	103.981	358.02	443.03

Table 4.2 Measured values of cutting force at depth of cut = 1 mm

NO.	Cutting Conditions		Cutting Forces (N)			F_C
	speed (S) rpm	Feed Rate (f) mm/rev	Longitudinal (F_L)	Radial (Fr)	Tangential (Ft)	
E17	250	0.1	209.307	168.93	327.36	423.69
E18		0.25	303.463	160.05	497.78	604.56
E19		0.4	485.342	272.32	767.25	947.83
E20		0.5	585.608	338.97	899.072	1125.24
E21	500	0.1	155.051	123.84	237.83	309.74
E22		0.25	298.03	129.49	425.87	535.68
E23		0.4	420.123	192.98	615.32	769.65
E24		0.5	521.166	246.23	780.1	969.95
E25	750	0.1	191.254	135.67	232.45	330.18
E26		0.25	283.125	134.34	379.21	491.94
E27		0.4	405.862	178.21	527.24	688.81
E28		0.5	482.376	195.43	658.25	839.15
E29	1000	0.1	204.318	149.054	225.65	338.94
E30		0.25	265.765	138.46	345.26	457.17
E31		0.4	396.125	165.12	498.34	657.66
E32		0.5	446.013	178.09	592.32	762.55

Table 4.3 Measured values of cutting force at depth of cut =1.5 mm

NO.	Cutting Conditions		Cutting Forces (N)			F_C
	speed (S) rpm	Feed Rate (f) mm/rev	Longitudinal (F_L)	Radial (Fr)	Tangential (Ft)	
E33	250	0.1	111.435	88.783	224.224	265.66
E34		0.25	495.951	362.97	715.11	942.92
E35		0.4	769.235	560.52	1075.2	1435.95
E36		0.5	956.1	773	1316.1	1801.05
E37	500	0.1	173.67	196.29	289.36	390.41
E38		0.25	455.937	387.32	679.71	905.48
E39		0.4	675.341	597.54	989.2	1338.53
E40		0.5	873.492	645.2	1210.7	1626.37
E41	750	0.1	110.243	225.35	275.23	372.41
E42		0.25	424.231	403.12	628.11	858.49
E43		0.4	587.123	611.21	880.2	1221.90
E44		0.5	799.185	523.23	1085.3	1445.80
E45	1000	0.1	105.1	277.68	221.54	370.45
E46		0.25	381.8	435.05	576.75	817.12
E47		0.4	499.21	635.54	765.2	1112.95
E48		0.5	695.506	494.022	962.17	1285.91

Figure 4.3(a,b) indicate the variations in cutting force with respect to the depth of cut and spindle speed to know how the cutting conditions are affected to the cutting force. It can be seen from Figure 4.3a, that increasing feed rates increase the cutting force. For example, the cutting force when the feed rate is 0.5 (mm/rev), rises to 1801 N for S=250 rpm, to 1626 N for S=500 rpm, to 1446 N for S=750 rpm, and finally to 1286 N for S=1000 rpm, respectively, while the depth of cut is equal to 1.5 mm. In addition, the force increases with increasing depths of cut. This is clearly shown in Figure 4.3 b, the spindle speed is affected on the cutting forces negatively.

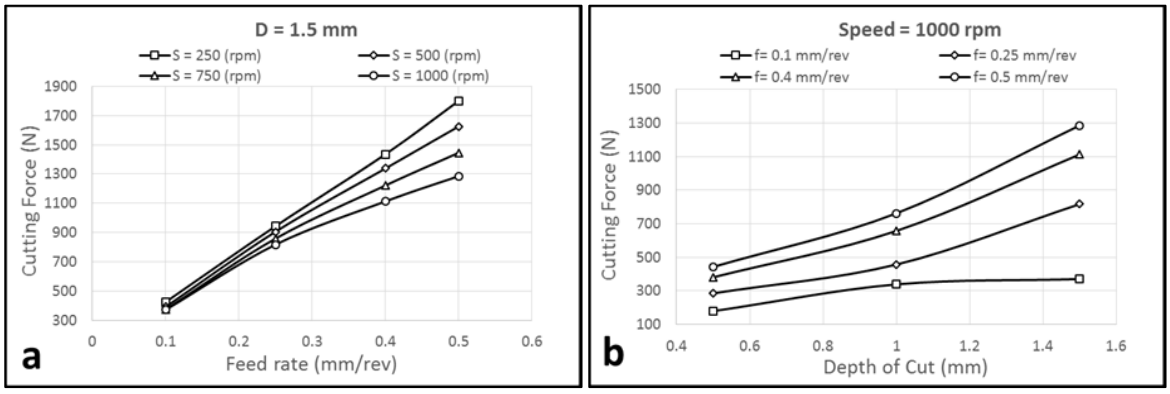

Figure 4.3 Variation in cutting force with respect to a) Feed rate at different speed and depth of cut 1.5 mm b) Depth of cut at different feed rate and speed 1000 rpm.

The measured cutting force for different feed rates and depth of cut behaves likewise for all cutting conditions. In other words, the effect of cutting speed on the cutting force is in the lower values compared to the feed rates and depths of cut. This could be explain in relation to the federate/tooth value which is shown in Eq. 4.2. The cutting force is increasing with the increase of the feed rate/tooth value. However, from Eq. 4.2 it can be seen that the feed rate/tooth values are also function of the (F) Feed rate (mm/min), the spindle seed (N) (r.p.m) and the number of tooth (Z) which is equal to one in turning operation. Hence

whenever the cutting speed is increased the feed/tooth is decreased and the cutting force is also decrease (Yau & Kuo, 2001).

$$R(\frac{mm}{tooth})=\frac{F}{Z\times N} \tag{4.2}$$

Which; *R*, is feed per tooth or depth of cut per tooth (mm/tooth), and *Z*, is number of teeth that in turning it is only one. *N*, is the spindle speed (rpm). *F,* is feed speed (mm/min).

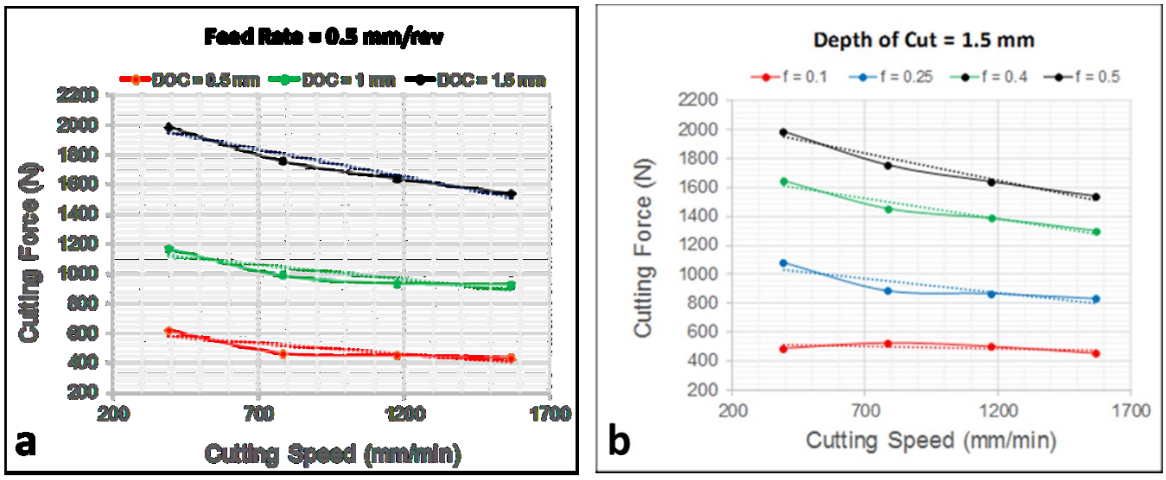

Figure 4.4 Changes in cutting force with respect to cutting speed a) at different depth of cut and feed rate 0.5 mm/rev b) at different feed rate and depth of cut 1.5 mm.

Change in cutting force with respect to cutting speed is illustrated in Figure 4.4. The figure shows that there is minor effect of cutting speed on the cutting force. An increase in the cutting speed generally leads to a reduction in the cutting forces.

4.3 Estimation of Friction Force in Guideways Using Measured Cutting Force

Friction between contact points in linear guideways and carriages is problematic for achieving machining precision and accuracy. Friction forces on machine tool linear guideways are mainly influenced by cutting force values where the cost of machining maintenance and amount of machining accuracy are the most important factors to necessary of the friction force estimation.

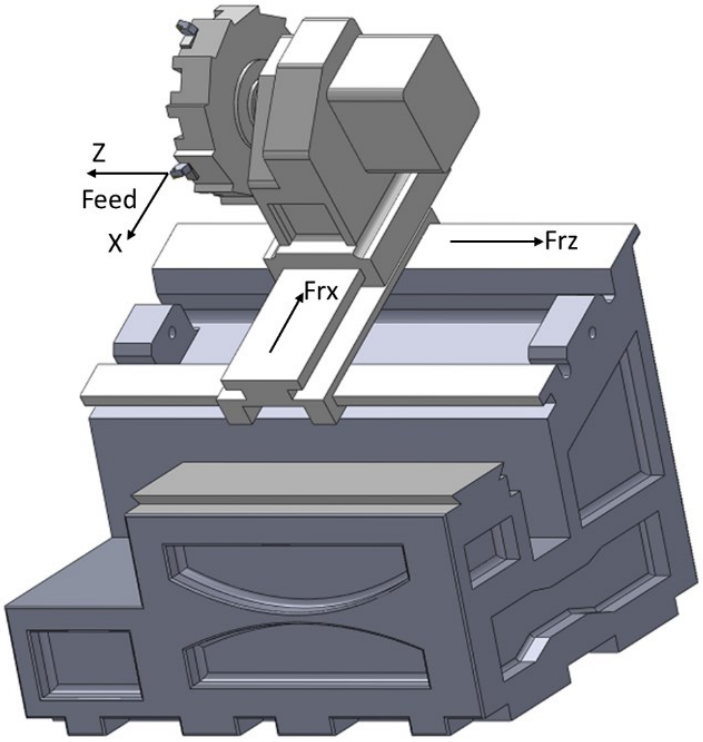

Figure 4.5 Friction force in linear guideways

Friction forces on the machine tool guideways, are calculated by the analysis of two set of forces, which are cutting force and normal force (Figure 4.5). The cutting forces components have some effects on a tip of cutting tool. The cutting force was divided to three vectors, F_t (tangential force), F_L (Longitudinal force), and F_r (Radial force) as shown in Figure 4.6.

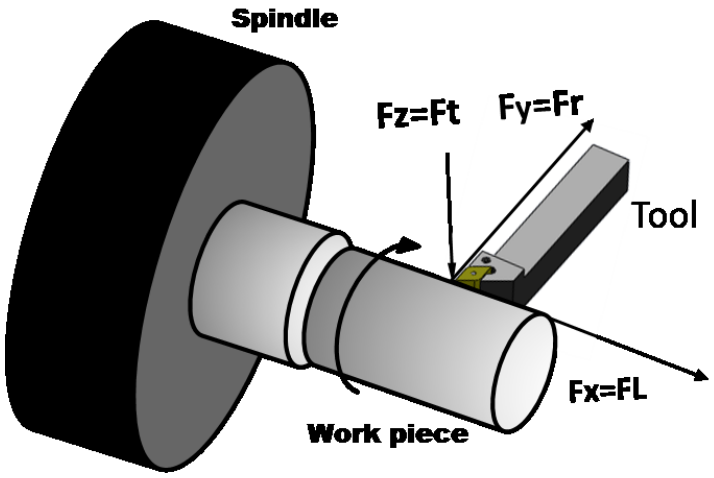

Figure 4.6 Cutting forces on workpiece during turning

As mentioned in Chapter 3, the moving table has a 25˚ degree slope, relative to horizontal line in side view of CNC machine (refer to Figure 3.3). The cutting force angle matching the inclined angle. However, the normal force is required to divide under α˚ angle as shown in Figure 4.7. Normal force is obtained from weight of moving table with belongings, such as, turret, tool changer, cutting tools, and so on, will be analyzed (projected) to F1 and F2 under α degree.

$$F_1 = W.\cos\alpha \tag{4.3}$$

$$F_2 = W.\sin\alpha \tag{4.4}$$

Where here; F_1, F_2 are, the components of the weight, and W, is weight of moving table.

It is necessary to transfer the moment of the forces due to cutting forces and normal force, to the machine's center of gravity in order to calculate the forces acting on the linear guideways.

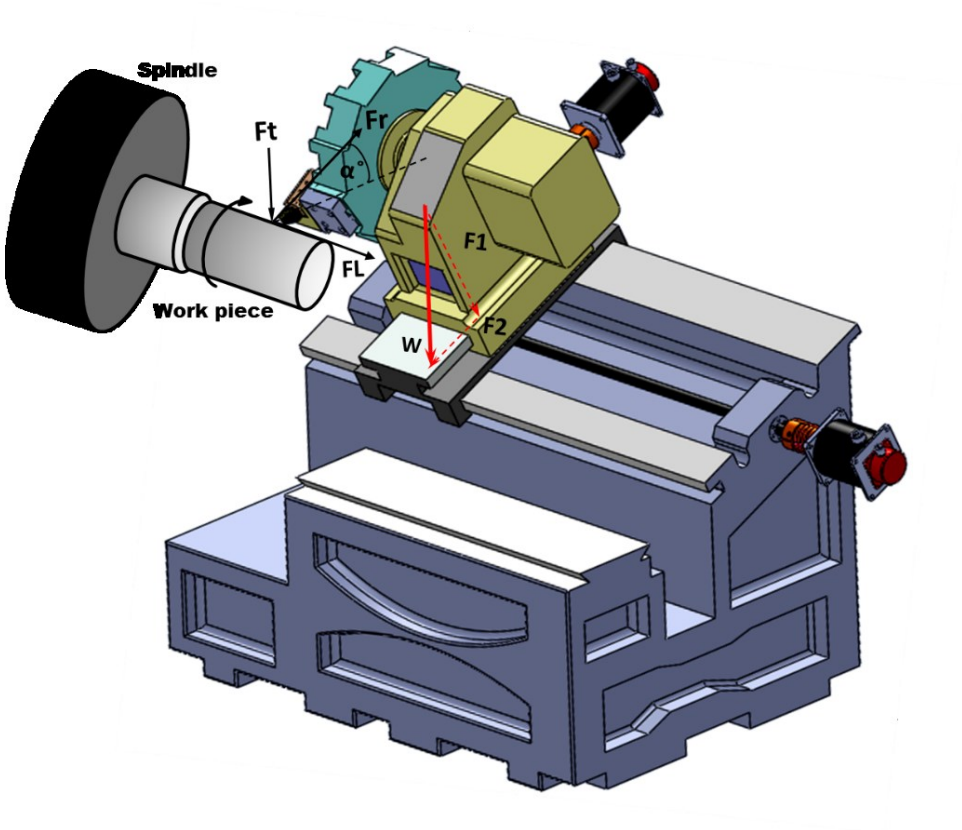

Figure 4.7 Directions of force application and analysis them

4.3.1 Analysis of Effective Forces

Cutting force and normal force as effective forces were explained above and they are affected the linear guideways in both X, and Z- axes simultaneously. Analyzing them is required to estimate the friction force.

Another effective force is the weight of moving table (W_1 and W_2), that is composed of two main parts. Figure 4.8 shows the Turret body and belongings including housing body, tool changer, cutting tool and installed dynamometer on the tool changer part B, which the weight of part B is called, W_1. The W_1, is used to estimate the friction force in X-axis. The other part is X- axis carriage, which is slides on Z- axis linear guideways. Whereas the turret can be reciprocating motion in the X-axis direction part C. The assembly of part B, and part C, is represented as part A. the weight of part A is called W_2, that is used in calculation of friction force in Z-axis.

It should be mentioned, the weight of moving parts has been calculated via density of the material in solid work software with respect to the real dimensions, which has been adapted from user manual of CNC lathe machine.

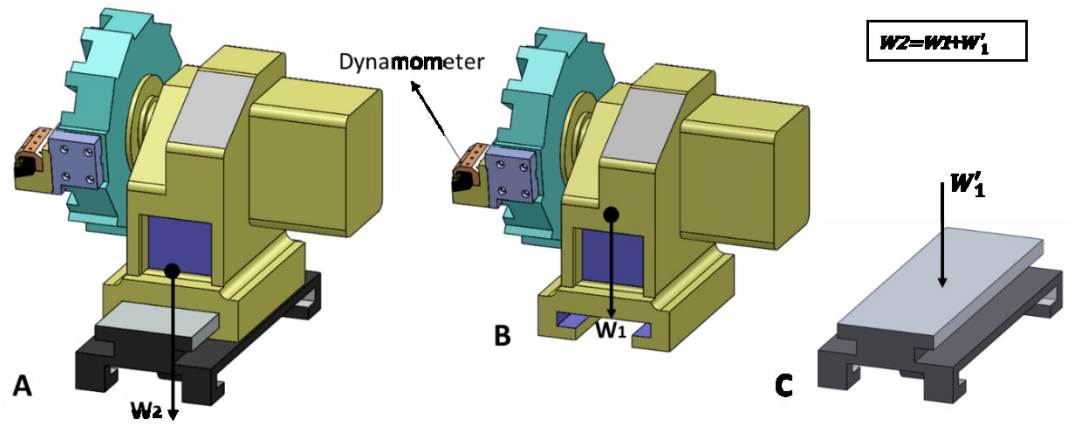

Figure 4.8 Main parts of moving table

Figure 4.9 Shows force vectors on X, and Z- axes moving tables, with accurate dimensions of design. For a precise positioning of forces, first calculate the center of gravity

of moving table with belongings, which is acquired via mathematical methods using solid work software. Afterwards, that point to be considered as a load point in the normal force. Secondly, it should be measured longitudinal and lateral distance of this point until the exact location of the cutting forces at the tip of cutting tool, and distance from the machine bed according to real dimensions of the CNC machine. The $\bar{X}, \bar{Y}$ values are shown in Figure 4.9. These values are distances from center of gravity (G).

$$\bar{X} = \frac{\sum_{i=1}^{n} m_i \bar{x}_i}{m} \tag{4.5}$$

$$\bar{Y} = \frac{\sum_{i=1}^{n} m_i \bar{y}_i}{m} \tag{4.6}$$

Where here; m is the total mass of system.

Figure 4.9, and Figure 4.10 , illustrates the center of gravity, dimensions of "Turret belongings" as mention to Figure 4.8.

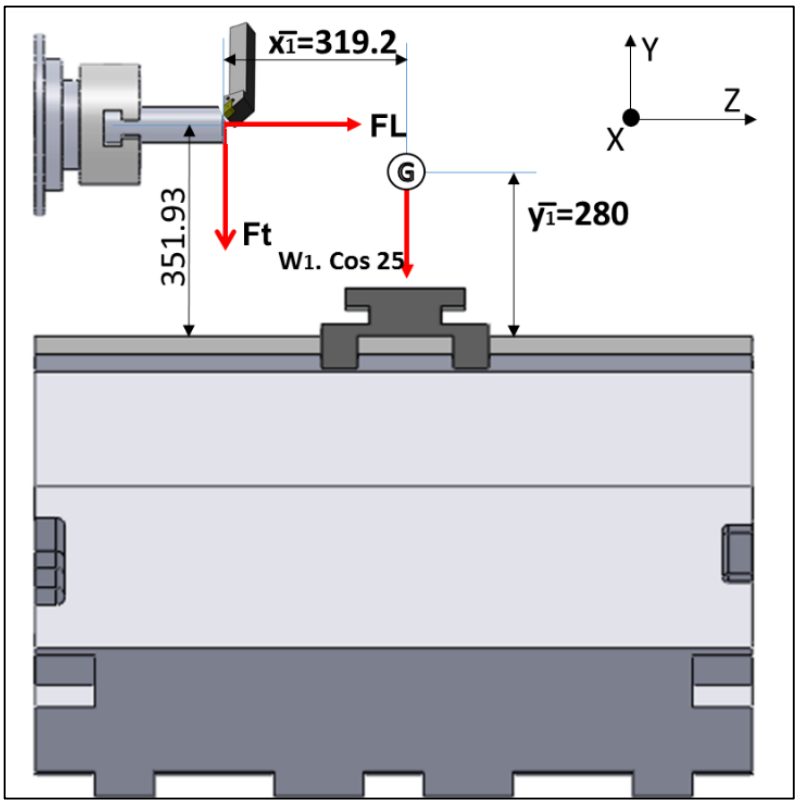

Figure 4.9 Center of gravity distance from linear guideways in X- axis

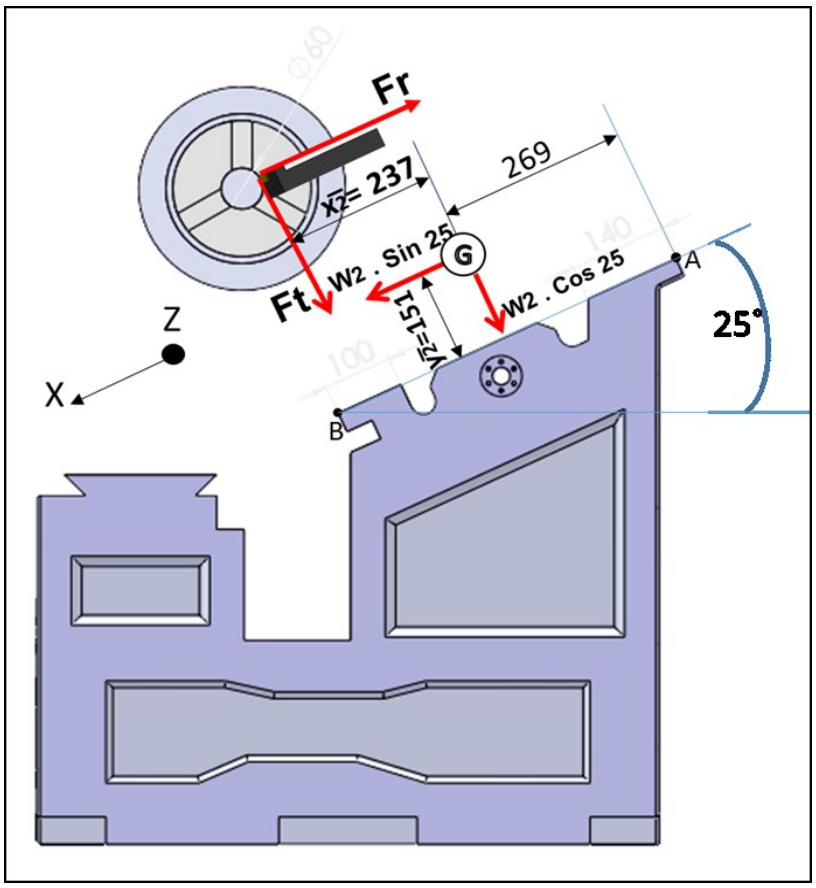

Figure 4.10 Center of gravity distance from linear guideways in Z- axis

4.3.2 Friction Force Estimation in X- axis

The load points of cutting force and the weight force on X-axis are necessary to calculate normal force at contact surfaces. Figure 4.11 a-c, shows the forces and their distance from the certain points relative to coordinate axes.

According to Figure 4.11 to Figure 4.13, as a rigid body model, the system of forces can be projected to each point on a body with the corresponding moment.

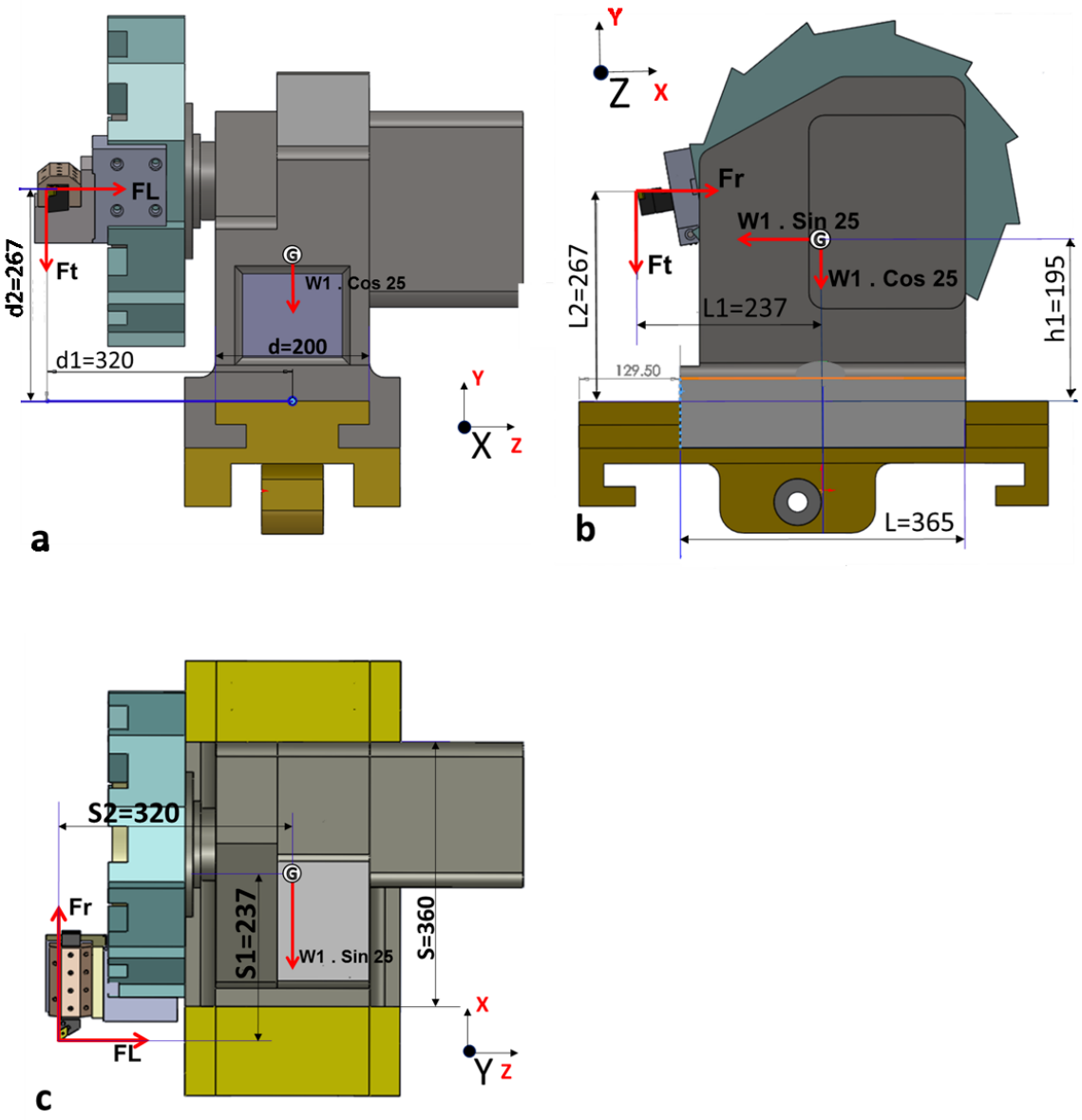

Figure 4.11 Forces and their distances from certain load points on X- axis coordinate

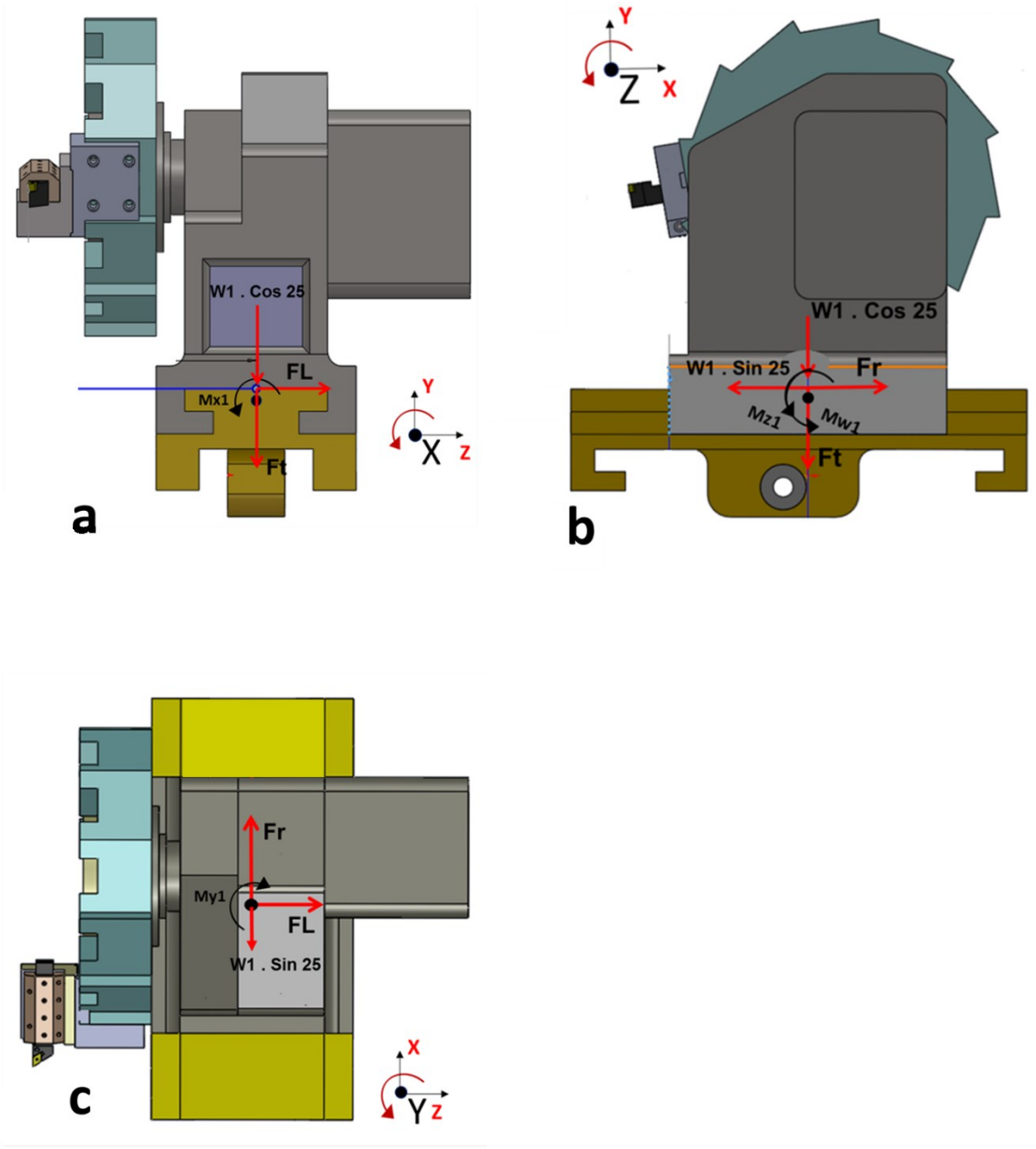

Figure 4.12 Torques and forces affected on X-axis linear guideways

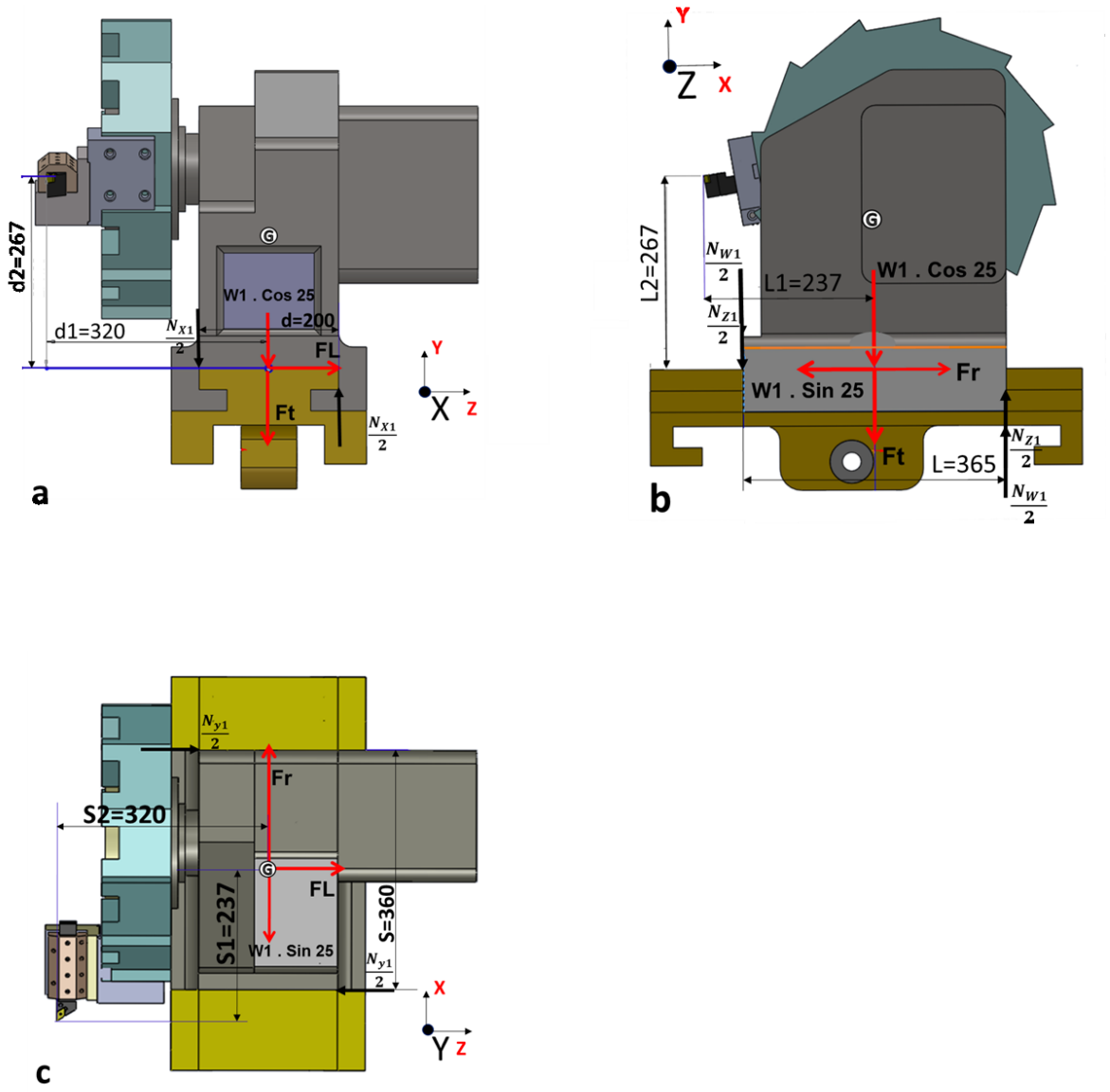

Figure 4.13 Reaction force vector based on torque analysis on X-axis linear guideways

Torque, moment or moment of force, is a force to rotate an object around an axis. Just as a force is a push or a pull, a torque can be thought of as a twist to an object. Mathematically, torque is defined as the cross product of the distance vector and the force vector, which tends to produce rotation.

The force vector of cutting force components and weight force creates a torque or couple around the center of gravity. This torque causes reaction forces on the contact surfaces, which is illustrated in Figure 4.13. The reaction forces increase the friction forces

as depicted in Figure 4.14. The exerted torques and forces can be calculated form the following equations for any component in X, Y and Z directions:

From fig. 4.11 to 4.13 (a), $M_{X1} = \mathrm{F_t}.\mathrm{d_1} - \mathrm{F_L}.\mathrm{d_2}$

$$N_{X1} = \frac{M_{X1}}{d} = \frac{320F_t - 267F_L}{200} = 1.6F_t - 1.34F_L$$

From fig. 4.11 to 4.13 (b), $M_{Z1} = F_t.L_1 - F_r.L_2$

$$N_{Z1} = \frac{M_{Z1}}{L} = \frac{237F_t - 267F_r}{365} = 0.65F_t - 0.73F_r$$

From fig. 4.11 to 4.13 (b), $M_{W1} = W_1.\sin 25\,.h_1$

$$N_{W1} = \frac{M_{W1}}{L} = \frac{82.4W_1}{365} = 0.23W_1$$

From fig. 4.11 to 4.13 (c), $M_{y1} = \mathrm{F_L}.\mathrm{S_1} - \mathrm{F_r}.\mathrm{S_2}$

$$N_{y1} = \frac{M_{y1}}{S} = \frac{237F_L - 320F_r}{360} = 0.66F_L - 0.89F_r$$

Because of the forces affecting on the objects in the stationary state. Then:

STATIC State $\begin{Bmatrix} \sum F_X = 0 \\ \sum F_Y = 0 \\ \sum M_O = 0 \end{Bmatrix}$

The free body diagram shown in Figure 4.14.

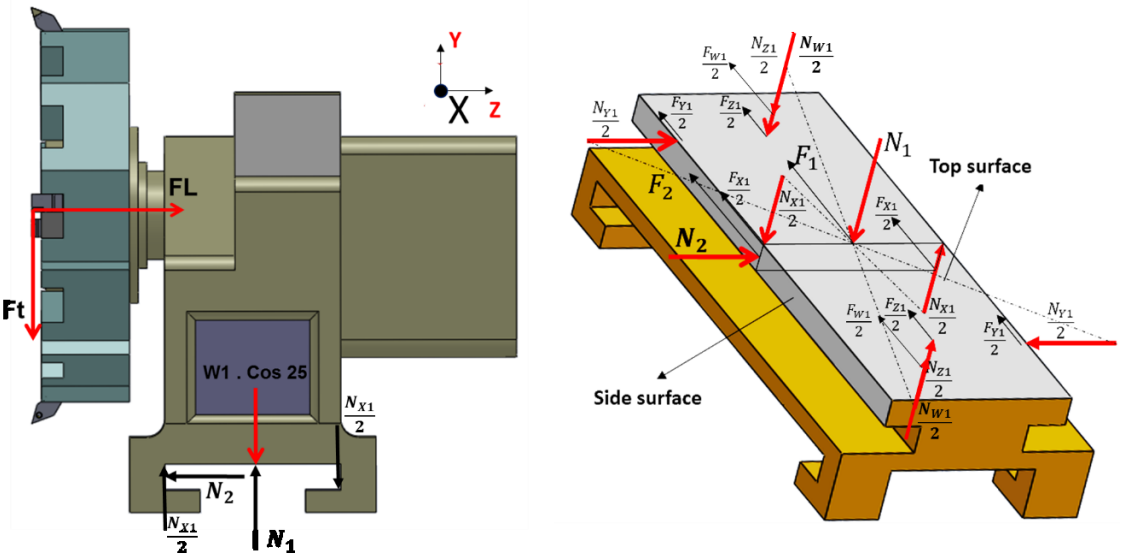

Figure 4.14 Free body diagram for X-axis linear guideways

The total friction force in X-axis is as following:

$$F_X = F_1 + F_2 + 2(\frac{F_{X1}}{2} + \frac{F_{Y1}}{2} + \frac{F_{Z1}}{2} + \frac{F_{W1}}{2}) \quad (4.7)$$

$F_1 = \mu.N_1 = \mu.(W_1.cos\,25 + F_t)$

$F_2 = \mu.N_2 = \mu(F_L)$

$F_{X1} = \mu.N_{X1} = \mu.(1.6F_t - 1.34F_L)$

$F_{Y1} = \mu.N_{Y1} = \mu.(\,0.66F_L - 0.89F_r)$

$F_{Z1} = \mu.N_{Z1} = \mu.(0.65F_t - 0.73F_r)$

$F_{W1} = \mu.N_{W1} = \mu.(\,0.23W_1)$

$F_X = \mu[0.906W_1 + F_t + F_L + (1.6F_t - 1.34F_L) + (0.66F_L - 0.89F_r) + (0.65F_t - 0.73F_r) + 0.23W_1]$

$F_X = \mu(1.14W_1 + 3.25F_t + 0.32F_L - 1.62F_r)$

Where; $W_1 is\ the\ weight\ of\ part\ B$(refer to Figure 4.8).

The static and kinetic coefficient friction ($\mu_S\ and\ \mu_K$) are considered to identify the friction force in X- axis in both of stationary and moving table on the guideways.

$$F_{SX} = \mu_S.(1.14W_1 + 3.25F_t + 0.32F_L - 1.62F_r) \quad (4.8)$$

$$F_{KX} = \mu_K.(1.14W_1 + 3.25F_t + 0.32F_L - 1.62F_r) \quad (4.9)$$

Where, F_{SX} is a total static friction force and F_{KX} is total kinetic friction forces in X-axis linear guideways.

4.3.3 Friction Force Estimation in Z- axis

The cutting force and normal force result in the friction force on Z direction during cutting operations are shown in Figure 4.15.

Figure 4.16 shows the force and torque affected on Z-axis direction.

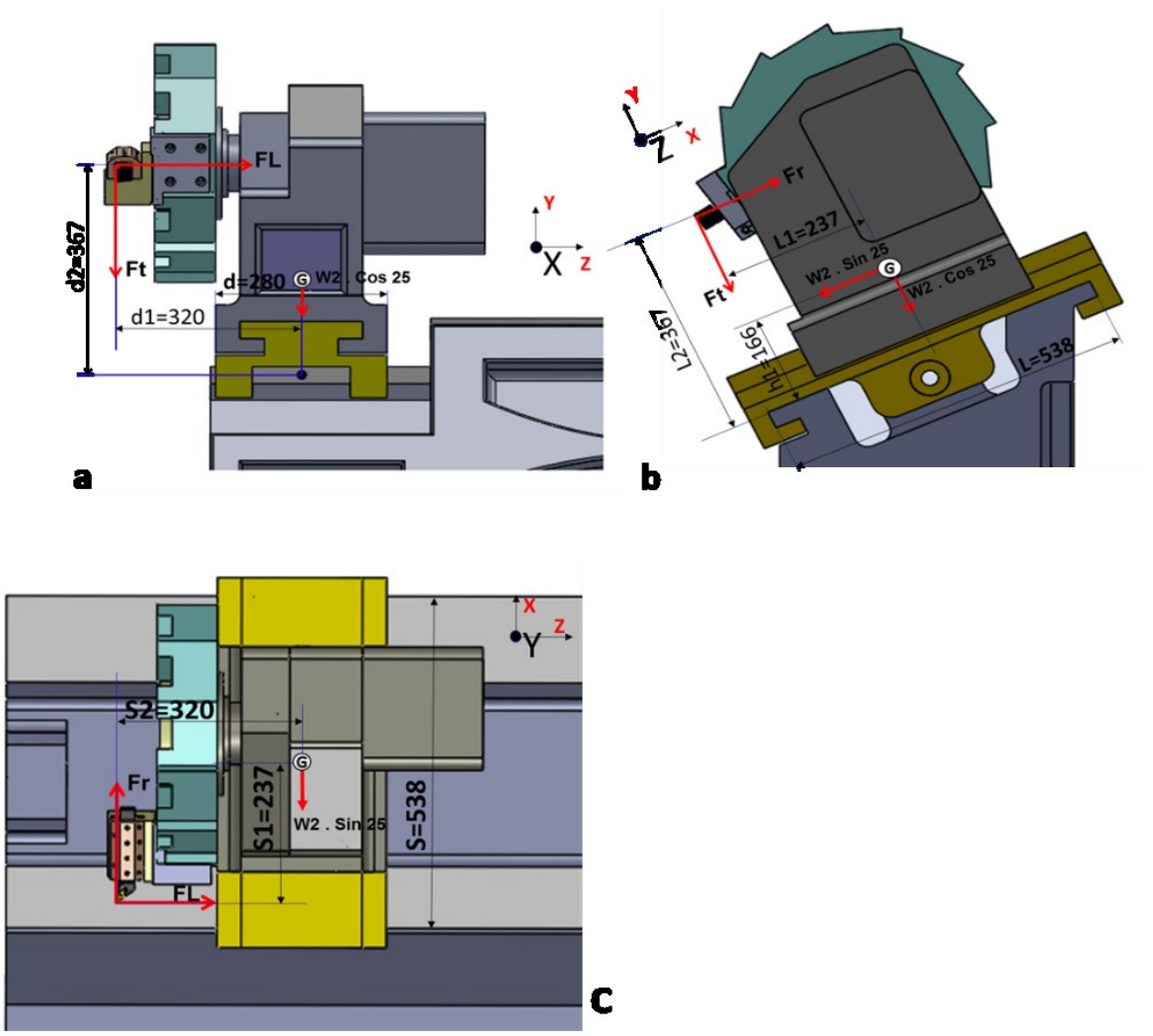

Figure 4.15 Forces and distances from load points on Z- axis coordinate

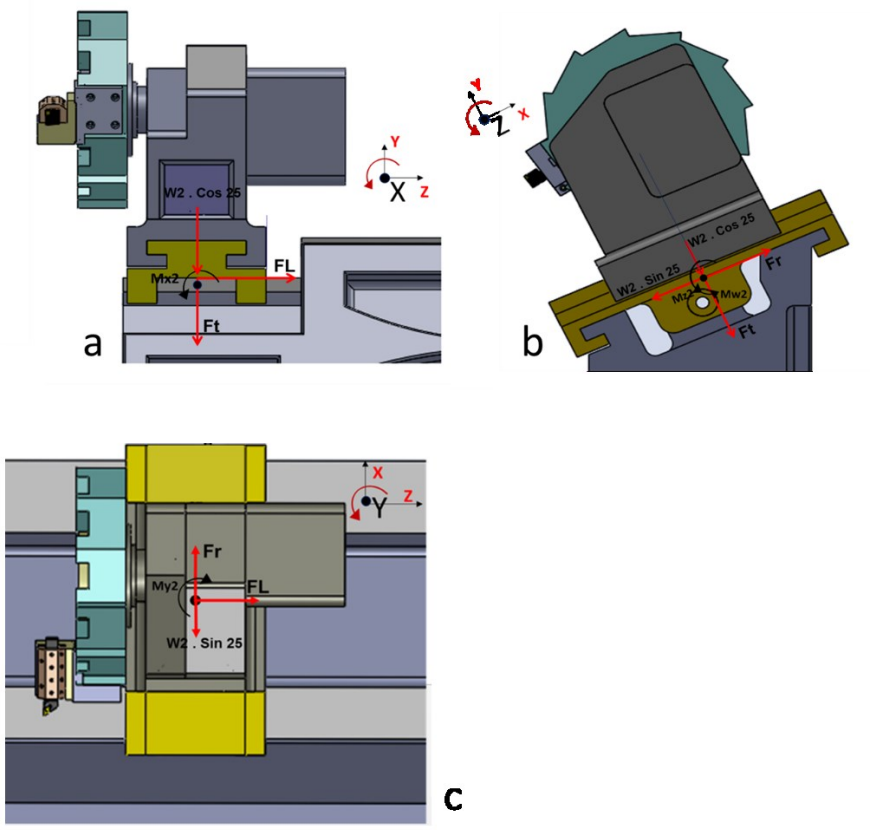

Figure 4.16 Torques and forces affected on Z-axis linear guideways

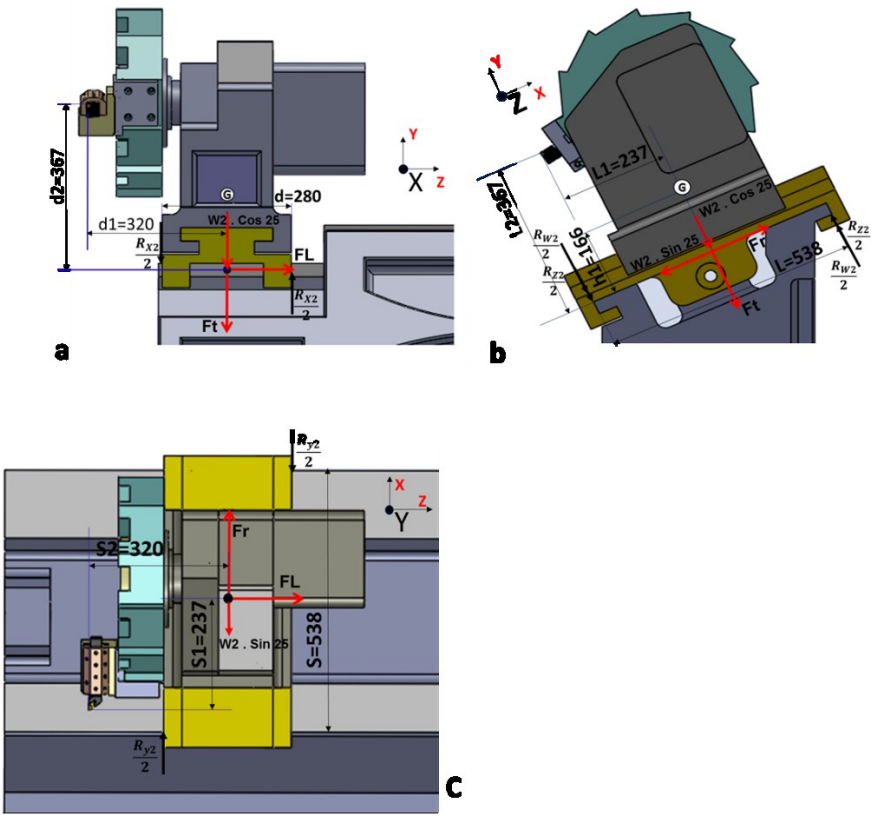

Figure 4.17 Reaction force vector based on torque analysis on Z-axis linear guideways

From Figure 4.15 to Figure 4.17 (a), $M_{X2} = \mathrm{F_t}.\mathrm{d_1} - \mathrm{F_L}.\mathrm{d_2}$

$$R_{X2} = \frac{M_{X2}}{d} = \frac{320F_t - 367F_L}{280} = 1.14F_t - 1.31F_L$$

From Figure 4.15 to Figure 4.17 (b), $M_{Z2} = F_t.L_1 - F_r.L_2$

$$R_{Z2} = \frac{M_{Z2}}{L} = \frac{237F_t - 367F_r}{538} = 0.44F_t - 0.68F_r$$

From Figure 4.15 to Figure 4.17 (b), $M_{W2} = W_2.\sin 25\,.h_1$

$$R_{W2} = \frac{M_{W2}}{L} = \frac{70.15W_2}{538} = 0.13W_2$$

From Figure 4.15 to Figure 4.17 (c), $M_{Y2} = \mathrm{F_L}.\mathrm{S_1} - \mathrm{F_r}.\mathrm{S_2}$

$$R_{y2} = \frac{M_{y2}}{S} = \frac{237F_L - 320F_r}{538} = 0.44F_L - 0.59F_r$$

Free body diagram for Z-axis linear guide after analysis the forces is shown in Figure 4.18.

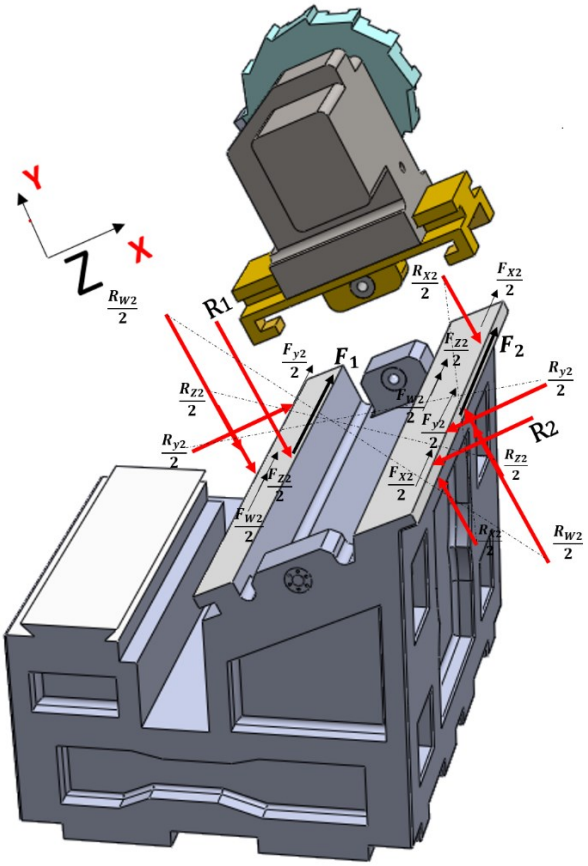

Figure 4.18 Free body diagram for Z-axis linear guideways

$$F_Z = F_1 + F_2 + 2\left(\frac{F_{X2}}{2} + \frac{F_{Y2}}{2} + \frac{F_{Z2}}{2} + \frac{F_{W2}}{2}\right)$$

$$F_1 = \mu.(W_2.\cos 25 + F_t)$$

$$F_2 = \mu.(W_2.\sin 25 - F_r)$$

$$F_{X2} = \mu.R_{X2} = \mu.(1.14F_t - 1.31F_L)$$

$$F_{Y2} = \mu.R_{y2} = \mu.(0.44F_L - 0.59F_r)$$

$$F_{Z2} = \mu.R_{Z2} = \mu.(0.44F_t - 0.68F_r)$$

$$F_{W2} = \mu.R_{W2} = \mu.(0.13W_2)$$

$$F_Z = \mu[0.906W_2 + 0.422W_2 + F_t - F_r + (1.14F_t - 1.31F_L) + (0.44F_L - 0.59F_r) + (0.44F_t - 0.68F_r + 013W_2)]$$

$$F_Z = \mu.(1.46W_2 + 2.58F_t - 2.27F_L - 0.87F_r)$$

Where; $W_2 is\ the\ weight\ of\ part\ A$(refer to Figure 4.8).

The static and kinetic coefficient friction ($\mu_S\ and\ \mu_K$) will be used to identify the friction force in Z- axis.

$$F_{SZ} = \mu_S.(1.46W_2 + 2.58F_t - 2.27F_L - 0.87F_r) \quad (4.10)$$

$$F_{KZ} = \mu_K.(1.46W_2 + 2.58F_t - 2.27F_L - 0.87F_r) \quad (4.11)$$

Where, F_{SZ} is a static friction force on Z-axis, and F_{KZ} is kinetic friction forces on Z-axis linear guideways.

Generally material of linear guideways that has been used in moving table of CNC machines are from hardened Steel. The mass density of them is $\rho = 7.85\ \left(\frac{gr}{cm^3}\right)$, and the static coefficient of mixed (Dry and Greasy) mode of sliding friction between contact points of moving table for static and mixed kinetic will be identified according to measurements. The most commonly used classification for guideways is manufactured from AISI A4 tool steel.

4.3.4 Coefficient of Friction Measurement in Dry Lubrication Condition

Though in order to find the coefficients of friction can refer to engineer's handbooks, and apply the values of coefficients of friction materials but for more, accurate we decided to obtain the coefficient of friction experimentally in both static and kinetic mods. In friction coefficient measurement in CNC linear guideways, the mixed friction zone (II) is considered (Refer to Stribeck diagram in Figure 2.7). The coefficient of frictions test method is "flat block sliding down an inclined runway" (IS).

Figure 4.19, shows a piece of test block with specifications given in Table 4.4 is used for measuring coefficient of friction.

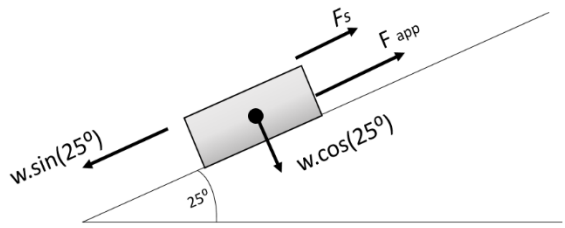

Static:

$$F_S = w.\sin 25 - F_{app1}$$

$$F_S = \mu_S.w.\cos 25$$

Kinetic:

$$F_K = w.\sin 25 - F_{app2}$$

$$F_K = \mu_K.w.\cos 25$$

$$\left.\begin{matrix}\mu_S = 0.095\\ \mu_K = 0.075\end{matrix}\right\}$$

Figure 4.19 Test method used to obtain the coefficient of friction

The coefficient of static friction in dry lubrication condition that achieved was equal to 0.095 ($\mu_S = 0.095$). While this value for kinetic friction was 0.075 ($\mu_K = 0.075$).

Where: $F_{app1,}\ and\ F_{app2}$, are static and kinetic applied force for measuring, respectively.

Table 4.4 Specification of test method for coefficient of frictions in dry condition

Material of test block	Hard Steel
Density	7.60 gr/cm3
Size	100*100*50 mm
Slope angle	25 °
Mass of test block	3.80 kg
Weight of test block	37.28 N (W)
Static force applied	18.98 N (F_{app1})
Kinetic force applied	13.24 N (F_{app2})

Coefficient of friction values in engineer's handbook is according to the below table (Table 4.5) (Shackelford & Alexander, 2010).

Table 4.5 Applied coefficient of friction

Material 1	Material 2	Coefficient of friction			
		Dry		Greasy	
		Static	Sliding	Static	Sliding
Steel (Hard)	Steel (Hard)	0.78	0.42	0.05 - 0.11	0.29 – 0.12

Finally, a function model between cutting force and friction force can help us to calculate the magnitude of the friction forces during cutting in different cutting conditions (Refer to Eq. 4.8 to 4.11).

This model is the following:

$$F_{SX} = 0.095(1.14W_1 + 3.25F_t + 0.32F_L - 1.62F_r) \quad (4.12)$$

$$F_{KX} = 0.075(1.14W_1 + 3.25F_t + 0.32F_L - 1.62F_r) \quad (4.13)$$

$$F_{SZ} = 0.095(1.46W_2 + 2.58F_t - 2.27F_L - 0.87F_r) \quad (4.14)$$

$$F_{KZ} = 0.075(1.46W_2 + 2.58F_t - 2.27F_L - 0.87F_r) \quad (4.15)$$

During cutting operations, there is only static friction force on the X-axis (F_{SX}), and only kinetic friction force on the Z axis (F_{KZ}). According to Eq. 4.12, the static friction force in X-axis depends on the tangential, longitudinal and radial forces. In accordance with Eq. 4.13, the kinetic friction force in X-axis is related to tangential, longitudinal and radial forces.

This model is used for friction force calculation based on different cutting conditions. while the Eq. 4.14, and Eq. 4.15 are static and kinetic friction force calculated in Z-axis, respectively.

The friction forces are modeled by a set of two equations as above Eq. 4.12, to Eq. 4.15, as is the case of the linear model, depends on a state variable representing the cutting force components. The static friction force equation on X-axis guideways is obtained from the friction force based on the tangential force (F_t), longitudinal force (F_L), radial force (F_r), weight (W_1, W_2) and static coefficient of friction. In addition, the kinetic friction force equation on Z-axis guideways is obtained from the friction force based on the tangential force (F_t), longitudinal force (F_L), radial force (F_r), weight (W_1, W_2) and kinetic coefficient of friction. Table 4.6 shows the values of friction force in dry lubrication condition based on cutting conditions in X, and Z-axis that was calculated from the equations obtained from 48 experiments.

Table 4.6 The values of friction force based on cutting conditions

48 Seq.	Cutting conditions			Cutting Force (N)			Friction Force (N)			
	Speed(S) rpm	DOC(d) mm	Feed Rate (f) mm/rev	Longitudinal (F_L)	Radial (F_R)	Tangential (Ft)	F_{SX}	F_{KX}	F_{SZ}	F_{KZ}
E1	250	0.5	0.1	42.33	33.11	61.87	429.59	339.17	660.50	521.40
E2			0.25	145.245	50.83	243.821	486.17	383.84	681.44	537.93
E3			0.4	244.125	80.235	360.22	520.59	411.01	686.21	541.70
E4			0.5	319.4	98.235	461.58	551.40	435.34	693.34	547.33
E5	500	0.5	0.1	92.845	50.499	103.371	441.27	348.39	658.34	519.70
E6			0.25	156.415	55.086	222.583	479.30	378.42	673.47	531.65
E7			0.4	231.532	62.175	311.651	507.99	401.07	678.52	535.63
E8			0.5	265.157	72.96	362.832	523.16	413.04	682.92	539.10
E9	750	0.5	0.1	109.542	75.34	102.95	437.82	345.67	652.58	515.16
E10			0.25	176.254	78.34	219.5	475.37	375.31	666.52	526.15
E11			0.4	222.534	89.95	297.43	499.05	394.01	674.68	532.60
E12			0.5	264.123	97.53	360	518.47	409.34	680.42	537.13
E13	1000	0.5	0.1	125.481	85.923	95.312	434.32	342.90	646.40	510.27
E14			0.25	180.535	89.932	202.3	468.41	369.82	660.42	521.34
E15			0.4	225.425	92.321	293.1	497.44	392.74	672.80	531.11
E16			0.5	239.338	103.981	358.02	516.11	407.48	684.74	540.54
E17	250	1	0.1	209.307	168.93	327.36	495.74	391.39	678.34	535.49
E18			0.25	303.463	160.05	497.78	552.58	436.27	700.54	553.01
E19			0.4	485.342	272.32	767.25	624.03	492.68	718.08	566.86
E20			0.5	585.608	338.97	899.072	657.52	519.12	723.26	570.95
E21	500	1	0.1	173.67	196.29	289.36	478.71	377.95	674.45	532.42
E22			0.25	424.231	403.12	628.11	559.09	441.40	686.35	541.81
E23			0.4	587.123	611.21	880.2	609.85	481.48	695.81	549.28
E24			0.5	799.185	523.23	1085.3	693.16	547.25	707.62	558.60
E25	750	1	0.1	191.254	135.67	232.45	471.00	371.87	661.72	522.37
E26			0.25	283.125	134.34	379.21	519.31	410.01	677.99	535.21
E27			0.4	405.862	178.21	527.24	562.00	443.70	684.17	540.09
E28			0.5	482.376	195.43	658.25	602.12	475.38	698.36	551.30
E29	1000	1	0.1	204.318	149.054	225.65	467.24	368.90	656.13	518.95
E30			0.25	265.765	138.46	345.26	507.67	400.81	673.07	531.33
E31			0.4	396.125	165.12	498.34	554.79	438.02	680.27	537.01
E32			0.5	446.013	178.09	592.32	583.33	460.54	691.48	545.86
E33	250	1.5	0.1	111.435	88.783	224.224	473.25	373.64	680.79	537.42
E34			0.25	495.951	362.97	715.11	594.31	469.21	695.52	549.05
E35			0.4	769.235	560.52	1075.2	683.39	539.54	708.52	559.32
E36			0.5	521.166	246.23	780.1	633.10	499.84	715.66	564.95
E37	500	1.5	0.1	110.243	225.35	275.23	467.95	369.45	682.26	538.58
E38			0.25	455.937	387.32	679.71	578.41	456.66	693.46	547.43
E39			0.4	675.341	597.54	989.2	648.28	511.82	704.63	556.24
E40			0.5	873.492	645.2	1210.7	715.36	564.78	712.25	562.26
E41	750	1.5	0.1	155.051	123.84	237.83	467.95	369.45	682.26	538.58
E42			0.25	298.03	129.49	425.87	534.92	422.33	686.61	542.02
E43			0.4	420.123	192.98	615.32	587.35	463.72	701.47	553.75
E44			0.5	956.1	773	1316.1	730.75	576.93	709.70	560.25
E45	1000	1.5	0.1	105.1	277.68	221.54	443.16	349.88	665.88	525.66
E46			0.25	381.8	435.05	576.75	537.02	423.99	680.27	537.01
E47			0.4	499.21	635.54	765.2	567.92	448.38	684.57	540.41
E48			0.5	695.506	494.022	962.17	656.48	518.30	702.21	554.34

4.4 Summary

In this chapter, the friction force in CNC Machine linear guideways in dry lubrication condition was estimated using cutting force values. For this purpose, the values of the cutting force components including tangential, longitudinal, and radial forces were measured based on the different cutting conditions. The cutting conditions, including depth of cut, feed rate and spindle speed, were applied in 48 individual experiments. The parameters were applied to achieve the effective forces on the machine linear guideways. Consequently, the effective forces including cutting force and normal force on linear guideways in both X, and Z-axis, were analyzed to estimate the friction force.

The static and kinetic coefficient of friction ($\mu_S \; and \; \mu_K$) were considered to identify the friction force in X, and Z- axis in both of stationary and moving table on the guideways. Mathematical friction models were formulated as Eq. 4.12 to 4.15 for the static and kinetic friction force. These models were obtained based on the measured static and kinetic friction coefficients in dry condition. It was observed in this chapter, that the friction force values on linear guideways, on X- axis generally was less than Z- axis at the same cutting conditions. For example, Table 4.6 demonstrated F_{SX}, and F_{SZ} were almost 656 N, and 702 N, respectively when the depth of cut was equal to 1.5 mm, feed rate 0.5 mm/rev, and 1000 rpm for spindle speed. Amongst these, the tangential force was increased more than the other two longitudinal and radial components.

The collected information and developed mathematical friction models will be used in the following chapters as a training and testing data to predict the friction force in CNC guideways using Adaptive Neuro-Fuzzy Inference System (ANFIS) modeling.

CHAPTER 5: ANFIS MODELING TO PREDICT THE FRICTION FORCE AND SERVOMOTOR CURRENT AT DRY LUBRICATION CONDITIONS

5.1 Introduction

The friction force in the CNC machine linear guideways was calculated in chapter 4, using cutting force values. The static and kinetic friction coefficient were measured on linear guideways in dry lubrication conditions. The cutting force components including, F_l, F_r, and F_t, are measured during cutting process. These cutting force values are corresponding to different cutting conditions. Spindle speed, depth of cut, and feed rate are effective for friction conditions in machine linear guide ways in order to the changing of cutting force values.

In this chapter, Adaptive Neuro-Fuzzy Inference System (ANFIS) modeling to predict the friction force in guideways and servomotor current in the feed drive system at dry lubrication conditions are implemented to be employed in the lubrication control system.

Two sets of training data are loaded in two models of ANFIS to predict the 1- friction force in guideways and 2- servomotor current in dry lubrication conditions. In model 2, The training data are including the cutting conditions as inputs, and the measured servomotor current signals in 48 experiments as an output. The calculated friction force and measured servomotor currents are compared with predicted friction force and predicted servomotor currents for evaluate the percentage of errors and accuracy.

5.2 Servomotor Motion and Force Analysis in X, and Z- axis Directions

The both X, and Z- axis servomotor drives collects signals from the control system, amplifies the signals, and transfers electrical current to the servo motors in order to produce motion proportional to the signals (Figure 5.1). Usually, the command signals generates a

favorable feed motion for machine table, but can also generates a favorable torque or position.

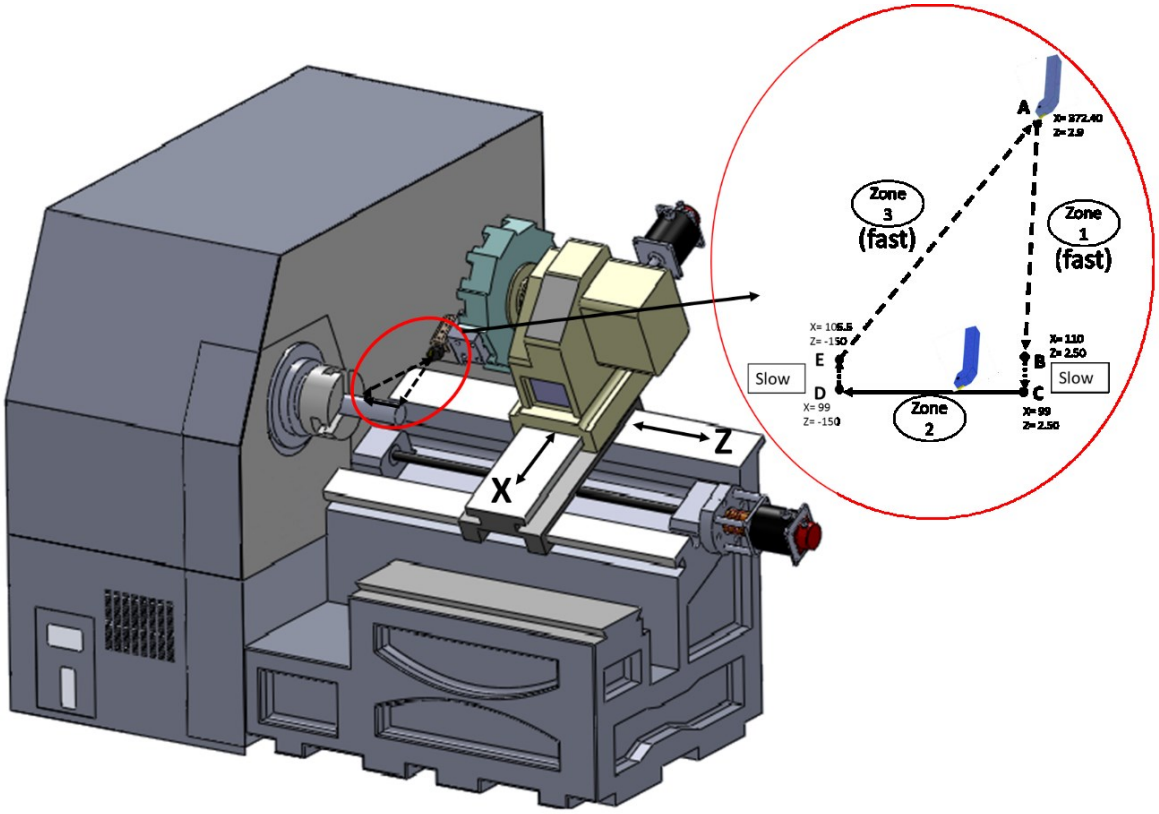

Figure 5.1 Schematic of tool servomotor motion in X, and Z-axis directions

The servomotor motion zones are as following:

Zone 1: before cutting (no loading): The cutting tool moves forward and stops near the workpiece very quickly.

Zone 2: during cutting (with load): Cutting tool is in contact with the workpiece. This cutting procedure is based on the depth of cut, feed rate and spindle speed.

Zone 3: after cutting (no loading): The cutting tool returns backward very fast and stops at the initial position.

5.2.1 Motion and Force Analysis in X-axis Direction

Figure 5.2 shows the force analysis in zone 1 at no loading condition during downward movements to set tool on the cutting point with workpiece.

Figure 5.3 shows the force analysis in Zone 2 during cutting operation in X- axis. During this zone, there is not moving and motion for table in Z direction. Figure 5.4 shows the force analysis in zone 3 at no loading condition of the cutting tool operation during upward movements for come back to the initial position.

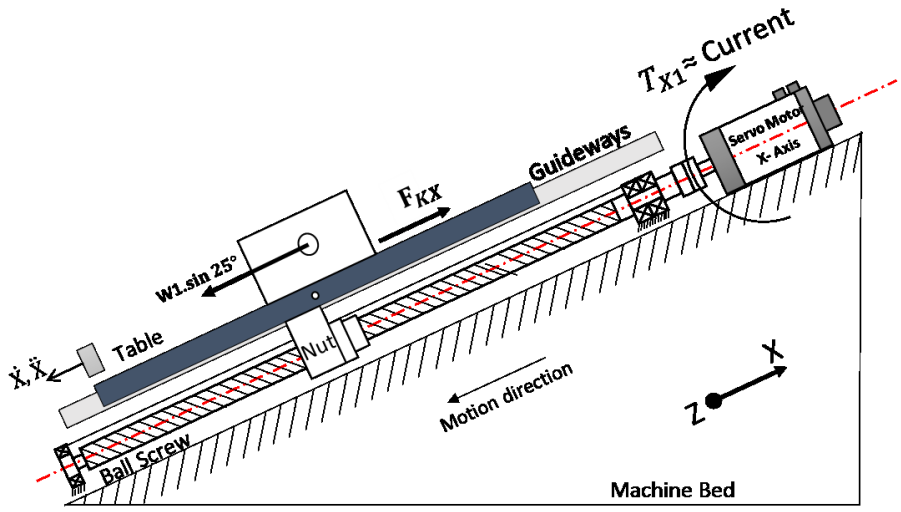

Figure 5.2 The schematic of cutting during downward movement in X-axis

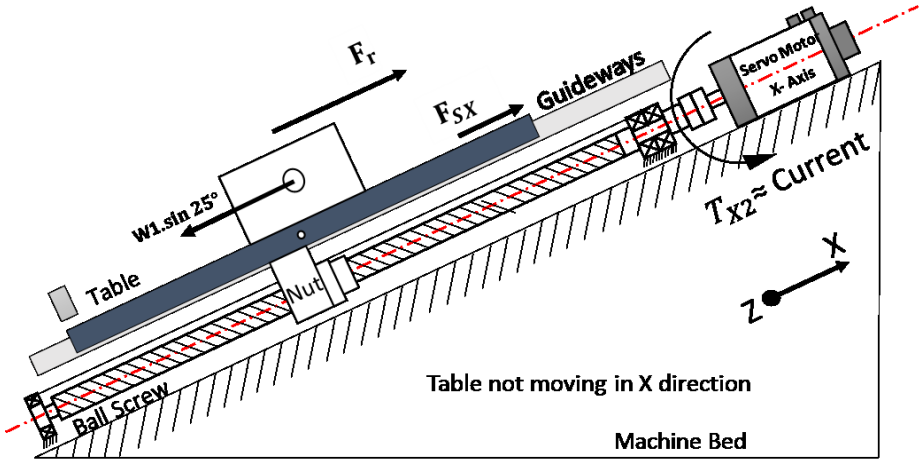

Figure 5.3 The schematic of cutting during cutting in X-axis

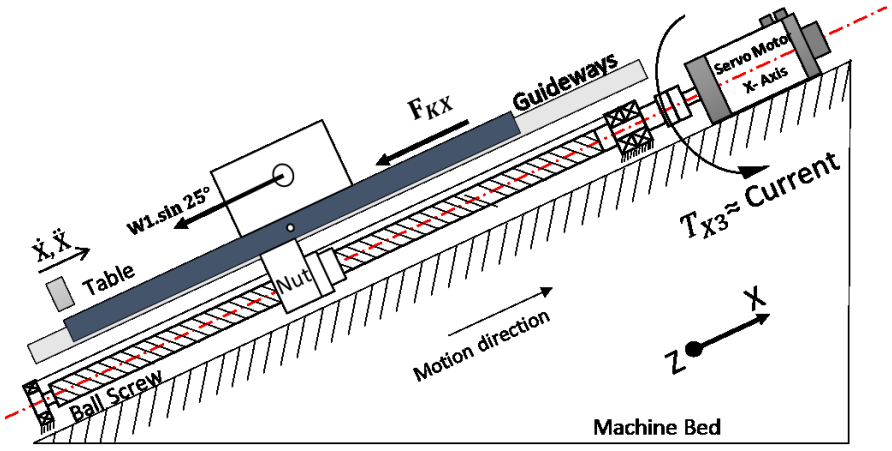

Figure 5.4 The schematic of cutting during upward movement in X-axis

5.2.2 Motion and Force Analysis in Z-axis Direction

Figure 5.5 shows the force analysis in the zone 1, and 3. no loading condition during forward and backward movements. Figure 5.6 shows the zone 2. loading condition of cutting tool operation for Z-axis, during cutting in terms of T_{Z2}

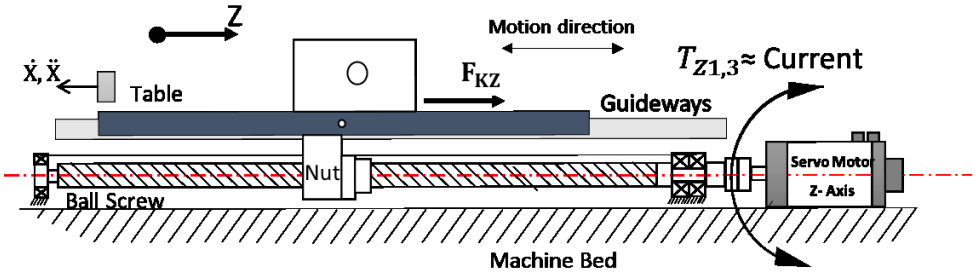

Figure 5.5 The schematic of cutting during forward and backward movement in Z-axis

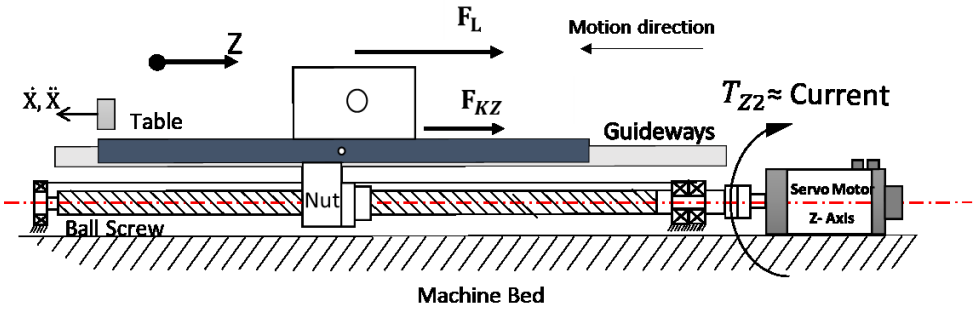

Figure 5.6 The schematic of component forces of cutting during cutting in Z-axis

5.3 Servomotor Current Measurement

In a cycle of cutting operations (Figure 5.7), the servomotor current amplitude can be different for every axis. The servomotor current for X and Z-axes, are measured based on designed model of current block diagram, are shown in Figure 5.8 and Figure 5.9.

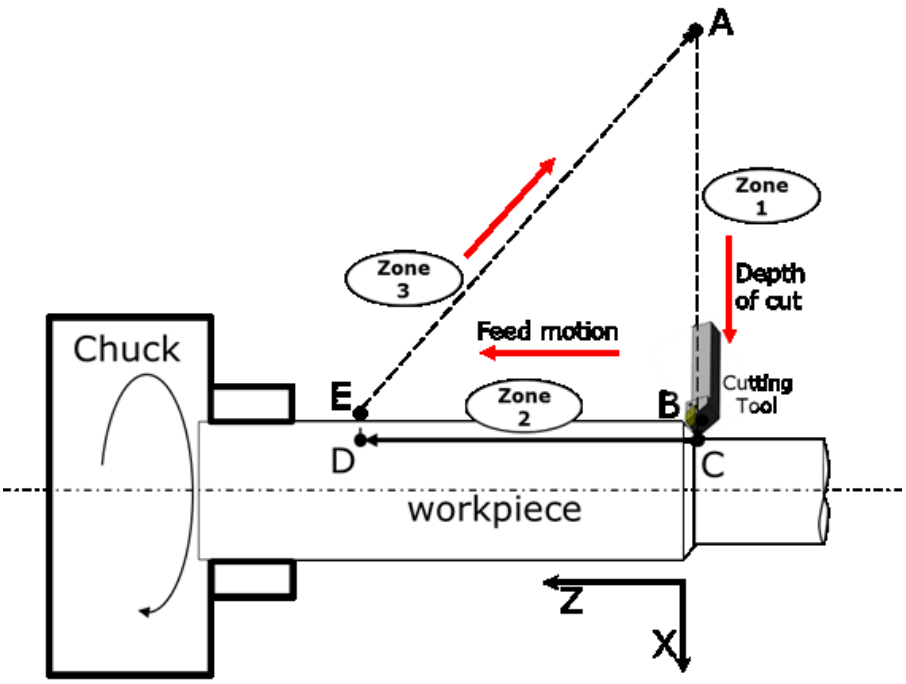

Figure 5.7 Cutting operation cycle

According to the tool moving model, which was shown in Figure 5.7, and the values of movement in Table 3.5, Figure 5.8, and Figure 5.9, are explained as following:

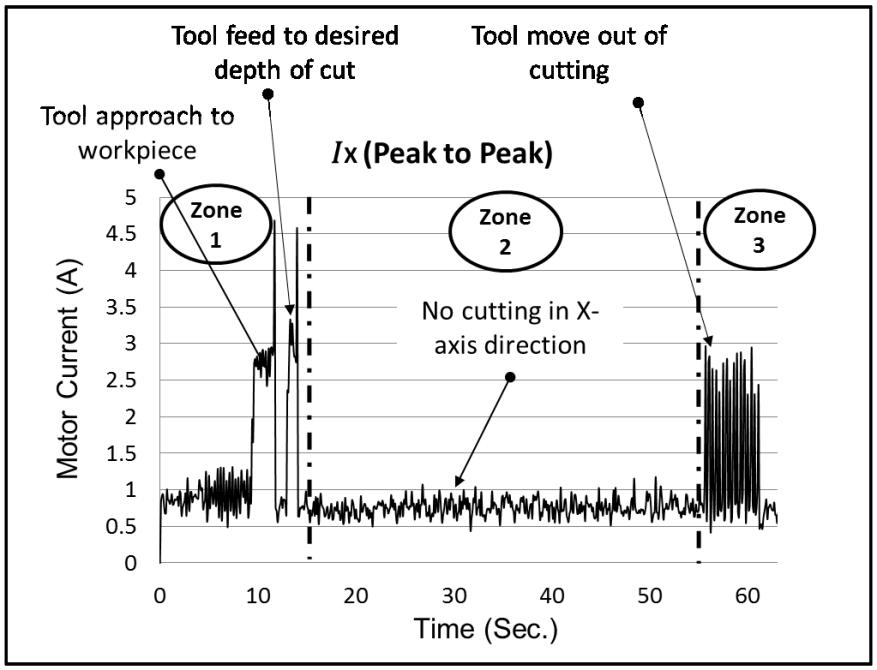

Figure 5.8 Peak to peak X- axis servomotor current in 3 stages of motion

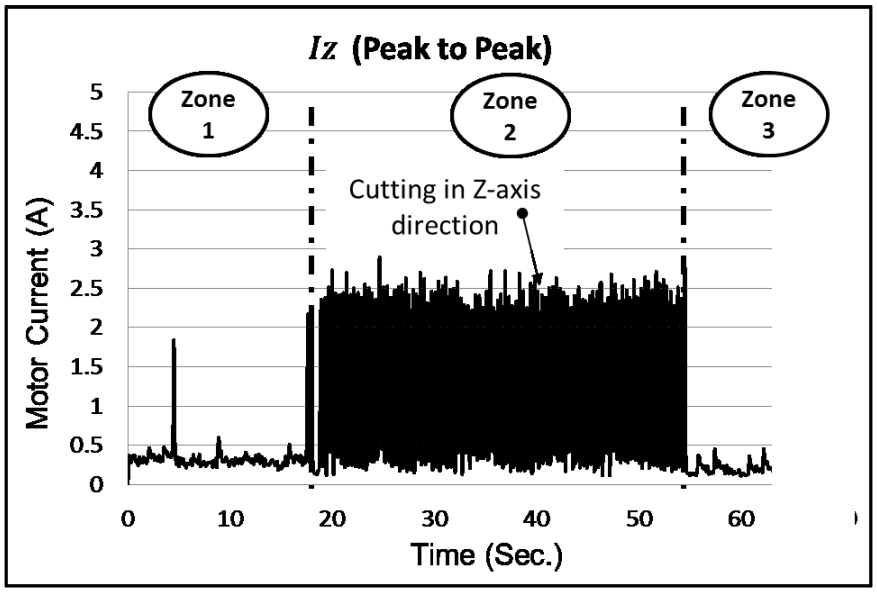

Figure 5.9 Peak to peak Z- axis servomotor current in 3 stages of motion

5.3.1 Measured Servomotor Current in X-axis Direction

Zone 1: Before relocating the X- axis servomotor from initial point, during 5 second the motor current average indicates 0.8 Ampere. This current is enough to maintain the weight of moving table under 25 degree slope relative to the horizontal line of the machine

bed. From this time until tenths of seconds and before big fluctuations, the motor current is almost 1 Ampere. During this time the tool has to move in X direction quickly to get to the B point. This is exactly 262.4 mm distance. Whereas, very slight movement in the Z direction is done simultaneously.

During the first big fluctuation, the servomotor current indicates about 2.75 Ampere, on average when the tool is moving from location B to location C, slowly. The tool moving 11 mm distance along the X direction until tip of tool engage to the workpiece and is stopped. The motor current is in terms of kinetic friction force in linear guideways and weight of part B (refer to Figure 4.8, in chapter 4).

For a seconds afterwards, the motion along with the penetration in the workpiece is done to create the depth of cut. During penetration time the current slightly increase and reaches to value of 3 amps. This increase is caused by the cutting force exerted on the surface of the linear guideways.

From end of penetration until dash dot line, which indicates the cutting zone, is the pause time before beginning of cutting. Because there is no motion in the X direction, so the load of current has been taken from the servomotor.

$$I_{X1}(A) = k.|(W_1.sin25° - F_{KX})| \tag{5.1}$$

Where, I_{X1} is servomotor current for X–axis during big fluctuation, k is the equivalent constant current coefficient, and F_{KX}, is kinetic friction force in X-axis (Figure 5.2).

Zone 2: There is no relative motion during cutting in X direction in zone 2. Therefore, the amount of current servomotor is low. The cutting distance during this time is exactly 147.5 mm distance (from location C to location D in Z-axis direction).

The servomotor current is in terms of weight of part B, the radial force, and the static friction force in X axis.

$$I_{X2}(A) = k.\ |[(W_1.sin25°) - (F_r + F_{SX})]| \tag{5.2}$$

Where,I_{X2} is servomotor current for X–axis during cutting, k is the equivalent constant current coefficient, F_r is radial force, andF_{SX}, is static friction force in X-axis (Figure 5.3).

Zone 3: The tool is return back after cutting process from D to point E, slowly. And then from E is return back to initial point (A point) very fast. The average of motor current increases to 2.5 amps in the period between 55 to 60 seconds. During this time we have the very fast motion in both X, and Z directions.

5.3.2 Measured Servomotor Current in Z-axis Direction

Similar to X-axis, there are three zone such as 1, 2, 3. However, the difference is that: in zone 1, there is no significant motion in Z direction. Therefore, motor current does not increase noticeably and the motor current average value indicates 0.3 amps.

In zone 2 that is enclosed between two dash dot lines, indicates the motor current values during cutting operation. There is motion only in Z direction and the cutting tool operations along 147.5 mm distance with real cutting speed. Therefore, the feed motor current is high level. The current value is duo to the longitudinal force and kinetic friction force on linear guideways in Z-axis. The average feed motor current in zone 2 is almost 2.45 amps.

$$I_{Z2}(A) = k.(F_L + F_{KZ}) \tag{5.3}$$

Where, I_{Z2} is servomotor current for Z–axis during cutting, k is the equivalent constant current coefficient, F_L is longitudinal force, andF_{KZ}, is kinetic friction force in Z-axis.

At zone 3 and according to tool moving model the tool is return to back after cutting process very fast. Therefore, there is no considerable load current in Z-axis servo motor. Figure 5.9 shows, the current amplitude for Z axis servomotor is different compared with X-axis. The Peak to peak current amplitude for this axis is higher during cutting in zone 2, where cutting is running and tool feed motion in Z- axis direction.

Table 5.1 shows the measured motor current values based on cutting conditions (refer to the experiment design section 4.3.4).

Table 5.1 Measured servomotor current based on cutting conditions

48 Seq.	Cutting conditions			Measured Motor Current (A)	
	Speed(S) rpm	DOC(d) mm	Feed Rate (f) mm/rev	I_X	I_Z
E1	250	0.5	0.1	1.71	1.78
E2			0.25	1.98	2.1
E3			0.4	2.5	2.17
E4			0.5	2.62	2.24
E5	500	0.5	0.1	1.67	1.58
E6			0.25	1.97	1.66
E7			0.4	2.32	1.94
E8			0.5	2.51	2.11
E9	750	0.5	0.1	1.57	1.45
E10			0.25	1.87	1.55
E11			0.4	2.11	1.81
E12			0.5	2.36	1.96
E13	1000	0.5	0.1	1.53	1.23
E14			0.25	1.84	1.25
E15			0.4	2.1	1.61
E16			0.5	2.34	2.15
E17	250	1	0.1	1.85	1.87
E18			0.25	2.66	2.39
E19			0.4	3.22	2.75
E20			0.5	3.49	2.75
E21	500	1	0.1	1.77	2.1
E22			0.25	2.68	2.18
E23			0.4	315	2.45
E24			0.5	3.95	2.65
E25	750	1	0.1	1.85	1.25
E26			0.25	2.45	1.85
E27			0.4	2.75	2.11
E28			0.5	315	2.45
E29	1000	1	0.1	1.74	1.15
E30			0.25	2.23	1.63
E31			0.4	2.68	1.95
E32			0.5	2.96	2.23
E33	250	1.5	0.1	2.05	1.98
E34			0.25	2.99	2.54
E35			0.4	3.6	2.98
E36			0.5	4.41	3
E37	500	1.5	0.1	1.9	2.25
E38			0.25	2.88	2.35
E39			0.4	3.35	2.62
E40			0.5	3.95	2.95
E41	750	1.5	0.1	1.85	1.58
E42			0.25	2.6	2.19
E43			0.4	2.78	2.58
E44			0.5	3.41	2.85
E45	1000	1.5	0.1	1.68	1.5
E46			0.25	2.52	1.95
E47			0.4	2.97	2.15
E48			0.5	3.25	2.6

In order to realize the objectives of this section, different effects from the cutting process are observed. The calculated friction force will be increased by increasing the feed rate (Figure 5.10 a) in different spindle speed. Moreover, the friction force values are increased by increasing the depth of cut (Figure 5.10 b) in different spindle speed, inevitably (Sparham & al., 2012).

According to Figure 5.11, the servomotor current may changes due to changes in the cutting conditions such as depth of cut, cutting feed rate, cutting speed and workpiece material. Besides, the amount and time of improper lubrication (PRI) of motion ways and moving parts of machine mainly affect to the feed motor current. Therefore, non-lubricated conditions or dry lubrication is performed to measure the servomotor currents (Sparham & al., 2013). This figure shows the feed rate, depth of cut and cutting speeds directly have impacts on the variations of feed motor current, accordingly.

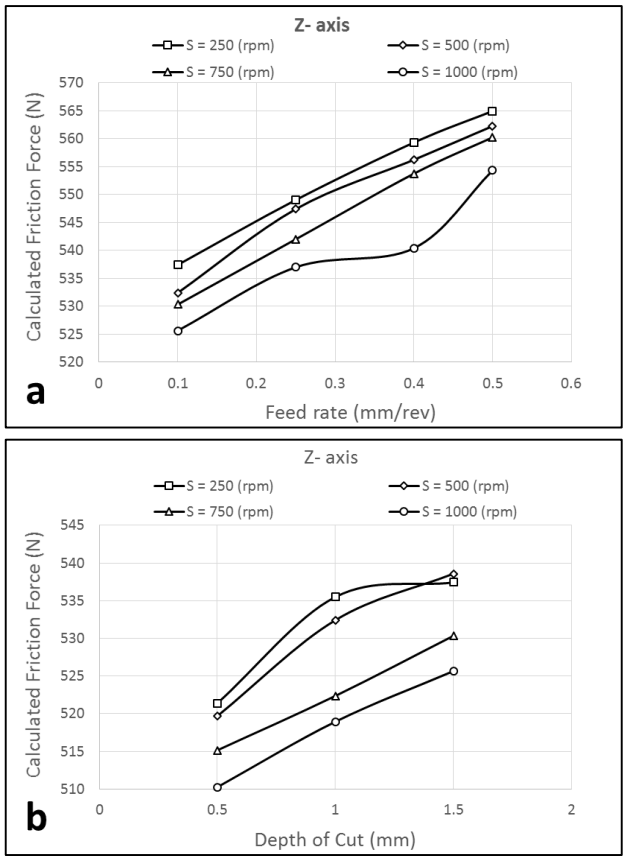

Figure 5.10 Friction force with respect to the a) Feed rate b) Depth of cut

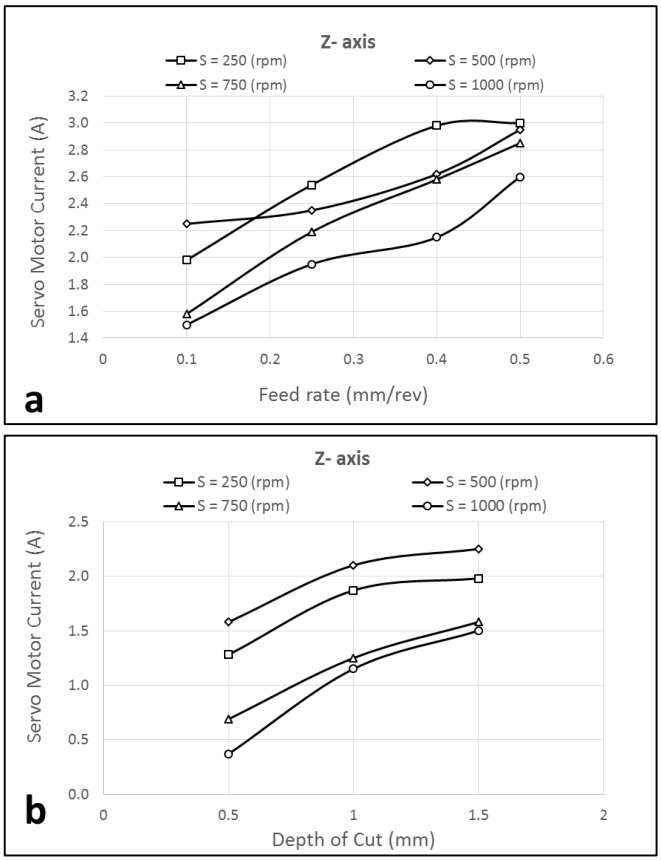

Figure 5.11 Servomotor current with respect to the a) Feed rate b) Depth of cut

5.4 ANFIS Modeling to Predict Friction Force and Servomotor Current in Dry Lubrication Condition

Because soft computing techniques are useful when exact mathematical information is not available and these differ from conventional computing in that it is tolerant of imprecision, uncertainty, partial truth, approximation, and met heuristics. Adaptive Neuro - Fuzzy Inference System (ANFIS) is one of the soft computing techniques that play a significant role in input-output matrix relationship modeling. It is used when subjective knowledge and suggestion by the expert are significant in defining objective function and decision variables. ANFIS is preferred in to predicting friction force and servomotor current signals based on the input variables due to nonlinear condition in cutting process. This research work applies the ANFIS Modeling technique to develop the rule model in order to

predict the friction forces in the CNC linear guide ways and motor current in feed drive system based on parameter and performance interaction. This relation, which is non-linear, can help us to obtain a predicted friction and motor current models. The predicted friction and motor current values are achieved from adapting of training data and testing data. The training data actually is including values of cutting parameters, and measured current of servomotor or calculated friction force, which are determined as input/output data.

To start training in ANFIS editor graphical user interface GUI:

1. First, we need to have a training data set that contains desired input/output data pairs of the target system to be modeled.
2. Sometimes we also want to have the optional testing data set that can check the generalization capability of the resulting fuzzy inference system, and/or a checking data set that helps with model over fitting during the training.
3. Over fitting is accounted for by testing the FIS trained on the training data against the checking data, and choosing the membership function parameters to be those associated with the minimum checking error if these errors indicate model over fitting.
4. We will have to examine our training error plots fairly closely in order to determine this.
5. Usually these training and checking data sets are collected based on observations of the target system and are then stored in separate files.

5.4.1 ANFIS Modeling to Predict Friction Force

The relationship of the friction force and the cutting conditions is important so cutting conditions could be used as parameter to indicate the friction force in CNC guideways. Adaptive Neuro-Fuzzy Inference System (ANFIS) is used to predict the friction force by

using the different cutting conditions during 48 experiments. The field of fuzzy logic has been making great strides motivated by its practical success in modeling and control of industrial process (Lin & al., 2008; Parlak & al., 2006). The ANFIS can be used as a modeling tool. The model provides appropriate outputs based on real experimental data sets. ANFIS model use a form of quantification of imprecise information (input fuzzy sets) to generate output by an inference scheme (Tinkir & al., 2010; Xia & al., 2014).

The number of inputs and outputs are determined from experiments of a CNC linear guideways. Fuzzy logic model membership functions and rules are obtained based on actual experimental data set results. Figure 5.12, describes the fuzzy logic prediction-modelling workbench based on friction force.

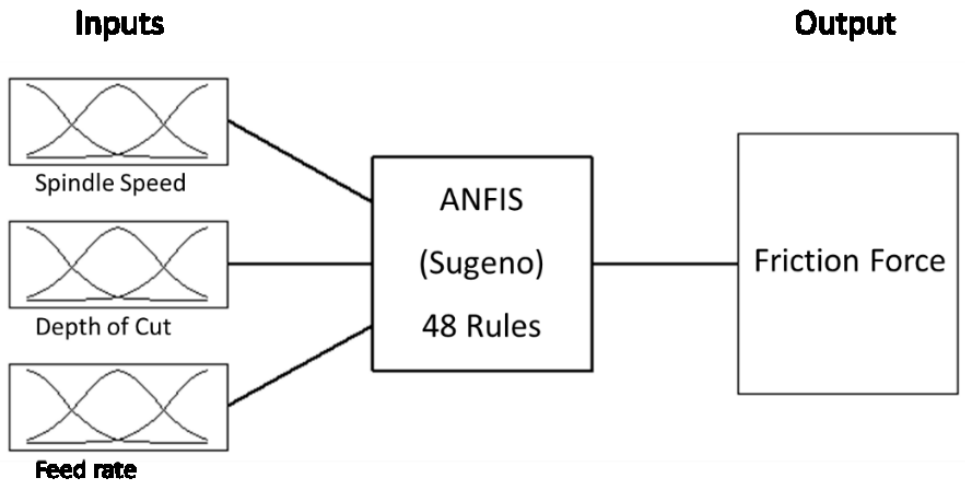

Figure 5.12 The structure of adaptive network based on FIS in friction force

In ANFIS model structure of logical operations, four main components are made including: (1) inputs; (2) membership functions of inputs and rules; (3) membership function of output or fuzzy reasoning, and (4) output. The basic model structure of the fuzzy system which was used in this study is shown in Figure 5.13.

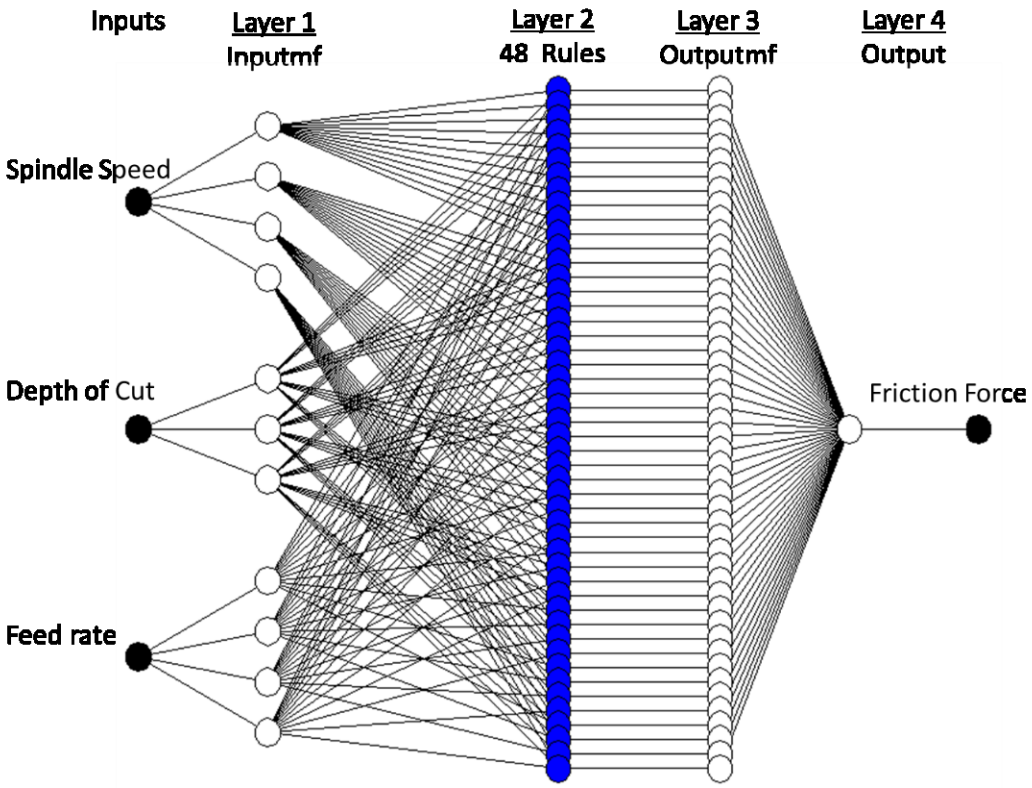

Figure 5.13 The optimum model structure of ANFI for friction force

Inputs: In fuzzy logic systems (FLS) linguistic variables as an inputs, are utilized to give a "value" to the element. The variables in this model are spindle speed (w), depth of cut (x), feed rate (y) (Figure 5.14). The structure of proposed ANFIS model is designed for multi input and single output (MISO) system. In this study, the MISO system has three inputs and one output. The inputs of the model are spindle speed (S), depth of cut (DOC) and feed rate (f), while one output of the model denoted is the friction force. The input values are including the spindle speed in four level (250, 500, 750 and 1000 rpm), the depth of cut in three level (0.5, 1, and 1.5 mm), and finally the feed rate in four level (0.1, 0.25, 0.4, and 0.5 mm/rev), regarding to loaded data. In addition, the output is the friction force (Fz) that depends on input parameters. This work used ANFIS modeling in order to improve the simulation results.

FLS require the linguistic variables in relation to their numeric values, their quantification and the connections between variables and the possible implications.

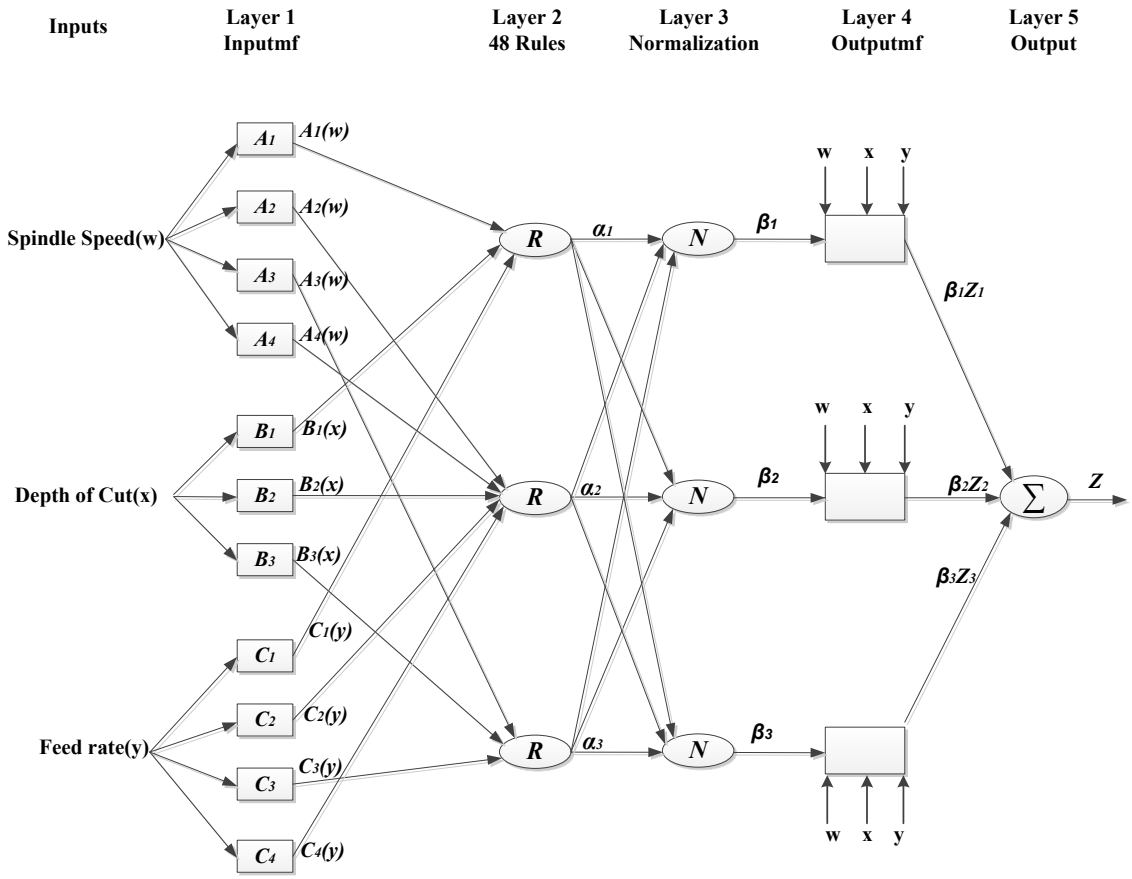

Figure 5.14 Simplification model of ANFIS architecture in Sugeno fuzzy

Layer 1: In FLS the input membership functions are utilized to find the degree of membership of the element in a given set as a particular inputs. The parameters in this layer which is called; $A_1, A_2, \ldots to\ C_4$, are as conditions of the parameters.

Layer 2: This layer is rules node which is fixed, with the node function to multiply input signals whose output is the product of all the incoming signals:

$$\alpha_1 = \sum A_1\,(w) \times \sum B_1\,(x) \times \sum C_1\,(y)$$

$$\alpha_2 = \sum A_2\,(w) \times \sum B_2\,(x) \times \sum C_2\,(y)$$

$$\alpha_3 = \sum A_3\,(w) \times \sum B_3\,(x) \times \sum C_3\,(y)$$

In this layer, there are 48 rules to fuzzification the every membership functions regarding to above explanation.

Layer 3: Every node *i* in this layer is a fixed node which is labelled *N* to indicate the normalization of the firing levels. The *ith* node computes the ratio of the *ith* rule's firing strength to the sum of all rule's strengths.

$$\beta_1 = \frac{\alpha_1}{(\alpha_1+\alpha_2+\alpha_3)}$$

$$\beta_2 = \frac{\alpha_2}{(\alpha_1+\alpha_2+\alpha_3)}$$

$$\beta_3 = \frac{\alpha_3}{(\alpha_1+\alpha_2+\alpha_3)}$$

Layer 4: in this layer each node *i* is an adaptive node of a function:

$$\beta_1 Z_1 = \beta_1(a_1 w + b_1 x + c_1 y)$$

$$\beta_2 Z_2 = \beta_2(a_2 w + b_2 x + c_2 y)$$

$$\beta_3 Z_3 = \beta_3(a_3 w + b_3 x + c_3 y)$$

β_i: is a normalized firing strength from previous layer. (a_i, b_i, c_i) Is the parameter set of this node, which is referred to the consequent parameters.

Layer 5: The single node in this layer is a fixed node labelled $\sum$, that calculates the overall output as the summation of incoming signals (Eq. 5.4):

$$Z = \beta_1 Z_1 + \beta_2 Z_2 + \beta_3 Z_3$$

$$\sum_i \overline{\beta_i Z_i} = \frac{\sum_i \beta_i Z_i}{\sum_i \beta_i} = \frac{\beta_1 Z_1+\beta_2 Z_2+\beta_3 Z_3}{\beta_1+\beta_2+\beta_3} \quad (5.4)$$

The ANFIS architecture has been constructed, so we can apply a learning procedure to find its parameters for achieving a minimal error measurement. A hybrid learning algorithm is adopted as follows:

In the forward pass, node outputs go forwards until layer four and the consequent parameters are identified by using the Least Square technique while in backward pass, the error signals propagate backward and the set of premise parameters is updated by Gradient

Descent method. The advantage of this hybrid learning versus the pure gradient descent method, the rapid convergence to the global minimum is guaranteed.

The developed modeling has a generalized bell-shaped membership function, and [4 3 4] is the number of membership function for three inputs including spindle speed, depth of cut and feed rate, respectively.

Usually, generalized bell-shaped membership function are chosen to represent the linguistic terms because the relationship between the cutting parameters and friction force is not linear. Figure 5.15 Figure 5.15(a-c) confirm that the system training based on ANFIS has an input with different rate of membership functions.

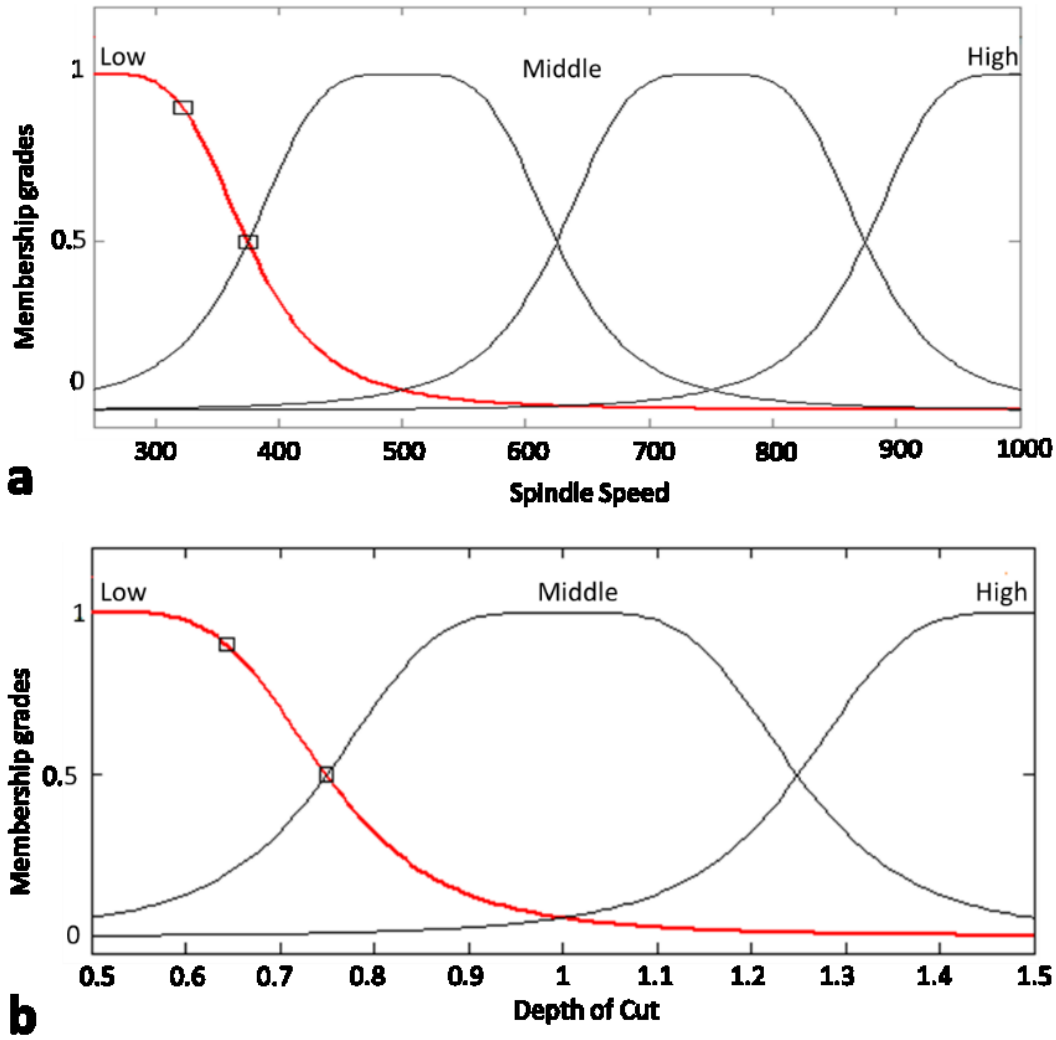

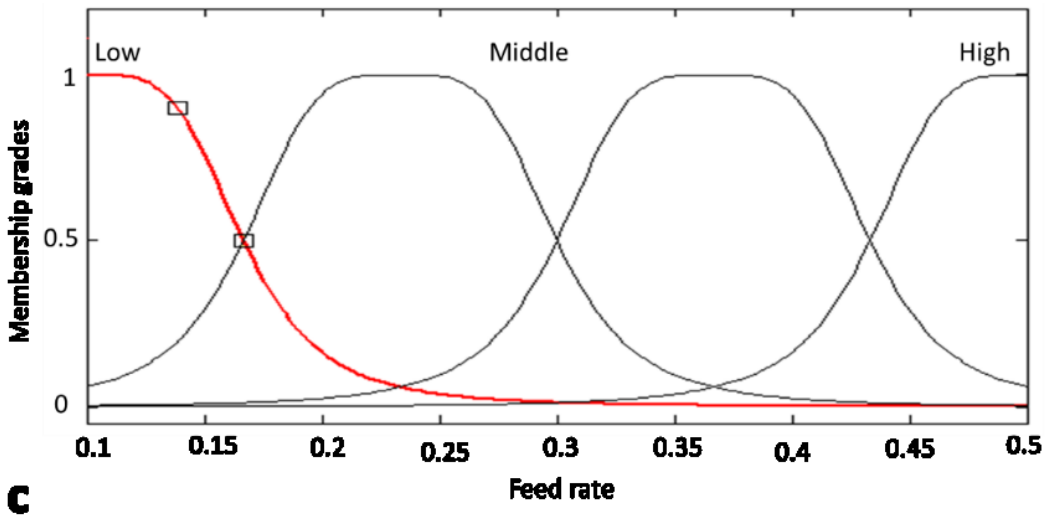

Figure 5.15 Membership function of the ANFIS model for different cutting parameters.

Figure 5.16 shows 3D view of the surface plats for different inputs combinations respect with friction force as an output in Z direction. In Figure 5.16 (a), at high level of spindle speed (1000 rpm) and low level of feed rate (0.1 mm/rev), it can be seen that the friction force decreases. Also in Figure 5.16 (b), with increasing depth of cut and feed rate the friction force as an output increases, proportionally.

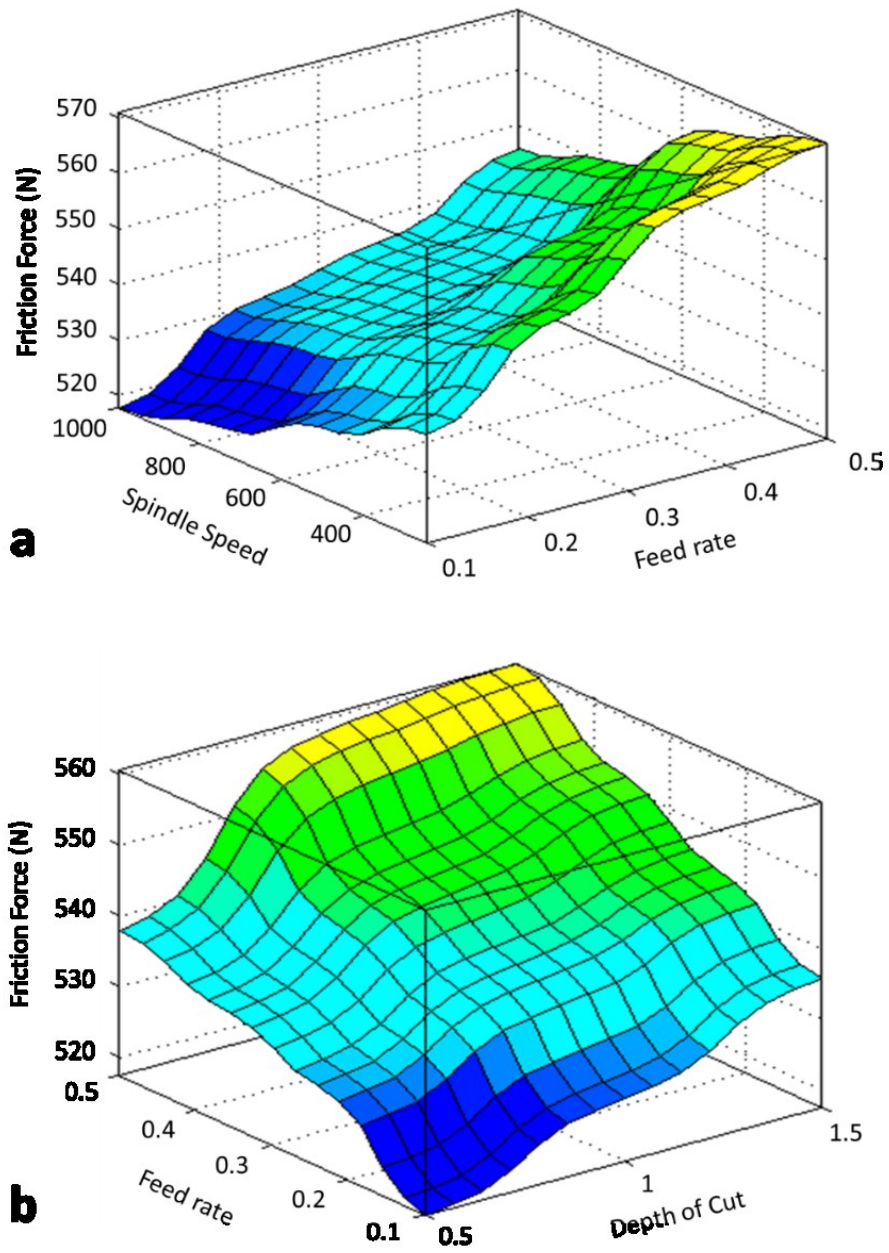

Figure 5.16 Surface plot of friction force a) (DOC=1mm) b) (S=625 rpm)

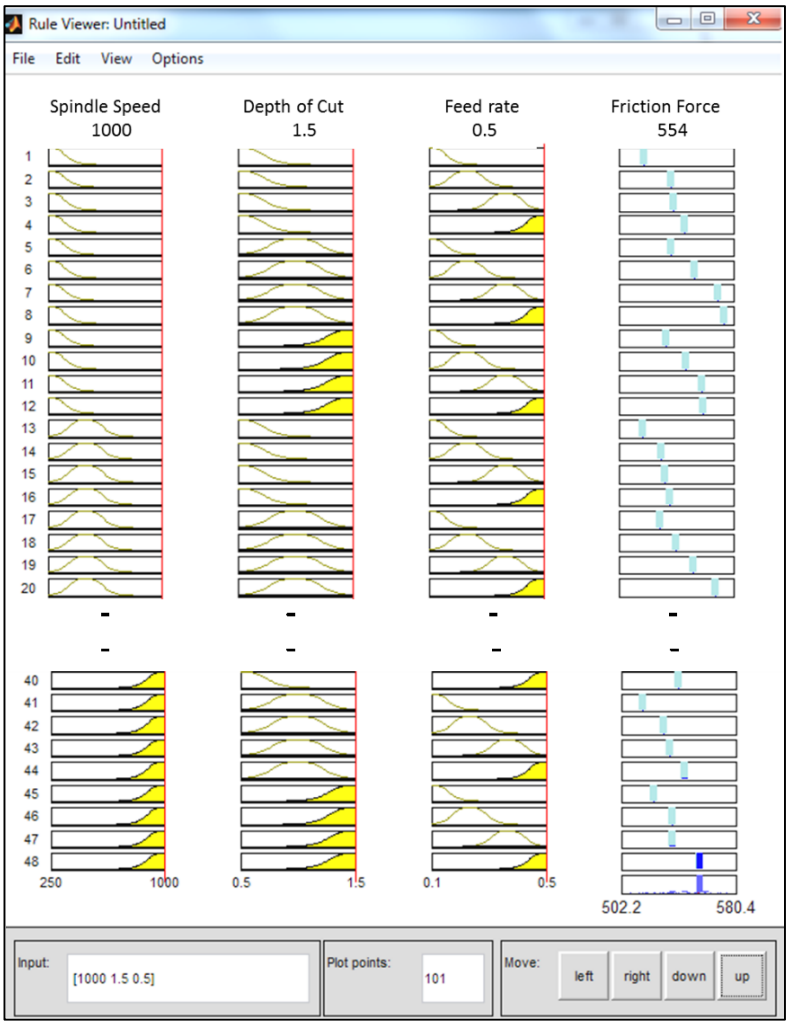

Figure 5.17 The friction force using the rule viewer of ANFIS toolbox

Figure 5.17, presents the printed screen for ANFIS modeling. It shows an example of friction force 554 N in Z- axis, using a spindle speed of 1000 rpm, a depth of cut 1.5 mm and a feed rate 0.5 mm/rev. The predicted friction force values are carried using this rule viewer, by apply the different values in the range of cutting parameters, to fuzzification the every membership functions.

5.4.1.1 Investigation the prediction error and accuracy for friction force

To investigate the errors and accuracy in ANFIS modeling prediction for friction force, another 18 experiments are carried out. Table 5.2 shows the conditions of the new 18-

experiments. According to this Table the calculated friction force increases influenced by increasing the depth of cut and feed rate. Nevertheless, the spindle speed has an inverse relationship with friction force.

The errors between the proposed ANFIS modeling and experimental is acceptable for 18 steps. The equations 5.5, and 5.6, show the percentage of error E and average error E_{av} for friction force, respectively.

$$E = \frac{|F - F_P|}{F} \times 100 \tag{5.5}$$

$$E_{av} = \frac{1}{m}\sum_{i=1}^{m} E \tag{5.6}$$

Table 5.2 ANFIS model prediction error and accuracy for friction force

Exp.	Cutting Condition			Calculated Friction Force(N) F	Predictive Friction Force(N) $F_{P(dry)}$	Error % $\%E_Z$	Accuracy %
	Spindle Speed	DOC	Feed Rate				
1	375	0.75	0.2	543.13	539	0.76	99.24
2			0.3	546.63	545	0.30	99.70
3			0.45	554.79	554	0.14	99.86
4		1.25	0. 2	563.60	576	2.20	97.80
5			0.3	566.26	553	2.34	97.66
6			0.45	572.80	564	1.54	98.46
7	625	0.75	0.2	541.89	532	1.83	98.17
8			0.3	542.42	536	1.18	98.82
9			0.45	542.89	546	0.57	99.43
10		1.25	0. 2	558.46	540	3.31	96.69
11			0.3	560.17	545	2.71	97.29
12			0.45	560.50	557	0.62	99.38
13	875	0.75	0.2	525.11	527	0.36	99.64
14			0.3	531.58	531	0.11	99.89
15			0.45	536.22	541	0.89	99.11
16		1.25	0. 2	541.89	535	1.27	98.73
17			0.3	555.37	538	3.13	96.87
18			0.45	557.52	549	1.53	98.47
Average						1.38	98.62

Figure 5.18, shows the comparison results between calculated friction force, and ANFIS modeling methods in Z- axis direction. For this case, the average of errors has a 1.38% value for Z-axis of the friction force (Figure 5.19). Accordingly, it is apparent that the proposed ANFIS modeling has much better accuracy to use in new technique for lubrication control.

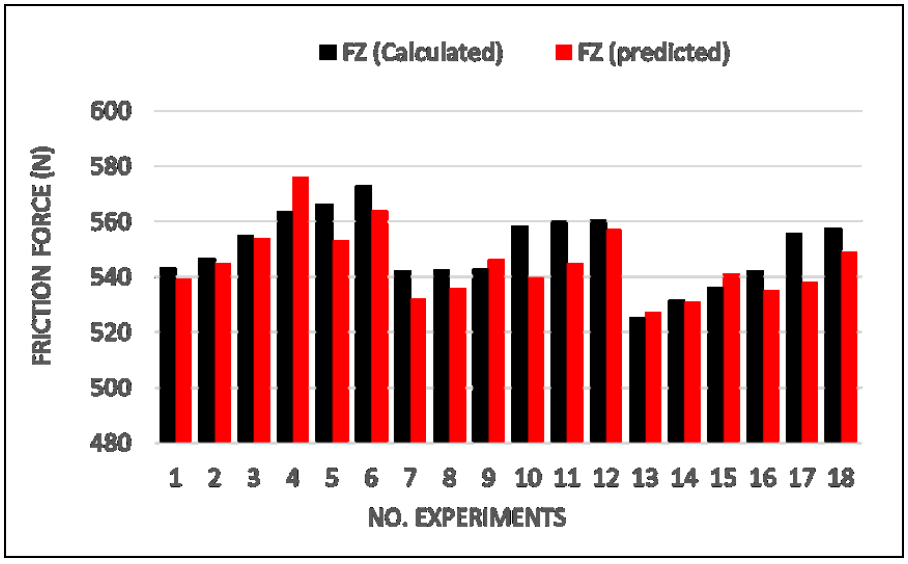

Figure 5.18 Results comparison of friction force between calculated and predicted

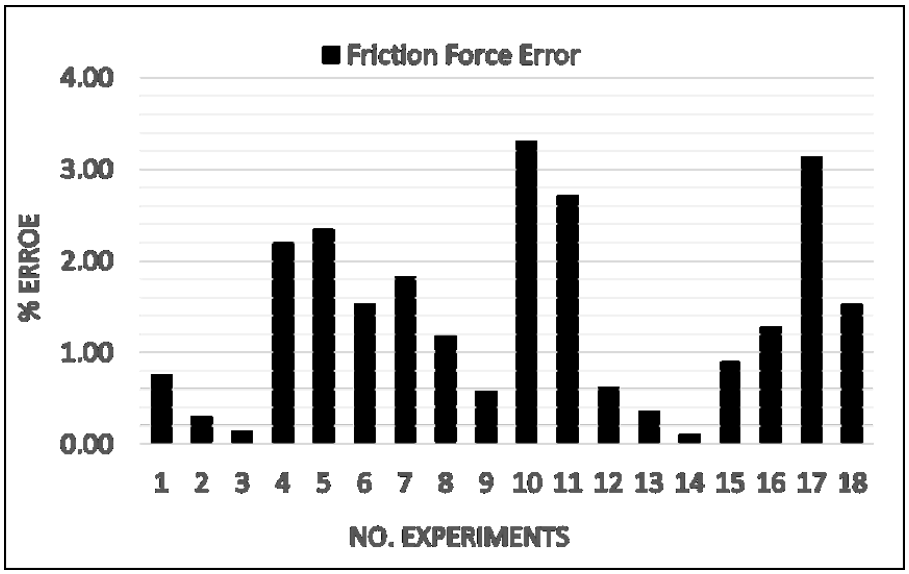

Figure 5.19 Errors in friction force using ANFIS modeling

5.4.2 ANFIS Prediction Model for Servomotor Current

The relationship of the servomotor current signals in dry lubrication condition and the cutting conditions is important to comparison with real measured motor current in lubrication mode. So cutting conditions could be used as parameter to indicate the motor current in CNC feed drive system. Adaptive Neuro-Fuzzy Inference System (ANFIS) is used to predict the motor current by using the different cutting conditions during 48 experiments.

The number of inputs and outputs are determined from experiments of a CNC linear guideways. Fuzzy logic model membership functions and rules are obtained based on actual experimental data set results.

Figure 5.20, describes the fuzzy logic prediction-modelling workbench based on feed drive servomotor current.

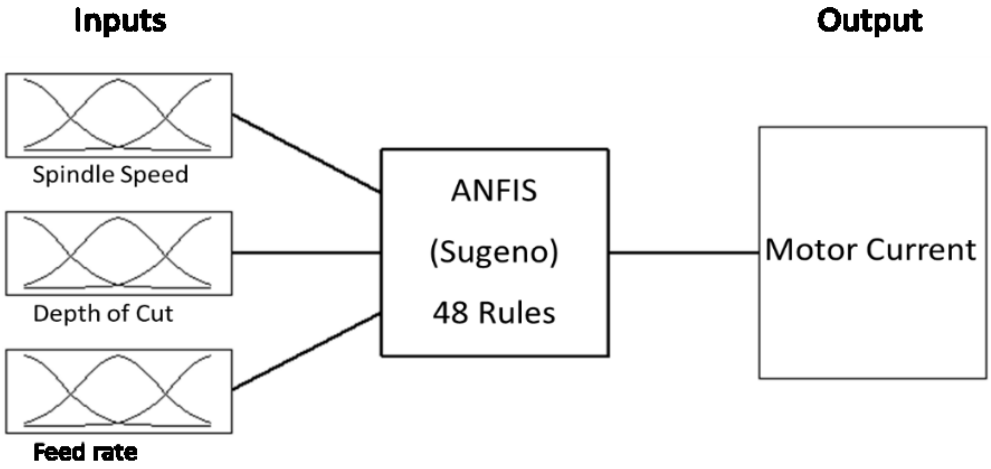

Figure 5.20 The structure of adaptive network based on FIS in motor current

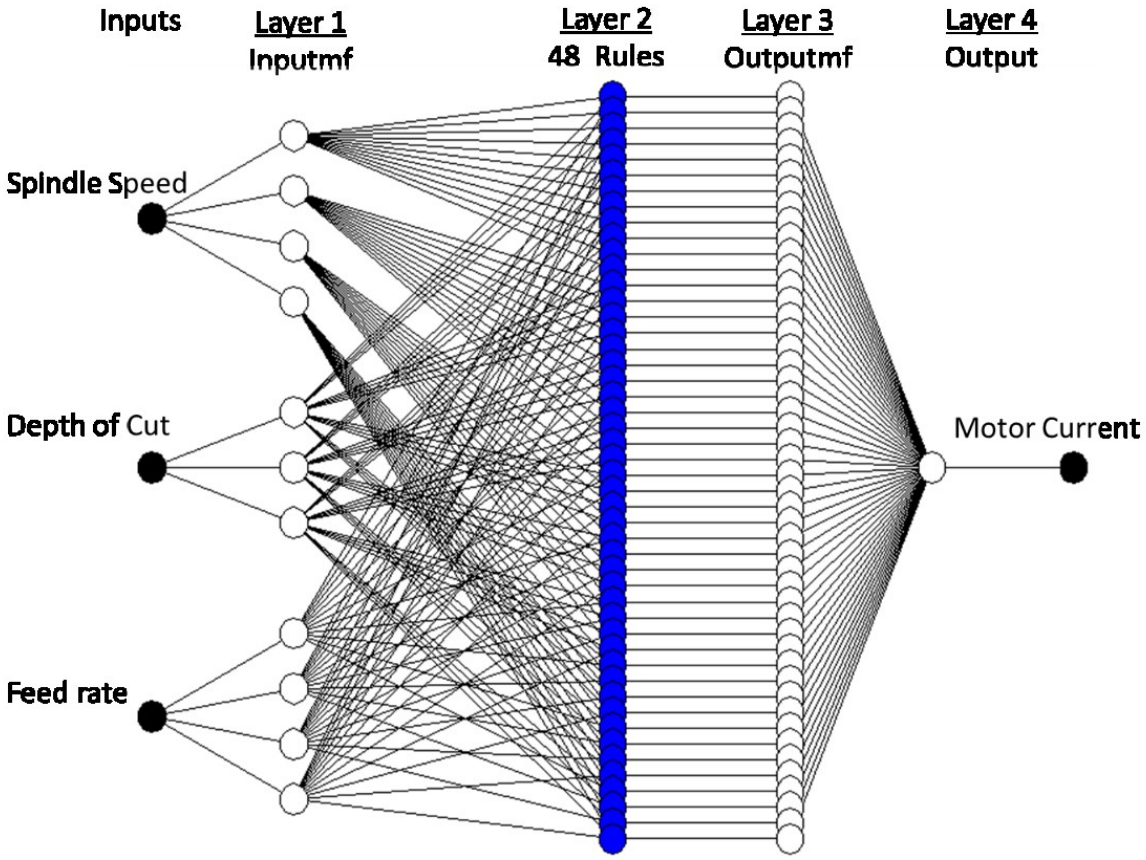

Figure 5.21 The optimum model structure of ANFI for servomotor current

In ANFIS model structure of logical operations, four main components are made including: (1) inputs; (2) membership functions of inputs and rules; (3) membership function of output or fuzzy reasoning, and (4) output. The basic model structure of the fuzzy system which was used in this study is shown in Figure 5.21.

The simplification model of ANFIS structure for servomotor current is as same as structure for friction force, which was discussed in last section (refer to section 5.4.1). According to the model there are five layer that were introduced as before, to perform the following fuzzy interface steps as shown in Figure 5.22: 1- input fuzzification, 2- fuzzy set database construction, 3- fuzzy rule base construction, 4- decision making, 5- output defuzzification.

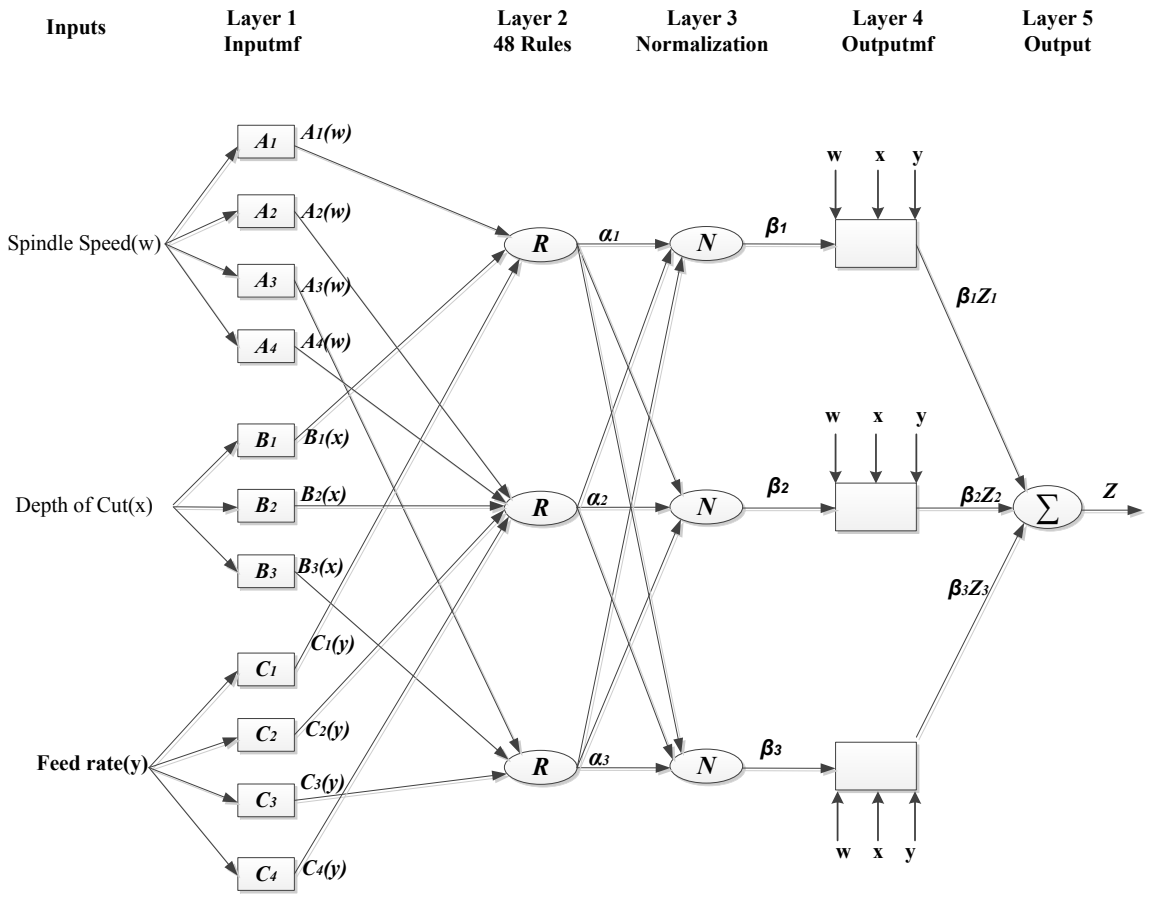

Figure 5.22 Simplification model of ANFIS architecture for motor current

Figure 5.23 shows 3D view of the surface plats for different inputs combinations respect with motor current as an output in Z direction. In addition, in Figure 5.23 (a), at high level of spindle speed (1000 rpm) and low level of feed rate (0.1 mm/rev), it can be seen that the motor current increases. In Figure 5.23 (b), with increasing depth of cut and feed rate the motor current as an output increases, proportionally.

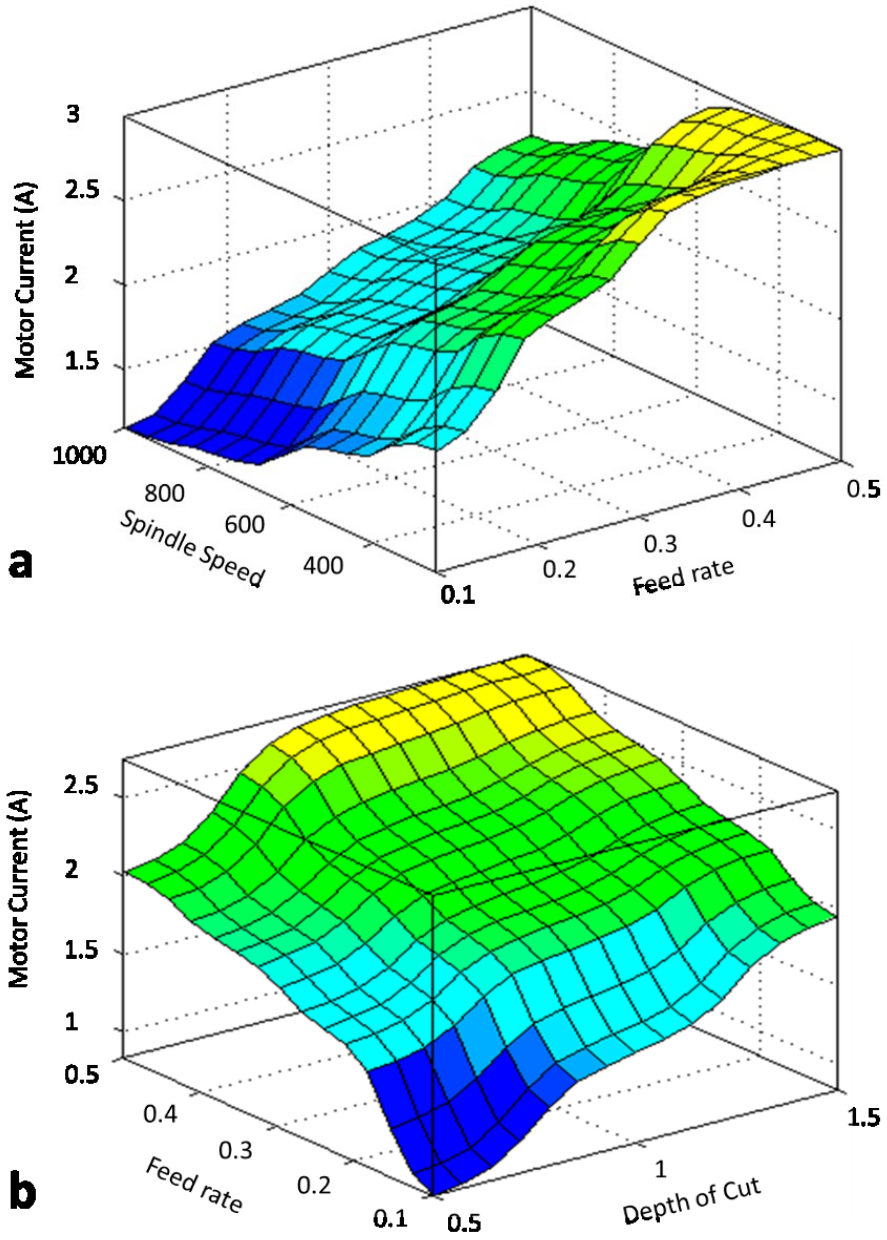

Figure 5.23 Surface plot of servomotor current a) (DOC=1mm) b) (S=625 rpm)

Figure 5.24, presents the printed screen for ANFIS modeling. It shows an example of servomotor current 2.6 Ampere in Z- axis, using a spindle speed of 1000 rpm, a depth of cut 1.5 mm and a feed rate 0.5 mm/rev. The predicted motor current values are carried using this rule viewer; by apply the different values in the range of cutting parameters, to fuzzification the every membership functions

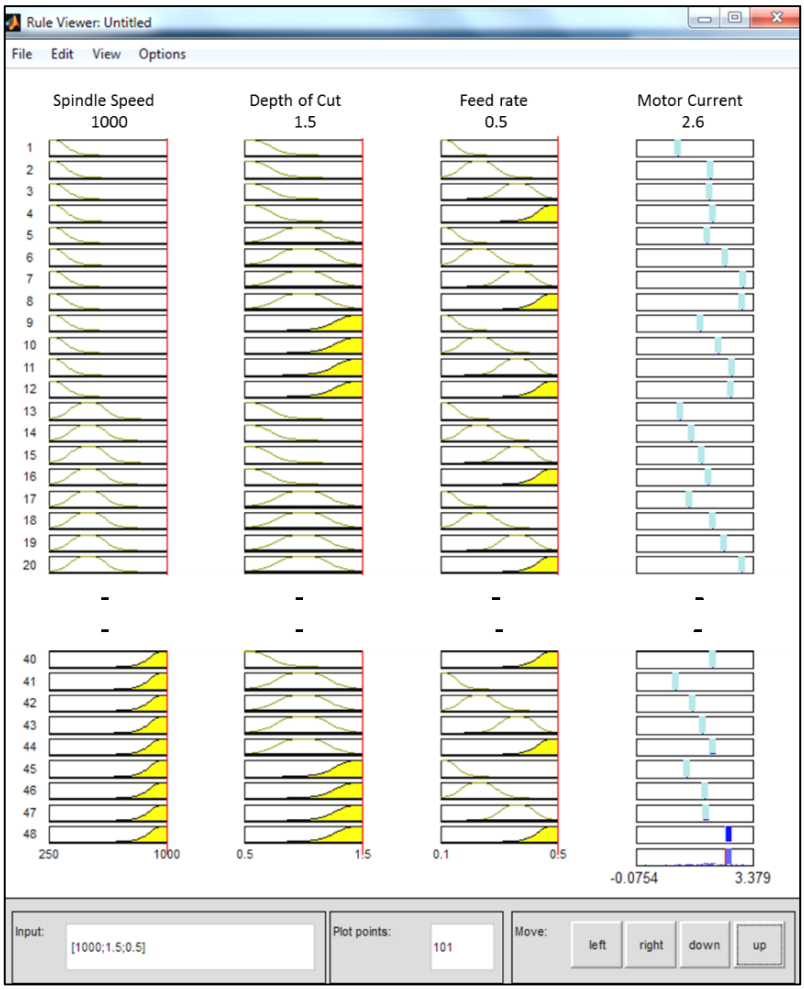

Figure 5.24 The motor current using the rule viewer of ANFIS toolbox

5.4.2.1 Investigation the prediction error and accuracy for motor current

To investigate the error and accuracy in the ANFIS modeling prediction, another 18 experiments are carried out. Table 5.3 shows the conditions of the new 18-experiments. According to this table, the measured motor current increases influenced by increasing the depth of cut and feed rate. However, the spindle speed has an inverse relationship with friction force.

The errors between the proposed ANFIS modeling and experimental is acceptable for 18 steps. The equations 5.5, and 5.6, were shown the percentage of error E and average error E_{av} for friction force, respectively (Refer to section 5.4.1.1).

Table 5.3 ANFIS model prediction error and accuracy for motor current

Exp.	Cutting Condition			Measured Motor Current(A) I	Predictive Motor Current (A) $I_{P(dry)}$	Error % $\%E_Z$	Accuracy %
	Spindle Speed	DOC	Feed Rate				
1	375	0.75	0.2	1.98	2.05	3.54	96.46
2			0.3	2.19	2.27	3.65	96.35
3			0.45	2.47	2.55	3.24	96.76
4		1.25	0. 2	2.21	2.3	4.07	95.93
5			0.3	2.45	2.55	4.08	95.92
6			0.45	2.79	2.87	2.87	97.13
7	625	0.75	0.2	1.66	1.74	4.82	95.18
8			0.3	1.87	1.93	3.21	96.79
9			0.45	2.41	2.31	4.15	95.85
10		1.25	0. 2	1.98	2.09	5.56	94.44
11			0.3	2.15	2.27	5.58	94.42
12			0.45	2.55	2.67	4.71	95.29
13	875	0.75	0.2	1.43	1.49	4.20	95.80
14			0.3	1.59	1.68	5.66	94.34
15			0.45	1.99	2.11	6.03	93.97
16		1.25	0. 2	1.79	1.86	3.91	96.09
17			0.3	1.98	2	1.01	98.99
18			0.45	2.32	2.4	3.45	96.55
Average						4.10	95.90

Figure 5.25, shows the comparison results between motor current measured, and ANFIS modeling methods in Z- axis direction. For this case, the average error has a 4.10% value for Z-axis of the motor current (Figure 5.26). Accordingly, it is apparent that the proposed ANFIS modeling has much better accuracy to use in new technique for lubrication control.

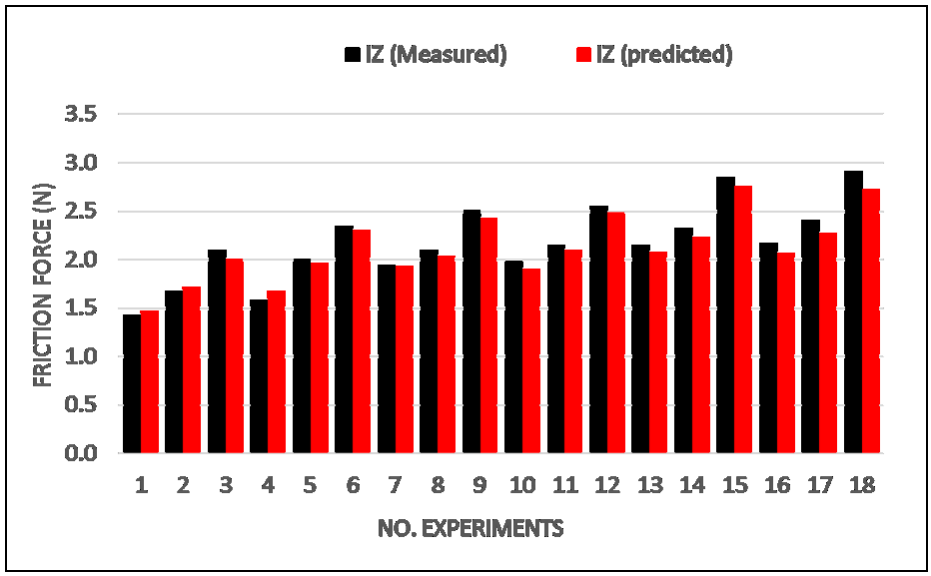

Figure 5.25 Results comparison of servomotor current between measured and predicted

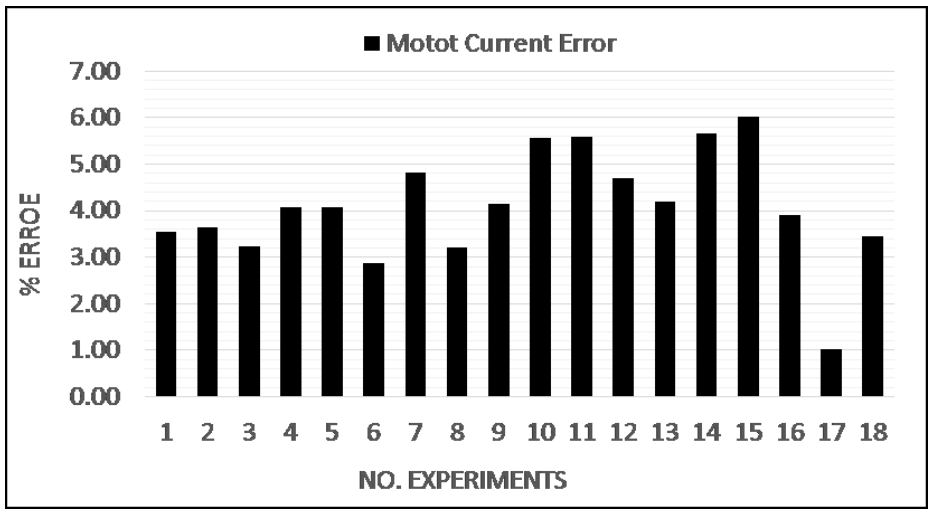

Figure 5.26 Errors in servomotor current using ANFIS modeling direction

5.5 Summary

In this chapter, prediction errors and accuracy in servomotor current and friction forces in CNC machine linear guideways in dry lubrication condition, using ANFIS modeling was considered.

The three significant purpose were considered in this chapter. First, the servomotor forces of affecting forces were calculated in the cutting tool movement ways during machine operations. These forces of the A, B, C modes in such a way that, in two A, and C were calculated non-cutting. Therefore, the servomotor forces result in non-cutting mods were constant values. Nevertheless, during cutting (B mode), the value was a function of the cutting forces.

Second, current consumption of each feed servomotor was measured during a full cutting cycle (refer to Figure 3.28). These values were compared at each of three zone of cutting process. The most significant output is current values, which measured during cutting operation, as shown in Table 5.1.

In third section of this chapter, the measured servomotor current signals and the calculated friction force of linear guideways were analyzed. Friction force that exerted on the linear guideways was calculated by taking into account the equations of X, Z-axes. The motor current ($I_{P(dry)}$) and friction force estimation ($F_{P(dry)}$) were modeled via Adaptive Neuro-Fuzzy Inference System (ANFIS) methods in dry lubrication condition. These methods were compared with mathematical model, which was obtained in previous chapter. A significant reduction errors in ANFIS model was observed. Therefore, these models will be used to control lubrication in the next chapter. This work used ANFIS modeling in order to improve the simulation results. The developed modeling has three inputs including spindle speed, depth of cut, and feed rate, besides one output based on friction force or motor current. ANFIS method was used to obtain a reliable correlation between the parameters. It was observed that the depth of cut, cutting feed rate, and spindle speed, have an effect on the motor current in feed drive system and friction force that exerted on the CNC linear guideways.

CHAPTER 6: LUBRICATION CONTROL SYSTEM BASED ON FRICTION CONDITIONS

6.1 Introduction

In the previous chapter, ANFIS modeling was used to predict servomotor current in feed drive systems and the friction force on linear guideways in dry condition. The two models developed in the last chapter are as follows:

Model 1: ANFIS model to predict the motor current in a feed drive system in dry lubrication condition (I_{dry}).

Model 2: ANFIS model to predict the friction force in linear guideways in dry lubrication condition (F_{dry}).

In this chapter, a lubrication control for CNC machine linear guideways is proposed based on the predicted friction conditions and real measured motor current. In this process, the lubrication amount and time are decided based on the friction force values in the linear guideways (F_{dry}) and servo motor current ratio ($R = \frac{I_M}{I_{dry}}$).

This chapter starts with the proposed algorithm for the lubrication control system (LCS). Next, the LCS stages are introduced and explained in detail. After that, the overall process of measuring and controlling is presented and discussed accordingly. Finally, the experimental setup for the lubrication control system in ordinary lubrication mode and the new lubrication mode technique are consequently confirmed and compared.

6.2 Algorithm of lubrication control system

The ANFIS model is used to build the oil feedback form LCS to be able to predict friction force values at different online servomotor current signals and cutting conditions. Hence, the LCS sends a signal to the actuators to trigger the oil pump to inject oil. The oil

injection amount and time (pump response interval (PRI)) is identified based on the ANFIS-predicted friction force values in linear guideways. The predicted friction force values are categorized in five levels corresponding to five friction force conditions. At each level, the PRI is defined optimally to protect the guideways. Finally, the controller performance is verified trough a new set of experiments where the results of the new proposed lubrication technique are compared with the ordinary lubrication system results. In these tests, several parameters are monitored in both lubrication systems, including servomotor current, cutting force, PRI, and oil consumption.

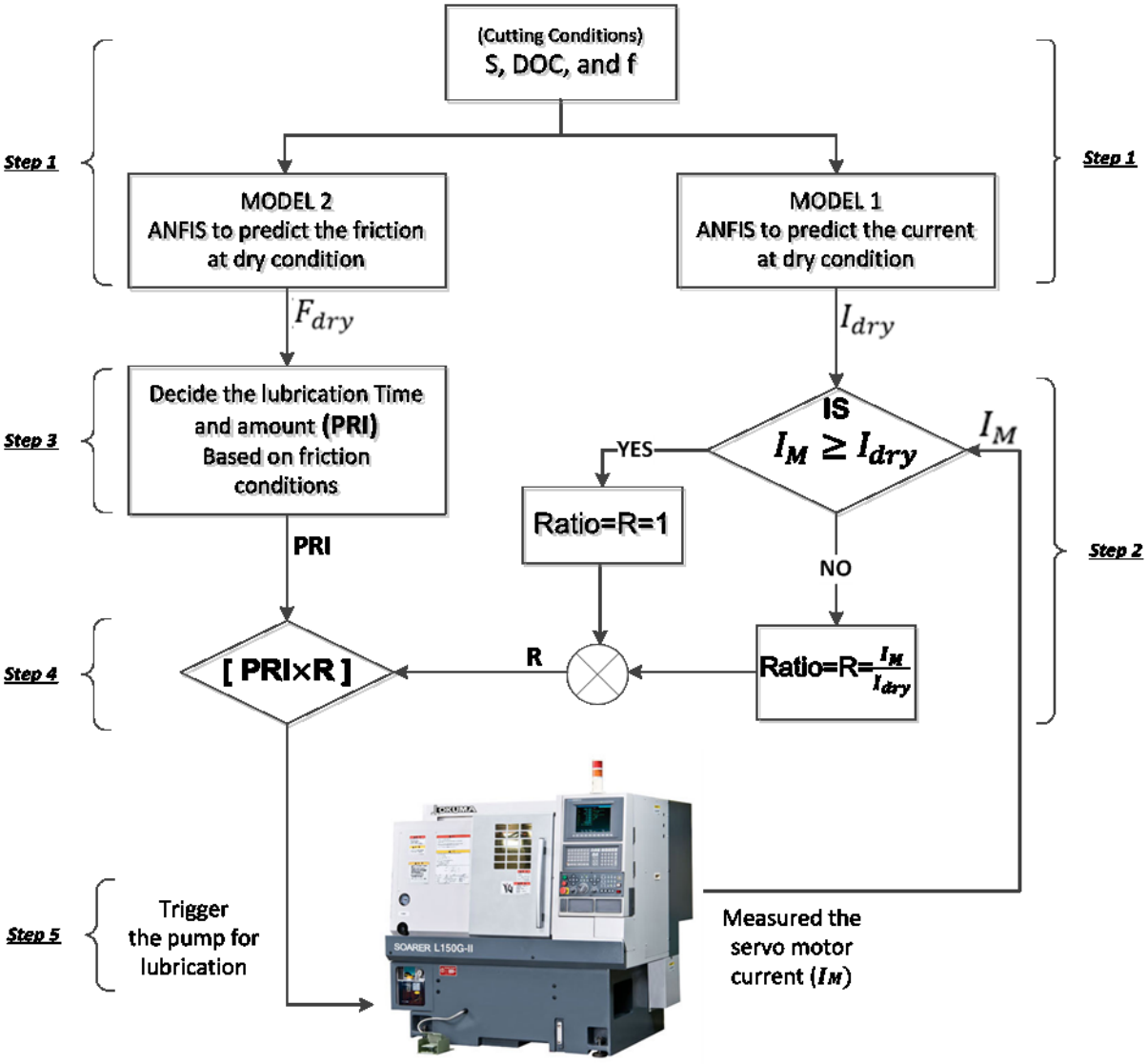

Figure 6.1 Proposed algorithm for the structure of the lubrication control system

The verification experiments were prepared for five cutting levels to ensure the correctness and confirm the control accuracy at different machining conditions. The experiments were repeated three times at each cutting level to prove the reproducibility of the method.

According to the flowchart shown in Figure 6.1, the structure of the lubrication control process includes five (5) steps as follows:

Step 1: Predicting the friction force (F_{dry}) and motor current in dry lubrication condition (I_{dry}); this step was done in the last chapter (refer to sections 5.4.1, and 5.4.2). In that case, ANFIS model 1 was used to predict the motor current in the feed drive system in dry lubrication condition. The relationship between the servomotor current signals in dry lubrication condition and the cutting conditions is important for comparison with real measured motor current in lubrication mode. Therefore, cutting conditions such as spindle speed, depth of cut, and feed rate (S, DOC, and f), were used as inputs to indicate the motor current in the CNC feed drive system as an output in ANFIS model 1.

ANFIS model 2 was used to predict the friction force in linear guideways in dry lubrication condition. The relationship between the friction force in dry lubrication condition and the cutting conditions is important for comparison with the calculated friction force. Therefore, cutting conditions such as spindle speed, depth of cut, and feed rate (S, DOC, and f), could be used as inputs to indicate the friction force in CNC linear guideways as an output in ANFIS model 2.

Step 2: Evaluate the lubrication condition based on the measured servomotor current (I_M): the online measurement of servomotor current has two very significant benefits for the lubrication control system. First, according to the moving tool model (refer to section 3.3.4, Figure 3.28) the cutting operation stages are known for the tool motion model during the

experiments. In other words, increased motor current values represent the state of the cutting operation. Second, the lubrication condition in the guideways is defined using motor current values. For example, for high motor current values, more time and amount of lubricant (PRI) are needed for injection into the machine linear guideways.

In this step, the motor current measured online is compared with that predicted in dry lubrication condition to evaluate the lubrication condition. In fact, the predicted servo motor current in dry lubrication condition (I_{dry}) is the current in machine's overload. If for any reason, such as different cutting conditions, the measured motor current is equal to or greater than the predicted motor current in dry condition ($I_M \geq I_{dry}$), this ratio is assumed to be equal to 1 (R=1). Nevertheless, if the I_M is not greater than I_{dry}, then the real value of the ratio ($R = \frac{I_M}{I_{dry}}$) will be considered in the step5.

Step 3: In this step, the predicted friction force that was previously proposed in ANFIS model 2 is classified. In accordance with the classification, the time and amount of oil injection to the linear guideways is decided. The manufacturers of commercially available CNC machines provided an operation and preventive maintenance plan regarding oil injection interval time (OKUMA, 1998). Therefore, the currently proposed algorithm in Figure 6.2 has five output modes for oil pump operation that are designed as the defined timeout intervals (T= 10, 15, 20, 25, and 30 sec). The oil injection interim time and amount are called the Pump Response Interval (PRI). Lower friction has a lower PRI and higher friction is defined by higher PRI. After every PRI, the pump is turned off for a fixed period of 5 minutes. Pump operations P1 to P5 are defined based on PRI as follows:

$P_1 \rightarrow \text{Injection Time On} = 10 \text{ sec}$

$P_2 \rightarrow \text{Injection Time On} = 15 \text{ sec}$

$P_3 \rightarrow \text{Injection Time On} = 20 \text{ sec}$

$P_4 \rightarrow$ Injection Time On $= 25$ sec

$P_5 \rightarrow$ Injection Time On $= 30$ sec

Based on this, the control algorithm for step 4 is shown in Figure 6.2.

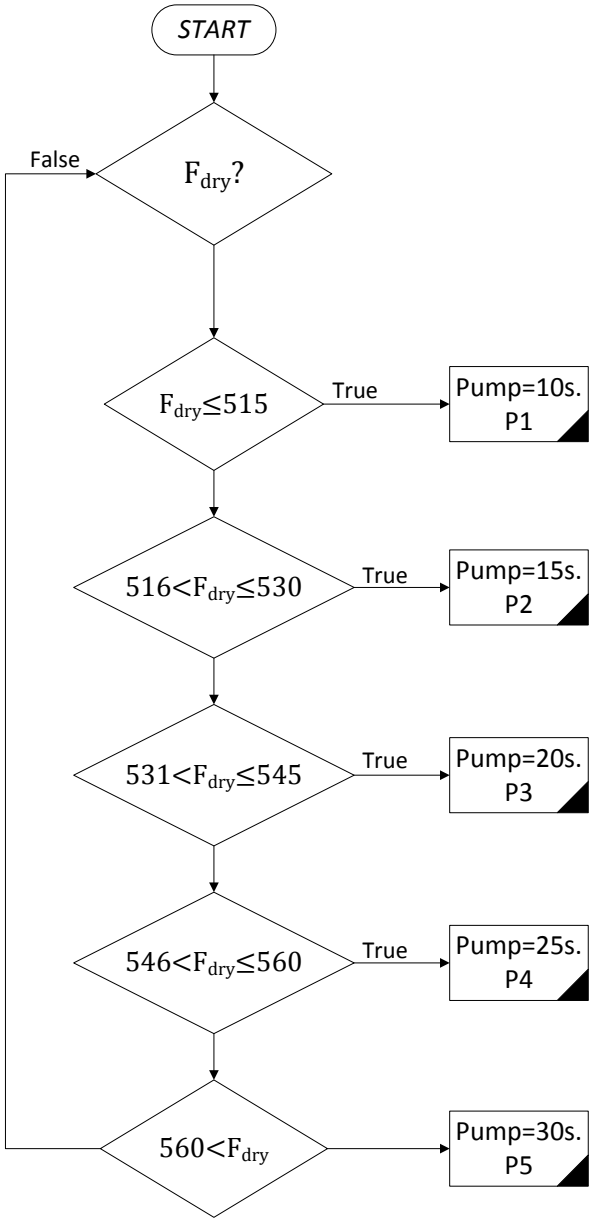

Figure 6.2 Algorithm to select the PRI

According to Figure 6.2, F_{dry} in the first level is selected as less than 515 N. This is because the value is the kinetic friction force in the Z direction (F_{KZ}) that was carried out at low levels of cutting and in dry lubrication condition during machining (refer to chapter 5,

Table 5.1). Additionally, the F_{dry} of the last level is considered bigger than 560 N. This is because the value is the kinetic friction force in the Z direction (F_{KZ}), which was carried out at high levels of cutting and in dry lubrication condition during machining. The other values between 515 N and 560 N are settings based on equal cutting levels.

Step 4: Decided the real PRI based on current ratio: in this step, the PRI that was previously is defined based on friction force levels, is multiplied to ratio of measured servo motor current and predicting the motor current in dry lubrication condition ($\frac{I_M}{I_{dry}}$). The value is rounded for fixing the time to trigger the pump for lubrication.

Step 5: Trigger the pump for oil injection: two ANFIS control system models for converting multi-input to single output are considered in the last section. The names of the single outputs are servomotor current and friction force.

6.3 Visual instrument programs for the lubrication control system

As explained in the methodology chapter on programming design, two main components are the block diagram and front panel windows, which are used simultaneously (refer to section 3.3). The front panel window is a user interface (UI) for the visual instrument (VI). It has controls and indicators with input and output terminals respectively. In the block diagram window, a series of graphical codes called “function pallets” graphically show the design created in the front panel. It can be used to control the front panel components via graphical symbols of functions.

The lubrication control system contains a number of loops. Each of these loops is responsible for specific tasks in the overall process of measuring and controlling. These tasks include measuring system parameters, reading and writing of text files and lubrication operation control. These loops are described next.

6.3.1 Lubrication operation control loop

To design the lubrication operation control loop a simulation of this model is needed for graphical testing before connecting to the CNC machine for the final test. According to the block diagram in Figure 6.3, the control model is connected to DAQ Assistant Express VI. The output of this while loop would be appropriate to trigger a relay 12 DC V and maximum 1 Amp for lubrication operation.

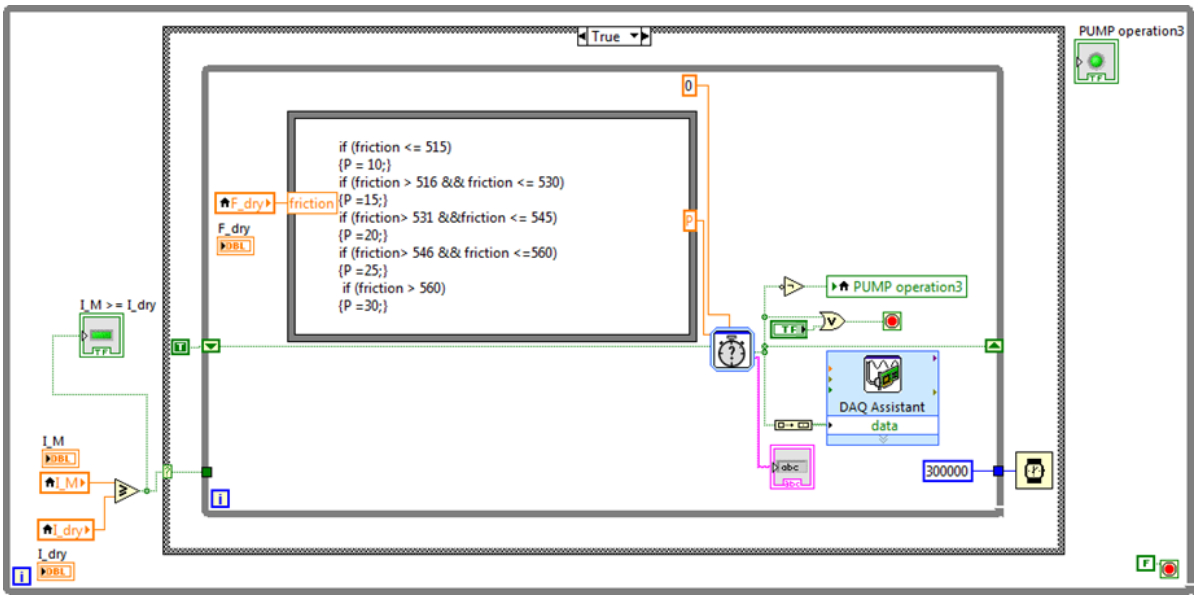

Figure 6.3 Block diagram of friction control with digital output

Actually, the control model is designed as a timer for lubrication control. This timer works based on the predicted friction force range. The range is obtained from many experiments in training and testing mode (refer to section 5.4.2). According to the algorithm in Figure 6.3, the minimum and maximum values of friction force on linear guideways are divided into 5 parts based on the experimental and manufacturer's instructions. This classification can be modified depending on different types of servo drive system and CNC cutting parameters. As already described, the cutting parameters and variations in servomotor current consumption can definitely change the friction force values directly.

In this structure, an input is created based on local variables of friction force data. After writing commands such as coding regarding algorithm control, an output (P) is created based on five states of injection time. Then a while loop with a stop button is required around the formula node and the controls. The start time will be zero, and the output will be 5 minutes (300.000 msec.) off for every output.

For example, if the friction force value is fixed at 525 N in this program the control design will be:

If (friction > 516 && friction <= 530) (P =15).

Therefore, the amount and time of oil injection (pump response interval (PRI)) will be 15 sec.

6.3.2 The overall process of measuring and controlling

As previously mentioned, any CNC lathe machine has at least two axes of motion. The moving table and its accessories slide on these axes via servomotor support. This sliding generates friction at contact points. The parameter that needs to be measured in the early stages of the experiments is cutting force. As explained in Section 4.2 on how to measure cutting forces, these forces have a direct effect on estimating the friction force. It must be noted that cutting force measurement is necessary only in early-stage experiments for designing a control model. In this stage, the measured and predicted friction forces can be compared. After designing the control model, only cutting parameters including spindle speed, depth of cut, and feed rate, must be manually recorded in that control. The cutting parameters do not always change, but they only change with machining changes based on the experience of the machine operator. These variations are recorded in the lubrication control model at any time.

In continuation of the above, in designing the lubrication control model, another parameter is necessary. With measuring the servomotor current and recording its moment variations, the control model inputs are completed. Since movement onto the Z-axis during machining with the CNC machine is far greater than the X-axis, controlling one axis produces similar results as other axes. Therefore, the control model was designed only for the Z-axis.

According to the overall diagram, which is shown in Figure 6.4 the peak-to-peak of motor current on the Z-axis was measured. The maximum value of motor current as one of four input data was stored in the text file. Therefore, three necessary input data for the control model include spindle speed, depth of cut and feed rate.

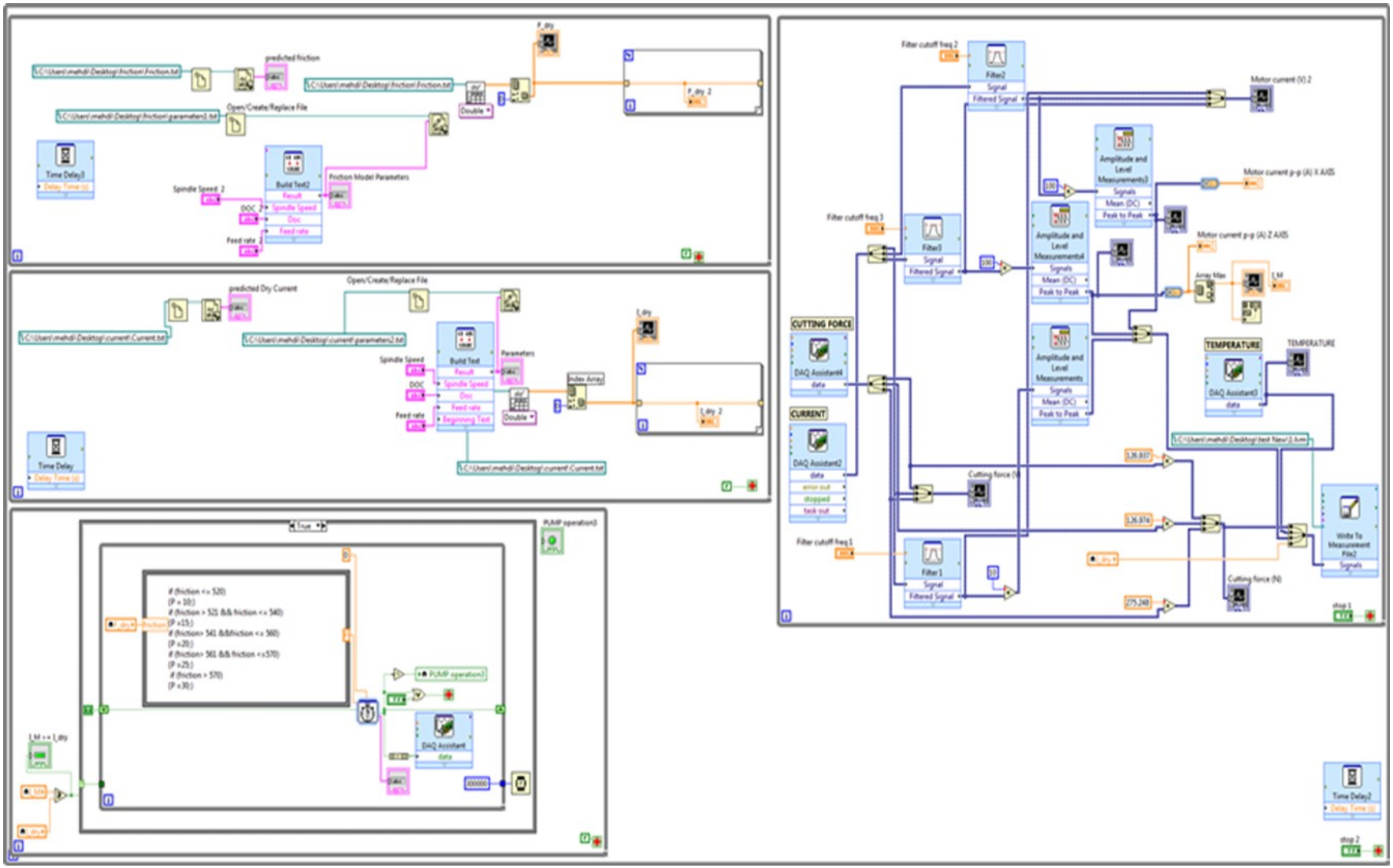

Figure 6.4 Overall block diagram for lubrication control based on friction condition

The block diagram above provides a front panel as shown in Figure 6.5. This panel consists of three Tab controls. In the first Tab, the temperature of the four thermocouples and cutting force values is designed as a waveform chart. In cutting force values, the components of voltage signals become force signals. The temperature of each thermocouple has a little variation.

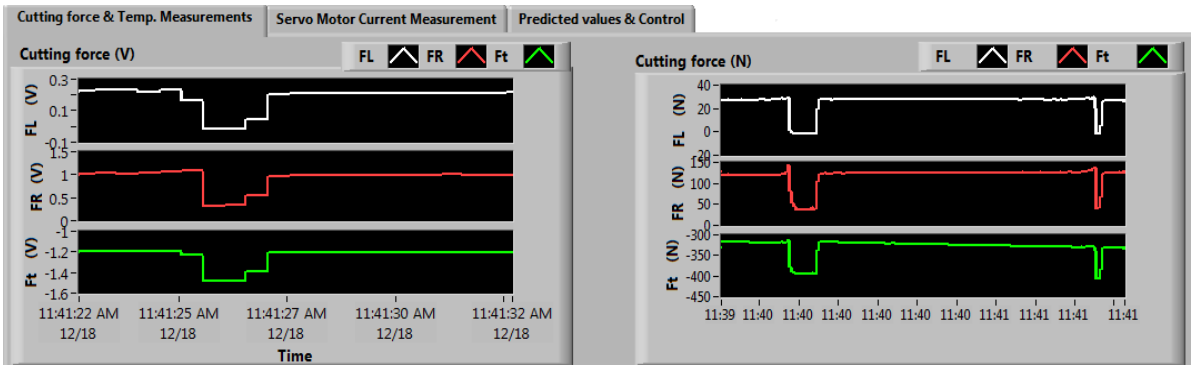

Figure 6.5 The first tab that displays and controls in the front panel

The second tab shows the filtered measured values of motor current for spindle X and the Z-axis. Low pass filtering signals with 150 (HZ) cutoff frequency were set to provide a smoother signal form, removing the short-term fluctuations, and leaving the longer-term trend. Moreover, in this tab, peak-to-peak amplitude measurements and the maximum current values for servo drivers are given (Figure 6.6). During the machining operation, whenever a change is in order for the tool, a sharp fluctuation is observed. Because of this, fluctuations are moment fluctuations, which is why they are not calculated in the measurement. As noted above, applying a filter can reduce these fluctuations.

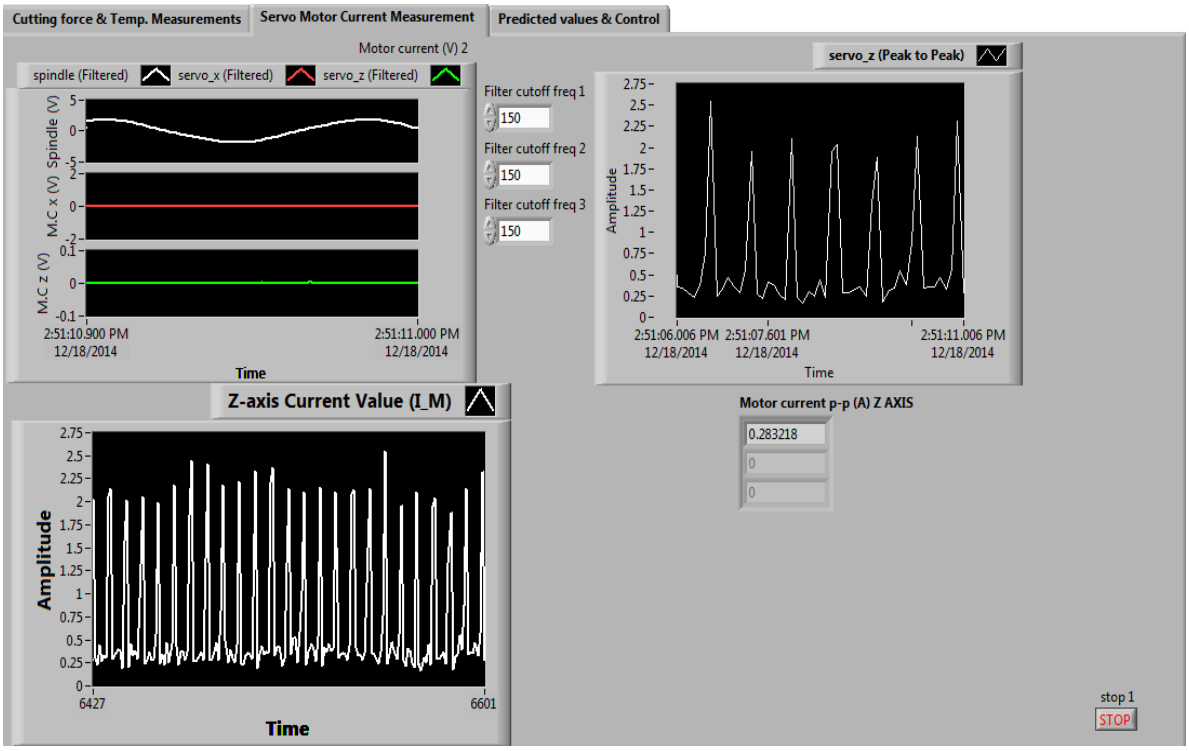

Figure 6.6 Servomotor Current Measurement tab in the front panel

Figure 6.7 shows the third tab, "Predicted values & Control," where current and friction value graphs are observed. Input numerical values consist of cutting conditions (spindle speed, depth of cut, feed rate) provided at the bottom of the graphs based on machining. Moreover, after measuring the maximum servomotor current, there will be another input signal for the control. These parameters are collected and stored in a text file. Predicted friction is obtained through the designed control as a single output. According to the maximum value of predicted friction, the Pump Response Interval (PRI) for oil injection to linear guideways is set by the lubrication control system. The oil injection time with fixed PRI is recorded in "loop iterations."

The green LED light will be ON during oil injection, and it turns off while the pump is not injecting.

The values shown in Figure 6.7 are an example of several experiments conducted. The oil injection time, or PRI, of 30 seconds is recorded (Elapsed time = 30 sec).

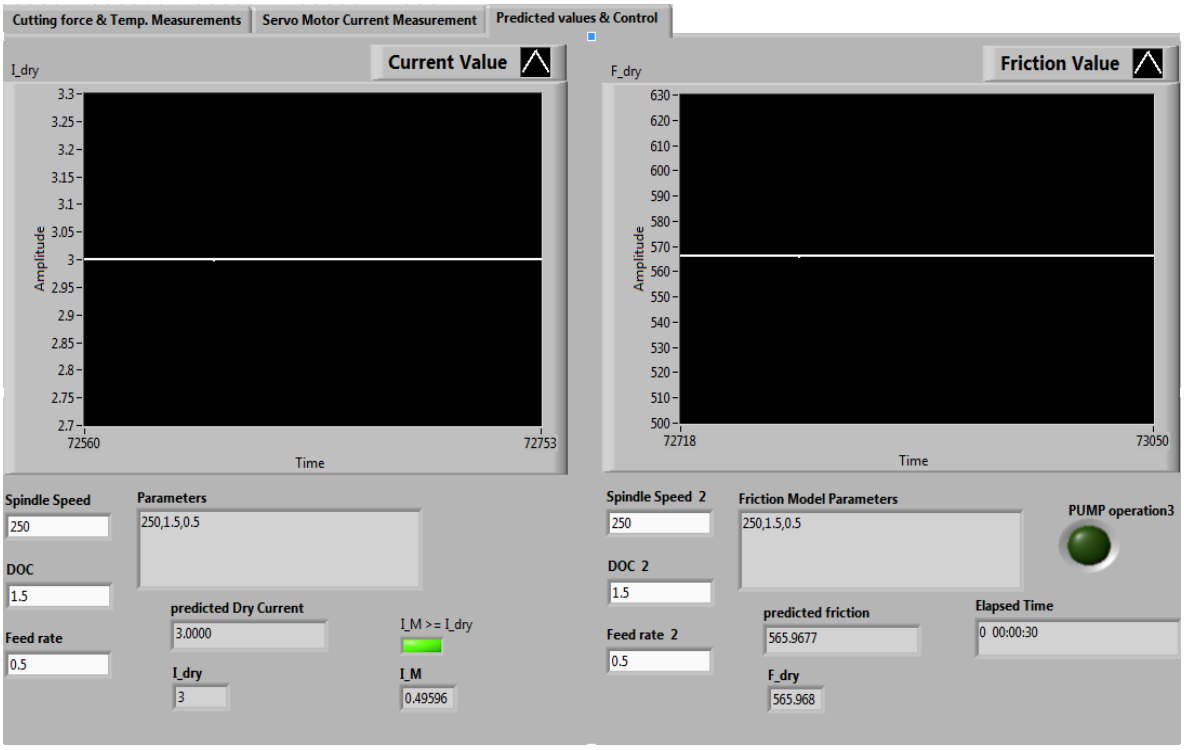

Figure 6.7 Predicted values and control tab in front panel

6.4 Experimental setup for the lubrication control system

The tool's movement model during finishing was discussed in chapter 3 (refer to Figure 3.28). Figure 6.8 schematically shows the tool's movement model during roughing in the experiments. According to Figure 6.8, the sample moving model of the cutting tool starts at point "A," undergoes the cutting process, and returns to point "A." Furthermore, regarding the behavior of the model, cutting takes place on the D-E path (220 mm). The depth of cut, feed rate and cutting speed, which are already defined in each experiment, are generated at this time. The moving part moves along the motion path and undertakes several forward and back motions. In each experiment, cyclic motions within the cyclic motions are repeatedly performed to obtain the average behavior of friction.

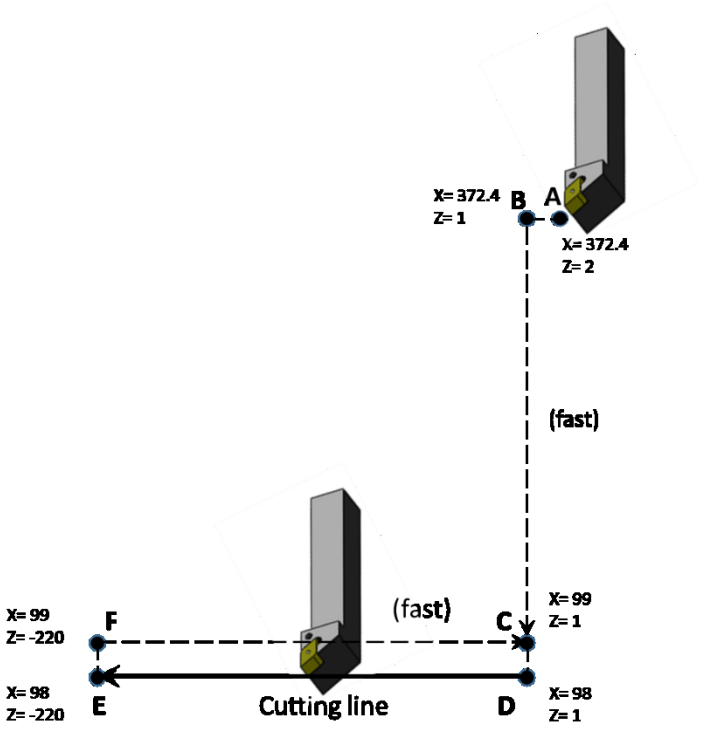

Figure 6.8 Tool movement model during roughing

Typically, friction on linear guideways is influenced by cutting force. Cutting force variations are caused by machining process changes. This process is normally called rough turning, medium turning, or finish turning. The decision to use the machining process is proportional to the material of the tools and workpiece. One correct method is to define these operations by the amount of remove chippings of cutting. However, there are other factors such as material, cutting conditions and other variables.

The experiments were prepared at five cutting force levels to ensure correctness and confirm the control accuracy in different machining conditions. The three main levels of cutting force are given in Table 6.1:

Table 6.1 The five levels of cutting force based on the experiments

Cutting Levels	Descriptions of experiments
Level 1 Low (Finishing Turning)	Low depth of cut and feed rate but high cutting speeds create a smooth and polished surface. According to the name of the turning level, it is the final phase of the operation. Although forces on the cutting tool are too little, there is still high cutting quality. At this level, the depth of cutting per side is less than 0.5 mm.
Level 2	Lower speed and higher feed rate than level 1 at the same depth of cut.
Level 3 Medium (Medium turning)	Standard range of depth of cut and feed rate with suitable cutting speed, create the best cutting operation. In this case, forces on the cutting tool are appropriate. It is the best operation in terms of time and cost. The depth of cutting per side is 0.5 – 1 mm. Many manufacturers make the mistake of applying a roughing tool when a medium turning tool is needed. Using an incorrect tool causes an increase in cycle time and direct tool cost, as well as a drop in profitability.
Level 4	Higher speed and lower feed rate than level 5 at the same depth of cut.
Level 5 High (Rough turning)	High depth of cut and feed rate but low cutting speed, create rough turning operation. In this operation, depth of cutting per side is more than 1.5 mm, and too much force is applied to the cutting tool.

6.4.1 Ordinary Lubrication Mode

According to the five levels of cutting force described above, the experimental results are compiled in Table 6.2 and Table 6.3. Maximum peak-to-peak servomotor current values in the Z direction are monitored. Moreover, the average is taken from three components of cutting force on the cutting tool. The kinetic friction force on the Z-axis linear guideways is achieved based on the cutting force. The calculated friction force is with respect to the mathematical model presented in Chapter 4 (refer to Eq. 4.14).

The motor current and friction force values predicted by the simulated model are shown in Table 6.3. However, the time of oil injection (PRI) is proportional to the ordinary mode of machine lubrication pump. The machine maker recommended this time, and it is fixed during ordinary mode machining. According to the oil pump specifications, the unit volume of oil transfer is 108 ml/min (refer to Table 3.3). Therefore, the oil consumption is fixed at 54 ml in all five cutting levels for one cycle of pump operation (ON/OFF time).

Table 6.2 Calculated friction force based on cutting forces

Cutting Level	Cutting conditions			Average Cutting Forces (N)			Calculated Friction Force (N)
	Speed rpm	DOC mm	Feed Rate mm/rev	Longitudinal (FL)	Radial (FR)	Tangential (Ft)	Z-Axis ***F***
1 (Low)	1000	0.5	0.1	125.481	85.923	95.312	510.27
2	750	0.5	0.25	176.254	78.34	219.5	526.15
3 (Medium)	500	1	0.25	424.231	403.12	628.11	541.81
4	500	1.5	0.4	675.341	597.54	989.2	556.24
5 (High)	250	1.5	0.5	521.166	246.23	780.1	564.95

Table 6.3 Oil consumption based on fixed PRI time in ordinary mode

Cutting Level	Cutting conditions			Measured Current	Predicted Current	Predicted Friction	injection time	Oil Consumption
	Speed rpm	DOC mm	Feed Rate mm/rev	I_M(A)	I_{dry}(A)	F_{dry}(N)	PRI	ml.
1 (Low)	1000	0.5	0.1	1.45	1.23	510.3	30Sec.	54
2	750	0.5	0.25	1.73	1.55	526.2	30Sec.	54
3 (Medium)	500	1	0.25	2.36	2.18	541.8	30Sec.	54
4	500	1.5	0.4	2.55	2.62	556.2	30Sec.	54
5 (High)	250	1.5	0.5	2.64	3	564.9	30Sec.	54

Peak-to-peak servomotor current curves for the five selected levels of cutting force include low, medium, and high as shown in Figure 6.9 to Figure 6.13 respectively. Extreme fluctuation is observed in all of these curves due to the moment of movement change in

servomotor direction. It should be mentioned that values of this big fluctuation could not be effected in current measurement and control of friction and lubrication in finally.

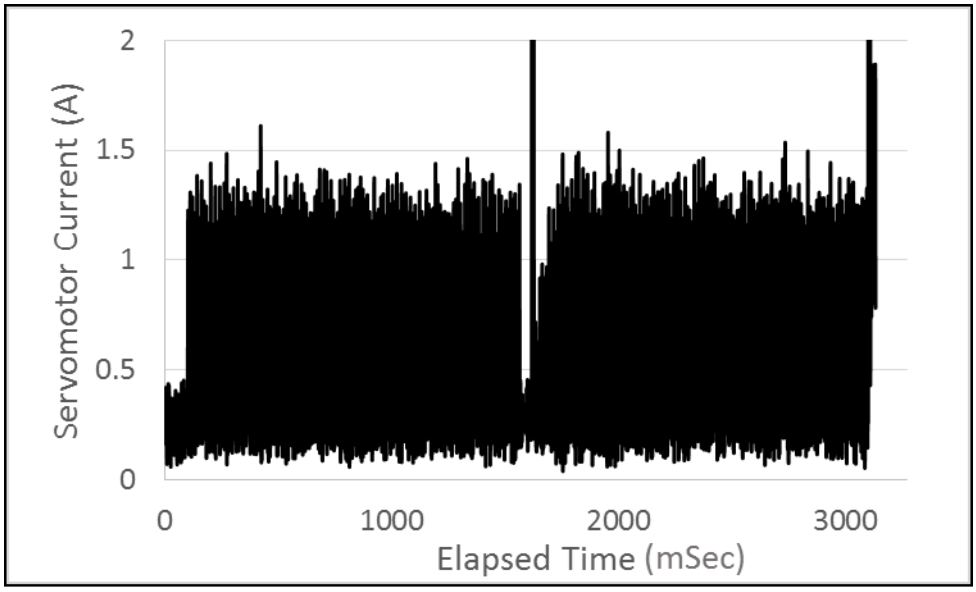

Figure 6.9 Measured servomotor current in ordinary mode at low level

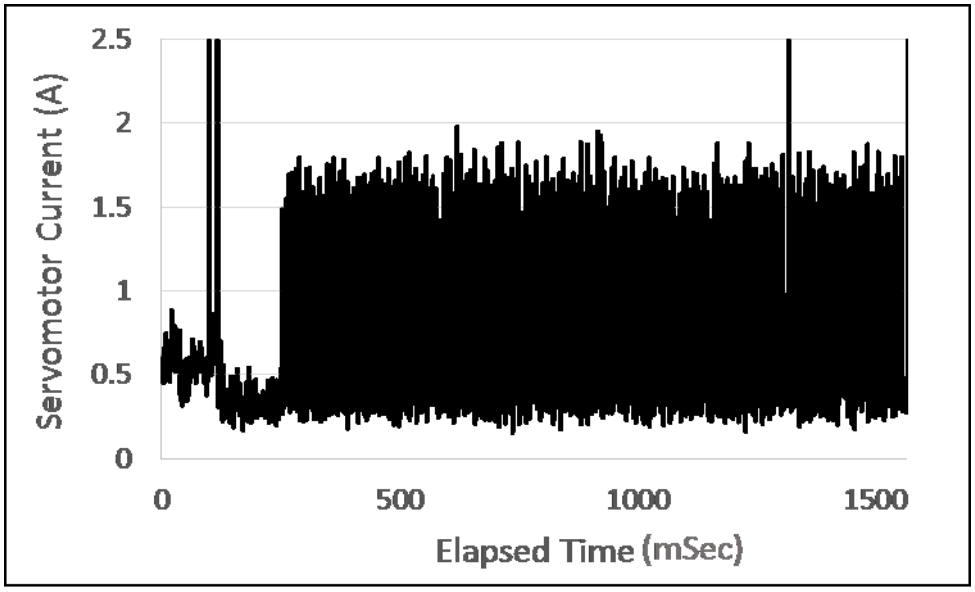

Figure 6.10 Measured servomotor current in ordinary mode at level 2

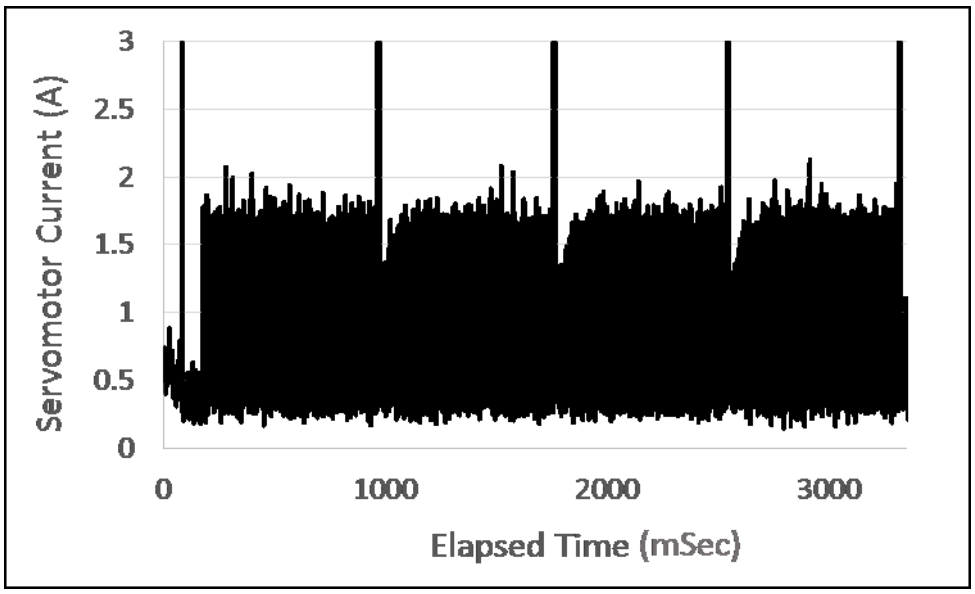

Figure 6.11 Measured servomotor current in ordinary mode at medium level

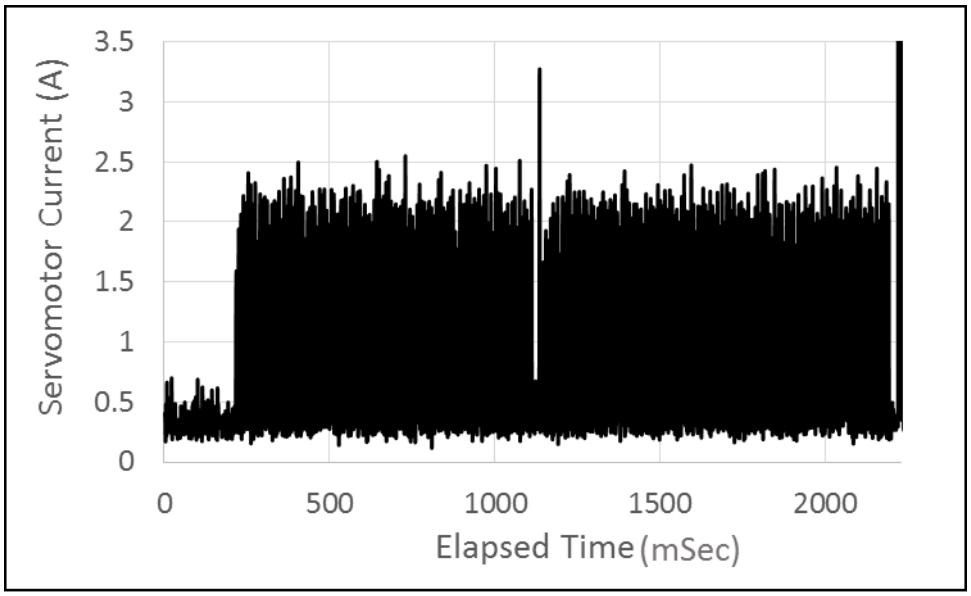

Figure 6.12 Measured servomotor current in ordinary mode at level 4

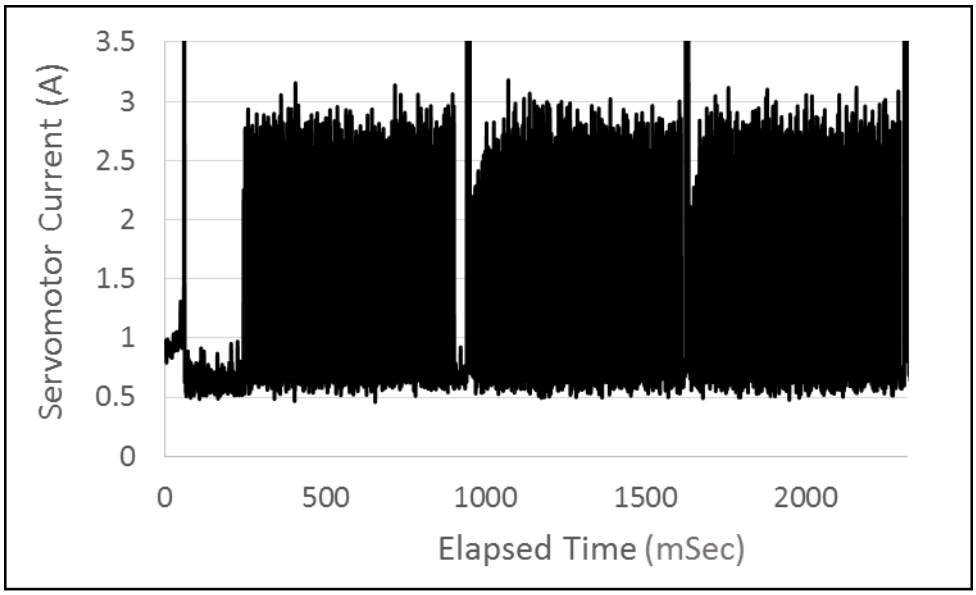

Figure 6.13 Measured servomotor current in ordinary mode at high level

6.4.2 New lubrication mode technique

Experiments that were performed in ordinary mode are repeated for this technique. In these tests, several parameters are monitored in the new lubrication technique, including temperature, servomotor current, cutting force, PRI, and oil consumption. The experiments were prepared for five levels of cutting force to ensure correctness and confirm the control accuracy in different machining conditions. There are three main cutting levels, namely low, medium, and high level, according to finishing turning, medium turning, and rough turning, respectively. The experimental results for these levels are compared. Temperature, servomotor current, and cutting force measurement are almost the same and not significantly different in each one of these levels. Meanwhile, PRI and oil consumption are different in both lubrication modes (ordinary and new technique) during a fixed machining time.

Table 6.4 Oil consumption based on variable PRI time in the new lubrication mode

Cutting Level	Measured Current I_M(A)	Predicted Current I_{dry}(A)	Is $I_M \geq I_{dry}$	R	Predicted Friction F_{dry}(N)	injection time PRI	Oil consumption ml.
1 (Low)	1.51	1.23	√	1	510.3	10sec.	18
2	1.78	1.55	√	1	526.2	15sec	27
3 (Medium)	2.47	2.18	√	1	541.8	20sec	36
4	2.58	2.62	×	0.98	556.2	24sec	43.2
5 (High)	2.78	3	×	0.92	564.9	28sec	50.4

As shown in Table 6.4, the predicted friction forces are obtained based on the simulated ANFIS model. In the new lubrication mode technique, the time and amount of oil injection (PRI) is not constant and it depends on the predicted friction variation and current ratio. This time follows the designed algorithm (refer to Figure 6.2). The PRI for low, medium, and high levels is 10, 20, and 28 seconds, respectively. Therefore, oil consumption was measured as 18, 36, and 50.4 ml, correspondingly (Table 6.4). However, according to the measured and predicted motor current, there is 43.2, and 50.4 ml oil injection at levels 4 and 5 respectively, because at these cutting levels the online measured current is less than the predicted motor current. This implies that there is lubricant in the linear guideways and additional oil injection based on servo motor current ratio is required. Thus, the oil injection time is multiplied to ratio of measured servo motor current and predicting the motor current in dry lubrication condition ($\frac{I_M}{I_{dry}}$). The value is rounded for fixing the time to trigger the pump for lubrication.

The curves of servomotor current for the new lubrication technique were measured at the five cutting force levels. The maximum peak-to-peaks of monitored motor current are shown in Figure 6.14 to Figure 6.18. In this technique, the motor current value is a little

higher than ordinary mode.

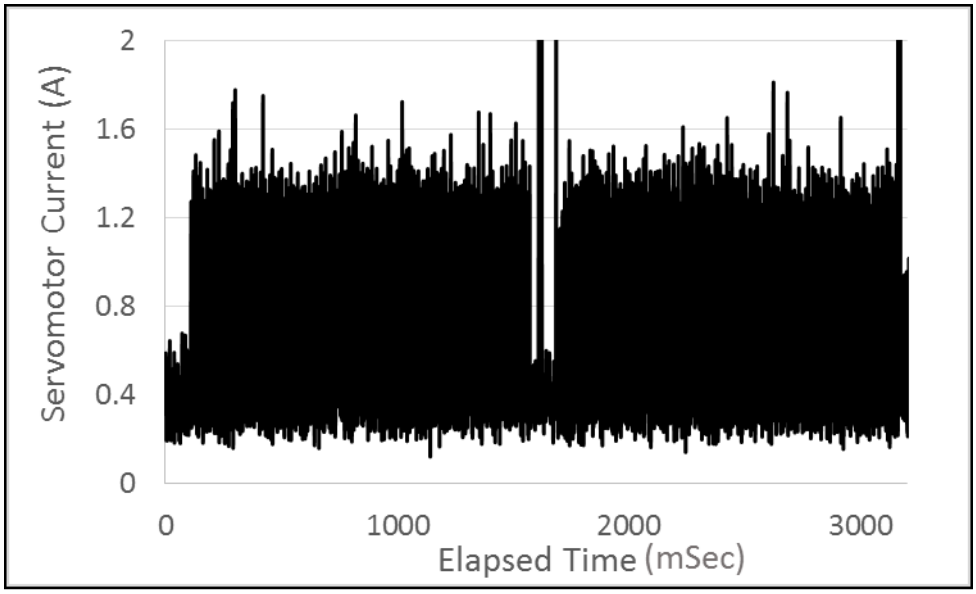

Figure 6.14 Measured servomotor current in new technique mode for low level

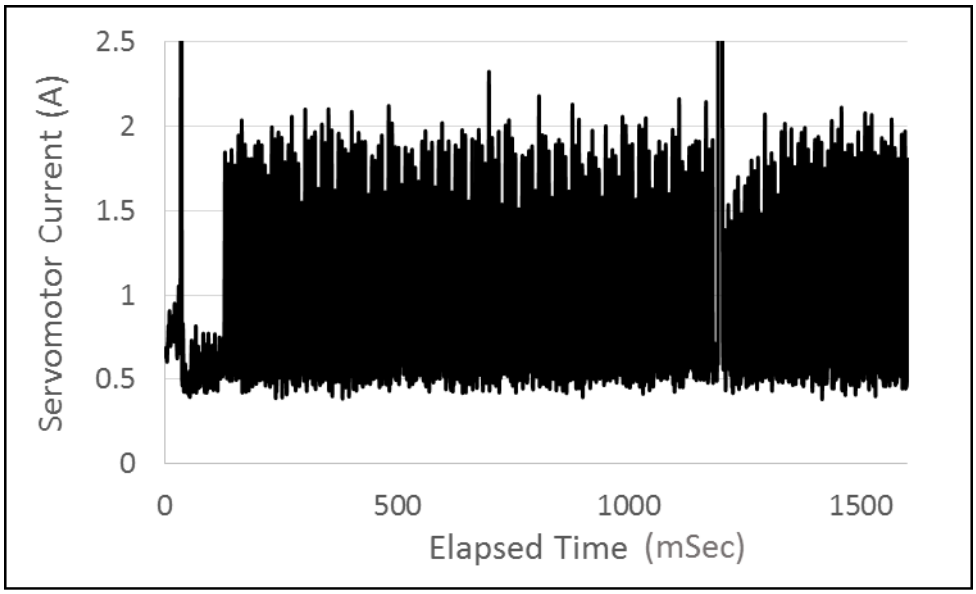

Figure 6.15 Measured servomotor current in new technique mode for level 2

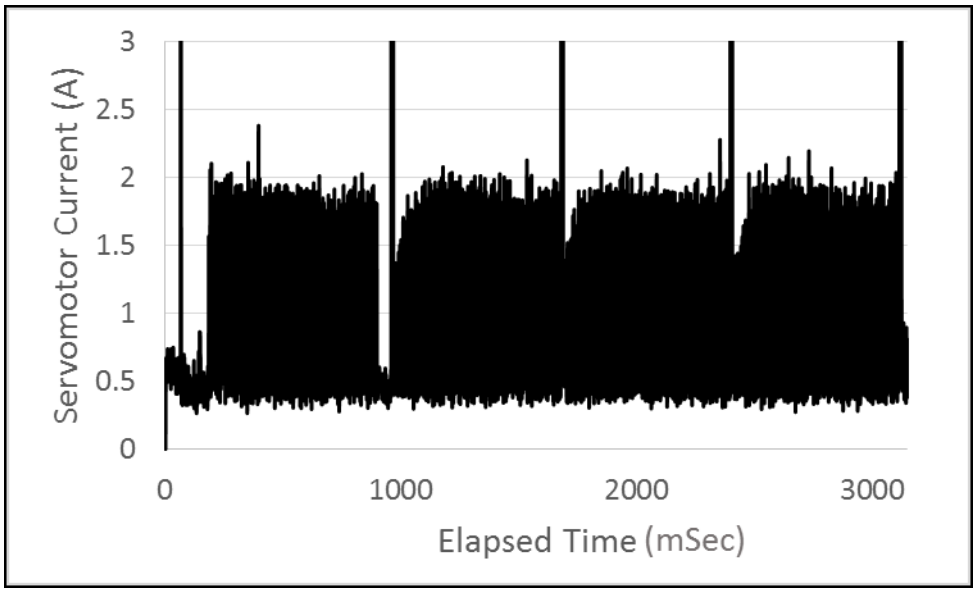

Figure 6.16 Measured servomotor current in new technique mode for medium level

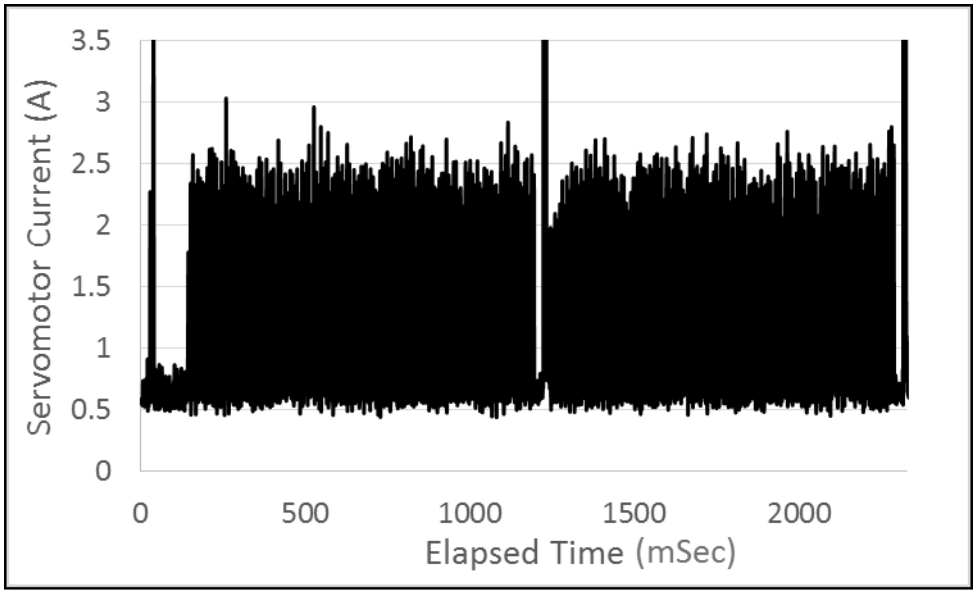

Figure 6.17 Measured servomotor current in new technique mode for level 4

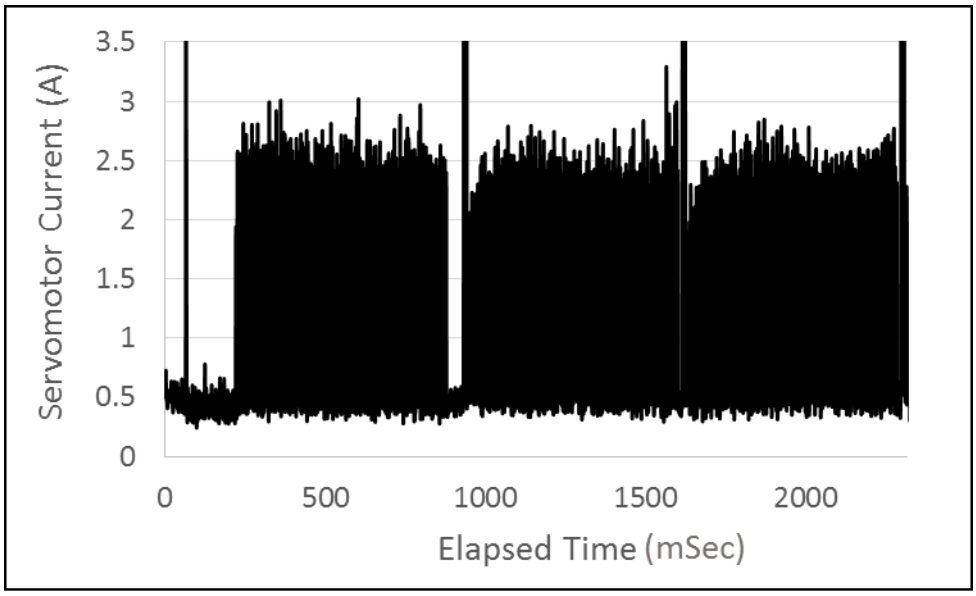

Figure 6.18 Measured servomotor current in new technique mode for high level

6.4.3 Comparison of Results

In this thesis, to achieve our objectives some results can be compared including servomotor current comparison, and time/amount of oil consumption comparison. These comparisons occurs between the ordinary and new lubrication technique modes.

The first cutting force level (low level) is shown in Figure 6.19. In this test, the amplitude fluctuations of motor current in ordinary mode are lower than the new lubrication mode. This change is not significant. Indeed, the friction force in linear guideways in ordinary mode is less than in the new technique because the oil consumption in ordinary mode is greater than the new technique. Meanwhile, Figure 6.19 shows that the servomotor current in the new technique increased negligibly compared with ordinary lubrication. Table 5.1 shows the measured motor current values based on cutting conditions, thus confirming this issue.

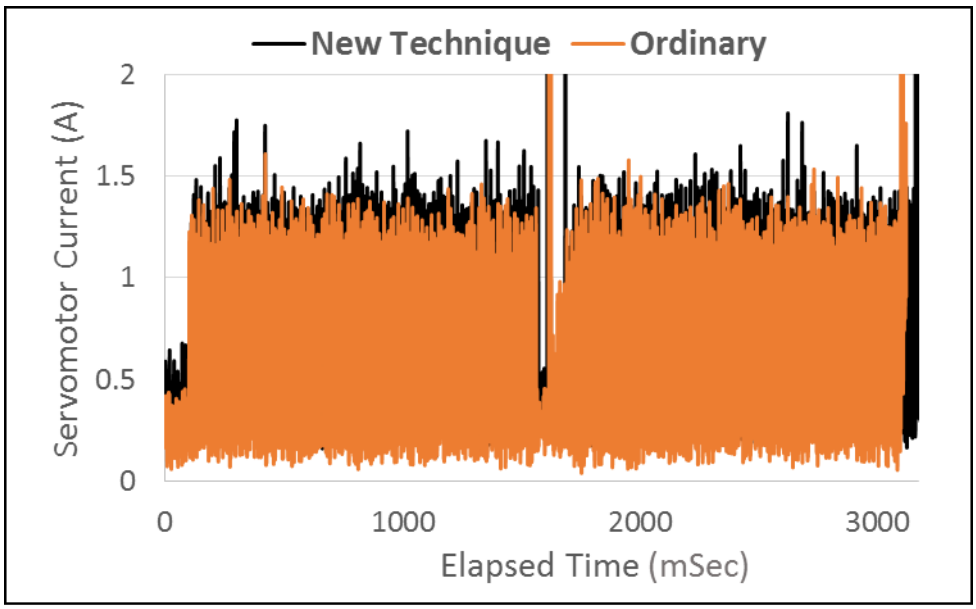

Figure 6.19 Measured servomotor current comparison (low level)

Figure 6.20 shows the second level of cutting force. Also in this level, the servomotor current in the new lubrication mode is higher than ordinary mode.

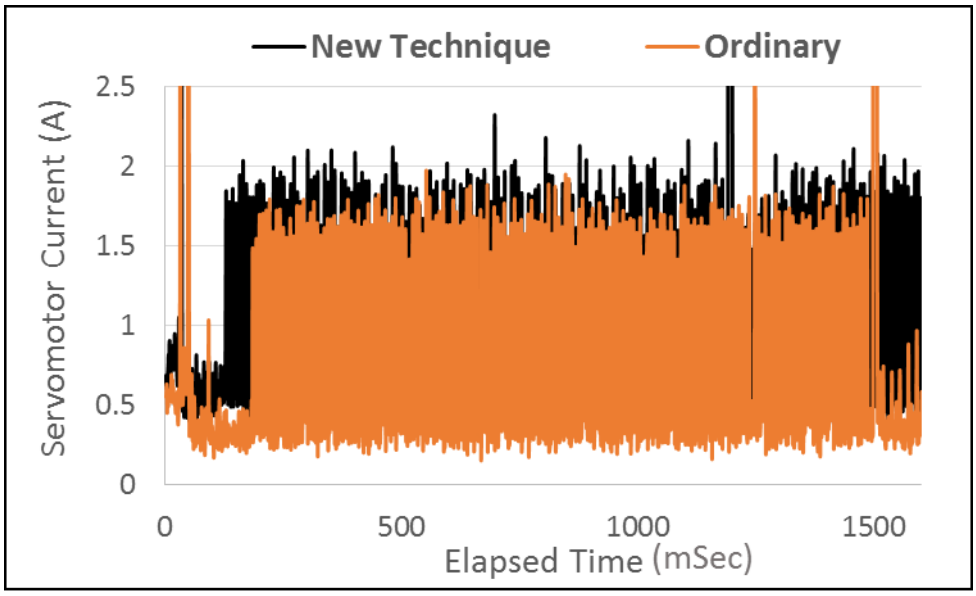

Figure 6.20 Measured servomotor current comparison for level 2

The medium level also confirms that the motor current in ordinary mode is lower than the new techniqe as illustrated in Figure 6.21.

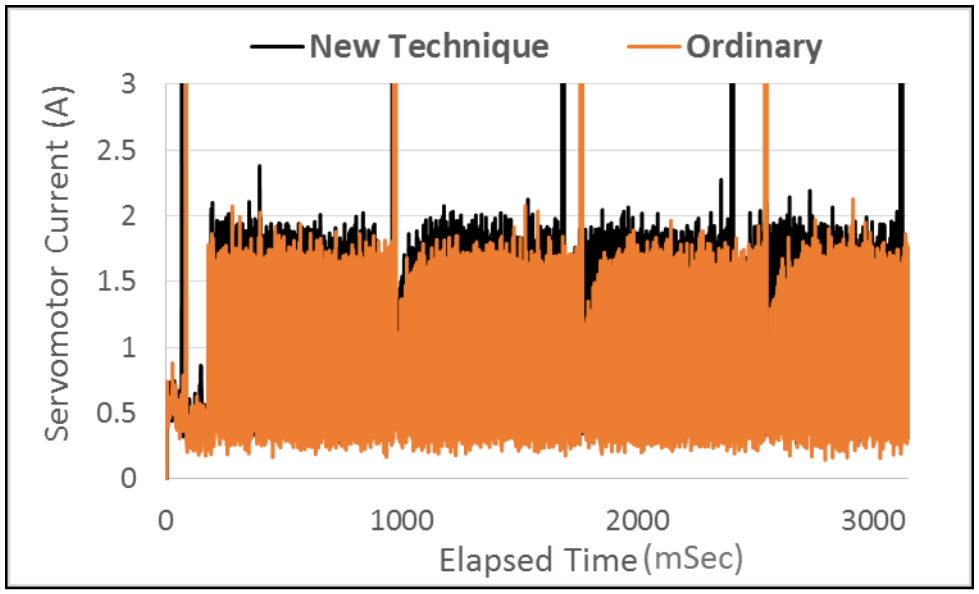

Figure 6.21 Measured servomotor current comparison (medium level)

There considerable fluctuations are evident in Figure 6.22. This demonstrates the cutting operation in workpiece levels in the experiment. In addition, motor current behavior is similar to previous levels.

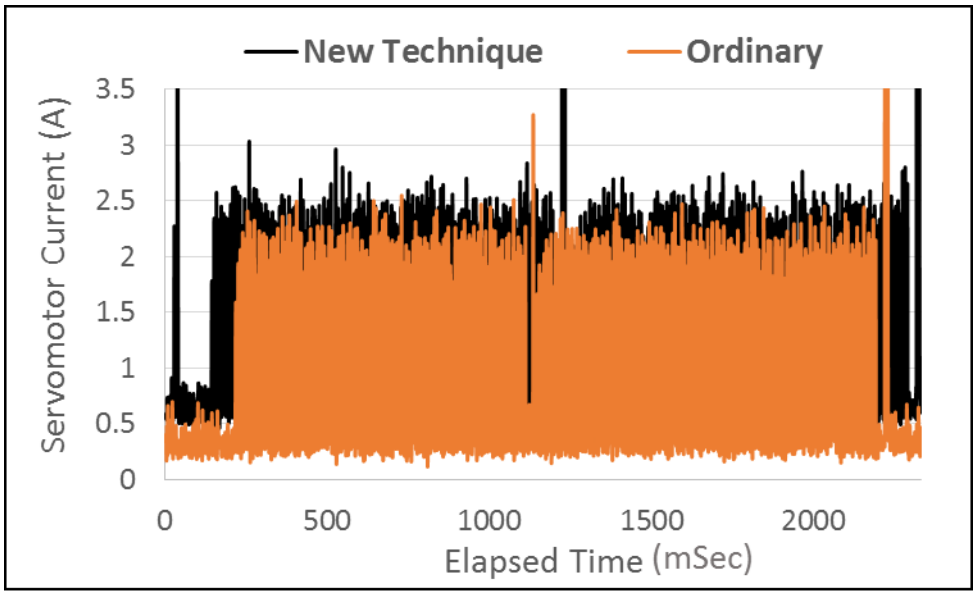

Figure 6.22 Measured servomotor current comparison for level 4

A high cutting force level is seen in Figure 6.23. In the high-level test, the amplitude

fluctuations of motor current in ordinary mode are lower than new lubrication mode. This difference is not significant. Indeed, the friction force in linear guideways in ordinary mode is less than the new technique mode because the time and amount of oil injection in ordinary mode is more than the new technique mode. Moreover, Figure 6.23 displays that the servomotor current increase in the new technique mode is negligible compared with ordinary lubrication.

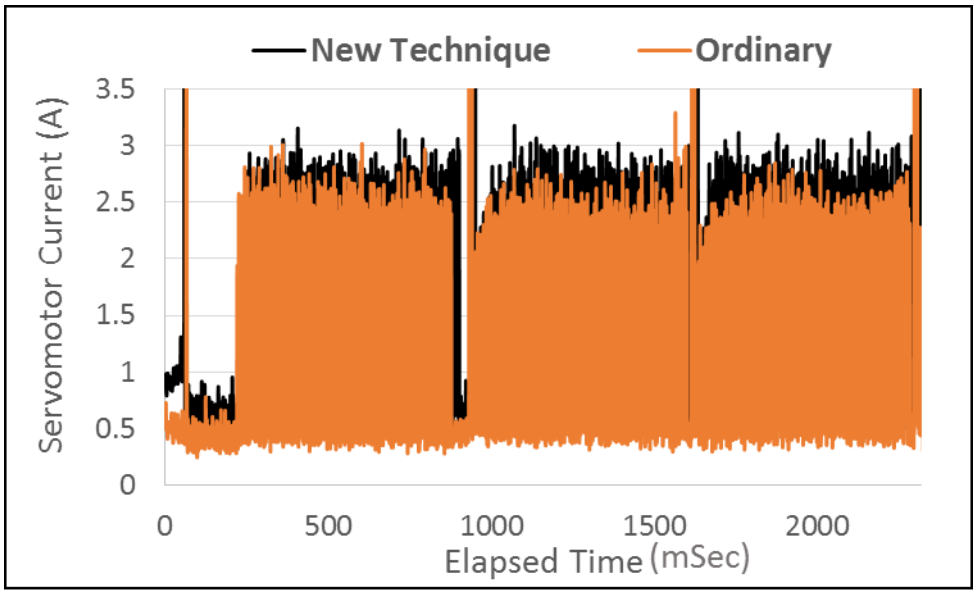

Figure 6.23 Measured servomotor current comparison (high level)

The maximum peak-to-peak servomotor current values are compared for different cutting force levels. The average values of these results are shown in the chart column of Figure 6.24. The maximum value is measured online via the control system for both ordinary and new technique modes for all cutting force levels. The average of the absolute deviations for motor current values at high level is 0.07, while at medium and low levels it is 0.01.

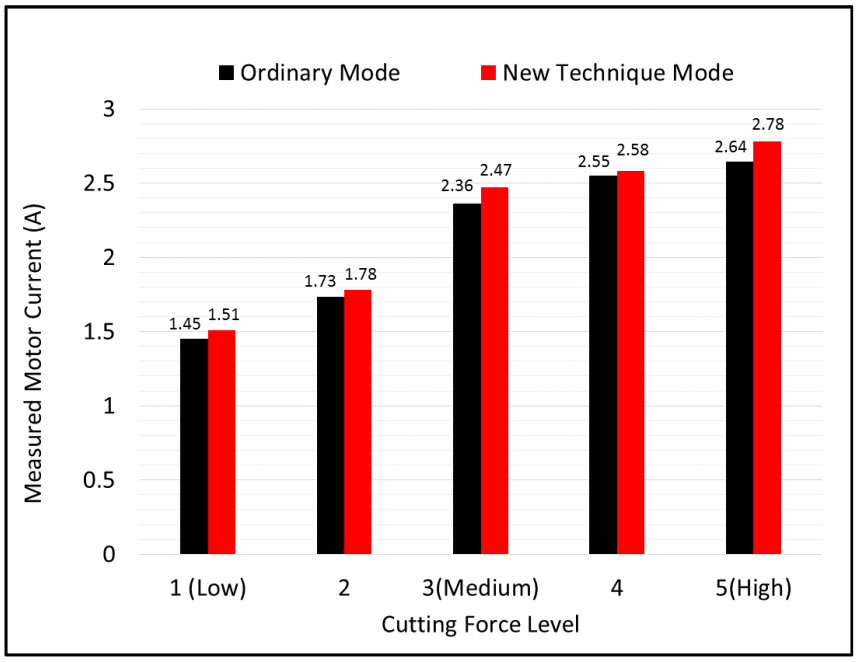

Figure 6.24 Comparison of motor current at different cutting force levels

Ordinary lubrication mode consumes 54 ml of oil, while the new designed technique mode reduces the oil consumption to 50.4 ml at high cutting force level, and 36 ml at medium cutting force level. This is an oil consumption reduction of 18 ml at low level of cutting force (Figure 6.25).

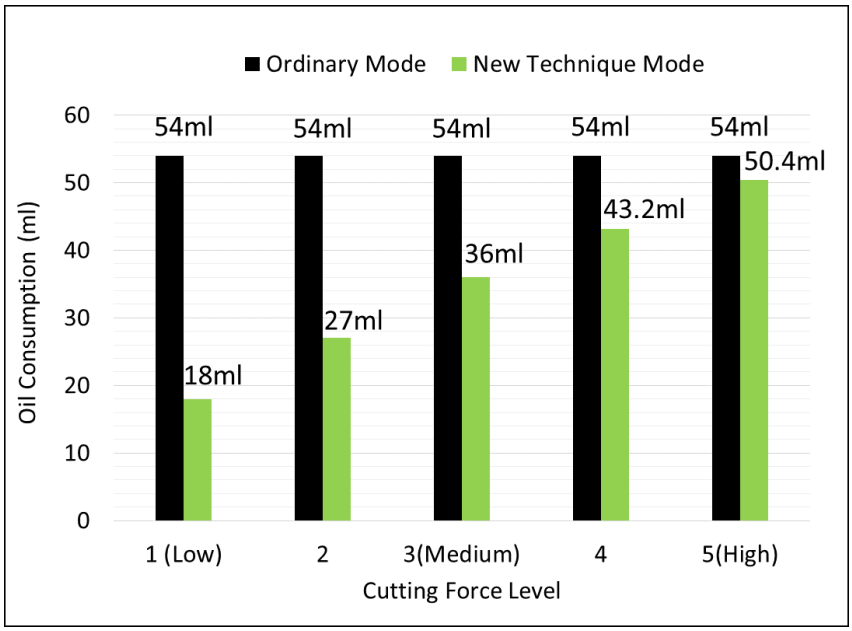

Figure 6.25 Comparison of oil consumption at different cutting force levels

Figure 6.25 shows the commercial machine as ordinary mode; do not provide any justification for lubrication. The lubrication is done regardless of cutting condition and friction. It is based on fixed time and amount of lubrication. The machine lubricate as a maximum to protect the guideways. However, our proposal system as a new technique mode have a this kind of less oil consumption in low level of cutting force and is based on friction conditions and servomotor current, which is, indicated the lubrication quality. It is much less lubrication compared with commercial machine.

Figure 6.24 shows the servo motor current in both ordinary and new lubrication mode after modified are almost same and values are closed together. The servomotor current indicate the lubrication quality. Even our lubrication is less but quality and performance is good. In addition, for sure of commercial machine, when they lubricate, they must ensure that maintaining accuracy and precision as long as our performance is almost same then, our system is ensuring the performance, accuracy and providing high quality

According to Table 6.4, 67% lubrication during machining was saved with the new technique when PRI = 10s, 50% when PRI = 15s, 33% at PRI = 20s. In addition, the oil consumption reduction was 20%, and 6.7%, during machining at cutting levels 4 and 5 (Figure 6.26). Finally, the PRI introduced in the new technique for lubrication and friction control resulted in significant oil consumption reduction of 18 ml for finishing (67%), 36 ml (33%) for medium turning, and 50.4 ml (6.7%) for rough turning, compared with ordinary mode.

A comparison between servomotor current and PRI indicates that the small difference in motor current against the big difference in PRI for the lubrication method helps achieve the objectives of this thesis.

Figure 6.26 shows the comparison the oil consumption between ordinary mode and new technique with oil saving at different cutting levels.

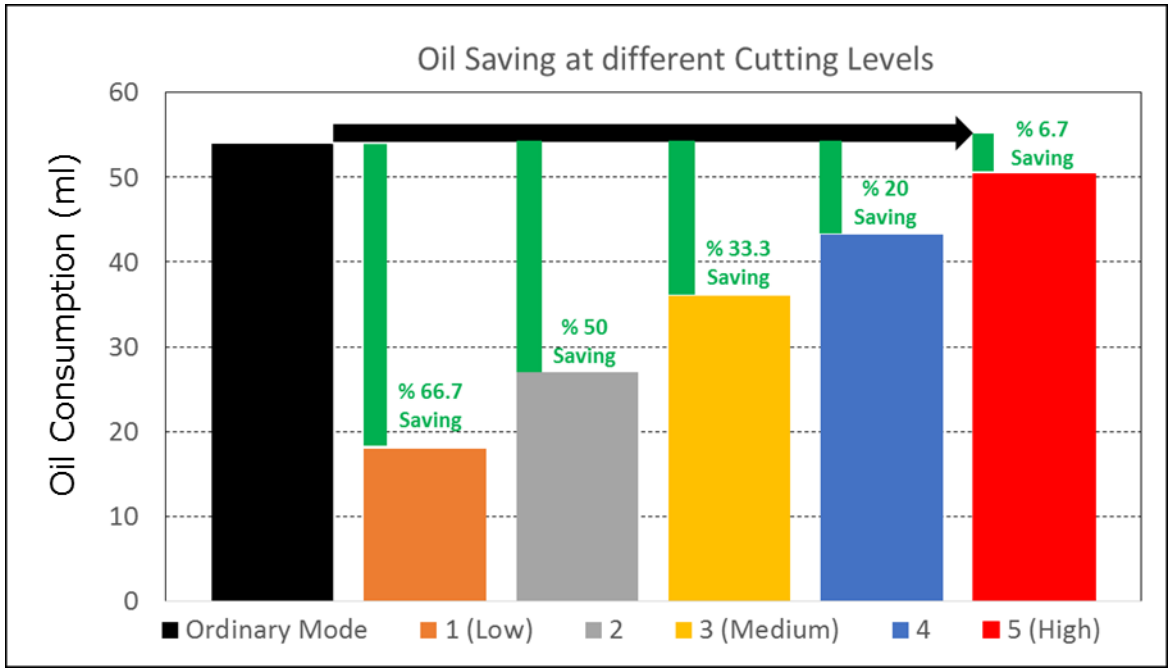

Figure 6.26 Comparison of oil saving at different cutting levels

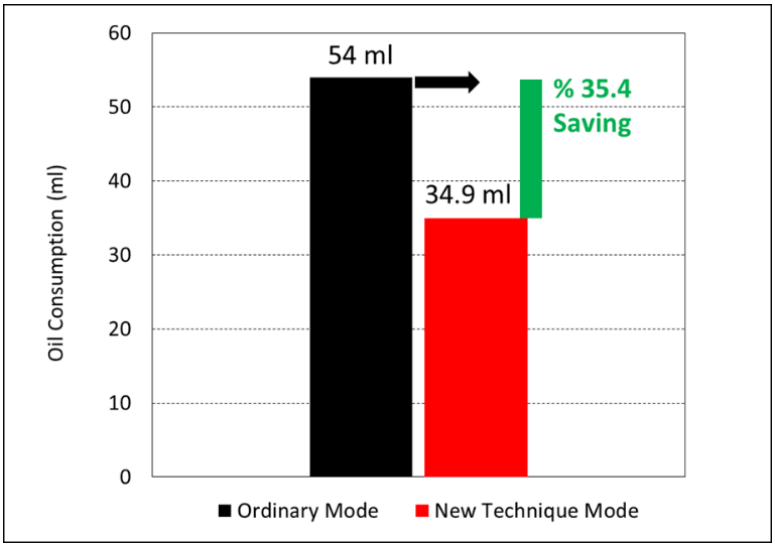

Figure 6.27 Oil saving comparison

6.5 Summary

This chapter addressed the process of lubrication control based on friction conditions using online servomotor current signals. A control algorithm was designed based on the predicted friction. The proposed algorithm was developed in accordance with the CNC machine specifications and default commands for machine lubrication. This algorithm was programmed in formula node structure with LabVIEW software so that the predicted friction is an input and time of injection (PRI) is an output for the control system. This program output as an actuator signal can launch the lubricating oil pump. The ON/OFF time of oil injection is controlled by the predicted friction force and a comparison between online measured servomotor current and predicted current in dry lubrication condition.

The whole process of measurement and control was described by designing an overall block diagram. The control/indicator elements used in the "while loop" of each circuit were configured according to the precise specification and calibration of sensors and modules. This block diagram collects, stores, monitors and analyzes the data as a control, and sends a signal of voltage to trigger the oil pump relay.

The final experiments were done to evaluate the system performance at five cutting force levels. A summary of these experiments is included in Table 6.3 for ordinary lubrication mode and in Table 6.4 for the new lubrication technique. According to the experiments, the servomotor current and oil consumption values were compared for the two lubrication methods introduced. The comparisons indicated that servomotor current in the new lubrication technique is a little higher than in ordinary mode. Because the friction force on linear guideways is controlled in the new method, the time and amount of oil injection change relative to the predicted friction. This represents the achievement of the objectives of this thesis. Meanwhile, oil consumption was reduced significantly.

CHAPTER 7: CONCLUSIONS AND RECOMMENDATIONS

7.1 Conclusions

In this research work, a newly designed lubrication control system for CNC machine tool guideways was introduced for controlling friction forces using online servomotor current signals in a feed drive system. It is a novel approach in machining technology, where the ideal lubrication condition during machining was identified through signals from sensitive sensors installed on the machine tools.

A significant contribution of this work is the analysis of motor current effects on the feed rate, depth of cut and spindle system compared to a substitute force sensor in the proposed method. The cutting force accuracy in predicting the usage of the cutting feed system under limited conditions was shown.

The experimental results indicate the extent of effects on friction, and ultimately on the variation of current in the feed servomotor. In addition, the results demonstrated the capability of the motion control system of feed motors with the friction model obtained in determining and tracking errors. Additionally, the effectiveness of the proposed method was observed in terms of creating smooth slideways and the nonstick-slip phenomenon, as compared to ordinary detection methods.

There was minuscule effect on frictional force due to the cutting conditions of spindle speed, depth of cut and cutting feed rate. The adaptive neuro fuzzy inference system (ANFIS modeling) was run to predict frictional force in guideways and servomotor current in the feed drive system in dry lubrication conditions, which were implemented in the lubrication control system. It was found that the ANFIS model used to build the oil feedback LCU is capable of predicting friction force values in servomotor current signal and cutting conditions.

The PRI was identified based on friction force values in the linear guideways. It can be seen that PRI and oil consumption are different in lubrication mode (ordinary mode and new technique) during fixed machining times. In the new lubrication technique, the PRI only for five levels of cutting force was achieved at 10, 15, 20, 24, and 28 seconds, respectively. Therefore, the oil consumption measured was 18, 27, 36, 43.2, and 50.4 ml, correspondingly. The PRI introduced in the new technique for lubrication and friction control resulted in significant reduction of oil consumption: 18 ml for finishing (67%), 36 ml (33%) for medium turning and 50.4 ml (6.7%) for rough turning compared with ordinary mode. The average reduction of total oil consumed over five levels of cutting force was 34.9 ml (35.4%).

The major findings of this research work are as follows:

- First, the friction force values in linear guideways were calculated using normal/cutting force analysis in the guideways.
- Second, the servo motor current was measured in dry lubrication condition.
- Third, ANFIS modeling was built to predict both, friction force and servo motor current in dry lubrication conditions.
- Finally, Build the Lubrication Control System based on Friction Conditions in Linear Guideways using Servomotor Current Signals in Feed Drive System.
- Reduction of oil consumption:
    - For finishing 67%,
    - For medium turning 33% ,
    - For rough turning 6.7% compared with ordinary mode.

7.2 Recommendations for future works

To improve and develop the project, the following recommendations are proposed:

1- This research not only helps control the friction in CNC machine linear guideways, but it is also useful for cost effectiveness and the prevention of environmental pollution. That is why it is called green technology.

2- The LCU can be simplified by removing the modules. Therefore, all data is directly sent to the controller. On the other hand, the controller monitors and sends the signals to the actuators. This means the LCU function becomes simpler.

3- Surface roughness can be considered as one of the parameters for the correlation between predicted friction force and measured surface roughness at different cutting force levels.

4- A sample, moving model of the cutting tool in roughing operation (rough turning) for cutting force evaluation was shown. Even though the validity of the model was shown through modeling, additional experimental studies on other moving models may be desirable for complete cutting force evaluation.

5- Friction force in linear guideways is problematic for achieving machining precision and accuracy. Hence, creating a suitable model to realize the relation between friction and machining precision/accuracy to offset this problem would definitely be helpful.

6- This research did not focus on the different models of programming and friction control for machine lubrication systems. Therefore, addressing the issue of software control methods can be considered as a topic for the future.

7- Finally, the workpiece material as an input is effective on predicting friction force and servomotor current using ANFIS modeling. It means that different workpiece materials change the value of friction force in linear guideways and servomotor current in feed drive systems.

REFERENCES

Adoko, A. C., & al., e. (2013). Knowledge-based and data-driven fuzzy modeling for rockburst prediction. *International Journal of Rock Mechanics and Mining Sciences, 61*, 86-95.

Al-Bender, F., & Symens, W. (2005). Dynamic characterization of hysteresis elements in mechanical systems. I. Theoretical analysis. *Chaos: An Interdisciplinary Journal of Nonlinear Science, 15*(1),

Altintas. (2012). *Manufacturing automation: metal cutting mechanics, machine tool vibrations, and CNC design*. Cambridge University Press.

Altintas, & Chicago. (1992). Prediction of cutting forces and tool breakage in milling from feed drive current measurements. *Journal of engineering for industry, vol. 114(4)*, pp. 386-392.

Altintas, & Dong, C. (1990). Design and analysis of a modular CNC system for machining control and monitoring. *Modeling of Machine Tools: Accuracy, Dynamics, and Control*, 199-208.

Anderson, J., Wiseman, S. B., Moustafa, A., Gamal El-Din, M., Liber, K., & Giesy, J. P. (2012). Effects of exposure to oil sands process-affected water from experimental reclamation ponds on Chironomus dilutus. *Water Research, 46*(6), 1662-1672.

Armstrong-Helouvry, B. (1993). Stick slip and control in low-speed motion. *Automatic Control, IEEE Transactions on, 38*(10), 1483-1496. doi: 10.1109/9.241562

Armstrong-Hélouvry, B., Dupont, P., & De Wit, C. C. (1994). A survey of models, analysis tools and compensation methods for the control of machines with friction. *Automatica, 30*(7), 1083-1138.

Åström, K. J., & Hägglund, T. (1984). Automatic tuning of simple regulators with specifications on phase and amplitude margins. *Automatica, 20*(5), 645-651.

Benhabib, B. (2003). Manufacturing: design, production, automation and integration. *CRC Press, vol. 63*.

Bramhane, R., Arora, A., & Chandra, H. (2014). Simulation of flexible manufacturing system using Adaptive Neuro Fuzzy Hybrid structure for efficient job sequencing and routing.

Bushuev, V. V., & Molodtsov, V. V. (2010). Role of the machine tool's kinematic structure in ensuring machining precision. *Russian Engineering Research, 30*(10), 1053-1059.

Byrne, G., Dornfeld, D., Inasaki, I., Ketteler, G., König, W., & Teti, R. (1995). Tool Condition Monitoring (TCM) — The Status of Research and Industrial Application. *CIRP Annals - Manufacturing Technology, 44*(2), 541-567.

Chen, G. S., Mei, X. S., & Tao, T. (2011). Friction compensation using a double pulse method for a high-speed high-precision table. *Proceedings of the Institution of Mechanical Engineers, Part C: Journal of Mechanical Engineering Science, 225*(5), 1263-1272.

Cheok, K. C., HONGXING, H., & Loh, N. K. (1988). Modeling and identification of a class of servomechanism systems with stick-slip friction. *Journal of dynamic systems, measurement, and control, vol. 110(3)*, pp. 324-328.

Chiu, G.-C., & al., e. (2001). Contouring control of machine tool feed drive systems: a task coordinate frame approach. *Control Systems Technology, IEEE Transactions on, 9*(1), 130-139.

Chow, J. H. Z., Z.W. and Lin, W. . (2010). Investigation of thermal effect in permanent magnet linear motor stage. *11th International Conference on Control, Automation, Robotics and Vision, Singapore*, pp.258e262.

d'Iribarne, A., & Lutz, B. (2014). *Work organisation in flexible manufacturing systems - first findings from international comparisons.* Paper presented at the Design of Work in Automated Manufacturing Systems: Proceedings of the IFAC Workshop, Karlsruhe, Federal Republic of Germany, 7–9 November 1983.

Desforges, X., & al., e. (2011). Design methodology for smart actuator services for machine tool and machining control and monitoring. *Robotics and Computer-Integrated Manufacturing, 27*(6), 963-976.

Dölen, M., & Lorenz, R.D.(2002).General Methodologies for Neural Network Programming. *International Journal of Smart Engineering System Design, 4*(1),63-73.

Freidovich, L., & al., e. (2010). LuGre-Model-Based Friction Compensation. *Control Systems Technology, IEEE Transactions on, 18*(1), 194-200.

Giri, F. (2013). *AC electric motors control: Advanced design techniques and applications*: John Wiley & Sons.

Goodwin, G. C., & al., e. (2001). *Control system design* (Vol. 240): Prentice Hall New Jersey.

Haitao, Z., & al., e. (2007). Simulation of thermal behavior of a CNC machine tool spindle. *International Journal of Machine Tools and Manufacture, 47*(6), 1003-1010.

Hsiao, Y. F., & al., e. (2009). Study of the lubrication oil consumption prediction of linear motion guide through the grey theory and the neural network. *WSEAS Transactions on Applied and Theoretical Mechanics, vol. (1)*, pp. 42-51.

Huo, F., & Poo, A.-N. (2013). Precision contouring control of machine tools. *The International Journal of Advanced Manufacturing Technology, 64*(1-4), 319-333.

Jeong, Y.-H., & al., e. (2002). Estimating cutting force from rotating and stationary feed motor currents on a milling machine. *International Journal of Machine Tools and Manufacture, 42*(14), 1559-1566.

Jin-Hyeon, L., & Yang, S.-H. (2002). Statistical optimization and assessment of a thermal error model for CNC machine tools. *International Journal of Machine Tools and Manufacture, 42*(1), 147-155.

Jong-Jin, K., & al., e. (2004). Thermal behavior of a machine tool equipped with linear motors. *International Journal of Machine Tools and Manufacture, 44*(7–8), 749-758.

Jywe, W.-Y., & Chen, C.-J. (2005). The development of a high-speed spindle measurement system using a laser diode and a quadrants sensor. *International Journal of Machine Tools and Manufacture, 45*(10), 1162-1170.

Karnopp, D. (1985). Computer Simulation of Stick-Slip Friction in Mechanical Dynamic Systems. *Transaction of ASME, Journal of Dynamic System Measurement and Control, 107*, 100-103.

Kasa Narasimha Murthy, A. (2014). Model driven product realization: A holistic demonstration of model driven product development.

Kato, S. Y., K. and Matsubayashi, T. . (1974). Stick-slip motion of machine tool slideway. *ASME J. Eng. Ind, vol. 96*, pp. 557-566.

Kim, & Chu, C. N. (1999). Indirect Cutting Force Measurement Considering Frictional Behaviour in a Machining Centre Using Feed Motor Current. *The International Journal of Advanced Manufacturing Technology, 15*(7), 478-484.

Kim, Kim, H. M., & Han, S. I. (2009). Precision position control of servo systems using adaptive back-stepping and recurrent fuzzy neural networks. *Journal of Mechanical Science and Technology, 23*(11), 3059-3070.

Kobayashi, K., & Fujita, E. (2006). Hydrostatic pressure linear guide devices. *U.S. Patent No. 7,101,080. Washington, DC: U.S. Patent and Trademark Office.*

Kok Kiong, T., & al., e. (2001). High precision linear motor control via relay-tuning and iterative learning based on zero-phase filtering. *Control Systems Technology, IEEE Transactions on, 9*(2), 244-253.

Kumar, S., & al., e. (2007). Process control in CNC manufacturing for discrete components: A STEP-NC compliant framework. *Robotics and Computer-Integrated Manufacturing, 23*(6), 667-676.

Lau, J. H., & al., e. (2013). A Comparative Study on Testing of Wide-Range Angles Precision 2-axis Digital Angular Measuring Instrument.

Lee, & al., e. (1995). Real-Time Tool Breakage Monitoring for NC Milling Process. *CIRP Annals - Manufacturing Technology, 44*(1), 59-62.

Lin, & al., e. (2008). *Improved fuzzy control method for temperature in water tank of intelligent viscometer.* Paper presented at the Information and Automation, 2008. ICIA 2008. International Conference on.

Lin, & Tzeng, C. S. (2008). Modeling and measurement of active parameters and workpiece home position of a multi-axis machine tool. *International Journal of Machine Tools and Manufacture, 48*(3), 338-349.

Liu, K., & Melkote, S. N. (2007). Finite element analysis of the influence of tool edge radius on size effect in orthogonal micro-cutting process. *International Journal of Mechanical Sciences, 49*(5), 650-660.

Maher, I., & al., e. (2014). Cutting force-based adaptive neuro-fuzzy approach for accurate surface roughness prediction in end milling operation for intelligent machining. *The International Journal of Advanced Manufacturing Technology*, 1-9.

Makino, H., & Ohde, T. (1991). Motion control of the direct drive actuator. *CIRP Annals-Manufacturing Technology, 40*(1), 375-378.

Mannan, M. A., & al., e. (1989). Monitoring and Adaptive Control of Cutting Process by Means of Motor Power and Current Measurements. *CIRP Annals - Manufacturing Technology, 38*(1), 347-350.

Mei, X., Tsutsumi, M., Yamazaki, T., & Sun, N. (2001). Study of the friction error for a high-speed high precision table. *International Journal of Machine Tools and Manufacture, 41*(10), 1405-1415.

Mickelson, D. (2006). *Guide to hard milling and high speed machining*: Industrial Press.

Molina, A., Ponce, H., Ponce, P., Tello, G., & Ramírez, M. (2014). Artificial hydrocarbon networks fuzzy inference systems for CNC machines position controller. *The International Journal of Advanced Manufacturing Technology, 72*(9-12), 1465-1479.

Nikolakopoulos, P. G., & Papadopoulos, C. A. (2008). A study of friction in worn misaligned journal bearings under severe hydrodynamic lubrication. *Tribology International, 41*(6), 461-472.

OKUMA. (1998). Operation & Maintenance Manual. In O. m. w. LTD. (Ed.), *Okuma LB15 CNC Lathe with OSP5000L-G CNC System*. Oguchi-Cho, Niwa-Gun, Aichi 480-01 JAPAN: OKUMA.

Olsson, H., & al., a. (1998). Friction models and friction compensation. *European Journal of Control, 4*(3), 176-195.

Park, K.-H., & al., e. (2010). A study on droplets and their distribution for minimum quantity lubrication (MQL). *International Journal of Machine Tools and Manufacture, 50*(9), 824-833.

Parlak, A., & al., e. (2006). Application of artificial neural network to predict specific fuel consumption and exhaust temperature for a diesel engine. *Applied Thermal Engineering, 26*(8), 824-828.

Pateloup, V., Duc, E., & Ray, P. (2010). Bspline approximation of circle arc and straight line for pocket machining. *Computer-Aided Design, 42*(9), 817-827.

Pérez-Canales, D., & al., e. (2011). Identification of dynamic instabilities in machining process using the approximate entropy method. *International Journal of Machine Tools and Manufacture*.

Persianoff, R., Ray, P., & Vidal, O. (2003). Comparison between an experimental study and a numerical model of the dynamic behaviour of machine-tool slideways. *Proceedings of the Institution of Mechanical Engineers, Part B: Journal of Engineering Manufacture, 217*(8), 1111-1115.

Persson, B. N. (2014). Sliding Friction, Experimental Results. *Encyclopedia of Lubricants and Lubrication*, 1841-1856.

Pfefferkorn, F. E., & al., e. (2009). A metric for defining the energy efficiency of thermally assisted machining. *International Journal of Machine Tools & Manufacture, 49*(5), 357-365.

Pretot, S., & al., e. (2000). Theoretical and experimental study of natural convection on a horizontal plate. *Applied Thermal Engineering, 20*(10), 873-891.

Prodan, D., Balan, E., Bucuresteanu, A., & Motomancea, A. (2013). Modeling and Simulation of Closed-Loop Counterbalancing Hydraulic Units for Heavy-Duty Machine-Tools. *Applied Mechanics and Materials, 332*, 417-422.

Ramesh, R., Mannan, M. A., & Poo, A. N. (2000). Error compensation in machine tools — a review: Part II: thermal errors. *International Journal of Machine Tools and Manufacture, 40*(9), 1257-1284.

Ribeiro, L., & Barata, J. (2011). Re-thinking diagnosis for future automation systems: An analysis of current diagnostic practices and their applicability in emerging IT based production paradigms. *Computers in Industry, 62*(7), 639-659.

Rubaai, A., Castro-Sitiriche, M. J., & Ofoli, A. R. (2008). Design and Implementation of Parallel Fuzzy PID Controller for High-Performance Brushless Motor Drives: An Integrated Environment for Rapid Control Prototyping. *Industry Applications, IEEE Transactions on, 44*(4), 1090-1098.

Schwenke, H., Knapp, W., Haitjema, H., Weckenmann, A., Schmitt, R., & Delbressine, F. (2008). Geometric error measurement and compensation of machines—An update. *CIRP Annals - Manufacturing Technology, 57*(2), 660-675.

Shackelford, J. F., & Alexander, W. (2010). *CRC materials science and engineering handbook*: CRC press.

Soundararajan, V., Zekovic, S., & Kovacevic, R. (2005). Thermo-mechanical model with adaptive boundary conditions for friction stir welding of Al 6061. *International Journal of Machine Tools and Manufacture, 45*(14), 1577-1587.

Sparham, M., & al., e. (2012). Smart lubrication via pump response interval (PRI) variation in the machining process. *The International Journal of Advanced Manufacturing Technology*, 1-10.

Sparham, M., & al.,e.(2013).Designing and manufacturing an automated lubrication control system in CNC machine tool guideways for more precise machining and less oil consumption.*The International JournalofAdvanced Manufacturing Technology*,1-10.

Stein, & al., e. (1986). Evaluation of dc servo machine tool feed drives as force sensors. *Journal of dynamic systems,measurement, and control, vol. 108*, pp. 279-288.

Stein, Wang, & al., e. (1990). Analysis of power monitoring on AC induction drive systems. *Journal of dynamic systems, measurement, and control, 112*(2), 239-248.

Stein JL, W. C. (1990). Analysis of power monitoring on AC induction drive systems. Systems. *Journal of Dynamic Measurement, and Control, vol. 112(2)*, pp. 239–248.

Suresh Kumar Reddy, N., & al., e. (2010). Development of electrostatic solid lubrication system for improvement in machining process performance. *International Journal of Machine Tools and Manufacture, 50*(9), 789-797.

Sutar, M. D., & Deshmukh, B. B. (2013). Linear Motion Guideways–A Recent Technology for Higher Accuracy and Precision Motion of Machine Tool. *3*(1).

Tabor, F. P. B. a. D. (2001). The friction and lubrication of solids. *Oxford university press, vol. 1*.

Tanabe, I., & Watanabe, M. (2011, 25-27 May 2011). *Development of cost-effective and eco-friendly permanent grease lubrication for the machine tool slildes.* Paper presented at the Assembly and Manufacturing (ISAM), 2011 IEEE International Symposium.

Tarng, Y. S., & Cheng, H. E. (1995). An investigation of stick-slip friction on the contouring accuracy of cnc machine tools. *International Journal of Machine Tools and Manufacture, 35*(4), 565-576.

Tawakoli, T., Hadad, M. J., Sadeghi, M. H., Daneshi, A., Stöckert, S., & Rasifard, A. (2009). An experimental investigation of the effects of workpiece and grinding parameters on minimum quantity lubrication—MQL grinding. *International Journal of Machine Tools and Manufacture, 49*(12–13), 924-932.

Tinkir, M., & al., e. (2010). Modelling of neurofuzzy control of a flexible link. *Proceedings of the Institution of Mechanical Engineers, Part I: Journal of Systems and Control Engineering, 224*(5), 529-543.

Tlusty, J., & Andrews, G. C. (1983). A Critical Review of Sensors for Unmanned Machining. *CIRP Annals - Manufacturing Technology, 32*(2), 563-572.

Tung, E., Anwar, G., & Tomizuka, M. (1991, 26-28 June 1991). *Low Velocity Friction Compensation and Feedforward Solution based on Repetitive Control.* Paper presented at the American Control Conference, 1991.

Wang, & al., e. (2001). Adaptive Friction Compensation for Servo Mechanisms. In G. Tao & F. Lewis (Eds.), *Adaptive control of nonsmooth dynamic systems* (pp. 211-248): Springer London.

Wang, L. (2014). *Dynamic Thermal Analysis of Machines in Running State*: Springer.

Watson, N. S. (2013). System for holding a linear motion guide track to a support base and method therefor: Google Patents.

Weck, M. (1983). Machine diagnostics in automated production. *Journal of Manufacturing Systems, 2*(2), 101-106.

Xia, Y., & al., e. (2014). Application of active disturbance rejection control in tank gun control system. *Journal of the Franklin Institute, 351*(4), 2299-2314.

Yau, H.-T., & Kuo, M.-J. (2001). NURBS machining and feed rate adjustment for high-speed cutting of complex sculptured surfaces. *International Journal of Production Research, 39*(1), 21-41.

Yeh, S.-S., & Su, H.-C. (2011). Development of friction identification methods for feed drives of CNC machine tools. *The International Journal of Advanced Manufacturing Technology, 52*(1-4), 263-278.

Yong-Sub, Y., Kim, Y., Choi, J., Yoo, J., Lee, D., Lee, S., & Lee, S. (2008). Dynamic analysis of a linear motion guide having rolling elements for precision positioning devices. *Journal of Mechanical Science and Technology, 22*(1), 50-60.

Yong, L., & al., e. (2014). A Wavelet Bicoherence-Based Quadratic Nonlinearity Feature for Translational Axis Condition Monitoring. *Sensors, 14*(2), 2071-2088.

Yukeng, H., Darong, C., & Linqing, Z. (1985). Effect of surface topography of scraped machine tool guideways on their tribological behaviour. *Tribology International, 18*(2), 125-129.

Yun, W. S., Kim, S. K., & Cho, D. W. (1999). Thermal error analysis for a CNC lathe feed drive system. *International Journal of Machine Tools and Manufacture, 39*(7), 1087-1101.

Zhiping, L., & al., e. (2013). Adaptive Robust Control of Servo Mechanisms With Compensation for Nonlinearly Parameterized Dynamic Friction. *Control Systems Technology, IEEE Transactions on, 21*(1), 194-202.

APPENDIX A

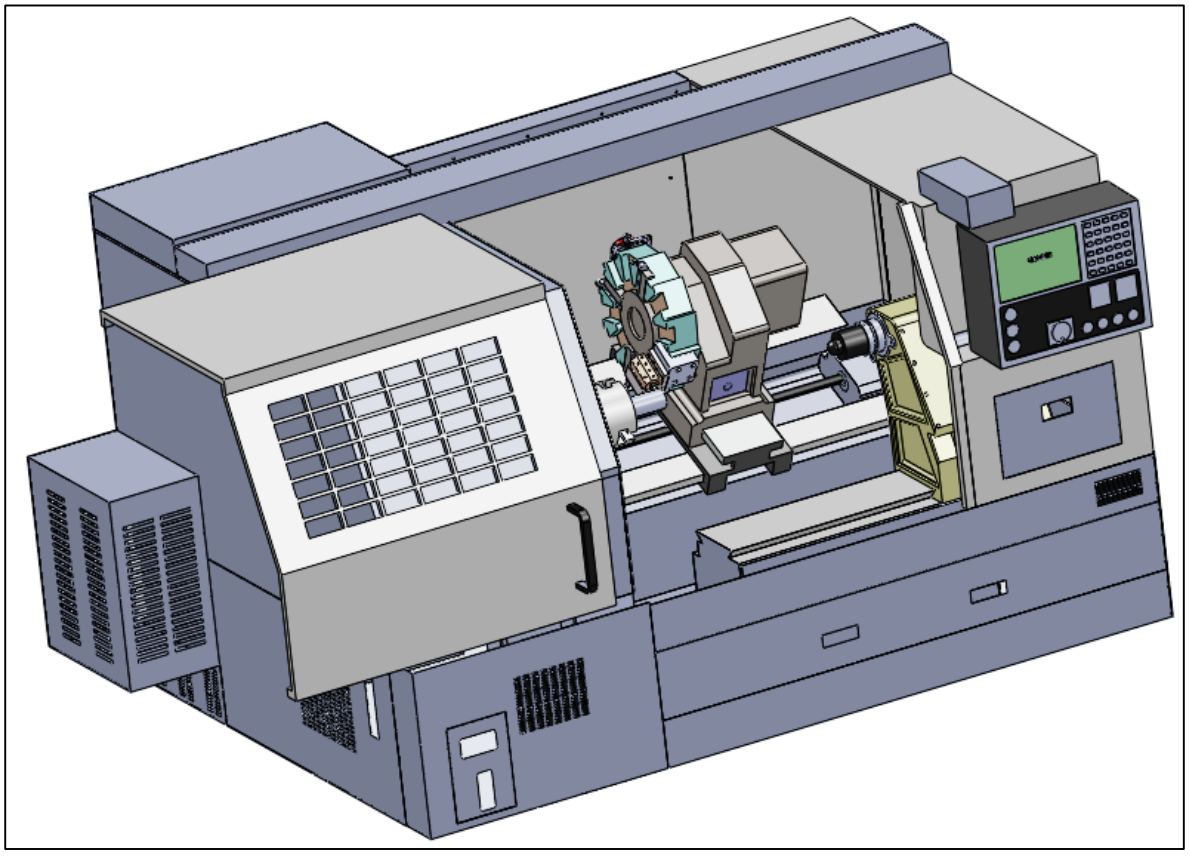

APPENDIX A1: Solid modeling of the OKUMA LB15 II CNC machine

APPENDIX A2: The images of preparations and experimental setup

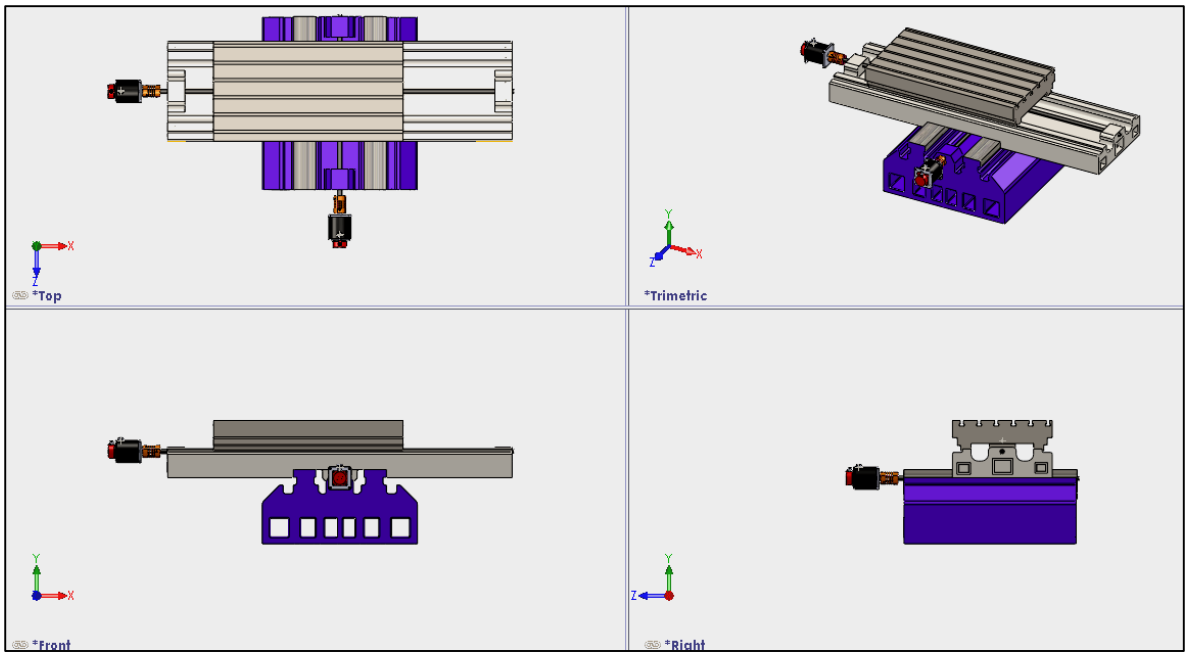

APPENDIX A3: Three different plans and Diametric view orientation of linear guideways.

APPENDIX B

Temperature 36 - Notepad

File Edit Format View Help

```
LabVIEW Measurement
Writer_Version  2
Reader_Version  2
Separator       Tab
Decimal_Separator       .
Multi_Headings  No
X_Columns       One
Time_Pref       Absolute
Operator        mehdi
Date    2012/11/20
Time    15:16:17.5183009999997828566
***End_of_Header***

Channels        4
Samples         100             100             100             100

Y_Unit_Label    Deg C           Deg C           Deg C           Deg C
X_Dimension     Time    Time    Time    Time

Delta_X         0.100000        0.100000        0.100000        0.100000
***End_of_Header***
X_Value         TA              TB              TC              TD
0.000000        29.900791       29.887625       29.497273       29.871167
0.100000        29.900791       29.887625       29.497273       29.871167
0.200000        29.900791       29.887625       29.497273       29.871167
0.300000        29.900791       29.887625       29.497273       29.871167
0.400000        29.877251       29.867847       29.497244       29.880543
0.500000        29.877251       29.867847       29.497244       29.880543
0.600000        29.877251       29.867847       29.497244       29.880543
0.700000        29.877251       29.867847       29.497244       29.880543
0.800000        29.886590       29.869662       29.488712       29.867311
0.900000        29.886590       29.869662       29.488712       29.867311
1.000000        29.886590       29.869662       29.488712       29.867311
1.100000        29.886590       29.869662       29.488712       29.867311
1.200000        29.895908       29.847945       29.491917       29.871456
1.300000        29.895908       29.847945       29.491917       29.871456
1.400000        29.895908       29.847945       29.491917       29.871456
1.500000        29.895908       29.847945       29.491917       29.871456
1.600000        29.886091       29.860699       29.473159       29.864931
1.700000        29.886091       29.860699       29.473159       29.864931
1.800000        29.886091       29.860699       29.473159       29.864931
1.900000        29.886091       29.860699       29.473159       29.864931
2.000000        29.888290       29.864779       29.496527       29.873243
2.100000        29.888290       29.864779       29.496527       29.873243
2.200000        29.888290       29.864779       29.496527       29.873243
2.300000        29.888290       29.864779       29.496527       29.873243
2.400000        29.915208       29.844205       29.466067       29.872889
2.500000        29.915208       29.844205       29.466067       29.872889
2.600000        29.915208       29.844205       29.466067       29.872889
2.700000        29.915208       29.844205       29.466067       29.872889
2.800000        29.895987       29.864012       29.473651       29.886113
2.900000        29.895987       29.864012       29.473651       29.886113
3.000000        29.895987       29.864012       29.473651       29.886113
3.100000        29.895987       29.864012       29.473651       29.886113
3.200000        29.882170       29.878408       29.488523       29.887342
3.300000        29.882170       29.878408       29.488523       29.887342
```

APPENDIX B1: A sample of data acquisition recorded for Temperature measurement

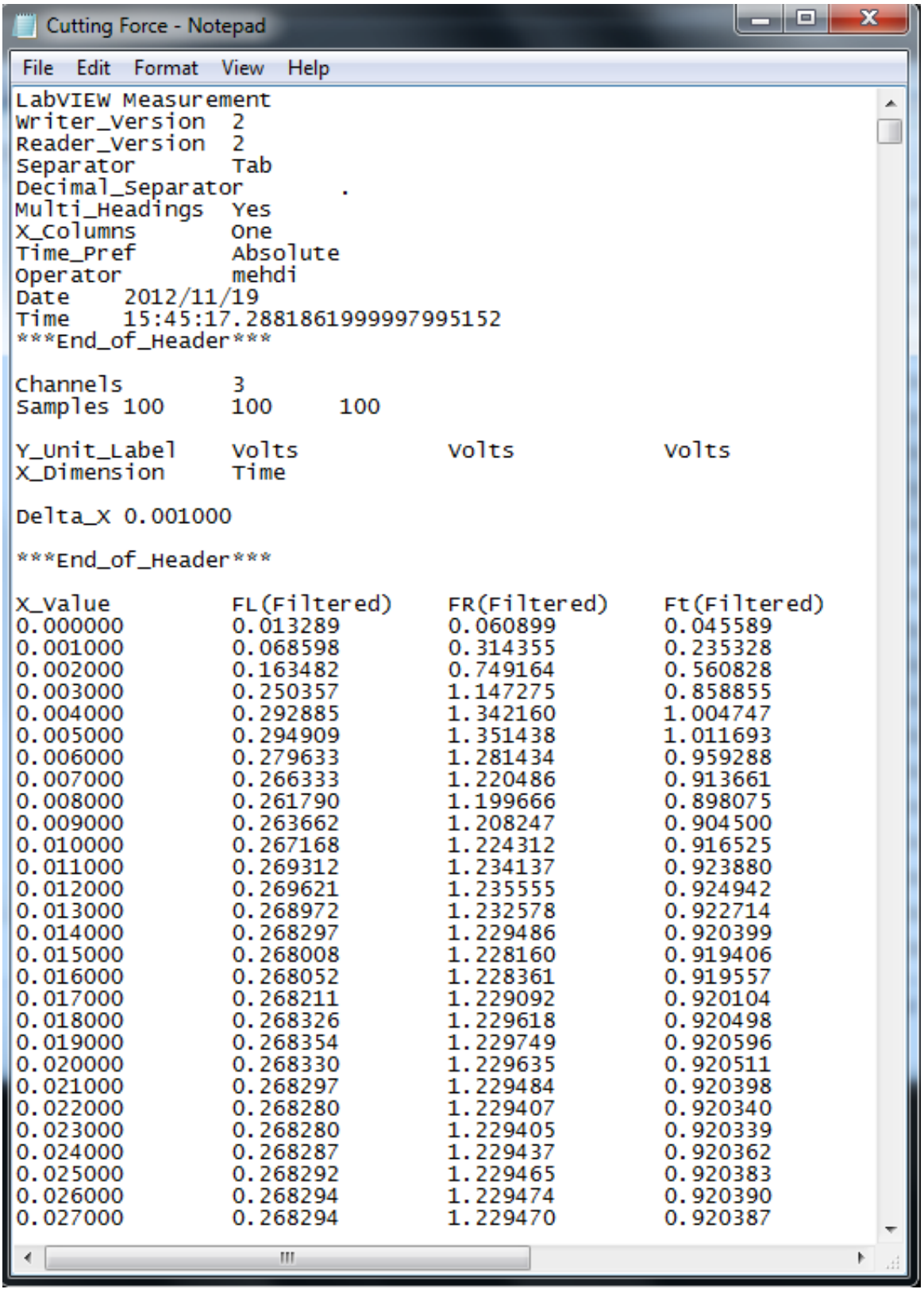

Cutting Force - Notepad

File Edit Format View Help

```
LabVIEW Measurement
Writer_Version  2
Reader_Version  2
Separator       Tab
Decimal_Separator       .
Multi_Headings  Yes
X_Columns       One
Time_Pref       Absolute
Operator        mehdi
Date    2012/11/19
Time    15:45:17.2881861999997995152
***End_of_Header***

Channels        3
Samples 100     100     100

Y_Unit_Label    Volts           Volts           Volts
X_Dimension     Time

Delta_X 0.001000

***End_of_Header***

X_Value         FL(Filtered)    FR(Filtered)    Ft(Filtered)
0.000000        0.013289        0.060899        0.045589
0.001000        0.068598        0.314355        0.235328
0.002000        0.163482        0.749164        0.560828
0.003000        0.250357        1.147275        0.858855
0.004000        0.292885        1.342160        1.004747
0.005000        0.294909        1.351438        1.011693
0.006000        0.279633        1.281434        0.959288
0.007000        0.266333        1.220486        0.913661
0.008000        0.261790        1.199666        0.898075
0.009000        0.263662        1.208247        0.904500
0.010000        0.267168        1.224312        0.916525
0.011000        0.269312        1.234137        0.923880
0.012000        0.269621        1.235555        0.924942
0.013000        0.268972        1.232578        0.922714
0.014000        0.268297        1.229486        0.920399
0.015000        0.268008        1.228160        0.919406
0.016000        0.268052        1.228361        0.919557
0.017000        0.268211        1.229092        0.920104
0.018000        0.268326        1.229618        0.920498
0.019000        0.268354        1.229749        0.920596
0.020000        0.268330        1.229635        0.920511
0.021000        0.268297        1.229484        0.920398
0.022000        0.268280        1.229407        0.920340
0.023000        0.268280        1.229405        0.920339
0.024000        0.268287        1.229437        0.920362
0.025000        0.268292        1.229465        0.920383
0.026000        0.268294        1.229474        0.920390
0.027000        0.268294        1.229470        0.920387
```

APPENDIX B2: A sample of data acquisition recorded for cutting force measurement

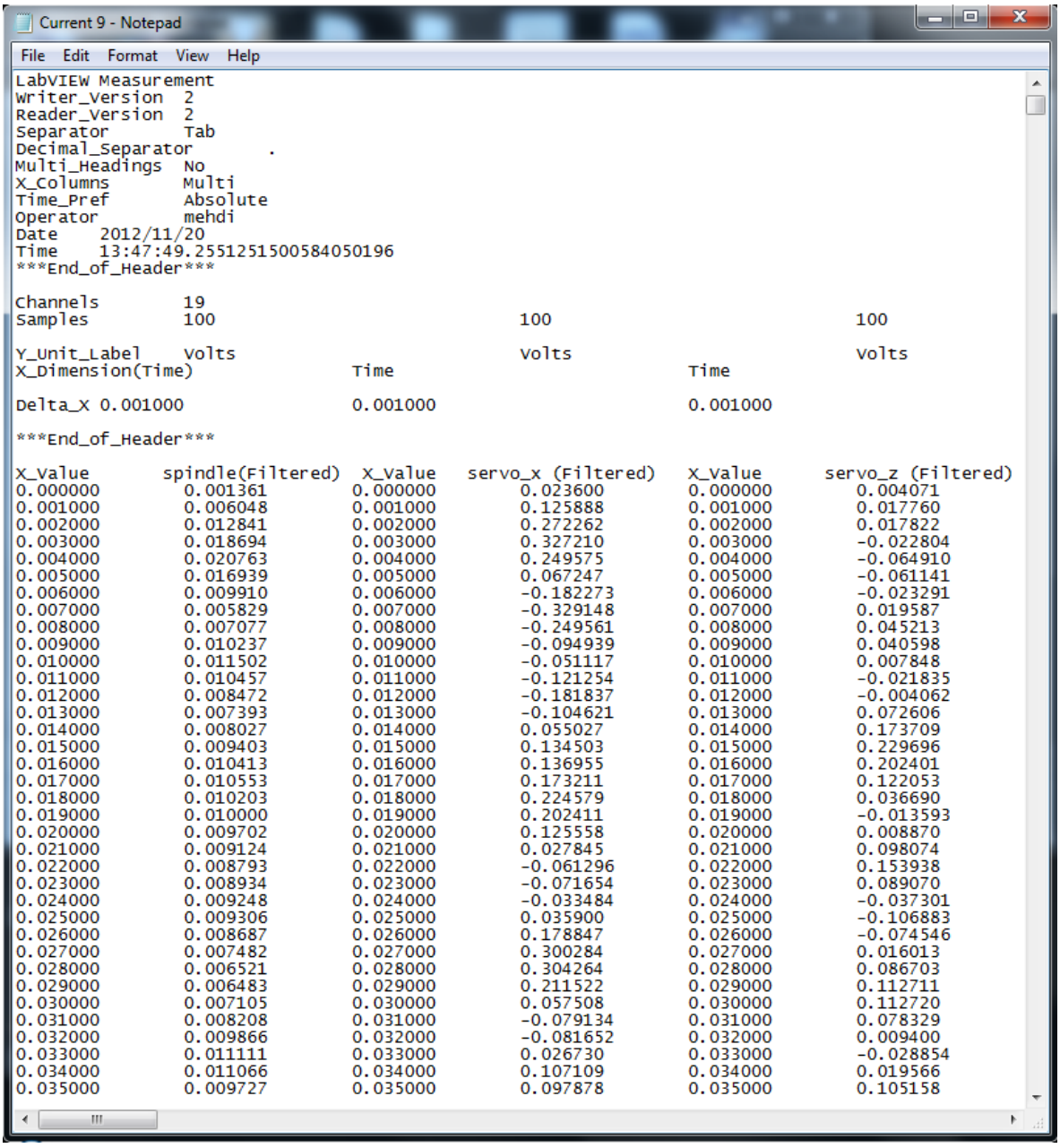

Current 9 - Notepad

File Edit Format View Help

```
LabVIEW Measurement
Writer_Version  2
Reader_Version  2
Separator       Tab
Decimal_Separator       .
Multi_Headings  No
X_Columns       Multi
Time_Pref       Absolute
Operator        mehdi
Date    2012/11/20
Time    13:47:49.2551251500584050196
***End_of_Header***

Channels        19
Samples         100                             100                             100

Y_Unit_Label    Volts                           Volts                           Volts
X_Dimension(Time)               Time                            Time

Delta_X 0.001000                0.001000                        0.001000

***End_of_Header***

X_Value       spindle(Filtered)  X_Value   servo_x (Filtered)   X_Value      servo_z (Filtered)
0.000000        0.001361        0.000000        0.023600        0.000000        0.004071
0.001000        0.006048        0.001000        0.125888        0.001000        0.017760
0.002000        0.012841        0.002000        0.272262        0.002000        0.017822
0.003000        0.018694        0.003000        0.327210        0.003000        -0.022804
0.004000        0.020763        0.004000        0.249575        0.004000        -0.064910
0.005000        0.016939        0.005000        0.067247        0.005000        -0.061141
0.006000        0.009910        0.006000        -0.182273       0.006000        -0.023291
0.007000        0.005829        0.007000        -0.329148       0.007000        0.019587
0.008000        0.007077        0.008000        -0.249561       0.008000        0.045213
0.009000        0.010237        0.009000        -0.094939       0.009000        0.040598
0.010000        0.011502        0.010000        -0.051117       0.010000        0.007848
0.011000        0.010457        0.011000        -0.121254       0.011000        -0.021835
0.012000        0.008472        0.012000        -0.181837       0.012000        -0.004062
0.013000        0.007393        0.013000        -0.104621       0.013000        0.072606
0.014000        0.008027        0.014000        0.055027        0.014000        0.173709
0.015000        0.009403        0.015000        0.134503        0.015000        0.229696
0.016000        0.010413        0.016000        0.136955        0.016000        0.202401
0.017000        0.010553        0.017000        0.173211        0.017000        0.122053
0.018000        0.010203        0.018000        0.224579        0.018000        0.036690
0.019000        0.010000        0.019000        0.202411        0.019000        -0.013593
0.020000        0.009702        0.020000        0.125558        0.020000        0.008870
0.021000        0.009124        0.021000        0.027845        0.021000        0.098074
0.022000        0.008793        0.022000        -0.061296       0.022000        0.153938
0.023000        0.008934        0.023000        -0.071654       0.023000        0.089070
0.024000        0.009248        0.024000        -0.033484       0.024000        -0.037301
0.025000        0.009306        0.025000        0.035900        0.025000        -0.106883
0.026000        0.008687        0.026000        0.178847        0.026000        -0.074546
0.027000        0.007482        0.027000        0.300284        0.027000        0.016013
0.028000        0.006521        0.028000        0.304264        0.028000        0.086703
0.029000        0.006483        0.029000        0.211522        0.029000        0.112711
0.030000        0.007105        0.030000        0.057508        0.030000        0.112720
0.031000        0.008208        0.031000        -0.079134       0.031000        0.078329
0.032000        0.009866        0.032000        -0.081652       0.032000        0.009400
0.033000        0.011111        0.033000        0.026730        0.033000        -0.028854
0.034000        0.011066        0.034000        0.107109        0.034000        0.019566
0.035000        0.009727        0.035000        0.097878        0.035000        0.105158
```

APPENDIX B3: A sample of data acquisition recorded for Current measurement

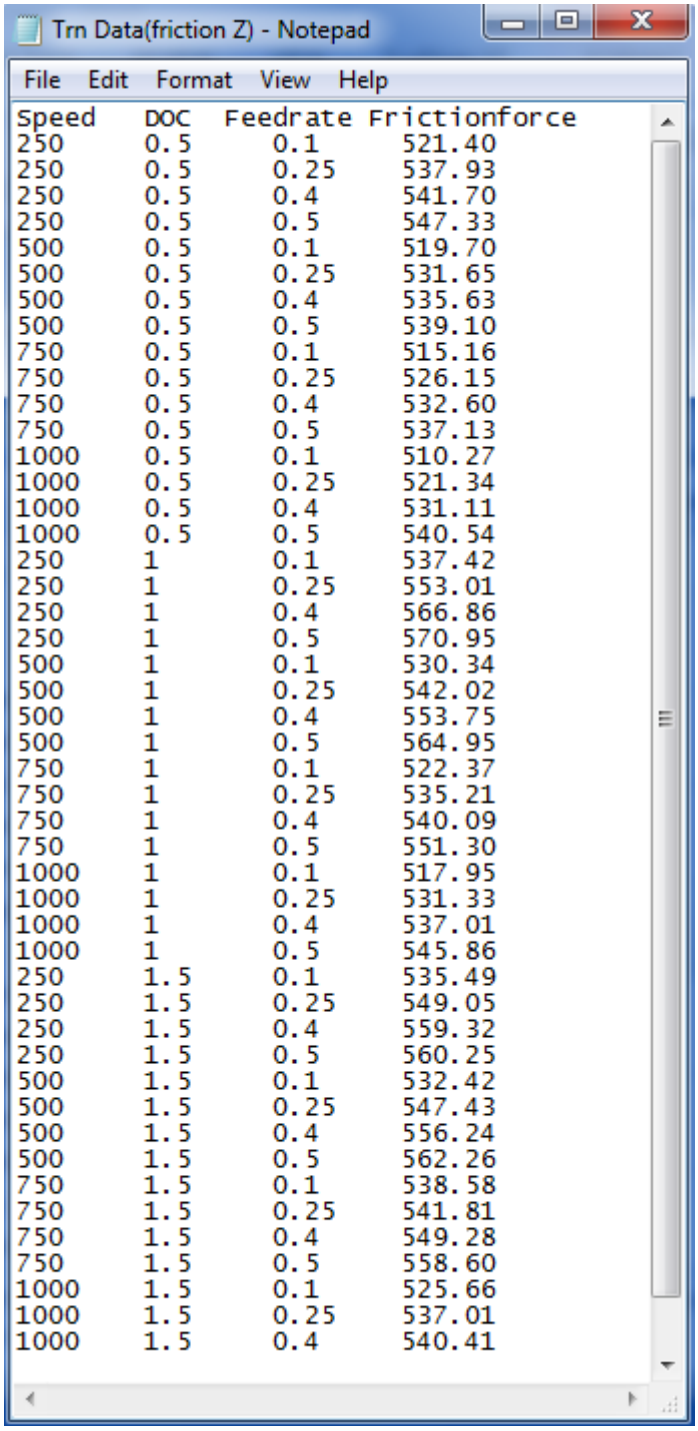

Speed	DOC	Feedrate	Frictionforce
250	0.5	0.1	521.40
250	0.5	0.25	537.93
250	0.5	0.4	541.70
250	0.5	0.5	547.33
500	0.5	0.1	519.70
500	0.5	0.25	531.65
500	0.5	0.4	535.63
500	0.5	0.5	539.10
750	0.5	0.1	515.16
750	0.5	0.25	526.15
750	0.5	0.4	532.60
750	0.5	0.5	537.13
1000	0.5	0.1	510.27
1000	0.5	0.25	521.34
1000	0.5	0.4	531.11
1000	0.5	0.5	540.54
250	1	0.1	537.42
250	1	0.25	553.01
250	1	0.4	566.86
250	1	0.5	570.95
500	1	0.1	530.34
500	1	0.25	542.02
500	1	0.4	553.75
500	1	0.5	564.95
750	1	0.1	522.37
750	1	0.25	535.21
750	1	0.4	540.09
750	1	0.5	551.30
1000	1	0.1	517.95
1000	1	0.25	531.33
1000	1	0.4	537.01
1000	1	0.5	545.86
250	1.5	0.1	535.49
250	1.5	0.25	549.05
250	1.5	0.4	559.32
250	1.5	0.5	560.25
500	1.5	0.1	532.42
500	1.5	0.25	547.43
500	1.5	0.4	556.24
500	1.5	0.5	562.26
750	1.5	0.1	538.58
750	1.5	0.25	541.81
750	1.5	0.4	549.28
750	1.5	0.5	558.60
1000	1.5	0.1	525.66
1000	1.5	0.25	537.01
1000	1.5	0.4	540.41

APPENDIX B4: Real training data for using ANFIS model to predict the friction force in Z- axis

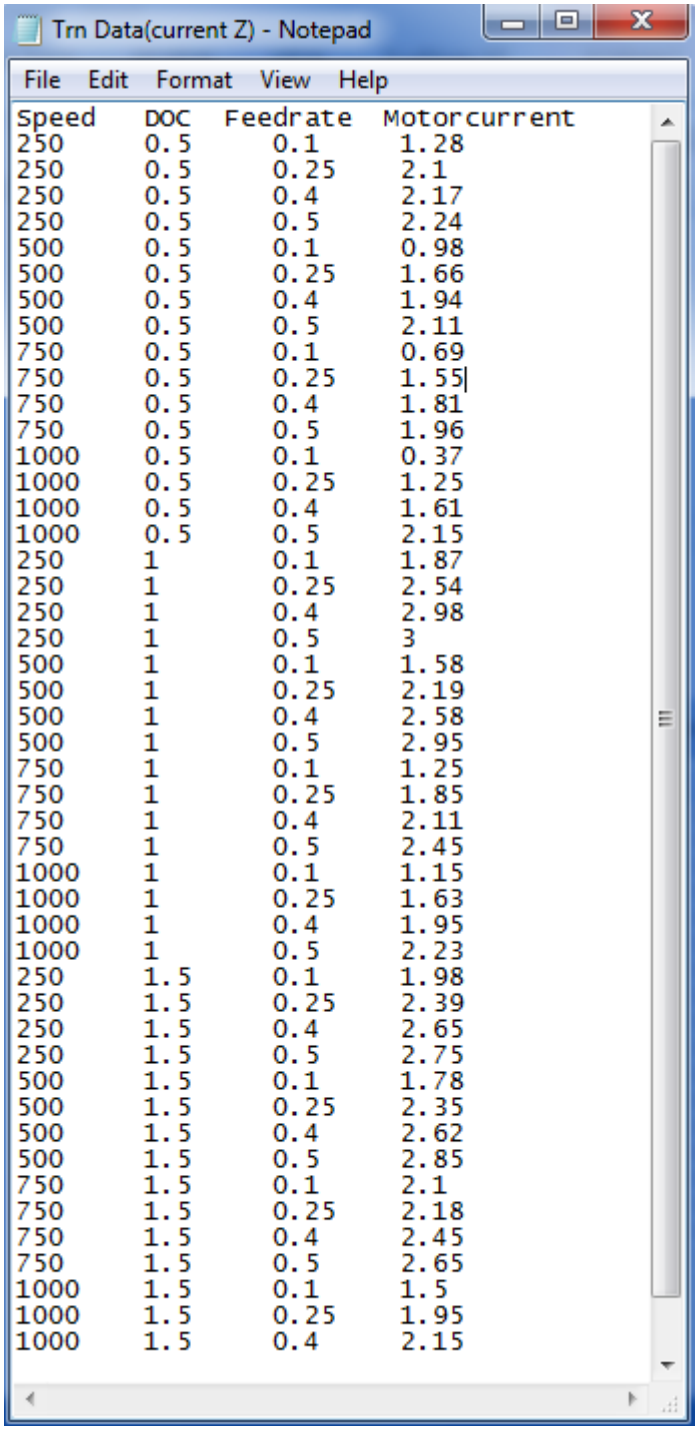

APPENDIX B5: Real training data for using ANFIS model to predict the motor current in Z- axis

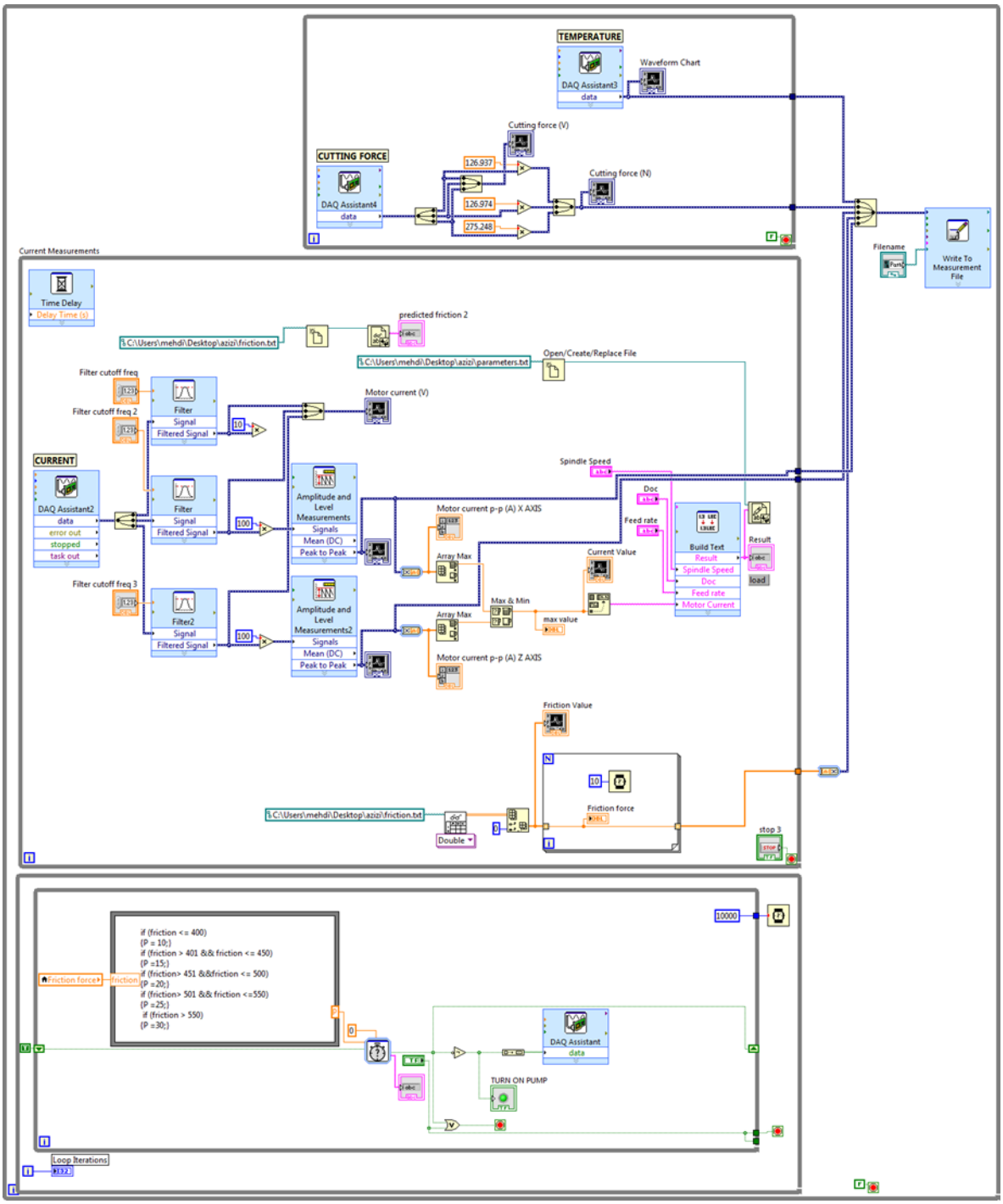

APPENDIX B6: A model of closed loop control for lubrication using LabVIEW

APPENDIX C

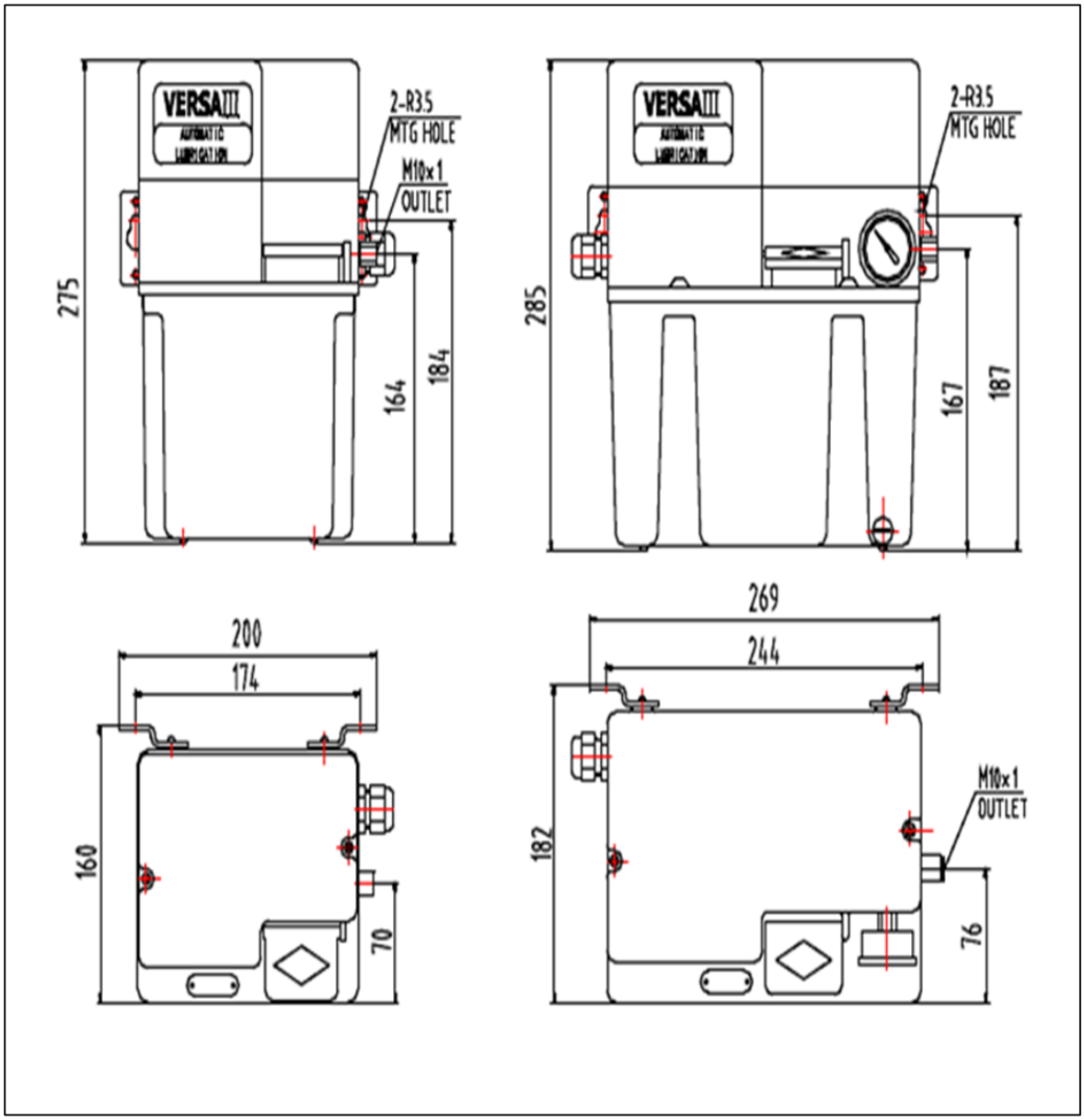

APPENDIX C1: Dimension of lubricating system used in new technique control

Dimensions & Specifications:

LCB4 0 1 1 C

Model		LCB4
Pump MLB01W,X	Discharge Vol.	100 cc/min
	Discharge Press.	12 kg/cm2
Tank Capacity	Gross	2 Liters
	Net	1.3 Liters
Timer / Controller		None
Weight		4.1 kg

0	2L Plas.
1	2L Alum.

0	FS, PS
1	FS
3	PS
4	None

0	PG
1	No PG

C	100V
B	200V

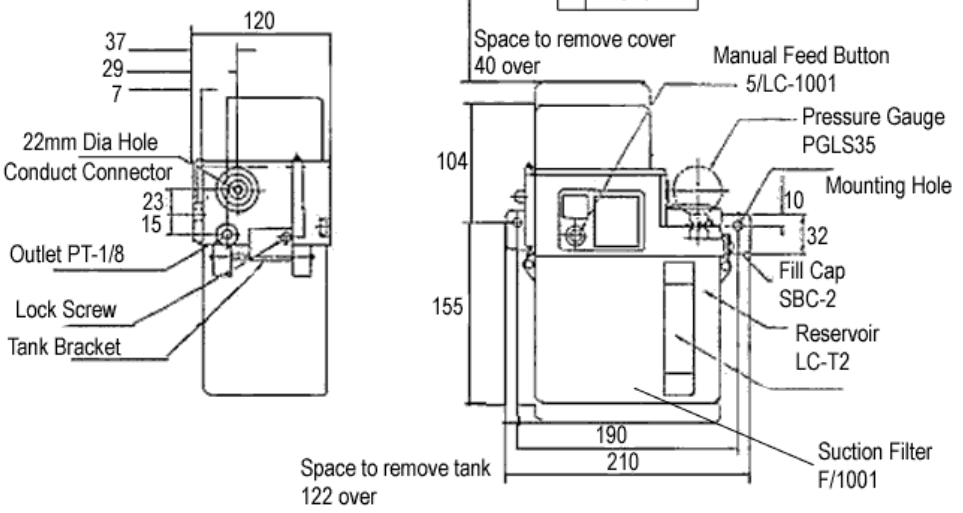

Specifications:

Pump No. MLB01W,X	Discharge Volume	100cc/min (50Hz) 120cc/min (60Hz)			
	Discharge Pressure	12 kg/cm2			
Motor M-B01-100 (100V) M-B01-200 (200V)	Voltage	M-B01-100 (100V)		M-B01-200 (200V)	
	Frequency	50Hz	60Hz	50Hz	60Hz
	Current	1.5A	1.2A	0.8A	0.6A
	RPM	2500	3000	2500	3000
	Output	17W x 2P			
	Insalation	E Type			
	Running Time	5 Minute Maximum			
	Resting Time	Running Time X2 Mins or more (Min 2 Min)			
Reservoir Capacity		Gross (2 Liters), Net (1.3 Liters)			
Float Switch (OLV01.02)		AC-0.33A, DC-0.5A			
Pressure Switch (GFB8-5)		AC-250V, 5A			
Oil Viscosity Range		50-800 cSt			

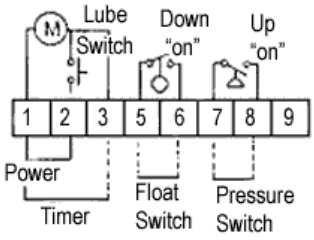

1-2: Power
1-3: Timer
4-5: Float Switch
6-7: Pressure Switch
(Engage when Pressure increases)

Do Not use Float Switch to Control Motor.

Circuit Diagram

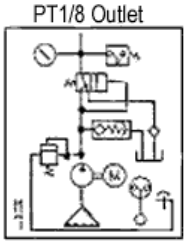

APPENDIX C2: Dimension and specification of lubricating system in CNC OKUMA LB15II (SHOWA LCB4)

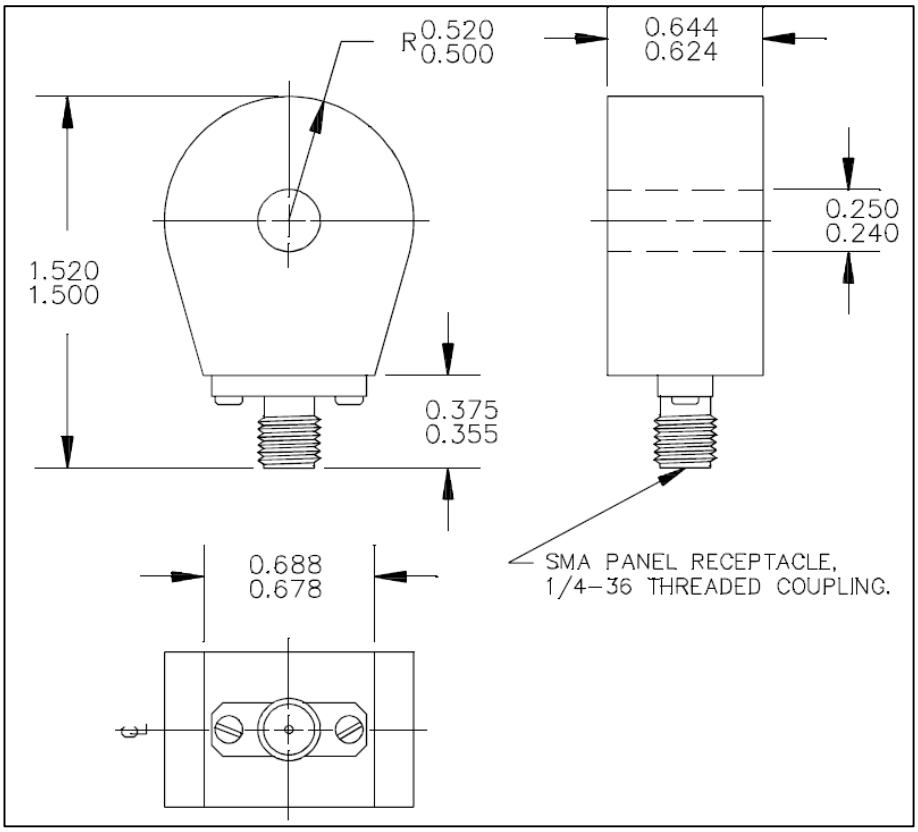

APPENDIX C3: Dimension of Current Clamp Model 2879

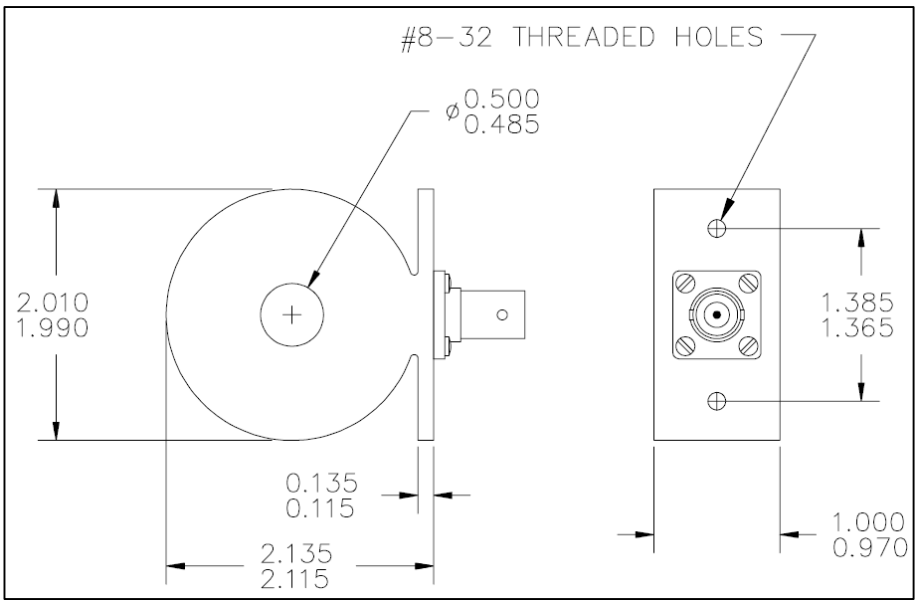

APPENDIX C4: Dimension of Current Clamp Model 410

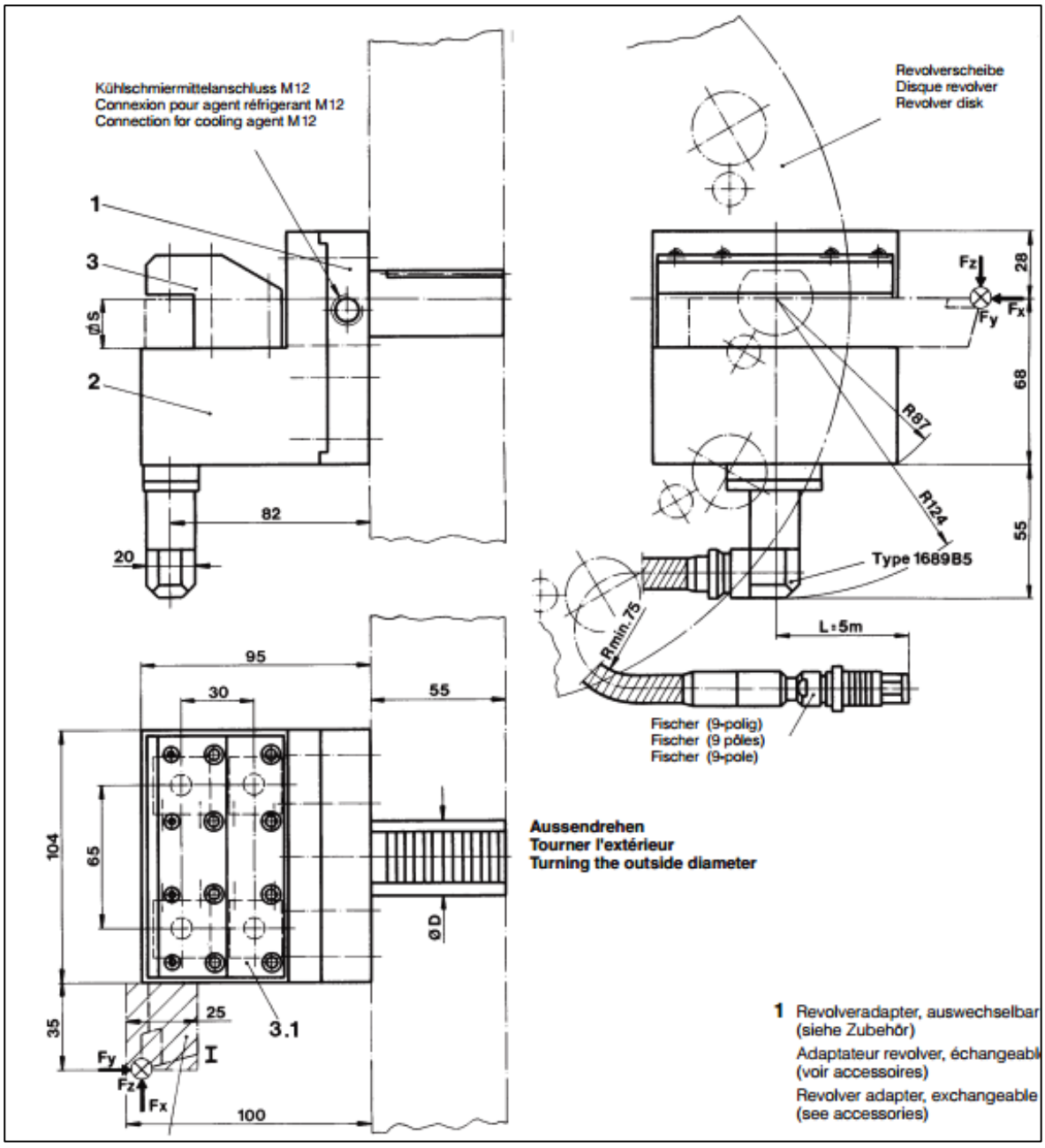

APPENDIX C5: Dynamometer 2D drawing (Model- Kistler 9121)

APPENDIX D

APPENDIX D1: specification of Surface Thermocouple with Self-Adhesive Backing

Thermocouple Calibration	**K** Type $\begin{Bmatrix} CHROMEGA: A\ chrominum - nickel\ alloy \rightarrow +(leg) \\ ALOMEGA: An\ aluminum - nickel\ alloy \rightarrow -(leg) \end{Bmatrix}$
Adhesive	Silicon based cement
Maximum Temperature	175°C (350°F) continuous
Minimum Temperature	-60°C (-75°F) continuous
Dimensions	25 L x 19 W x 0.3 mm (1 x 0.8 x 0.01")
Laminates	High temperature polymer, and fiberglass reinforced polymer layers
Wire	30 AWG PFA-coated
Adhesive Pad (TAP)	Polyamide Film with a silicone pressure sensitive adhesive,13% Polyamide, 32% Polymethyl phenylsiloxane, 54% Saturated Paper
Response Time	Better Than 0.3 Second
Accuracy	± 0.1 °C

APPENDIX D2: Pearson Current monitor specifications

	Model 2879	Model 410
Sensitivity	0.01 Volt/Ampere +1/-0%	0.1 Volt/Ampere +1/-0%
Output resistance	Output resistance 50 Ohms	50 Ohms
Maximum peak current	2,000 Amperes	5,000 Amperes
Maximum rms current	25 Amperes	50 Amperes
Droop rate	0.002 %/microsecond	0.06 %/microsecond
Useable rise time	20 nanoseconds	20 nanoseconds
Current time product	0.04 amp-seconds maximum*	0.25 Ampere-second maximum
Low frequency 3db point	Hz (approximate)	120 Hz (approximate)
High frequency 3db point	20 MHz (approximate)	20 MHz (approximate)
I/f figure	0.25 peak Amperes/Hz	1.7 peak Amperes/Hz
Output connector	SMA	BNC (UG-290A/U)
Operating temperature	0 to 65 °C	0 TO 65°C
Weight	1.12 ounces	8.7 ounces

APPENDIX D3: Table of friction coefficient between materials

MATERIAL 1	MATERIAL 2	Coefficient Of Friction			
		Dry		Greasy	
		Static	Sliding	Static	Sliding
Aluminum	Aluminum	1.05-1.35	1.4	0.3	
Brake Material	Cast Iron (Wet)	0.2			
Brass	Cast Iron		0.3		
Bronze	Cast Iron		0.22		
Bronze	Steel			0.16	
Cadmium	Cadmium	0.5		0.05	
Cadmium	Mild Steel		0.46		
Cast Iron	**Cast Iron**	**1.1**	**0.15**		**0.07**
Cast Iron	Oak		0.49		0.075
Chromium	Chromium	0.41		0.34	
Copper	Cast Iron	1.05	0.29		
Copper	Copper	1.0		0.08	
Copper	Mild Steel	0.53	0.36		0.18
Copper-Lead Alloy	Steel	0.22		-	
Diamond	Diamond	0.1		0.05 - 0.1	
Diamond	Metal	0.1 -0.15		0.1	
Glass	Glass	0.9 - 1.0	0.4	0.1 - 0.6	0.09-0.12
Glass	Metal	0.5 - 0.7		0.2 - 0.3	
Glass	Nickel	0.78	0.56		
Graphite	Graphite	0.1		0.1	
Graphite	Steel	0.1		0.1	
Graphite (In vacuum)	Graphite (In vacuum)	0.5 - 0.8			
Hard Carbon	Hard Carbon	0.16		0.12 - 0.14	
Hard Carbon	Steel	0.14		0.11 - 0.14	
Iron	Iron	1.0		0.15 - 0.2	
Lead	Cast Iron		0.43		
Magnesium	Magnesium	0.6		0.08	
Nickel	Nickel	0.7-1.1	0.53	0.28	0.12
Nickel	Mild Steel		0.64;		0.178
Nylon	Nylon	0.15 - 0.25			
Platinum	Platinum	1.2		0.25	
Plexiglas	Plexiglas	0.8		0.8	
Plexiglas	Steel	0.4 - 0.5		0.4 - 0.5	
Polystyrene	Polystyrene	0.5		0.5	
Polystyrene	Steel	0.3-0.35		0.3-0.35	
Polythene	Steel	0.2		0.2	
Silver	Silver	1.4		0.55	
Sintered Bronze	Steel	-		0.13	
Solids	Rubber	1.0 - 4.0		--	
Steel	Aluminium Bros	0.45			
Steel	Brass	0.35		0.19	
Steel(Mild)	Brass	0.51	0.44		
Steel (Mild)	Cast Iron		0.23	0.183	0.133
Steel	Cast Iron	0.4		0.21	
Steel	Copper Lead Alloy	0.22		0.16	0.145
Steel (Hard)	Graphite	0.21		0.09	
Steel	Graphite	0.1		0.1	
Steel (Mild)	Lead	0.95	0.95	0.5	0.3
Steel(Hard)	Polythened	0.2		0.2	
Steel(Hard)	Polystyrene	0.3-0.35		0.3-0.35	
Steel (Mild)	Steel (Mild)	0.74	0.57		0.09-0.19
Steel(Hard)	**Steel (Hard)**	**0.78**	**0.42**	**0.05 -0.11**	**0.029-0.12**
Steel	Zinc (Plated on steel)	0.5	0.45	-	-

APPENDIX D4: Data Sheet for Module of temperature measurement NI9211

Input Characteristics	Specifications
Number of channels	4 thermocouple channels, 1 internal autozero channel, 1 internal cold-junction compensation channel
ADC resolution	24 bits
Type of ADC	Delta-Sigma
Sampling mode	Scanned
Voltage measurement range	±80 mV
Temperature measurement ranges	Works over temperature ranges defined by NIST (J, K, T, E, N, B, R, S thermocouple types)
Conversion time	70 ms per channel; 420 ms total for all channels including the autozero and cold-junction channels
Common-mode voltage range	
Channel-to-COM	±1.5 V
COM-to-earth ground	±250 V
Common-mode rejection ratio (0 to 60 Hz)	
Channel-to-COM	95 dB
COM-to-earth ground	>170 dB
Input bandwidth (–3 dB)	15 Hz
Noise rejection (at 50 and 60 Hz)	85 dB min
Overvoltage protection	±30 V between any input and COM
Differential input impedance	20 MΩ
Input current	50 nA
Input noise	1 μV rms
Gain error	0.05% max at 25 °C, 0.06% type at –40 to 70 °C, 0.1% max at –40 to 70 °C
Offset error (with auto zero channel on)	15 μV type, 20 μV max
Gain error from source impedance	Add 0.05 ppm per Ω when source impedance >50 Ω
Offset error from source impedance	Add 0.05 μV typ, 0.07 μV max per Ω source impedance >50 Ω
Cold-junction compensation sensor accuracy	
0 to 70 °C	0.6 °C typ, 1.3 °C max
–40 to 70 °C	1.7 °C max
MTBF	633,012 hours at 25 °C; Bellcore Issue 2, Method 1, Case 3, Limited Part Stress Method

APPENDIX D5: Data Sheet for Module of servomotor current measurement NI9205

Analog Input Characteristics	Specifications
Number of channels	32 single-ended or 16 differential analog input channels, 1 digital input channel, and 1 digital output channel
ADC resolution	16 bits
DNL	No missing codes guaranteed
INL	Refer to the AI Absolute Accuracy Tables and Formulas
MTBF	775,832 hours at 25 °C; Bell core Issue 6, Method 1, Case 3, Limited Part Stress Method
Conversion time	
R Series Expansion chassis	4.50 µs (222 kS/s)
All other chassis	4.00 µs (250 kS/s)
Input coupling	DC
Nominal input ranges	±10 V, ±5 V, ±1 V, ±0.2 V
Minimum over range (for 10 V range)	4%
Maximum working voltage for analog inputs (signal + common mode)	Each channel must remain within ±10.4 V of common
Input impedance (AI-to-COM)	
Powered on	>10 GΩ in parallel with 100 pF
Powered off/overload	4.7 kΩ min
Input bias current	±100 pA
Crosstalk (at 100 kHz)	
Adjacent channels	–65 dB
Non-adjacent channels	–70 dB
analog bandwidth	370 kHz
Overvoltage protection	
AI channel (0 to 31)	±30 V (one channel only)
AISENSE	±30 V
CMRR (DC to 60 Hz)	100 dB

APPENDIX D6: Data Sheet for Module of cutting force measurement NI9219

Input Characteristics	Specifications
Number of channels	4 analog input channels
ADC resolution	24 bits
Type of ADC	Delta-sigma (with analog prefiltering)
Sampling mode	Simultaneous
Type of TEDS supported	IEEE 1451.4 TEDS Class II (Interface)
Overvoltage protection	
Terminals 1 and 2	±30 V
Terminals 3 through 6, across any combination	±30 V
Input impedance	
Voltage and Digital In modes (±60 V, ±15 V, ±4 V)	1 MΩ
Current mode	<40 Ω
All other modes	>1 GΩ
Input bias current	<1 nA
INL	±15 ppm
CMRR ($f$in = 60 Hz)	>100 dB
NMRR	
Best 60 Hz rejection	90 dB at 60 Hz
Best 50 Hz rejection	80 dB at 50 Hz
High resolution	65 dB at 50 Hz and 60 Hz

APPENDIX D7: Data Sheet for Module of A/D converter NI9474

Output Characteristics	Specifications
Number of channels	8 digital output channels
Output type	Sourcing
Power-on output state	Channels off
External power supply voltage range (Vsup)	5–30 VDC
Output impedance (R0)	0.07 Ω
Typical	0.13 Ω
Maximum	0.75 A max
Continuous output current (I0), per channel	1 A max
Output voltage (V0)	Vsup – (I0 · R0)
I/O protection	
Voltage	30 VDC max
Reversed voltage	None
hort-circuit trip time	10 μs at 13 A
Output delay time (full load)	1 μs max
MTBF	479,889 hours at 25 °C; Bellcore Issue 2, Method 1, Case 3, Limited Part Stress Method
Power consumption from chassis	
Active mode	660 mW max
Sleep mode	0.6 mW max
Thermal dissipation (at 70 °C)	
Active mode	1.5 W max
Sleep mode	0.6 mW max

APPENDIX D8: Technical data for multi-channel charge amplifier
(Model 5019 B 141, Kistler)

Charge amplifier		Specifications
Number of measuring channels		3 ... 4
Measuring range		pC ±10 ... 999'000
Sensor sensitivity		pC / M.U. 0,01 ... 9'990
Scale		M.U. / V 0,001 ... 9'990'000
Output voltage		V ±10
Output current (short-circuit protected)		mA 0 ... ±5
Output impedance		Ω 10
Frequency limit (–3dB, Filter off)		kHz ≈ 0 ... 200
Low-pass filter Butterworth 2 pol., 8 stages 10, 30, 100 ... (–3dB)		KHz 0,01 ... 30 (±10 %)
Time constant	Long	DC-mode
High-pass filter	Medium	s 1 ... 10'000
	Short	s 0,01 ... 100
Linearity		% ≤ ±0,05
Measuring error		
≤ ±99,9 pC FS		% ≤ ±3
≥ ± 100 pC FS		% ≤ ±1
Output interference		mV rms < 1,5
Drift (input current MOSFET) at 25 °C		pC/s < ±0,03
Temperature range		°C 0 ... 50
Power supply (switchable)		V AC 230 / 115
		% +15 / –22
		Hz 48 ... 62
Power consumption		VA 35
Dimensions (DIN 41494, part 5)		
Width		TE 63
Height		HE 4
With case and handle		Mm 396 x 187 x 280
Weight		Kg 8